This material may be protected by copyright law (Title 17 U.S. Code).

The University of Wisconsin Library
Manuscript Theses

Unpublished theses submitted for the Master's and Doctor's degrees and deposited in The University of Wisconsin Library are open for inspection, but are to be used only with due regard to the rights of the authors. Bibliographical references may be noted, but passages may be copied only with the permission of the authors, and proper credit must be given in subsequent written or published work. Extensive copying or publication of the thesis in whole or in part requires also the consent of the Dean of the Graduate School of The University of Wisconsin.

This thesis by MARY ANN KELLY has been used by the following persons, whose signatures attest their acceptance of the above restrictions.

A Library which borrows this thesis for use by its patrons is expected to secure the signature of each user:

NAME AND ADDRESS DATE

LITHOLOGIES, CARBONATE BUILDUPS, AND CYCLICITY OF THE LOWER DESMOINESIAN BARKER CREEK INTERVAL, PARADOX BASIN, SE UTAH

by

MARY ANN KELLY

A thesis submitted in partial fulfillment of the requirements for the degree of

MASTER OF SCIENCE
(GEOLOGY)

at the

UNIVERSITY OF WISCONSIN - MADISON

1994

UCH
MWO
K259
U378

AFRA691

Abstract

The field area is located on the southwestern shelf of the Pennsylvanian Paradox Basin, a northwest - southeast trending basin, formed in conjunction with the uplift of the "Ancestral Rocky Mountains" during the late Paleozoic. Outcrops are exposed along deeply incised entrenched meanders on the San Juan River between river miles 39 and 43 (Baars and Stevenson, 1986).

The upper 40 meters of the Barker Creek interval of the Paradox Formation consist primarily of shallow water carbonates with minor sandy dolomites and siltstones. This stratigraphic interval contains thirteen shallowing upward sequences, which are included within eight sea level cycles separated by exposure surfaces. Evidence of exposure found at these surfaces includes rhizoliths, paleosols, fissures, and conglomerates with blackened clasts. There are two types of cycles in the study area. Cycles of the first type progress from high energy to low energy environments and are capped by an algal laminite. Cycles of the second type progress from low energy to high energy environments, and are again capped by either an algal laminite or stromatolites.

A bioherm-rich zone is present within the Barker Creek interval. All bioherms appear to have initiated growth at the same time. The beds making up the bioherms can be divided into two distinct zones. The lower, Zone A, is made up of wacke-, pack-, and grainstones, contains no Chaetetids, and appears to have been mechanically

reworked. The orientation and syndepositional relief of mounds within Zone A is interpreted to be a product of wave and tidal currents, with a possible transport direction from the northwest. The upper, Zone B, is made up of wacke-, pack-, grain-, and boundstones, contains Chaetetids, and is interpreted to have been biologically formed. Mounds within Zone B always grew above a Zone A mound, and in the same orientation. Zones A and B are interpreted to have been deposited during separate shallowing upward sea level cycles.

Mounds within Zones A and B are elongated, oriented with the long axis trending between N10°W and N60°W. They appear to be form patches, rather than ribbons or bands with a SE-NW orientation as previously described by Wengerd (1955). The bioherm orientation is roughly parallel to the southwestern shore of the Paradox Basin. The bioherms vary in height from 3 to 20 m. It is unclear why there is such a discrepancy in bioherm size. There is an increase in bioherm size to the southwest in the field area. If it is assumed that all bioherms grew to fill accommodation space, and that bioherm height reflects paleo-water depth, the trend in bioherm height indicates that the sea floor was sloping 1.0° to the southwest. This is the opposite slope expected on the southwestern shelf of the basin. This slope may reflect local perturbations in topography rather than the regional trend.

Acknowledgments

This project offered an incredible opportunity for classic field geology in one of the most beautiful places to which I have ever traveled. I would like to thank my advisor, Toni Simo, for introducing me to the project, and for his patience and advice as I experienced the trials of "big science". I owe much to Gary Gianniny for introducing me to the field area, and for the invaluable assistance he gave me on the river. I now know more about rubberized raft repair than I ever would have wanted to know! Gary has also kindly allowed me to use several of his figures in this thesis.

My assistant during my summer of field work was Kathy O'Neil, who showed extreme fortitude, as well as patience as we experienced situations that neither of us ever dreamed we would be in. She made great pancakes on rainy mornings, and taught me splendid songs which echoed through the canyons. I wish her luck in her upcoming adventures through central Europe.

A very embarrassed thanks must go out to the members of the Arizona Wilderness Club who helped me out when my very small raft hit a very big rock in the San Juan. This is a story whose time to be told has not yet come.

Thanks, and a jaunt to House on the Rock, must be given to Mary A. K. Lee, who showed me that it is actually possible to complete ones thesis in a reasonable amount of time. I also thank my comrades in

stress, Tuffy Peare and Meredith Westover, who managed to make me laugh and keep me sane during the past two years. These friendships, forged in the fire known as grad school, are some of the strongest I have ever shared.

Finally, I would like to acknowledge my father, James J. Kelly, who never stopped encouraging me whenever I thought of giving up. I would never have gotten as far as I have today without his confidence and pride backing me up.

Funding for this project was provided by grants from the Geological Society of America (Grant No. 4966-92), The American Association of Petroleum Geologists (Grant No. 201-12-00), ARCO, the University of Wisconsin Geology Department, and the USGS.

Table of Contents

Abstract ii

Acknowledgments iv

Table of Contents vi

Chapter 1 - Introduction 1

- Introduction 1
- Introduction to the Paradox Basin 5
- Formal and Informal Stratigraphic Nomenclature 7
- Pennsylvanian Bioherms and their Composition 11
- Cyclicity within the Paradox Basin 13
- Rock Types in the Study Area 14
- Organization of Thesis 25

Chapter 2 - BC1 Interval 26

- Introduction 26
- Rock Types in the BC1 Interval 26
- Cycles in the BC1 Interval 41

Chapter 3 - BC2 Interval 45

- Introduction 45
- Rock Types in the BC2 Interval 46
- Cycles in the BC2 Interval 84
- Bioherms in the BC2 Interval 91
  - Zonation of Lithofacies within Bioherm H 95
  - Zonation of Lithofacies within Other Bioherms 99

Geometry and Distribution of Bioherms....106
Growth History of Bioherms in the BC2 Interval....109
Chapter 4 - BC3 and Akah Intervals....113
Introduction....113
Rock Types in the BC3 and Akah Intervals....114
Cycles in the BC3 and Akah Intervals....131
Chapter 5 - Conclusions....135
Introduction....135
Lithologic Trends in the Stratigraphic Column....135
Cyclicity in the Stratigraphic Column....138
Growth History of the Bioherm Community....142
Bioherm Orientation and Distribution....143
Control of Bioherm Size....144
References....146
Appendix A - Measured Sections....149
Appendix B - Description of Hand Samples....180

Chapter 1

Introduction

- INTRODUCTION -

The objective of this thesis is to provide a detailed field description of a bioherm community in Pennsylvanian age rocks in the Paradox Basin, southeastern Utah. Field work was conducted during the summer of 1992. Thin section and hand sample descriptions were made in 1992 and 1993. The objects of this study were 1) to verify lithologic repetition and cyclicity in the stratigraphic column examined, 2) to establish the growth history of the bioherm community, 3) to document and explain bioherm orientation and distribution, and 4) to determine the controls of bioherm size.

The field area is located in southeastern Utah, in the four corners area of the United States (Figures 1.1 and 1.2). Outcrops are exposed along deeply incised entrenched meanders on the San Juan River between river miles 39 and 43 (river miles after Baars and Stevenson, 1986) (Figure 1.3). Exposures along the San Juan River are excellent, with approximately 10% of the stratigraphic interval under cover.

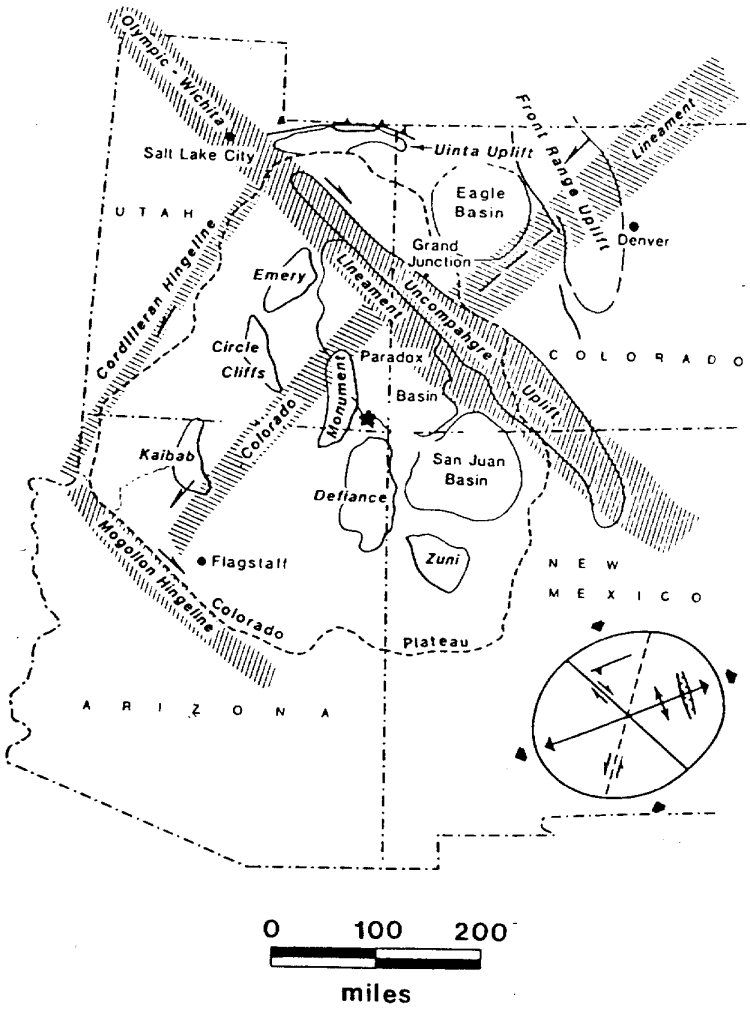


Figure 1.1 - Regional map, showing location of Paradox Basin. The Paradox Basin is a pull-apart basin, aligned along right-lateral NW-SE faults and NE-SW faults. The star marks the location of the field area in southeastern Utah, on the southwestern margin of the Paradox Basin. (From Baars and Stevenson, 1981, p 26.)

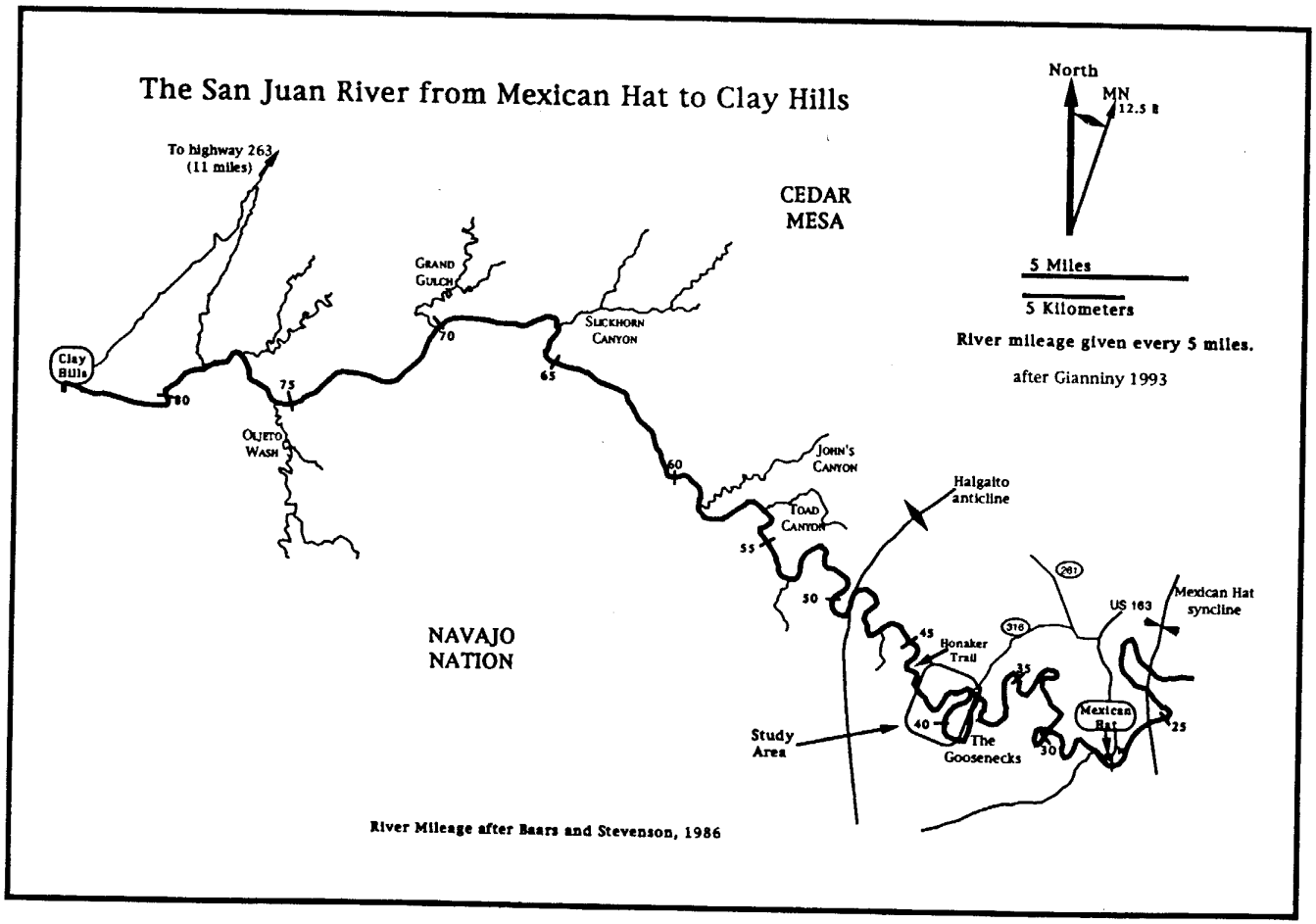


Figure 1.2 - Map of the San Juan River showing location of the field area.

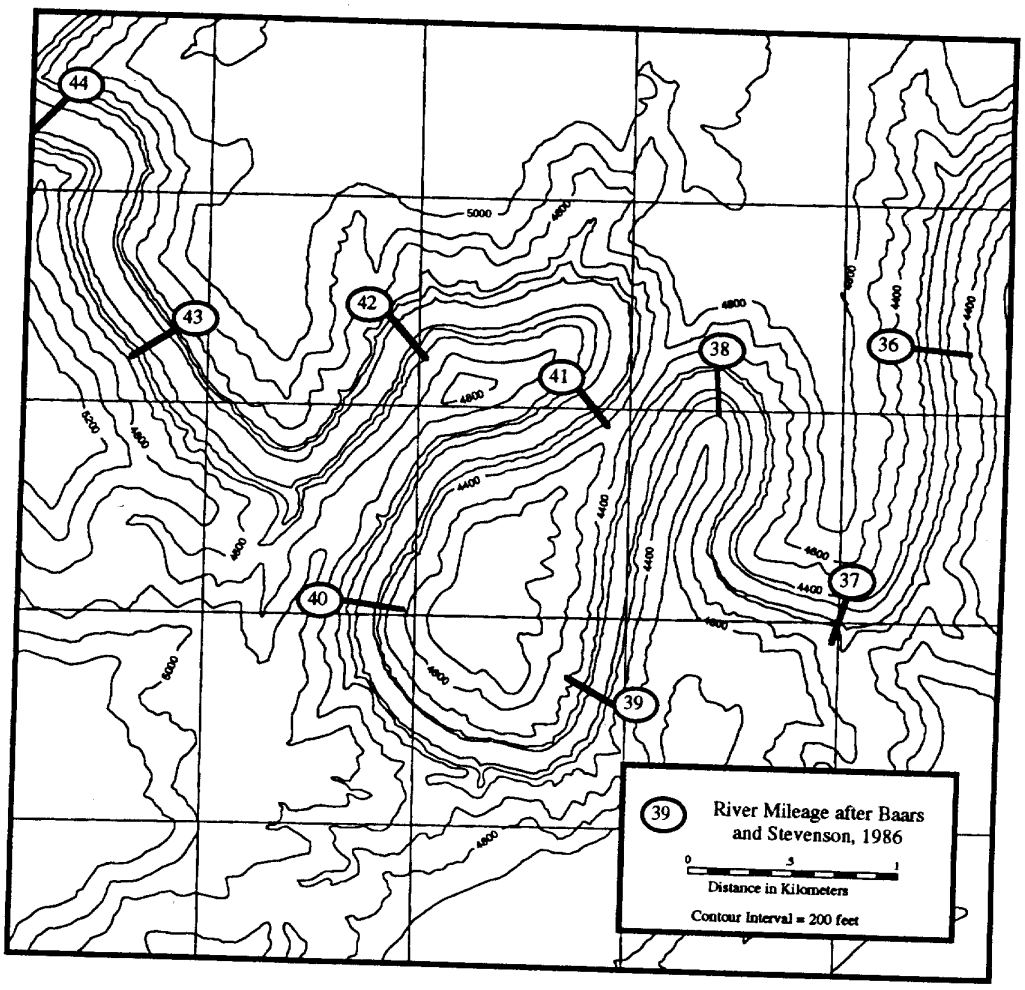


Figure 1.3 - Topographic map of study area within "Goosenecks" of the San Juan, from river mile 36 to 44.

- INTRODUCTION TO THE PARADOX BASIN -

The field area is located on the southwestern shelf of the Pennsylvanian Paradox Basin (Figure 1.1). This is a northwest - southeast trending basin, formed in conjunction with the uplift of the "Ancestral Rocky Mountains" during the late Paleozoic. During the Pennsylvanian, the basin was bordered to the northeast by the Uncompaghre uplift, to the south by the Defiance upwarp, and to the west by the Monument upwarp (Figure 1.1). The basin is asymmetrical in cross-section. The deepest part of the basin is adjacent to the Uncompaghre uplift (Baars and Stevenson, 1981) (Figure 1.4). Water circulation was restricted during parts of the Pennsylvanian, resulting in a thick accumulation (up to 8,000 feet or 2,500 m; Baars and Stevenson, 1981) of evaporites and black shales in the deepest portion of the basin. The northeastern edge of the basin is dominated by coarse siliciclastic sediments shed off the Uncompaghre uplift, and contains numerous internal unconformities; both a reflection of the tectonically active Uncompaghre Uplift. Mixed carbonate and siliciclastic rocks were deposited in the relatively shallow southwestern portion of the basin.

The structural features in the area of the Paradox Basin, including the Monument Upwarp, were all in place by the Pennsylvanian, formed in relation to deep basement faults (Baars and Stevenson, 1981). These features continued to be tectonically active throughout the Pennsylvanian. These structures were rejuvenated during the Laramide orogeny. Flowage of the salts within the basin

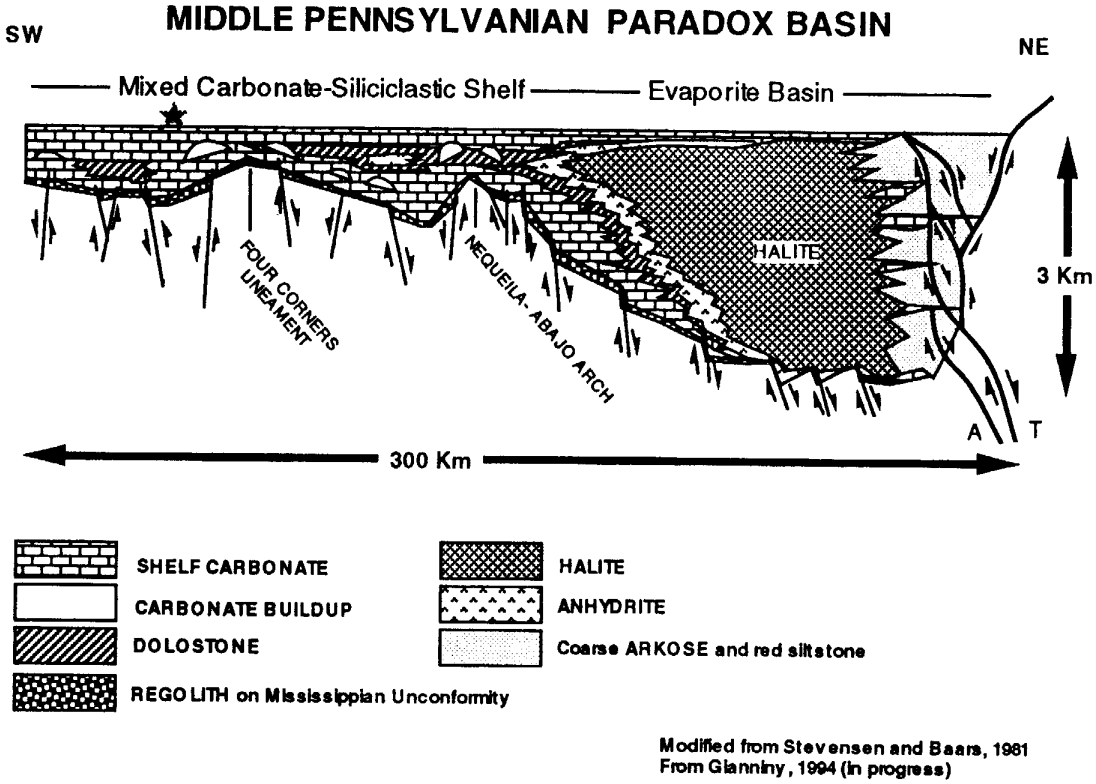


Figure 1.4 - Cross section of the Paradox Basin, showing its assymetric nature. Coarse siliciclastic sediments are found adjacent to the Uncompaghre uplift. A thick evaporite package (up to 8000 feet, 2500 m thick) is found in the deepest portions of the basin. Mixed carbonate and siliciclastic sediments are located on the shallow southwestern margin of the basin. The star marks the approximate location of the field area, within the Paradox shelf carbonates. (Modified from Baars and Stevenson, 1981, p. 28.)

has created numerous salt anticlines within the four corners area. Uplift of the Colorado Plateau during the Eocene had little effect upon the structure of the study area. It did cause increased surface erosion however, creating the "Goosenecks", or entrenched meanders of the San Juan river, along which the field area is exposed. The field area is located within the Cedar Mesa Anticline (part of the Monument Upwarp) which brings the older strata up to river level. Strata in the field area are roughly horizontal, dipping very gently to the north (N4W, 1.6°NE).

- FORMAL AND INFORMAL STRATIGRAPHIC NOMENCLATURE -

The rocks studied are Desmoinesian (Pennsylvanian) in age, approximately 300 MY old. The rocks of the Paradox Formation are informally divided into four intervals; from oldest to youngest they are the Barker Creek, Akah, Desert Creek, and Ismay intervals (Peterson and Ohlen, 1963; and See, 1963) (Figure 1.5). The intervals are related to productive oil and gas intervals in the Paradox Basin (See, 1963). The stratigraphic interval studied is within the Barker Creek and Akah intervals. Only the upper half to third of the Barker Creek interval is exposed in the field area. The stratigraphy outcropping in the study area has been further informally subdivided into three intervals (Figure 1.6): 1) the BC1, 2) the BC2, and 3) the BC3 and the lower part of the Akah. It should be noted that this subdivision of the Barker Creek interval is <u>not</u> formal and merely divides the interval according to my emphasis of study.

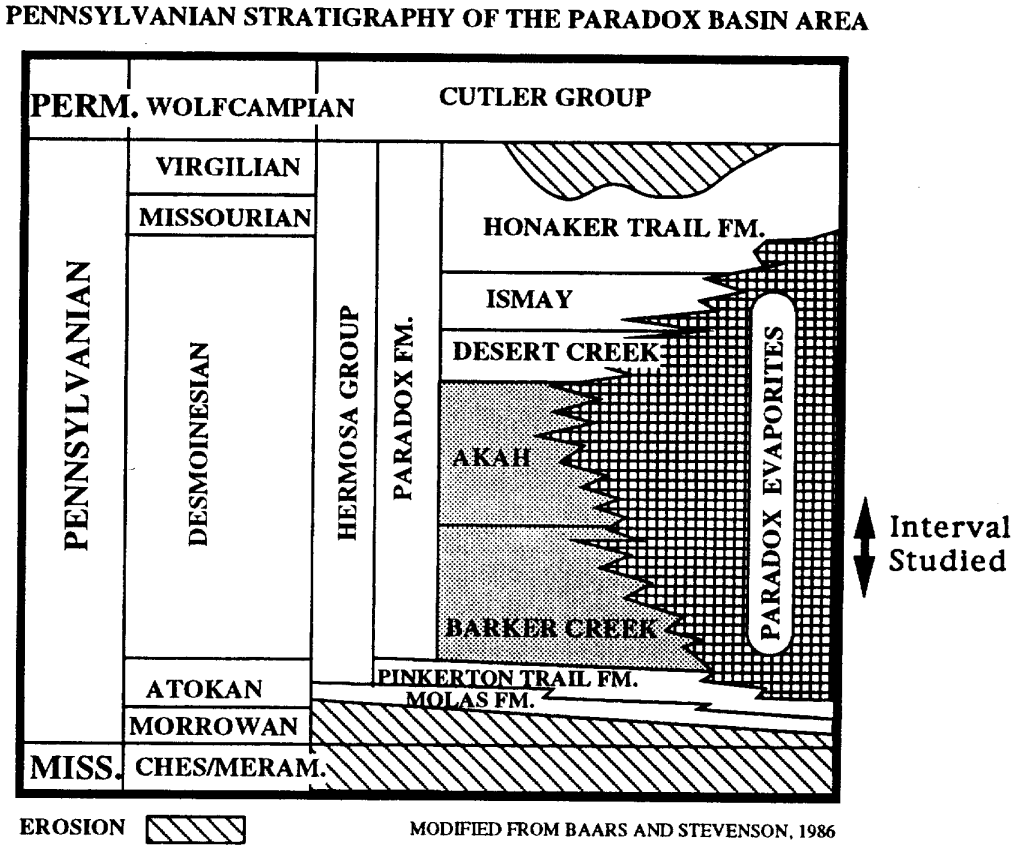


Figure 1.5 - Pennsylvanian stratigraphy within the Paradox Basin. The two intervals of interest, the Barker Creek and Akah, are shaded. (From Gianniny, 1994, in progress.)

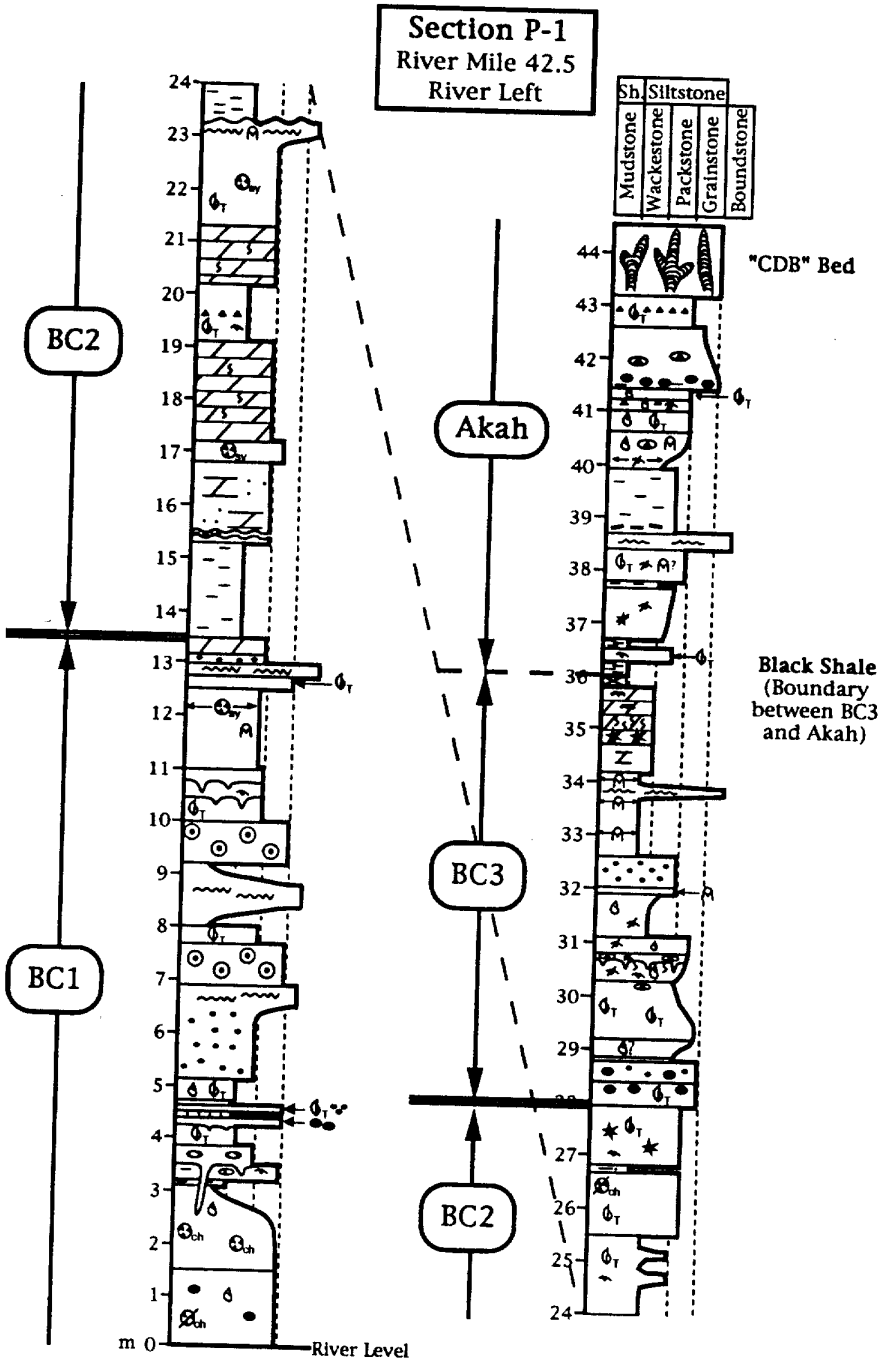


Figure 1.6 - Section P-1 showing subdivision of stratigraphic section within study area into three informal intervals (BC-1, BC-2, and BC-3 and Akah).

The BC1 interval is defined as the section exposed from river level to the base of a green siltstone (often covered in the study area) which marks the base of the BC2 interval. This green siltstone is a marker bed which can be traced throughout the exposed Barker Creek along the San Juan River. The BC2 interval is defined as a bioherm rich zone which extends from the base of the green siltstone to the upper surface of the bioherms, below the overlying conglomerate (or the equivalent surface in an inter-bioherm position). The BC3 and lower Akah interval is defined as the section from the base of the conglomerate overlying the bioherms to the upper surface of a distinctive digitate boundstone layer within the Akah, referred to as the continuous digitate bed or "CDB". The BC3 and Akah subdivisions are discussed together because the stratigraphic boundary between them (a black shale) does not correspond to a cycle boundary.

Four sections were measured through the BC1 interval, which ranges from 3.2 m (Section M-1) to 11.7 m (Section P-1) thick. Seventeen sections were measured through portions of the BC2. Section P-1 is the only section which extends through the BC2. The thickness of the interval in Section P-1 is 14.5 m. The thickness of the BC2 is greater when measured through a bioherm than between bioherms. Estimates of thickness range from 7 m (Section G-1) to 30.7 m (Section P-4) in a bioherm position and from 6 m (Section G-2) to 14.5 m (Section P-1) in a between-bioherm position. Eight measured sections contain portions of the BC3 and lower Akah, but generally they are incomplete because of covered intervals. Estimates of complete thickness range from 9.5 m (Section P-7) to 16.5 m (Section

P-1). All measured sections, as well as a key to the symbols used, can be found in Appendix A.

- PENNSYLVANIAN BIOHERMS AND THEIR COMPOSITION -

The Pennsylvanian was a time of limited reef growth (James, 1983). There were no skeletal metazoans present at that time to create the resistant skeletons necessary to survive in the turbulent zone in which reefs form. Organic mounds, or bioherms, did grow during this time. In this study the term "bioherm" describes lens-like biogenic buildups which formed areas of relief at the time of deposition. These low relief bioherms grew in quiet water environments, such as downslope environments on shallow platform margins, in deep basins, and widely spread within reef lagoons (James, 1983). The shallow carbonate shelf on the southwestern margin of the Paradox Basin was one such site of bioherm growth in the Pennsylvanian.

Common organisms found in Pennsylvanian bioherms include the following (Wilson, 1975; and West and Clark, 1987):

1) Phylloid Algae: plate-like codiacean(?) algae which are believed to have acted as baffling organisms.
2) Tubular Foraminifera: Opthalmidid and Calcitornellid forms, generally encrusting, forming small masses.
3) Tubiphytes: encrusting, laminated growths of unknown biological affinity, often containing areas of clear calcite.

4) Komia: a red algae, usually found as small broken twig-like forms.
5) Palaeoaplysina: a possible hydrozoan, occurs as thin plates with internal branching tubules.
6) *Chaetetes* - a sclerosponge, generally silicified in the field, showing concentric growth lines. For a discussion on why these are considered to be sclerosponges, see West and Clark (1987 pp. 130-140).

West (1988) describes the Paradox Basin bioherms as being formed dominantly by Chaetetid sponges and phylloid algae (*Ivanovia*). In the study area, three of the above six organisms are seen: tubular foraminifera, Chaetetid sponges, and phylloid algae. Tubular foraminifera are very common both within bioherms and in a between-bioherm position. Chaetetid sponges are found within the bioherms, and appear to have been framebuilding or baffling organisms. Numerous phylloid algae - like organisms have been seen within the bioherms, but no definite phylloid algae have been seen in this study. However other researchers (including West, 1988) however have seen phylloid algae in the bioherms within the study area.

Two organisms in addition to those mentioned above are common within bioherms in the study area. These are:

1) Brachiopods - various species of brachiopods are found, both within bioherms and in a between-bioherm position.

2) Echinoderms - fragmented echinoderm fragments, especially crinoid columnals are found both within bioherms and in a between-bioherm position.

These four (tubular foraminifera, *Chaetetid* sponges, brachiopods, and echinoderms) are the most common organisms found in the study area.

- CYCLICITY WITHIN THE PARADOX BASIN -

The examination of cyclic sedimentation within the Paradox Basin began in 1960 with the work of Hite (1960) in the evaporites and black shales of the Paradox Formation, and Pray and Wray (1963) in the shelf carbonates describing porous algal facies. This work was followed by that of Goldhammer *et al.* (1991) and Atchley and Loope (1993). Goldhammer *et al.* (1991) interpreted the cyclicity to be due to eustatic sea level changes, caused by Milankovich orbital forcing. Atchley and Loope (1993) interpreted higher order cycles to be driven by eustatic sea level changes, and lower order cycles to be caused by tectonic activity. Today the work continues at the University of Wisconsin - Madison, with the study of the mixed carbonates and siliciclastics on the southwestern shelf. Research includes that of Gianniny (1994) and this thesis.

The stratigraphic interval within the study area has been divided into several shallowing upwards cycles. The cycle breaks are defined as surfaces or beds which contain compelling evidence of

exposure. These exposure features include fissures, roots and rhizoliths, paleosols, and conglomeratic beds with blackened clasts.

The repetition of cycles within the study area indicates a fluctuation of relative sea level. It is impossible to determine, at this level of analysis, whether these relative sea level fluctuations are due to eustatic or regional tectonic causes. The fact that the Paradox Basin was tectonically active during the Pennsylvanian strongly suggests that the fluctuations are due at least in part to regional tectonic forces. The repetition of lithofacies, without separation by an exposure surface, may be due to either sea level fluctuations or to environmental fluctuations. The Paradox Basin was a saline environment, with periodic influx of normal marine waters to "replenish the salt supply" (Baars and Stevenson, 1981). This change in salinity would have affected the regional biota, and could have caused a drastic change in carbonate sedimentation without a change in relative sea level.

- ROCK TYPES IN THE STUDY AREA -

The rocks within the study area are quite varied and can change character drastically over a short distance, either vertically or horizontally. To facilitate description of these lithologies, they have been grouped into nine different rock types (Table 1.1). The relative abundance of each rock type within the study area, determined from Section P-1, is shown in Table 1.2. In addition minimum, maximum, and average bed thicknesses within Section P-1 are shown. Data from

Rock Type	Occur-rence	Color	Texture	Dominant Grain Type	Grain Size	Sorting	Dominant Fossils	Porosity	Sedimentary Structures
Bioclastic Limestone	all	light to dark grey	wackestone to packstone	bioclasts	variable	variable	tubular foraminifera, brachiopods, crinoids	variable	grainy laminations
Peloidal Limestone	BC1, BC2, BC3	medium to dark grey	wakestone to packstone	peloids	fine-medium sand, mud	variable	tubular foraminifera, brachiopods	variable	burrows
Oolitic Limestone	BC1	light to medium grey	grainstone	oolites	fine-medium sand	good	-	excellent	trough cross bedding, burrows
Algal Boundstone (Algal Mats)	all	light to medium grey	mudstone or boundstone	carbonate mud, (also bioclasts, peloids)	mud	good	algal binding organisms	poor	algal laminations
Algal Boundstone (Stromatolitic Heads)	BC2, BC3	heads are dark grey to black, matrix is variable	boundstone	mud, bioclasts	mud, granules	poor to moderate	stromatolite-like binders, brachiopods	poor	algal laminations
Oncolitic	all	oncoids are dark grey to black, matrix is light to medium grey	wackestone to packstone	oncolites, also bioclasts, peloids	pebbles, cobbles, matrix variable	poor	encrusting algae and/or foraminifera	poor	-
Clastic (Conglomerate)	all	dark grey to black clasts, matrix variable	-	subangular to subrounded clasts, matrix variable	coarse sand, granules, pebbles, matrix variable	poor	-	poor	-
Clastic (Intraclasts)	all	matrix and clasts, light to medium grey	-	intraclasts, matrix variable	coarse sand, pebbles, matrix variable	poor	-	poor	-
Fine Sandstone/ Siltstone	all	tan, grey, greenish grey	-	quartz silt or fine sand, (also carbonate mud, bioclasts)	silt - fine sand	good	-	moderate to good	-
Dolostone	all	tan, light grey	wackestone to packstone	dolomite rhombohedra, (also fine sand, silt, bioclasts)	silt - vfs	good	-	moderate to good	burrows
Black Shale	BC2 and Akah	black	-	argilaceous mud	mud	well sorted	-	poor	-

Table 1.1 - Characteristics of the nine rock types found in the study area.

Rock Type	Number of Beds	Total Thickness (in meters)	Percentage of Section (Thickness)	Minimum Bed Thickness (in meters)	Average Bed Thickness (in meters)	Maximum Bed Thickness (in meters)
Bioclastic Limestone (1)	26	21.13	48.9	0.18	0.81	1.88
Peloidal Limestone (2)	4	2.41	5.6	0.07	0.60	1.73
Oolitic Limestone (3)	2	1.60	3.7	0.76	0.80	0.84
Algal Boundstone (Algal Mat) (4a)	4	1.85	4.3	0.10	0.46	1.22
Algal Boundstone (Stromatolitic Heads) (4b)	0	0	0	-	0	-
Oncolitic (5)	5	4.11	9.5	0.15	0.82	1.68
Clastic (Conglomerates) (6a)	4	1.41	3.3	0.07	0.35	0.61
Clastic (Intraclasts) (6b)	1	0.10	0.2	-	0.10	-
Fine Sandstone/ Siltstone (7)	10	4.61	10.7	0.07	0.46	1.91
Dolostone (8)	7	5.56	12.9	0.20	0.79	1.52
Black Shale (9)	3	0.40	0.9	0.02	0.13	0.23
Total:		43.18				

Table 1.2 - Relative abundance of rock types in the study area. Data from section P-1.

only Section P-1 is shown because this is the only section which extends through the entire stratigraphic interval. The nine rock types are as follows:

1) Bioclastic Limestone Rock Type: Beds made up of this rock type make up approximately 50% of all beds found in the study area (Table 1.2). They are found in all four stratigraphic intervals. These light to dark gray units are characterized by an abundance of biotic grains, but are otherwise quite varied. They include wackestones, packstones, and grainstones. Peloids are commonly found among the bioclasts. Biotic grains include both in place fossil grains as well as reworked and fragmented material. The fossils most commonly found in these units are tubular foraminifera (encrusting or non-encrusting forms), brachiopods (either in place or reworked, either whole or fragmented), and crinoids (found as discrete crinoid columnals). Other fossils found include *Syringipora* corals, fusulinid foraminifera, Chaetetid sclerosponges, phylloid algae, and unidentifiable fossil hash. Grain size of any bioclast depends on both the fossil and the bed which one is examining. Sorting and porosity also vary from bed to bed. Within the BC2, dissolution of biotic grains has created moldic porosity. Grainy laminations are common, but other sedimentary structures are rare in this rock type. Cross bedding is suggested in one bioclastic packstone in the BC2,

but is not seen elsewhere. This rock types makes up the bulk of the bioherms. Beds which are bioclastic but also contain large oncolites are included in the oncolitic rock type.

The variety of bioclasts and abundance of peloids in the bioclastic limestones suggest the presence of an abundant normal marine fauna. The presence of some mud and the lack of sedimentary structures in the majority of these beds suggests that they were deposited in quiet water environments. Clean grainstones between and grainy laminations within the wackestones and packstones indicate episodic current activity, such as that caused by storm events. The majority of these beds however are interpreted to have been deposited in low-energy subtidal environments.

2) Peloidal Limestone Rock Type: Peloid-rich beds are found only in the BC1, BC2, and BC3 intervals. This medium to dark gray rock type includes both wackestones and packstones. The majority of the grains in these beds are peloids, but other grain types, most commonly bioclasts, may be present. Fossils are most commonly tubular foraminifera and brachiopod fragments. Peloids are generally very fine to medium sand sized. Generally rocks of this type are moderately to well sorted. Burrows have been seen both in the field and in thin section. No other sedimentary structures are seen. Porosity is poor. Beds which are peloidal but also contain large oncolites are included in the oncolitic rock type.

The abundance of peloids and the common presence of bioclastic material suggests that these limestones were deposited in normal marine, low-energy environments.

3) Oolitic Limestone Rock Type: Beds of this rock type are found only in the BC1 interval. These light to medium gray units are well sorted grainstones in which the great majority of grains are ooids. The ooids are very fine to medium sand sized. Fine sand sized fossils (including tubular foraminifera and brachiopod fragments) and peloids are found within one of the oolitic grainstones. Slender vertical burrows are also present in these beds. The grainstones are characterized by excellent porosity. Trough cross bedding is found in the majority of the oolite beds.

Oolitic limestones are interpreted to have been deposited in shallow subtidal, high-energy settings.

4) Algal Boundstone Rock Type: This includes both "algal" mats (Rock Type 4a) and stromatolitic heads (Rock Type 4b). Algal mats are found in all four stratigraphic intervals while stromatolitic heads are found only in the BC2 and BC3 intervals. Algal mats are characterized by very little relief. These light to medium gray boundstones contain trapped mud-sized sediments, and appear to be well sorted. Fenestral porosity is seen in two boundstones. The mats commonly grade either horizontally or vertically into mudstones. They

often contain burrowed intervals. With the exception of the rare fenestrae, the porosity of the algal mats / mudstones is very poor.

Stromatolitic heads are generally domed, hemispherical structures up to 20-30 cm in diameter and with relief of approximately 10-20 cm. These dark gray to black structures are surrounded by mud-rich wackestones or packstones. Fossils, most commonly granule-sized brachiopods, are found nestled in-place between stromatolites, as well as trapped within the stromatolitic heads. The stromatolitic units are more poorly sorted than the algal mat / mudstone units, but they are characterized by just as poor porosity.

The dominance of algal structures in this rock type suggests deposition in a restricted environment. Depositional environment is also restricted to the photic zone. Both algal mats and stromatolites are known to form both subtidally and intertidally. In modern environments, large columnar stromatolites are associated with high-energy settings, while low-relief algal structures are found in protected, low-energy settings (Hoffman, 1976).

5) Oncolitic Rock Type: All beds containing large (2-10 cm diameter) oncolites are included in this rock type, even if they are made up primarily of bioclasts or peloids. These beds are found within all four stratigraphic intervals of the

study area. The oncoids are biogenically formed, most probably by some encrusting algae or a combination of algae and encrusting foraminifera. The oncoids are dark gray to black in color, and may or may not display internal laminations. They are sparsely distributed within this matrix. They are roughly spherical in shape in the BC1 and BC2 intervals, but are disk to bladed in shape in the BC3 interval. The oncolites are found within light to medium gray mud-rich wackestones to packstones. These are poorly sorted units, characterized by poor porosity. Occasionally the oncoids occur along laminae. Usually the are found distributed through approximately 10 cm thick zones. Grainy laminations are found in some of the bioclastic beds.

The association of oncoids with normal marine bioclasts and peloids suggests that they are marine and not freshwater forms. The roughly concentric laminations in some of the oncoids suggests that they formed in an agitated environment, where there was frequent rolling of the grains, allowing equal algal growth on all sides of the oncoid. The massive oncoids, showing no internal laminations, more likely formed in quiet environments, where less turning of the grains occurred (Dahanayake 1983).

6) Clastic Rock Type: Both conglomerates (Rock Type 6a) and intraclast-containing units (Rock Type 6b) are included in this rock type. Conglomerates are found within all four

stratigraphic intervals. They contain dark gray or blackened clasts which range in size from very coarse sand to cobbles. The clasts are subangular to subrounded and commonly appear to be derived from underlying lithologies or nearby bioherms. The matrix is quite variable, ranging from tan to gray, from muddy to grainy, and from sandy to carbonate-rich. The conglomerates are clast supported. Interpenetration of clasts is common. Sorting and porosity of these units is generally poor. Conglomerates often overlie fissured surfaces.

Intraclast-bearing units are also found within all four stratigraphic intervals. The very coarse sand to pebble sized clasts are angular in shape. They are of the same texture and color as the underlying units from which they appear to be derived. The matrix of these units is light to medium gray and is generally quite muddy. These units are poorly sorted and non-porous.

The black color of the conglomerate clasts and the association with fissured surfaces (especially in the BC1 and BC2 intervals) suggests that the conglomerates mark periods of subaerial exposure. The intraclast-bearing units do not necessarily indicate exposure, although some units, such as mud crack related intraclasts, are interpreted to indicate desiccation. They do indicate an interval of high-energy in which either desiccation or scour occurred, and clasts were broken from the substrate and reworked.

7) Sandstone and Siltstone Rock Type: This rock type is found in all stratigraphic intervals. Sandstones and siltstones of appreciable thickness are rare. The majority are merely thin (<50 cm) recessive silty breaks. Rocks of this type are made up predominantly of quartz silt or fine sand, although they may contain carbonate mud or cement. They generally vary in color from tan to gray. They are moderately to well sorted and are moderately to highly porous. Rarely rip-up clasts or conglomerate clasts are seen at the base of the bed. No other sedimentary structures are seen. One thick (2 m) continuous green siltstone at the base of the BC2 interval is a key bed throughout the outcrop area.

The sandstone units can generally be correlated with conglomeratic units, suggesting that they indicate and/or postdate periods of subaerial exposure and terrestrial deposition. The siltstones appear to have been deposited in a variety of environments, depending upon the nature of the unit.

8) Dolostone Rock Type: Tan or light gray dolostones are found in all four stratigraphic intervals. The dolostones are fine-grained and composed of very finely crystalline dolomite rhombs (approximately 0.02 mm in diameter). Most contain a small percentage (1-10%) of quartz silt or fine sand. The dolostones are commonly moderately to well sorted, and are characterized by high porosity. Chert and anhydrite nodules

are common in the dolostones of the BC2 interval. Burrows are found in the BC2 and BC3 intervals.

The monotonously fine-grained dolostones containing chert nodules suggests deposition in a restrictive or perhaps deep environment. Dolostones are often found containing a normal marine fauna (reworked brachiopods and crinoid columnals) or are interbedded with grainy limestones. This suggests a relatively shallow, normal marine subtidal environment of deposition affected by storms. Alternatively, this could represent a series of shallowing upward successions, from mud-rich to mud-poor rocks.

9) Shale Rock Type: Black shales are found in the BC2 and Akah intervals. A relatively thick (7-30 cm) black shale marks the contact between the Barker Creek and Akah intervals. This fissile shale contains ramiform conodont elements. Other thin shales in the BC2 and Akah are fissile, but are otherwise unremarkable.

Black shales commonly indicate very quiet-water, anoxic environments, in which slow deposition of very fine-grained materials from suspension is allowed. The black shale found at the base of the Akah, as well as other black shales in the Paradox Basin, are interpreted to have been deposited in a deep subtidal environment, under low-energy, anoxic conditions (Goldhammer *et al.*, 1991).

- ORGANIZATION OF THESIS -

The body of this thesis is organized into four parts. A chapter is devoted to each of the informal intervals - the BC1, BC2, and the BC3 and lower Akah. A discussion of rock types and of cyclicity is contained within each of these chapters. The composition and distribution of bioherms found in the BC2 interval are described within that chapter. Finally, in Chapter 5 the depositional history of the stratigraphic column is summarized, as well as the orientation and distribution of the bioherms. The drafted measured sections are all shown in Appendix A, with a key to the symbols used as well as regional maps of the field area. Descriptions of samples taken from Navajo Nation land are included in Appendix B. All specimens referenced in this thesis are in the collections of the Department of Geology and Geophysics, University of Wisconsin - Madison, under file number U.W. 1884.

Chapter 2

BC1 Interval

- INTRODUCTION -

Four measured sections contain beds of the BC1 interval: A-2, C, M-1, and P-1 (Figure 2.1). Sections A-2, C, and P-1 are all within 0.3 km of each other, while Section M-1 is approximately 1 km to the SSE. The thickness of exposure at each of these sections is 11.7 m (Section A-2), 13.4 m (Section P-1), 8.0 m (Section C) and 3.2 m (Section M-1). The great variation in thickness is due to the lower boundary, defined as river level, occurring at different stratigraphic levels because of regional structural dip. The BC1 interval is characterized by shallow water carbonates, and has been divided into three cycles (see Cycles in the BC1 Interval, below). The abundance of different rock types within the BC1 interval in Section P-1, and the thickness of beds of each rock type within this section are displayed in Table 2.1.

- ROCK TYPES IN THE BC1 INTERVAL -

Bioclastic Limestone Rock Type

(Sections A-2, C, M-1, and P-1)

The bioclastic wackestone, packstone, and grainstone beds found in the BC1 interval are quite varied in character (Figure 2.1). Common

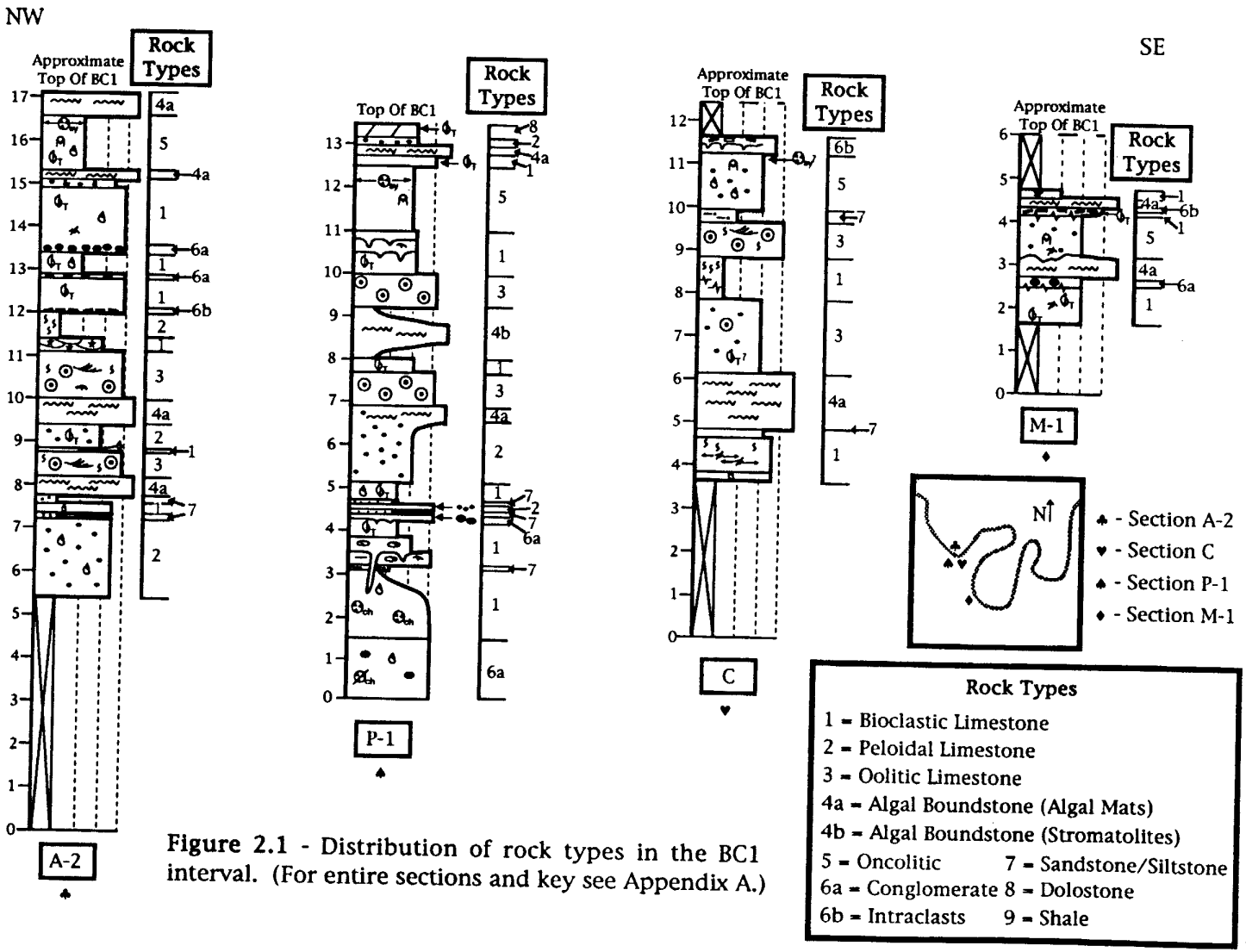


Figure 2.1 - Distribution of rock types in the BC1 interval. (For entire sections and key see Appendix A.)

Rock Type	Number of Beds	Total Thickness (in meters)	Percentage of Section (Thickness)	Minimum Bed Thickness (in meters)	Average Bed Thickness (in meters)	Maximum Bed Thickness (in meters)
Bioclastic Limestone (1)	9	6.86	50.4	0.18	0.76	1.75
Peloidal Limestone (2)	3	1.95	14.3	0.07	0.65	1.73
Oolitic Limestone (3)	2	1.60	11.7	0.76	0.80	0.84
Algal Boundstone (Algal Mat) (4a)	2	1.52	11.1	0.30	0.76	1.22
Algal Boundstone (Stromatolitic Heads) (4b)	0	0	0	-	0	-
Oncolitic (5)	1	1.15	8.4	-	1.15	-
Clastic (Conglomerates) (6a)	1	0.07	0.6	-	0.07	-
Clastic (Intraclasts) (6b)	0	0	0	-	0	-
Fine Sandstone/ Siltstone (7)	3	0.24	1.7	0.07	0.08	0.10
Dolostone (8)	1	0.23	1.7	-	0.23	-
Black Shale (9)	0	0	0	-	0	-
Total:	23	13.62				

Table 2.1 - Relative abundance of rock types in the BC1 interval. Data from Section P-1.

biotic grains include tubular foraminifera, fusulinids, brachiopods (whole and fragmented), and crinoid columnals. Tubular foram wackestones to grainstones are the most common of the bioclastic rocks found in the BC1 interval. Other bioclastic beds include crinoidal brachiopod-rich grainstones, a dolomitized tubular foram grainstone, and several grainstones containing unidentifiable fossil hash. Beds range from 10 cm to 1.7 m in thickness. The sorting varies from moderate to well. Tubular foraminifera and reworked bioclasts are generally fine to medium sand sized. Whole brachiopods and crinoid columnals are granule sized. The majority of the bioclastic beds contain some quantity of carbonate mud. Grainy laminations are common within these beds. Laminae of crinoid columnals separated by scoured surfaces are present in Section A-2.

Two beds composed of *Chaetetid*-rich wackestones to grainstones appear to form a small low-angle mound at the base of Section P-1. The mound is no wider than the side canyon in which it is exposed, approximately 8 m, and the relief of the mound does not exceed 50 cm. The maximum thickness of the mound is 3 m. These beds contain a fauna not found elsewhere in the BC1 interval, including bryozoans, horn corals, and silicified *Chaetetids*. The lower of the two *Chaetetid*-rich beds is a rudstone. It contains reworked brachiopods, bryozoans, and horn corals, as well as *Chaetetid* clasts up to 10 cm in diameter. The upper bed varies from a packstone at the base to a wackestone at the top. Grain size and sorting decreases as one moves up through this bed. Large *Chaetetid* heads (10 cm diameter) and in-place *Syringipora* are found in the lower half of the

upper bed. Fossil hash is predominant in the top half of the upper bed. The upper surface of the mound is fissured. The fissures are filled with material from overlying units. Porosity and secondary cementation are not notable in either bed.

The bioclastic limestones within the BC1 interval are interpreted to have been deposited in a normal marine, low-energy subtidal environment. The presence of grainstones, grainy laminations, and scour surfaces indicates episodic current activity.

Peloidal Limestone Rock Type

(Sections A-2 and P-1)

Six peloidal packstone beds are present within the BC1 interval, in Sections A-2 and P-1 (Figure 2.1). They vary in thickness from 7 cm to 1.8 m. Coarse sand sized fossil hash and tubular foraminifera are present within the peloidal rock at Section A-2.

These peloidal packstones are interpreted to have been deposited in a normal-marine, low energy environment, such as a protected carbonate shelf. The presence of coarse fossil hash suggests that either faunas from nearby normal marine environments were being transported in during high energy events, such as storms; or that these faunas were present in the same depositional environment as the peloids, and were reworked, sorted, and fragmented locally by high energy events.

Oolitic Limestone Rock Type

(Sections P-1, A-2, and C)

Two oolitic grainstone beds are present in the BC1 interval. The lower grainstone varies in thickness from 55 cm to 1.7 m and the upper varies from 85 cm to 1.3 m. The upper and lower contacts in both locations appear to be sharp, but there is no weathering break at either contact. Many of the ooids have been dissolved, resulting in an oomoldic texture. Slender vertical burrows (1 mm wide, approximately 5 mm long) are present through both oolite beds. Both the upper and lower oolite contain trough cross-beds at Section A-2, as does the upper oolite at Section C. Fine fossil molds, predominantly brachiopod molds, are present in the upper oolite at Section A-2. The lower oolite at Section C contains numerous fine sand sized peloids as well as fine sand sized tubular foraminifera and brachiopod fragments, in addition to ooids. The porosity of these two beds is excellent. There are no oolitic beds in Section M-1.

These oolitic limestones are interpreted to have been deposited in a shallow subtidal high-energy environment. The scarcity of fossils is due to the unstable substrate offered by an oolite shoal. The limited fauna found inhabiting modern ooid shoals is mostly limited to burrowing organisms, such as bivalves and other filter feeders. Such organisms probably formed the fine burrows present in these oolitic beds.

Algal Boundstone Rock Type

(Sections A-2, C, M-1, and P-1)

Algal laminites (Rock Type 4b) are present in all four sections. They range from 20 cm to 1.3 m thick. The grain size of these laminites is uniformly mud-sized. They grade laterally and vertically to mudstones, and contain burrowed intervals. No stromatolitic heads (Rock Type 4b) are found within the BC1 interval. The upper surface of a 40 cm thick laminite found in Section M-1 displays irregular relief up to 10 cm (Figure 2.2). This relief appears to be caused by later erosion or scour of the bed however, and is not the result of stromatolite growth. Several large stylolites are present within the laminites in Sections P-1 and C.

The lack of evidence of desiccation and the presence of burrowed intervals suggest that the laminated rocks were deposited subtidally. The large amount of mud trapped by the mats suggests that they were deposited in a quiet environment. The scoured surface above the laminite in Section M-2 indicates an increase in energy after this mat had formed.

Oncolitic Rock Type

(Sections A-2, C, M-1, and P-1)

A mud-rich wackestone to packstone containing large oncolites (up to 2 cm in diameter) can be correlated between all four sections, a distance of over 1.3 km. This unit ranges from 1.15 to 1.3 m thick, but the oncolites are found only within the upper meter of the bed. The oncolites contain roughly concentric internal laminations, but the

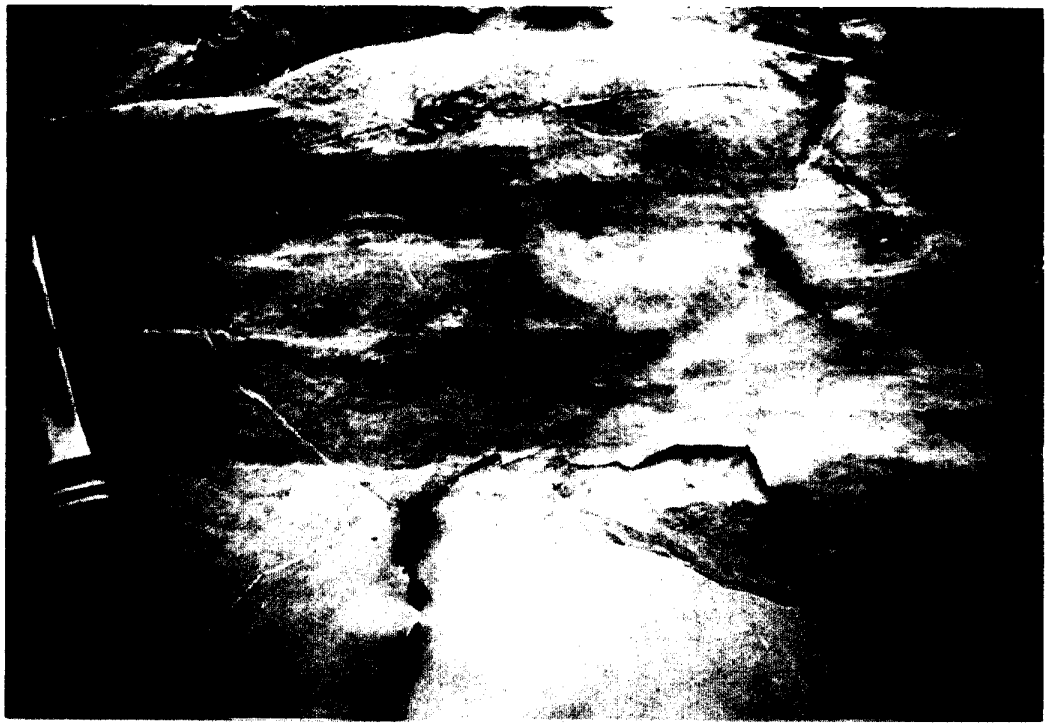


Figure 2.2 - Algal laminite (Section M-1, 4.4 m). Note the internal fine planar laminations. The undulatory upper surface appears to have been created by later scour.

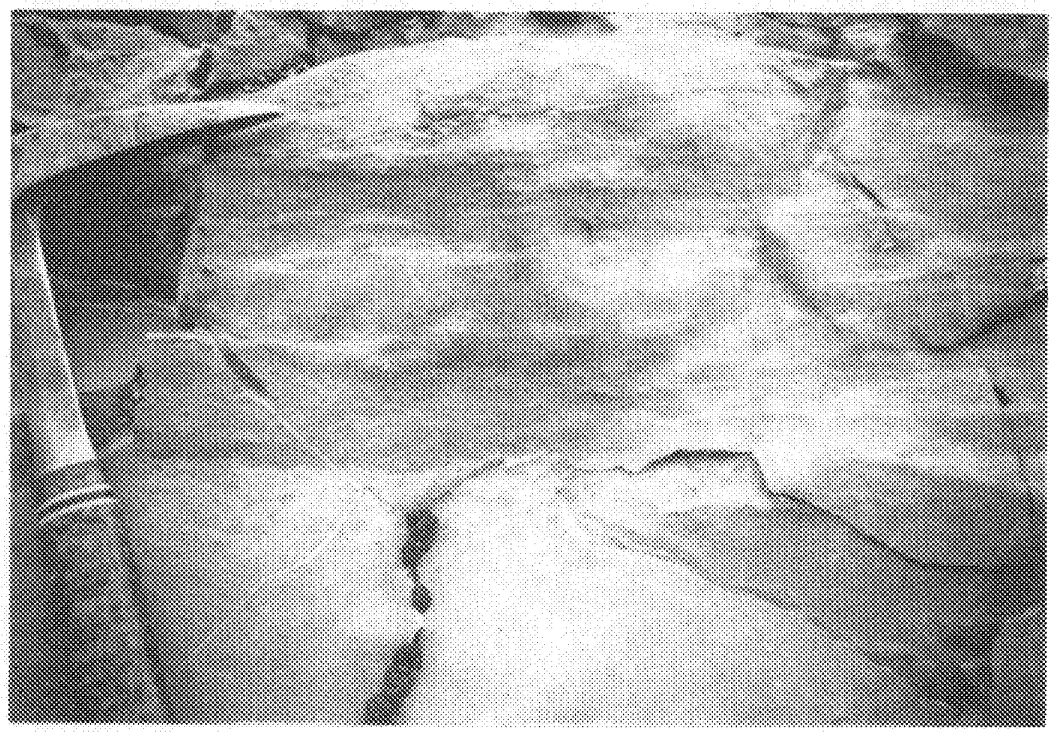


Figure 2.2 - Algal laminite (Section M-1, 4.4 m). Note the internal fine planar laminations. The undulatory upper surface appears to have been created by later scour.

individual laminations vary in thickness. They appear to have biotic grains or lithoclasts at their core. The oncoids occur within discrete zones, but are sparsely distributed within those zones (Figure 2.3). The matrix in which they are found is poorly sorted. This unit contains bioclasts such as tubular foraminifera (very fine sand sized), whole brachiopods (approximately 3-4 cm in diameter, Section P-1), and unidentifiable fossil hash (fine to medium sand sized). The top of this bed is marked by a remarkably continuous bed of in-place *Syringipora* (approximately 10 cm thick) which can be traced over 1 km (Figure 2.4). The *Syringipora* layer is not present at Section M-1, where the upper surface of this bed is marked by a stylolite. At Section C, there are very fine sand sized peloids present within the packstone.

The roughly concentric nature of the laminations around the oncoids suggests that they formed in an agitated environment, but the irregularity within the laminations suggests that the oncoids sat for long periods between agitation. The presence of lithoclasts in the cores of some oncoids supports the idea of an agitated environment, but the muddy nature of the beds supports the idea of a quiet environment. It is most probable that the environment was quiet (with minor turbulence, for rolling the oncoids) for long periods of time, and that episodic reworking of the beds, such as during a storm event, formed the individual mud-rich zones of oncoids.



Figure 2.3 - A zone of oncoids (Section A-2, 16.0 m).

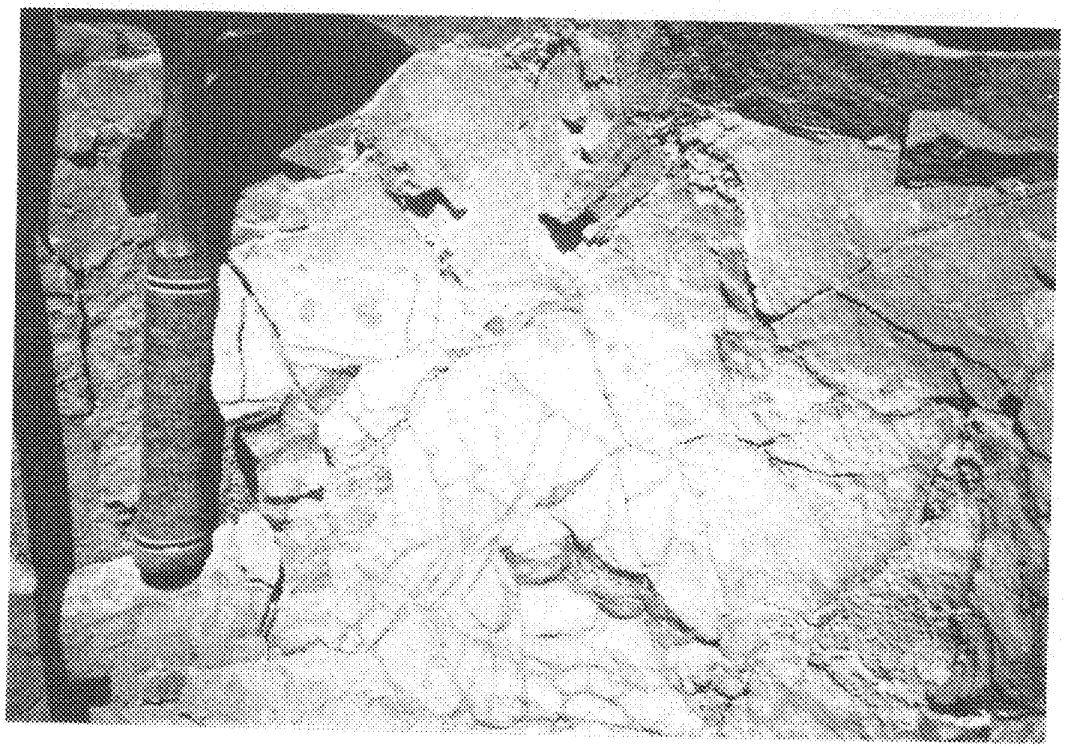


Figure 2.3 - A zone of oncoids (Section A-2, 16.0 m).

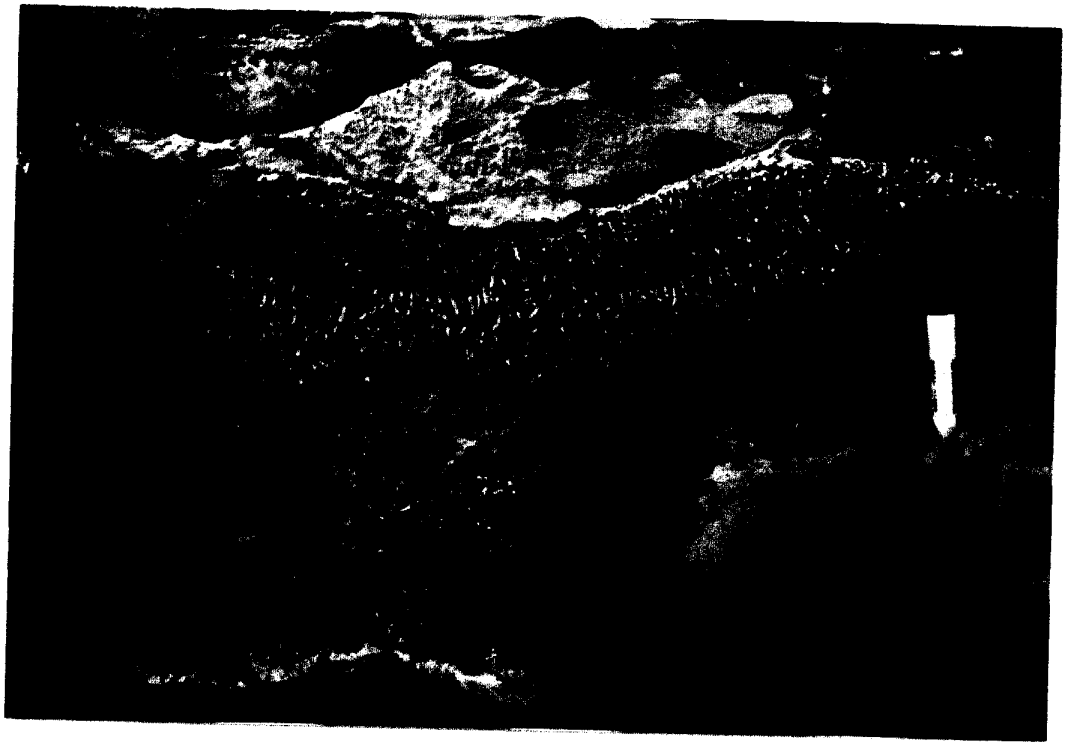


Figure 2.4 - Continuous *Syringipora* layer at the top of oncoid bed (Section P-1, 12.5 m). The oncoids below the Syringipora have either biotic grains or lithoclasts at their core.

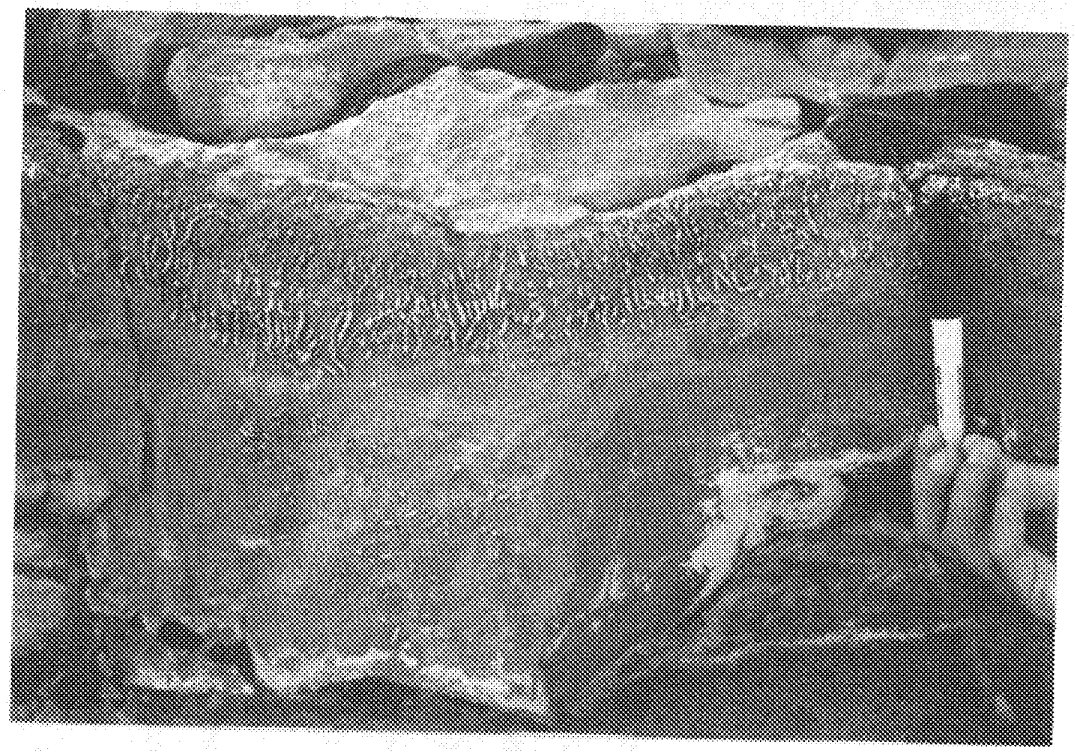


Figure 2.4 - Continuous *Syringipora* layer at the top of oncoid bed (Section P-1, 12.5 m). The oncoids below the Syringipora have either biotic grains or lithoclasts at their core.

Clastic Rock Type

(Sections A-2, C, M-1, and P-1)

Three thin conglomerate beds are present within the BC1 interval. They range in thickness from 7-10 cm thick. Of these four, one directly overlies a fissured surface and two others can be laterally correlated with a fissured surface. The lowest conglomeratic unit is found in Section P-1 at 4.2 m. It is moderately well sorted. The clasts are 3.5 to 4 cm in diameter and are fairly well rounded. The clasts are blackened and are surrounded by a light gray sandy matrix. This conglomerate overlies a fissured surface. A second and third conglomerate are located in Section A-2 at elevations of 12.8 m and 13.5 m respectively. Each are ten centimeters thick and contain blackened clasts. The lower conglomerate has a dark gray matrix. The upper conglomerate has an upper gradational contact with a bioclastic grainstone. A conglomerate in Section M-1 at an elevation of 2.5 m is in a laterally equivalent position with the two conglomerate beds in Section A-2 (Figure 2.5). Clasts are dark gray, found within a light gray matrix. Average clast size is pebble sized (approximately 5 mm), but ranges from very coarse sand up to pebble (3-4 cm) sized.

Two intraclast layers are found in the BC1 interval. The lower of these intraclast layers can be correlated between Section C (at an elevation of 11.5 m) and Section M-1 (at an elevation of 4.2 m). This intraclast layer contains very coarse sand, granule, and pebble sized (6-7 mm) clasts. The clasts are medium to dark gray in color. The matrix of the intraclast bed in Section C is light gray, while that in



Figure 2.5 - Plan view of the upper surface of a clast supported conglomeratic bed (Section M-1, 2.7 m). Clasts are dark gray in color and are very coarse sand sized to pebble sized. The matrix is a light gray bioclastic limestone. Clasts appear to be derived from the underlying lithologies.

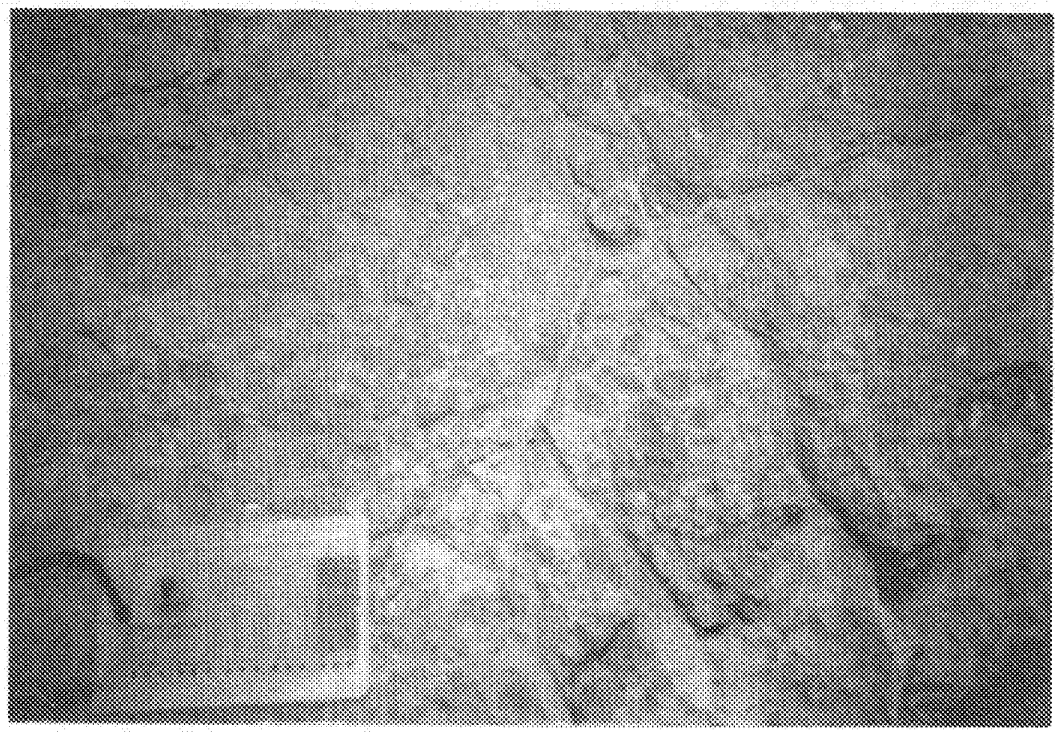


Figure 2.5 - Plan view of the upper surface of a clast supported conglomeratic bed (Section M-1, 2.7 m). Clasts are dark gray in color and are very coarse sand sized to pebble sized. The matrix is a light gray bioclastic limestone. Clasts appear to be derived from the underlying lithologies.

Section M-1 is medium gray and contains numerous tubular foraminifera. This intraclast bed is poorly sorted and is not porous. The intraclast layer in Section C is found directly above a medium gray grainstone. The upper intraclast layer (in Section A-2) does not have any equivalent in the other three sections. The intraclasts in this bed are found parallel to other grainy laminations.

The black color of the conglomerate clasts and the association of the lowest conglomerate with a fissured surface suggest that these beds have been subaerially exposed. The intraclast layer contain no desiccation features, suggesting that it was a high-energy event which caused the scour and rip-up of early lithified sediments.

Sandstone and Siltstone Rock Type

(Sections A-2 and P-1)

Three fine sandstone / siltstone beds are found in the BC1 interval. Two beds can be correlated between Sections A-2 and P-1 (Figure 2.1). These beds are tan and contain fine quartz sand. They also contain either carbonate mud or cement because the effervesce when exposed to hydrochloric acid. The lower sandstone is 7 cm thick, and is found overlying the lowest conglomerate in Section P-1. The upper sandstone is found 7 cm above the lower, and is 7 cm thick. These two beds are well sorted, but are not porous. A thin (30 cm) discontinuous silty recessive is found in Section C at 9.6 m. It appears to correlate with the upper conglomerates (Figure 2.1, Figure 2.6, boundary between cycles BC1-2 and BC1-3).

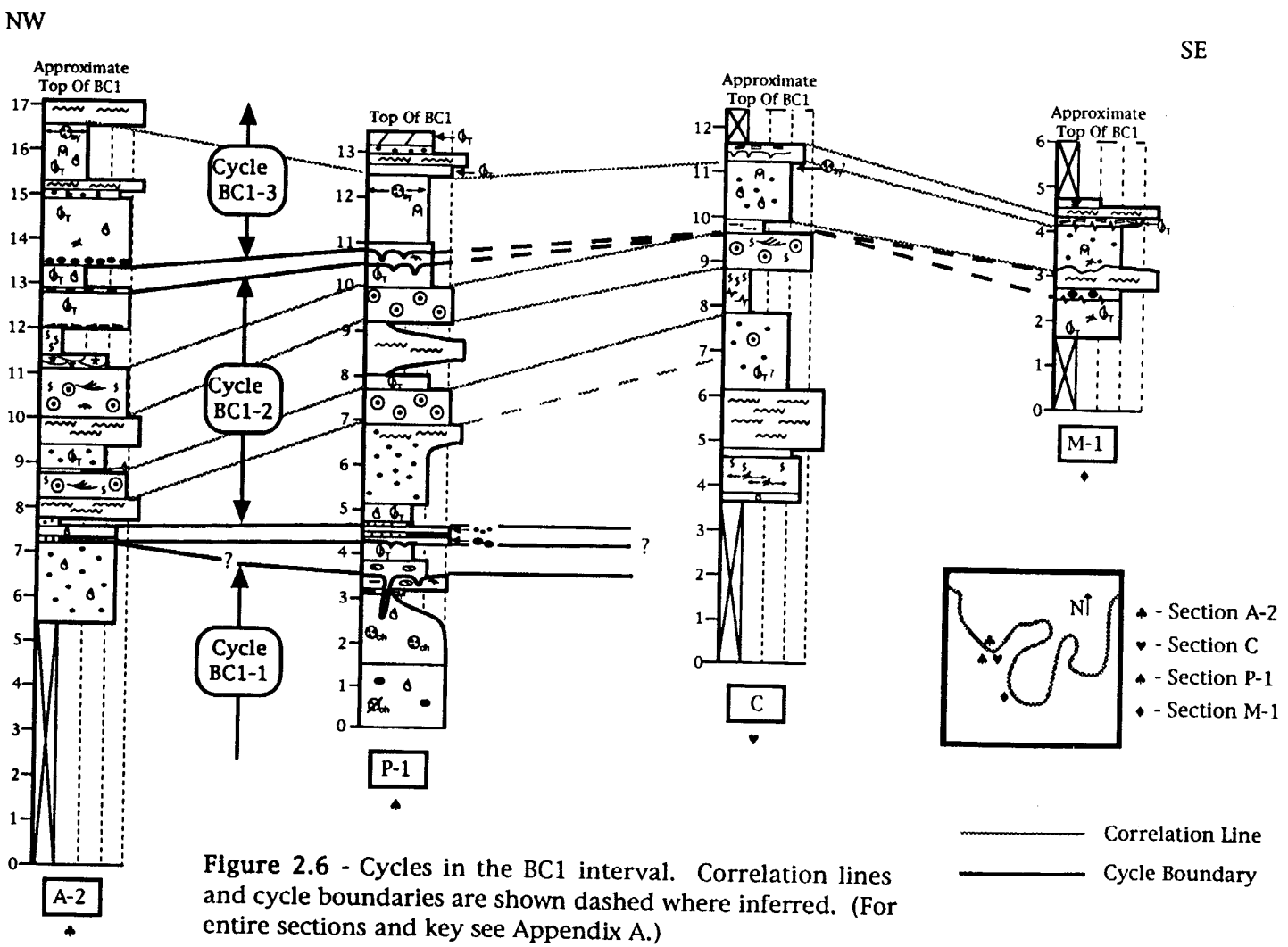


Figure 2.6 - Cycles in the BC1 interval. Correlation lines and cycle boundaries are shown dashed where inferred. (For entire sections and key see Appendix A.)

As all sandstone and siltstone beds in the BC1 interval appear to correlate with conglomerates containing blackened clasts, they are interpreted to record or postdate intervals of subaerial exposure.

Dolostone Rock Type

(Section P-1)

A 40 cm thick tan dolostone is found in Section P-1 at the very top of the BC1 interval. Upon close examination however, it is found to be a dolomitized packstone or grainstone. The secondary dolomitization has obscured the original texture of the rock, but it appears to have been bioclastic, containing numerous fine sand-sized foraminifera and fossil molds.

- CYCLES IN THE BC1 INTERVAL -

The sequence of different rock types in the BC1 interval can be divided into three cycles (cycles BC1-1, BC1-2, and BC1-3, Figure 2.6), using the criteria outlined in the introduction. Only fissured surfaces and conglomeratic beds with blackened clasts are present within the BC1 interval. The fissures are generally quite narrow and angular, and penetrate down into the underlying bed where they are filled with material from the overlying bed. The relief of the fissures may be as little as a few centimeters (surface at 4.3 m, Section P-1, Figures 2.1 and 2.6) or as much as a meter (surface at 3.5 m, Section P-1, Figures 2.1 and 2.6). Often these features are present in only one section, but may be correlated to similar, though less diagnostic

surfaces in the other sections. The sections have been correlated in Figure 2.6, which shows where the exposure features can be traced.

The cycle breaks occur within two zones, each containing multiple exposure surfaces or conglomerates within approximately a meter of section. It is unclear whether the multiple features of exposure contained within one of these zones indicate one period of exposure or multiple periods. Certainly multiple exposure surfaces can form during one major period of exposure. Apparent multiple exposure surfaces may also be formed during episodes of karsting, as dissolution occurs simultaneously along separate horizontal surfaces (Loucks and Handford, 1992). Alternately, it cannot be absolutely proved that each exposure surface or conglomerate was not deposited during a separate period of exposure, greatly separated in time from the other surfaces around it. The fact that a different number of exposure surfaces or conglomerates are at approximately the same stratigraphic level in each section suggests that each zone represents one period of exposure which is represented differently in different areas. If one considers each exposure zone as a cycle break, then there are three cycles (Figure 2.6).

The lowest cycle (BC1-1) is partially under river level, and is therefore incompletely exposed. It consists of the small low-relief mound found at the base of Section P-1, which appears to be laterally equivalent to the peloidal packstone in Section A-2. The exposure zone here is marked by two irregular, fissured surfaces (Section P-1), and a sandy conglomerate with blackened clasts (Section P-1). The lowest fissured surface (3.5 m above river level) extends down at

least one meter into the underlying beds. These deep fissures are filled with the fusulinid packstone found in the overlying bed. The upper fissured surface is marked by relief of only a few centimeters. It is overlain by a conglomerate with blackened clasts. This conglomerate is overlain by two sandy beds. The conglomerate/sandy beds and fissured surfaces correlate to a silty/sandy interval in Section A-2 (Figure 2.6).

The second cycle (BC1-2) contains several shallowing upward successions, but because there is no evidence of exposure between the different successions they are considered to be within one cycle (Figure 2.6). The lowest shallowing upward succession, exposed in Sections A-2, C, and P-1, consists of peloidal or bioclastic sediments capped by an algal laminite. The second shallowing upward succession, also exposed in Sections A-2, C, and P-1, consists of an oolitic grainstone and bioclastic or peloidal wacke/packstones, capped by a mudstone containing algal laminations (not present in Section A-2). An incomplete third shallowing upward succession is present in Sections A-2 and P-1 (and perhaps also M-1). This third succession consists of an oolitic grainstone overlain by bioclastic wackestones and packstones. It is truncated by the second exposure zone (Figure 2.6). This exposure zone is found interspersed within bioclastic wacke/packstones. It is marked by conglomerates (Sections A-2 and M-1), fissured surfaces (Section P-1), and silty intervals (Sections C and P-1). The fissured surfaces have only a few centimeters of relief. At Section M-1 the zone also appears to correlate with an algal boundstone with a scoured upper surface (Figure 2.6).

The upper cycle (BC1-3) consists predominantly of bioclastic pack/grainstones (Sections A-2 and P-1) and bioclastic wacke/packstones which contain oncolites (Sections A-2, C, M-1, and P-1) (Figure 2.6). The cycle in Sections A-2 and P-2 are capped by more bioclastic or peloidal rocks. A shallowing of the environment is suggested in Sections C and M-1 by the presence of an intraclast layer capping the cycle. The base of the continuous green siltstone is interpreted to be a cycle break and marks the contact between the BC1 and BC2 intervals.

Chapter 3

BC2 Interval

- INTRODUCTION -

The rocks of the BC2 interval contain the continuous zone of bioherms which is the focus of this study. The growth history of the bioherms, as well as their distribution within the field area is discussed below (see Bioherms in the BC2 Interval). The BC2 interval was well exposed in the study area. Of the nineteen sections measured in the study area, eighteen include portions of the BC2. Although exposure was good, parts of the BC2 interval formed steep cliffs, and some recessive beds formed persistent areas of cover. Section P-1 is the only section which extends through the entire BC2 interval. The thickness of the BC2 in this location is 14.5 m. The thickness of the BC2 interval is greater when measured through the core of a bioherm than when measured through the flank or between bioherms. Estimates of thickness when measured through a bioherm range from 7 m (Section G-1) to 30.7 m (Section P-4, Bioherm P). Estimates of thickness when measured between bioherms range from 6 m (Section G-2) to 14.5 m (Section P-1).

Because of the difference in thickness, sections are differentiated on the basis of whether they were measured through the core of a bioherm, or between or on the flanks of bioherms.

Between-bioherm sections are those in which the thickness of the "bioherm" beds has decreased to 25-50% of the maximum thickness of the bioherm. The distribution of rock types within seven sections measured through bioherms is shown in Figure 3.1. The distribution of rock types within four sections measured between or on the flanks of bioherms is shown in Figure 3.2. The abundance of different rock types within the BC2 interval in Section P-1, and the thickness of beds of each rock type within this section, are displayed in Table 3.1.

- ROCK TYPES IN THE BC2 INTERVAL -

Bioclastic Limestone Rock Type

(Sections A-1, C, D, F, G-1, G-2, H, M-1, M-2, P-1, P-2, P-3, P-4, P-5, P-6, and P-8)

Bioclastic limestones, ranging from wackestones to grainstones, are the most common rock type in the BC2 interval (52%, Table 3.1). Bioclastic limestones are found both below and within the bioherm rich-zone. Two bioclastic limestones ranging from wackestones to grainstones are present in the beds below the bioherms. The lower ranges from 30-70 cm thick, and the upper ranges from 70-160 cm thick. The dominant bioclasts include brachiopod and crinoid fragments (coarse sand to granule sized), non-encrusting tubular foraminifera (fine to medium sand sized), and fossil hash (very fine to medium sand sized). In place *Syringipora* are present within the lower bioclastic limestone in Section P-1. Probable phylloid algae are present in thin section. Peloids are found among the bioclasts. Beds

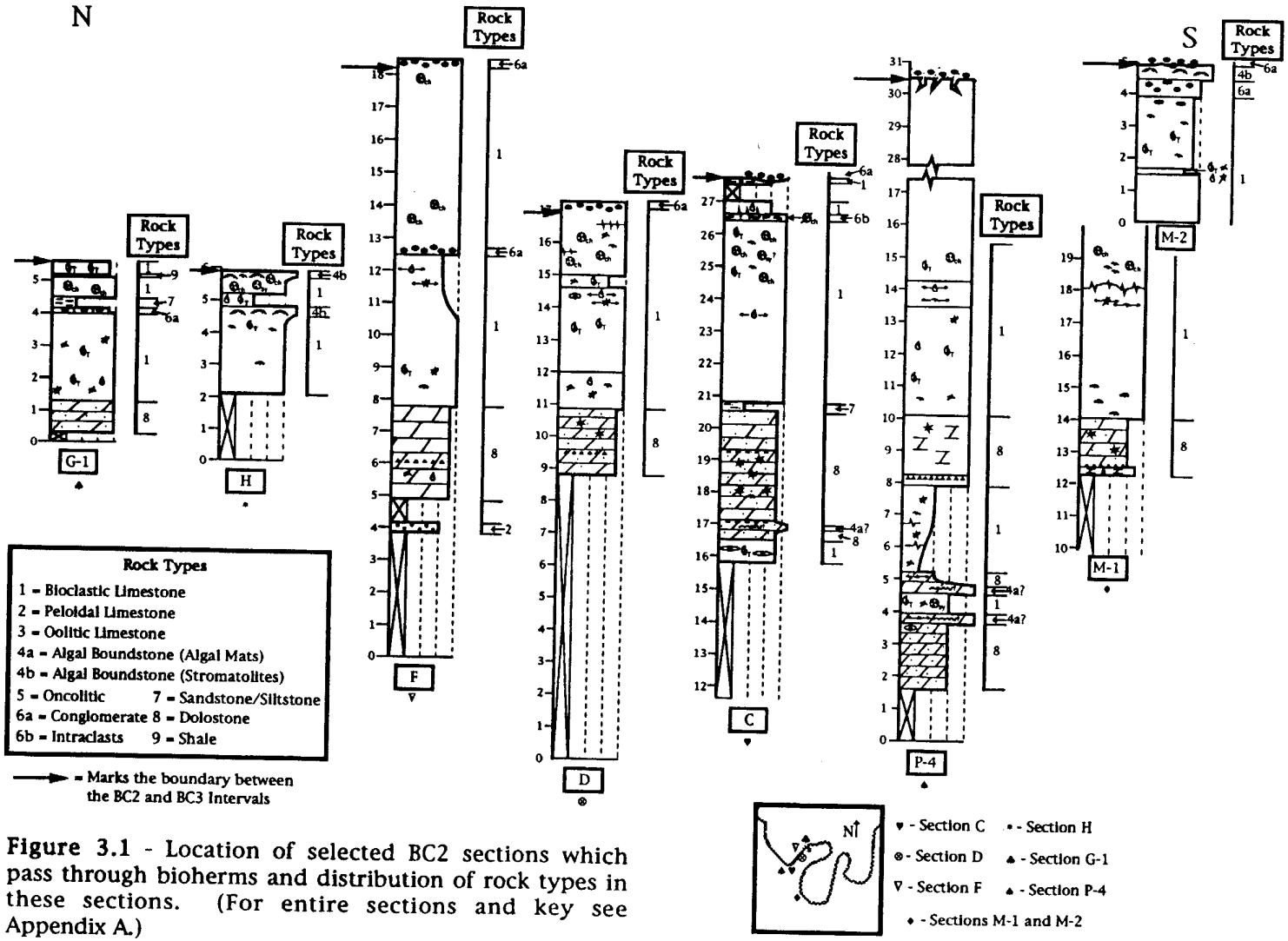


Figure 3.1 - Location of selected BC2 sections which pass through bioherms and distribution of rock types in these sections. (For entire sections and key see Appendix A.)

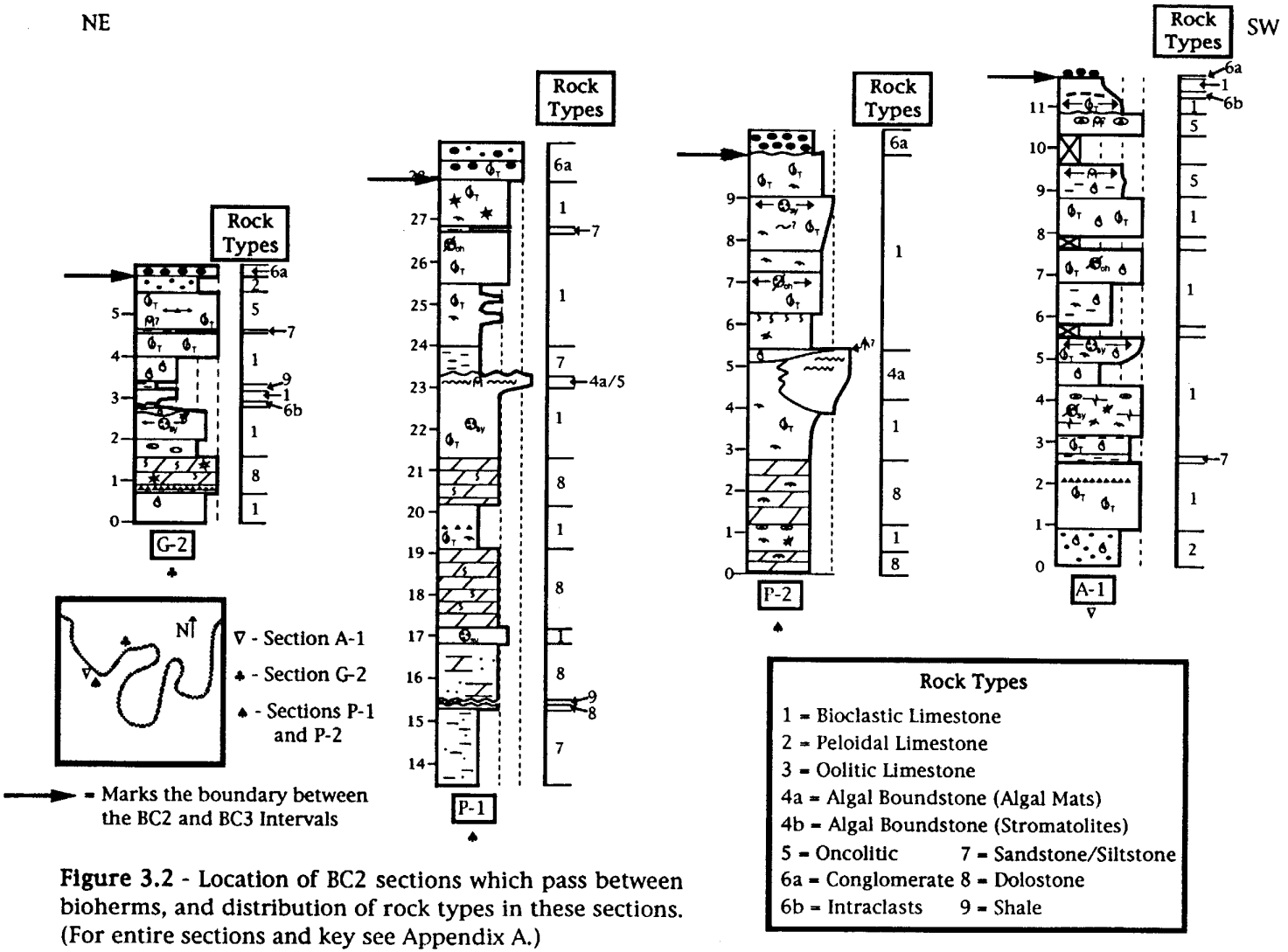


Figure 3.2 - Location of BC2 sections which pass between bioherms, and distribution of rock types in these sections. (For entire sections and key see Appendix A.)

Rock Type	Number of Beds	Total Thickness (in meters)	Percentage of Section (Thickness)	Minimum Bed Thickness (in meters)	Average Bed Thickness (in meters)	Maximum Bed Thickness (in meters)
Bioclastic Limestone (1)	6	7.14	52.0	0.30	1.19	1.88
Peloidal Limestone (2)	0	0	0	-	0	-
Oolitic Limestone (3)	0	0	0	-	0	-
Algal Boundstone (Algal Mat) (4a)	1	0.10	0.7	-	0.10	-
Algal Boundstone (Stromatolitic Heads) (4b)	0	0	0	-	0	-
Oncolitic (5)	0	0	0	-	0	-
Clastic (Conglomerates) (6a)	0	0	0	-	0	-
Clastic (Intraclasts) (6b)	0	0	0	-	0	-
Fine Sandstone/ Siltstone (7)	3	2.67	19.4	0.76	0.89	1.91
Dolostone (8)	4	3.80	27.8	0.20	0.95	1.52
Black Shale (9)	1	0.02	0.1	-	0.02	-
Total:	15	13.73				

Table 3.1 - Relative abundance of rock types in the BC2 interval. Data from Section P-1.

are moderately to moderately well sorted. Intragranular and moldic porosity is common within these two beds. Intergranular space and some fossil molds are filled with a microcrystalline calcite cement (Figure 3.3). Bioclasts commonly occur along grainy laminations. Stylolites and compressed fossil grains within these beds indicate late compaction (Figure 3.4).

Two different zones of bioclastic limestones can be distinguished within the bioherm-rich zone. The lower, Zone A, ranges from a wackestone to a grainstone, contains no Chaetetids, and appears to have been mechanically reworked. The upper, Zone B, ranges from wackestones to boundstones, contains Chaetetids, and does not appear to have been mechanically reworked.

The bioclastic limestones within Zone A range from wackestones to grainstones. They commonly contain peloids. Dominant bioclasts include crinoid columnals, broken or articulated brachiopods, encrusting and non-encrusting tubular foraminifera, and fossil hash. Accessory bioclasts include possible phylloid algae, rare *Syringipora*, and fusulinid and benthic porcellaneous foraminifera. Grain size varies from fine sand sized (tubular foraminifera and fossil hash) to coarse sand and granule sized (brachiopods and crinoids) material in a within-bioherm position, and from fine to medium sand (tubular foraminifera, brachiopods, crinoids, and fossil hash) to coarse sand (fusulinids) sized in a between/flanking bioherm position. Burrows are found within some of the beds. Overall sorting is poor, but it improves as one moves up through a bed. These bioclastic limestones are characterized by excellent enlarged moldic porosity (Figure 3.5).

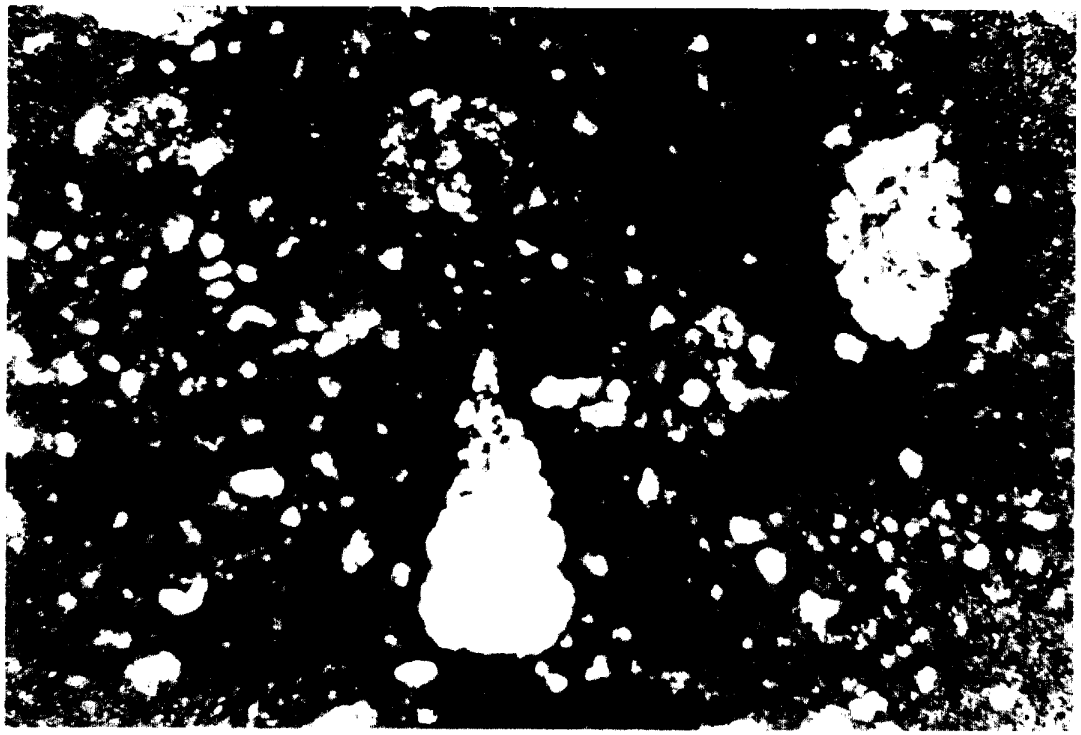


Figure 3.3 - Thin section microphotograph of a bioclastic packstone, showing moldic porosity filled with calcite spar. Note the (relatively) large gastropod mold in lower center of picture (Section P-3, 4.8 m, UW1884/107). (Width of view is 5 mm.)

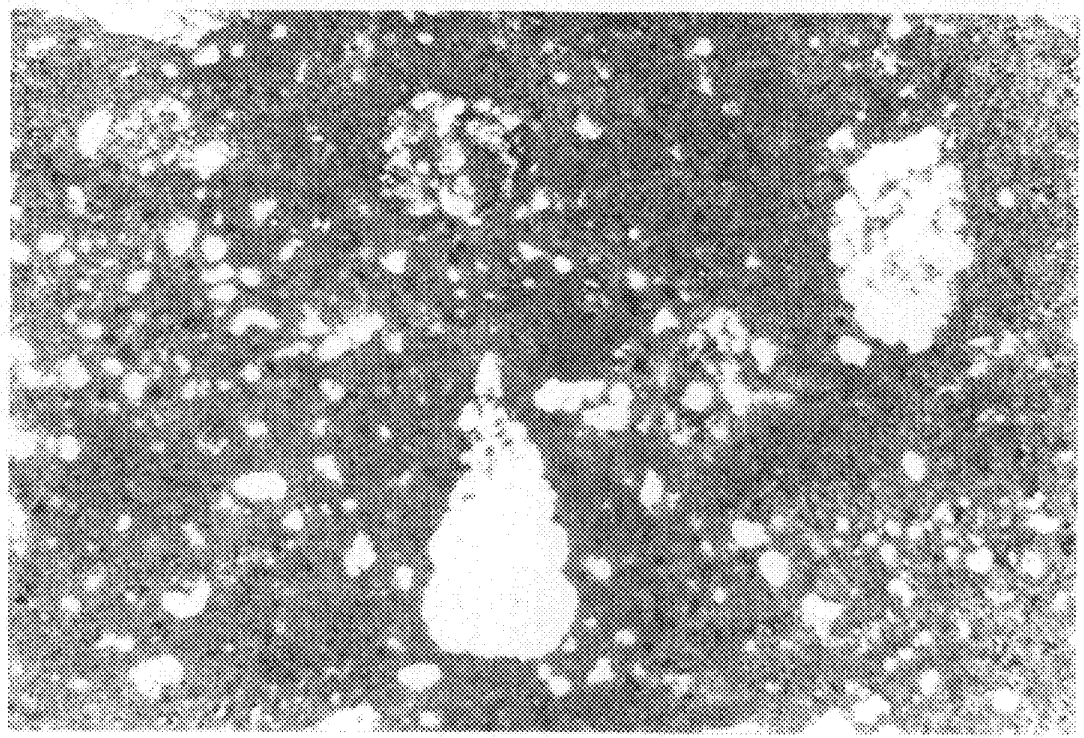


Figure 3.3 - Thin section microphotograph of a bioclastic packstone, showing moldic porosity filled with calcite spar. Note the (relatively) large gastropod mold in lower center of picture (Section P-3, 4.8 m, UW1884/107). (Width of view is 5 mm.)

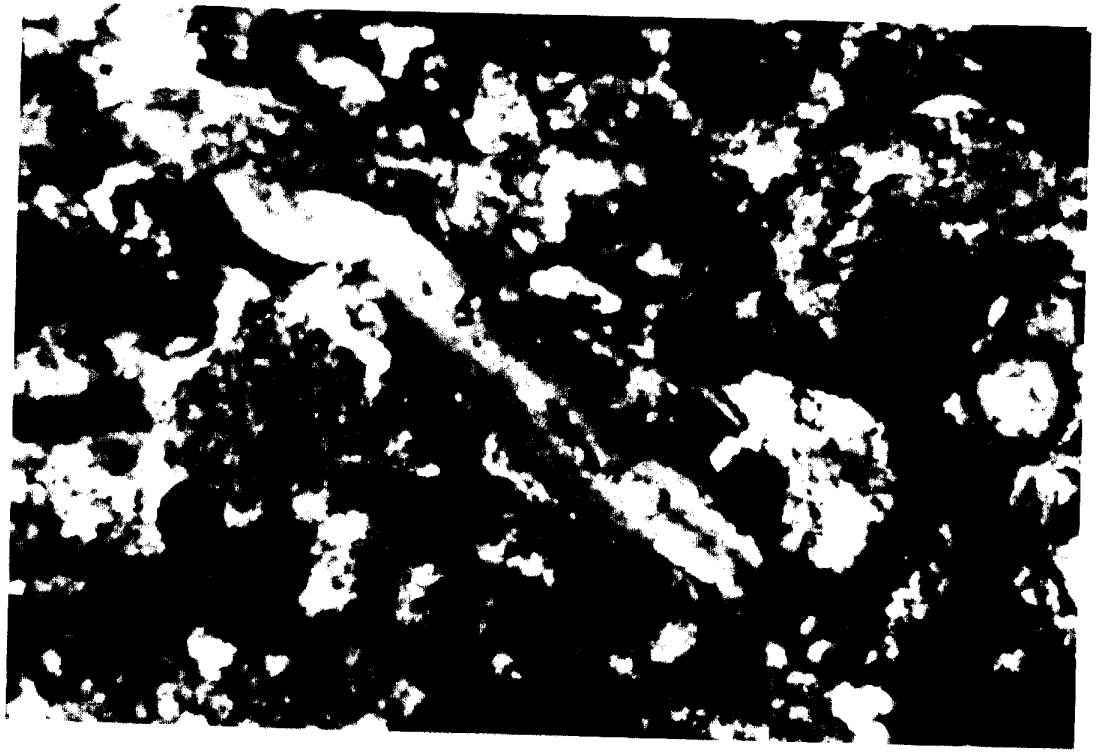


Figure 3.4 - Crushed brachiopod (center of photograph) showing evidence of compaction (Section P4, 4.3 m, UW1884/108). Bioclastic grains are coarse to medium sand sized. Other bioclasts include crinoid fragments and tubular foraminifera. (Width of view is 2.5 mm.)

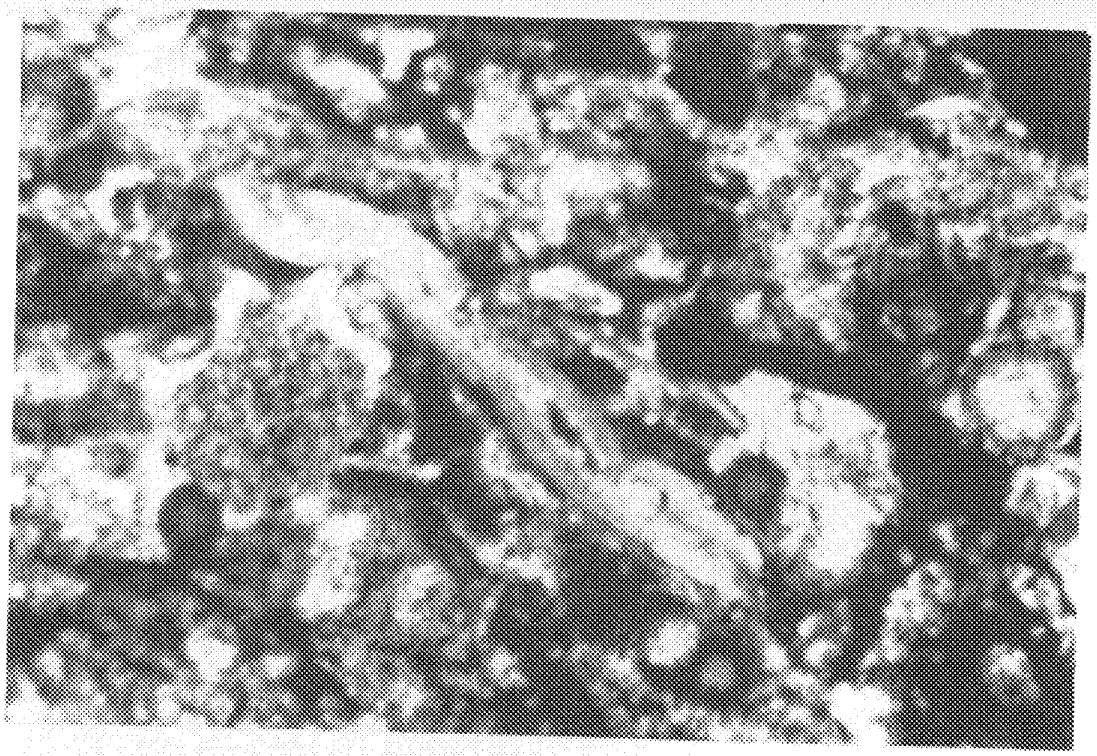


Figure 3.4 - Crushed brachiopod (center of photograph) showing evidence of compaction (Section P-2, 4.3 m, UW1884/108). Bioclastic grains are coarse to medium sand sized. Other bioclasts include crinoid fragments and tubular foraminifera. (Width of view is 2.5 mm.)



Figure 3.5 - Abundant enlarged moldic porosity in a bioclastic pack- to grainstone within Zone A (Section P-4, 12.0 m). The moldic porosity highlights subtle cross stratification. Here the apparent dip of the stratification is 1°-6° N11E.

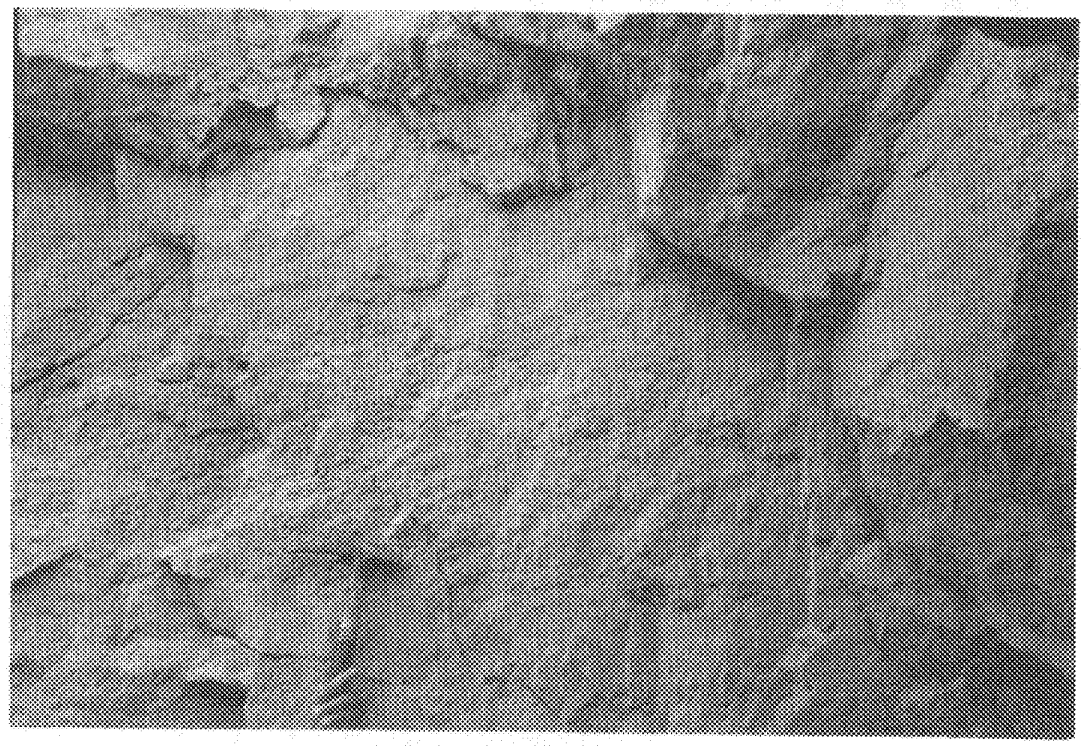


Figure 3.5 - Abundant enlarged moldic porosity in a bioclastic pack- to grainstone within Zone A (Section P-4, 12.0 m). The moldic porosity highlights subtle cross stratification. Here the apparent dip of the stratification is 1°-6° N11E.

The beds are commonly petroliferous, and the pores often contain dead oil (Figure 3.6).

Zone A can be subdivided into those rocks found within bioherms, and those laterally equivalent found in a between-bioherm or flank position. Beds within bioherms tend to be thick (up to 4.7 m, Section F). They weather massively, although upon closer examination one can see grainy laminations within the beds (Figure 3.7). Some of these laminations resemble hummocky cross bedding. Normal cross bedding is found within the basal bed of Bioherm P at Section P-4 (Figure 3.5, Figure 3.1). These cross beds have an apparent dip ranging from 1° to 6°, N11E. On the southeastern flank of Bioherm P, oolitic coatings are seen around biotic grains in an especially well sorted bed (Section P-1). Beds between and on the flanks of bioherms are generally thinner and more well bedded.

The bioclastic beds within Zone B include boundstones as well as wackestones, packstones, and grainstones. The binding organisms are tubular foraminifera (Figure 3.8). Dominant bioclasts include articulated, disarticulated, or fragmented brachiopods, encrusting and non-encrusting tubular foraminifera, in place or reworked Chaetetids (Figure 3.9), and fossil hash. Accessory bioclasts include crinoid columnals, *Syringipora* and fenestrate bryozoans. Again, grain size is greater within the bioherms than between or on the flanks of bioherms (medium and coarse sand and pebble sized versus fine to medium sand sized). Sorting is poor to moderate. Burrows are also seen within Zone B. Within-bioherm beds are characterized by excellent intragranular porosity, predominantly occurring within the



Figure 3.6 - Large enlarged mold in a bioclastic limestone within Zone A (Section P-4, 11.0 m, UW1884/109). The dark reddish-brown stain around the perimeter of the mold is dead oil. The cloudy material filling the mold is epoxy. (Width of view is 5 mm.)

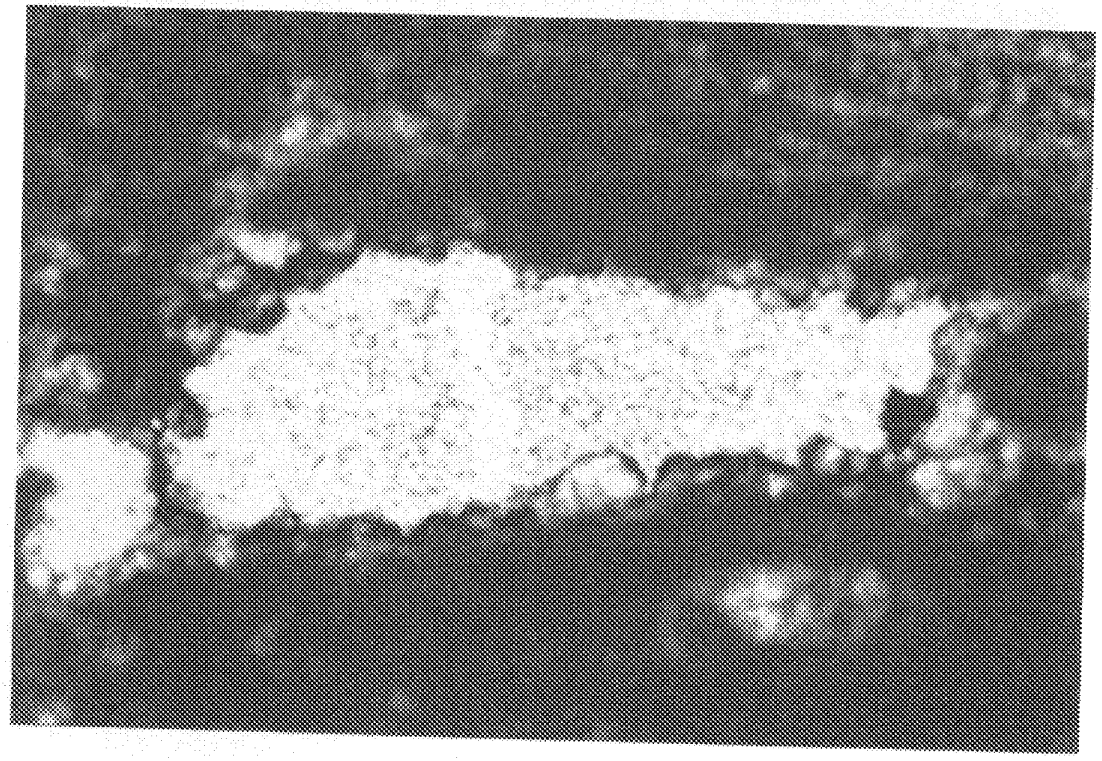


Figure 3.6 - Large enlarged mold in a bioclastic limestone within Zone A (Section P-4, 11.0 m, UW1884/109). The dark reddish-brown stain around the perimeter of the mold is dead oil. The cloudy material filling the mold is epoxy. (Width of view is 5 mm.)

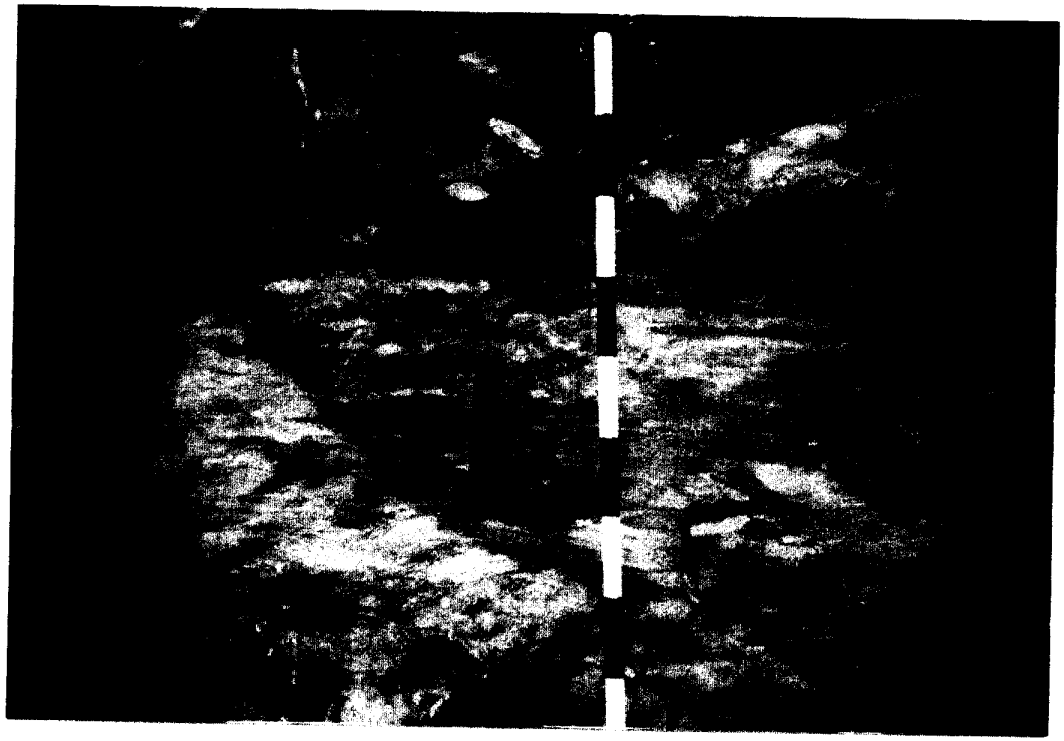


Figure 3.7 - Discontinuous grainy laminations in a bioclastic limestone within Zone A (Section M-1, 17.5 m). The undulations of some of these laminae resemble hummocky cross stratification.

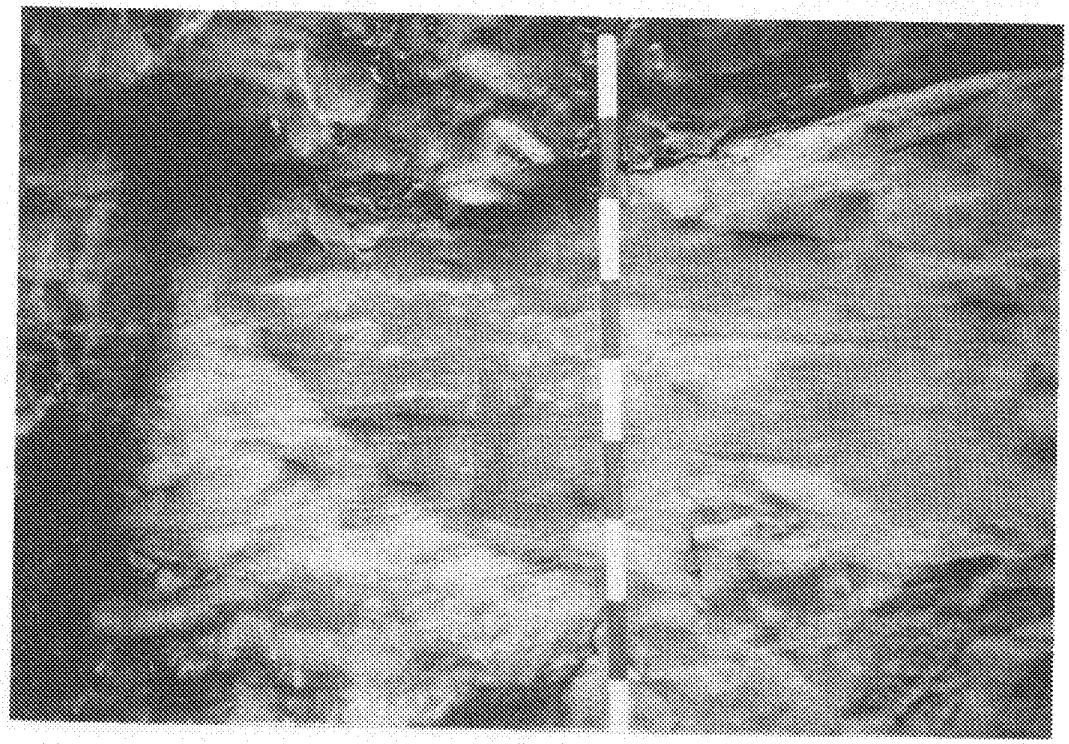


Figure 3.7 - Discontinuous grainy laminations in a bioclastic limestone within Zone A (Section M-1, 17.5 m). The undulations of some of these laminae resemble hummocky cross stratification.

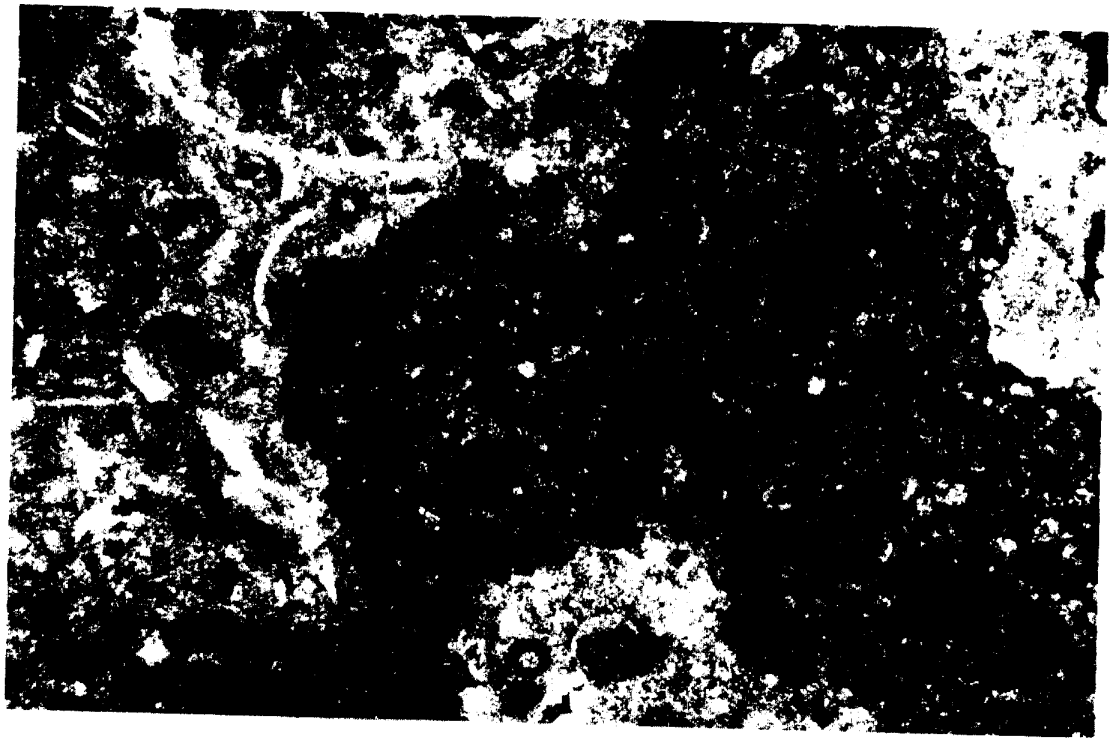


Figure 3.8 - Thin section showing encrusting tubular foraminifera surrounded by a bioclastic pack- to grainstone matrix (Section P-4, 14.9 m, UW1884/110). (Width of view is 2.5 mm.)

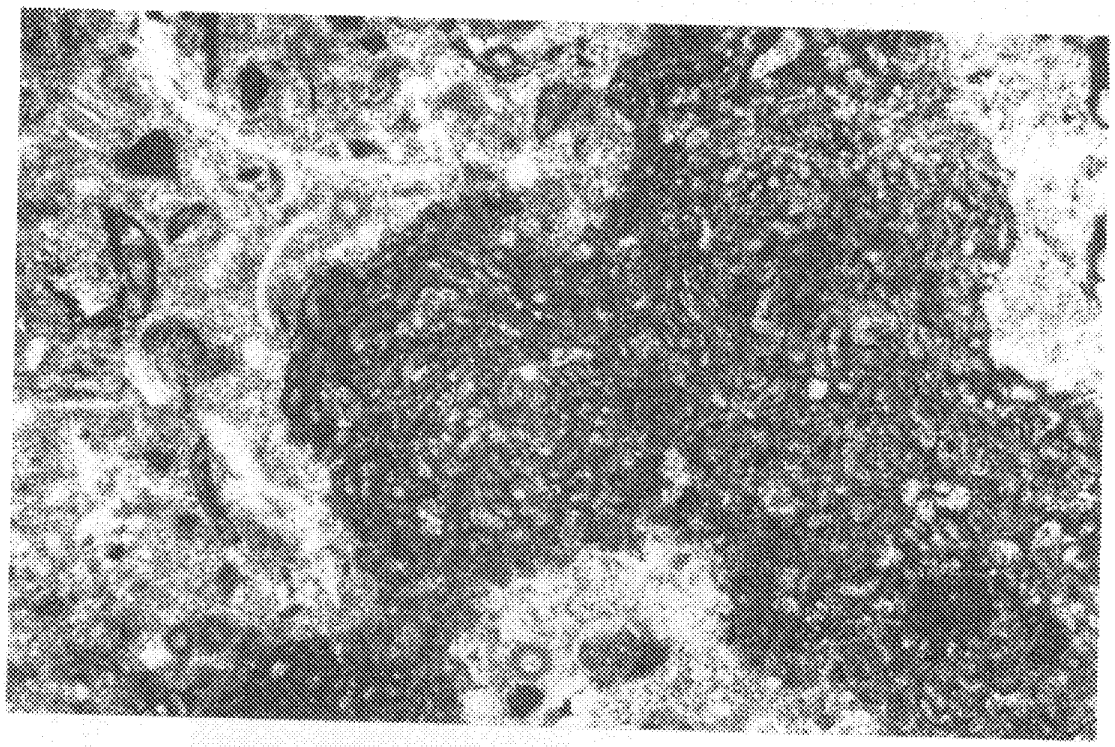


Figure 3.8 - Thin section showing encrusting tubular foraminifera surrounded by a bioclastic pack- to grainstone matrix (Section P-4, 14.9 m, UW1884/110). (Width of view is 2.5 mm.)



Figure 3.9 - Silicified Chaetetids (black) in a bioclastic packstone to grainstone within Zone B (Section H, 5.5 m).



Figure 3.9 - Silicified Chaetetids (black) in a bioclastic packstone to grainstone within Zone B (Section H, 5.5 m).

tubular foraminifera and Chaetetid heads. Porosity elsewhere in Zone B is not notable.

Zone B can also be subdivided into beds within bioherms and beds between or flanking bioherms. The bioclastic limestones found within bioherms are generally massive in character, while those between and on the flanks are well bedded and contain grainy laminations. Limestones within the bioherms are mud-lean while those between and on the flanks are often mud-supported.

The presence of a normal marine fauna in all of the bioclastic limestones suggests that they were deposited in normal marine waters. The lack of relief in the bioclastic limestones found below the bioherm-rich zone suggests that they formed on the shallow shelf, where they were occasionally affected by high-energy events (such as storms), forming the grainy laminations. For further interpretation of bioherm growth, see Growth History of Bioherms in the BC2 Interval below.

Peloidal Limestone Rock Type

(Sections A-1, F, P-3)

Peloidal packstones are found in three sections (Sections A-1, F, P-3) in the BC2 interval. Each section contains one peloidal packstone (Figures 3.1 and 3.2). All are found below the bioherm-rich zone. It is unclear whether these beds can be correlated between sections. They range from 10 to 90 cm thick. These three packstones contain very fine sand sized peloids. The beds in Sections A-1 and P-3 also contain very fine sand sized fossil hash. Brachiopod molds are found

in Section A-1. The abundance of peloids in conjunction with brachiopods and fossil hash suggests that these beds were deposited in a normal marine environment.

Algal Boundstone Rock Type

(Sections H, P-1, P-2, and P-4)

Both algal laminites and stromatolites are seen in the BC2 interval. Algal laminites are present in Sections P-4, P-1, and P-2 (Figures 3.1 and 3.2). The two "laminites" in Section P-4 are found within sandy dolomite beds below the bioherm-rich zone.

The laminites in Sections P-1 and P-2 are found at the top of Zone A. Both of these sections are found on the flanks of Bioherm P. The laminite in Section P-1 is a poorly sorted, grainy unit characterized by fenestral porosity (Figure 3.10). This laminite bed contains two small areas of positive topographic relief which measure approximately 40 cm wide and 20 cm high (Figure 3.11). These structures are visible, but not accessible in the field. They are believed to be algal growths. The laminite is found directly overlain by large (up to 10 cm diameter) black oncoids (see Oncoid Rock Type below). The laminite in Section P-2 has been silicified and is visible only where is it weathering out of the surrounding limestone (Figure 3.12). The laminite is found within an otherwise grainy bioclastic pack- to grainstone. Relief within this algal mat measures only 1-2 cm.

True stromatolitic heads are found within the bioherms at the tops of both Zones A and B, although they are most common at the top



Figure 3.10 - Algal laminite found at the top of Zone A on the southeastern flank of Bioherm P (Section P-1, 23.3 m). Note laminations in the central block in the photo.



Figure 3.10 - Algal laminite found at the top of Zone A on the southeastern flank of Bioherm P (Section P-1, 23.3 m). Note laminations in the central block in the photo.

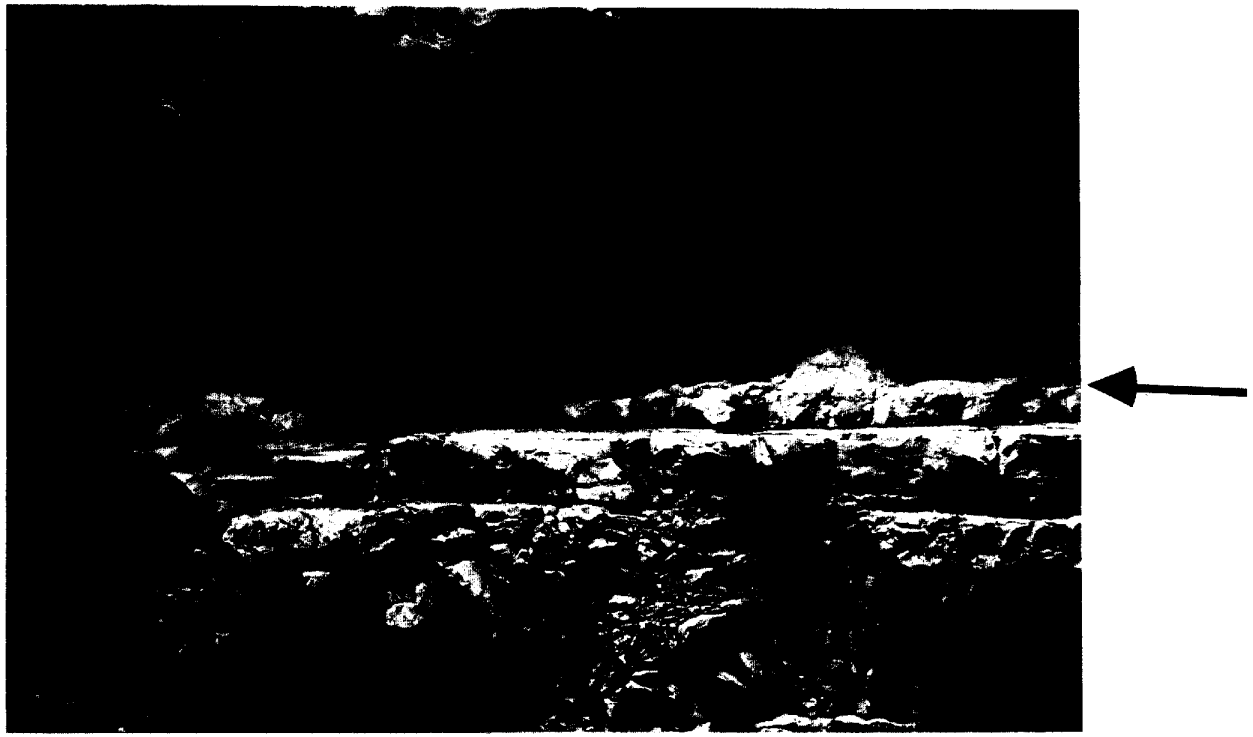


Figure 3.11 - Small areas of topographic relief (arrow), interpreted to be algal mounds. The mounds are located on the southeastern flank of Bioherm P, at the top of Zone A (Section P-1, 23.3 m).

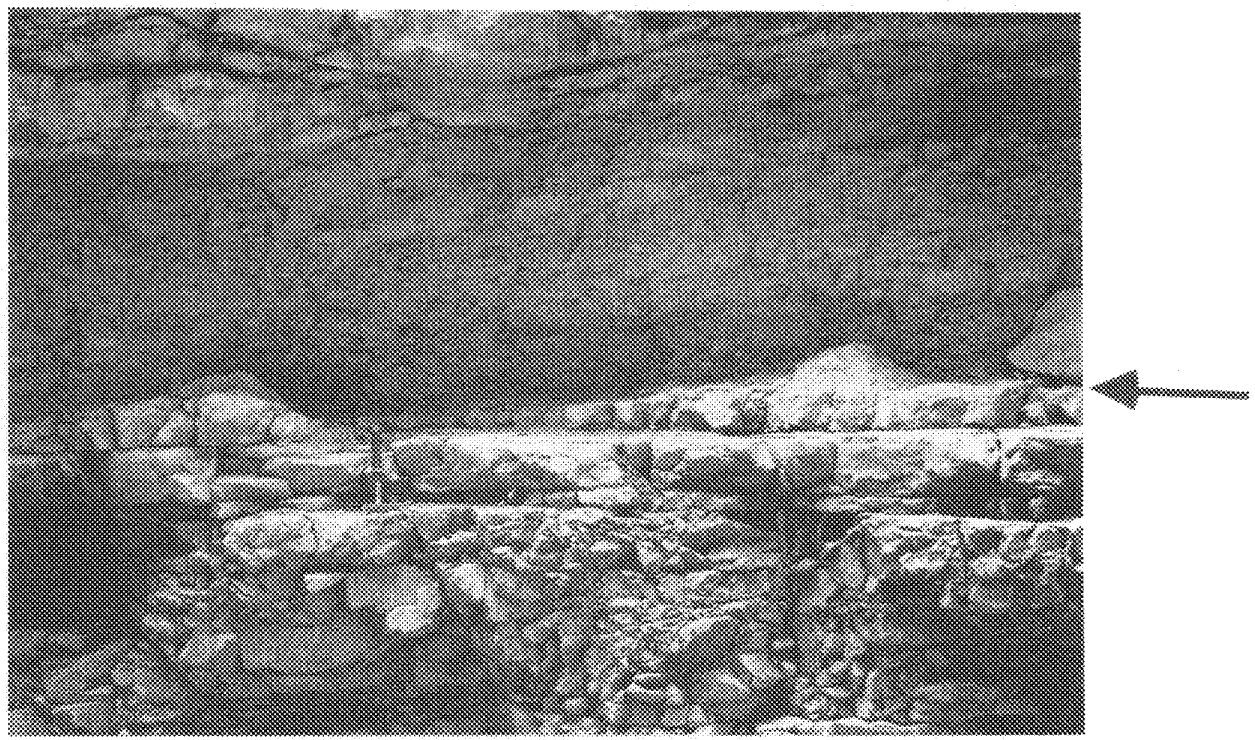


Figure 3.11 - Small areas of topographic relief (arrow), interpreted to be algal mounds. The mounds are located on the southeastern flank of Bioherm P, at the top of Zone A (Section P-1, 23.3 m).



Figure 3.12 - Algal laminite found at the top of Zone A in a mound peripheral to Bioherm P, found on the northwestern flank of Bioherm P (Section P-2, 5.0 m).

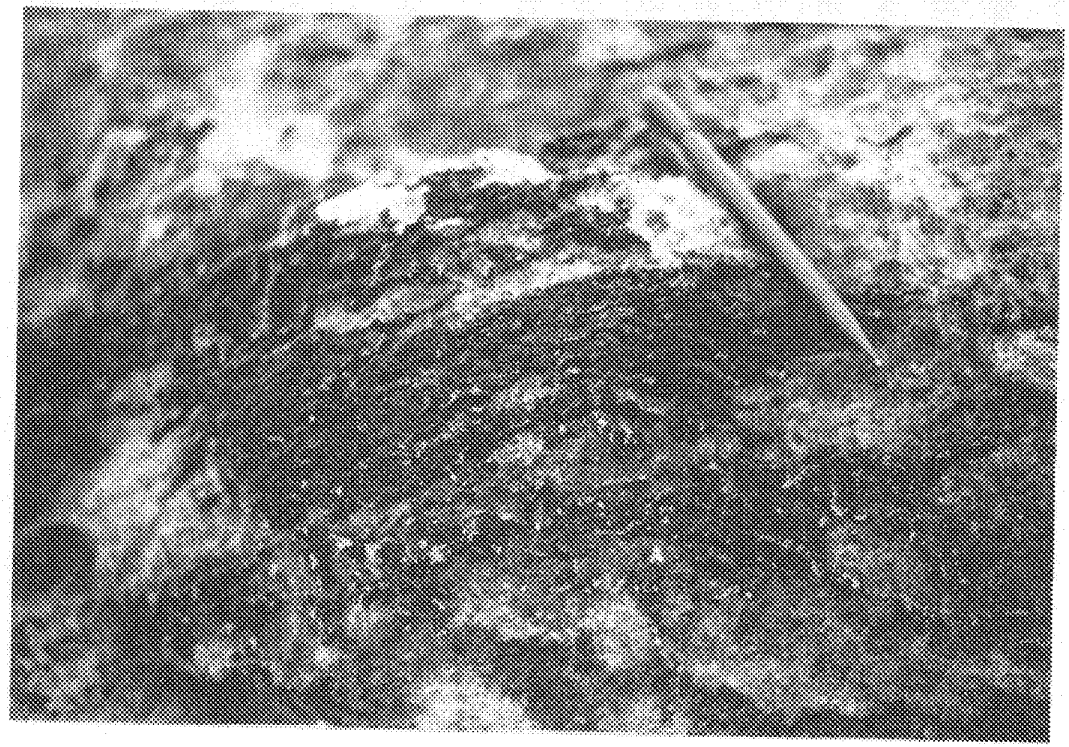


Figure 3.12 - Algal laminite found at the top of Zone A in a mound peripheral to Bioherm P, found on the northwestern flank of Bioherm P (Section P-2, 5.0 m).

of Zone B. The best exposure of stromatolites are seen in Bioherms H (Figure 3.1) and S. Stromatolites at the top of Zone B may or may not be silicified. If not silicified, they are a distinctive dark gray to black color, and have a concentric nature when seen along a weathered bedding plane (Figure 3.13). A bioclastic pack- to grainstone fills in the space around the heads. The stromatolites at the top of Zone B are found growing around Chaetetid heads at Bioherm H (Figure 3.14), although they are also present on their own (Figures 3.13 and 3.15). Concentric laminations are not always seen in these stromatolites, but they are always the distinctive dark gray to black color. These stromatolites are also found in association with bioclastic pack- to grainstones. All stromatolites are approximately 20 to 30 cm in diameter.

Algal growths are interpreted to represent a restricted depositional environment. Their presence at the top of bioclastic limestones suggests an increase in salinity, eliminating the normal marine fauna. The lack of grazing organisms allowed the growth of large stromatolite heads.

Oncolitic Rock Type

(Sections A-1, G-2, and P-1)

Oncoids are found at two stratigraphic intervals in the BC2 (Figure 3.2). Oncoids are found only in between-bioherm or flanking positions. The oncoids in Section P-1 are found within the upper 20 cm of the algal laminite bed at the top of Zone A (Figure 3.16). They can be found up to 7 cm in diameter, but are often fragmented into

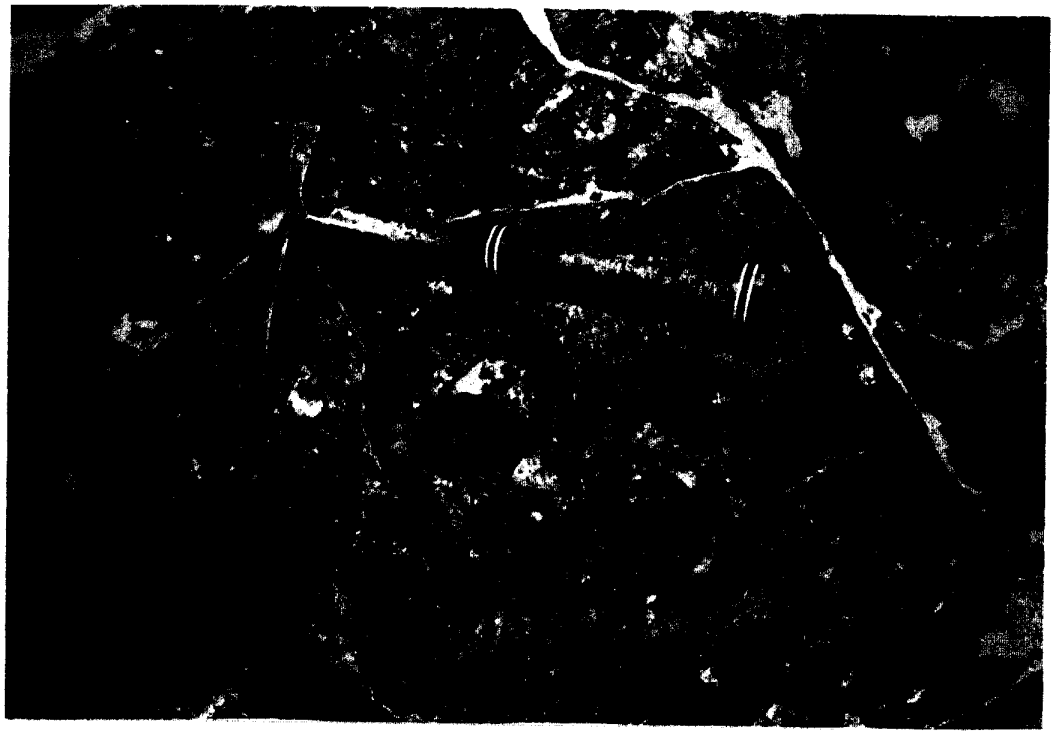


Figure 3.13 - Plan view of the upper surface of a stromatolite bed at the top of Zone A (Bioherm S). Note concentric laminations.



Figure 3.13 - Plan view of the upper surface of a stromatolite bed at the top of Zone A (Bioherm S). Note concentric laminations.

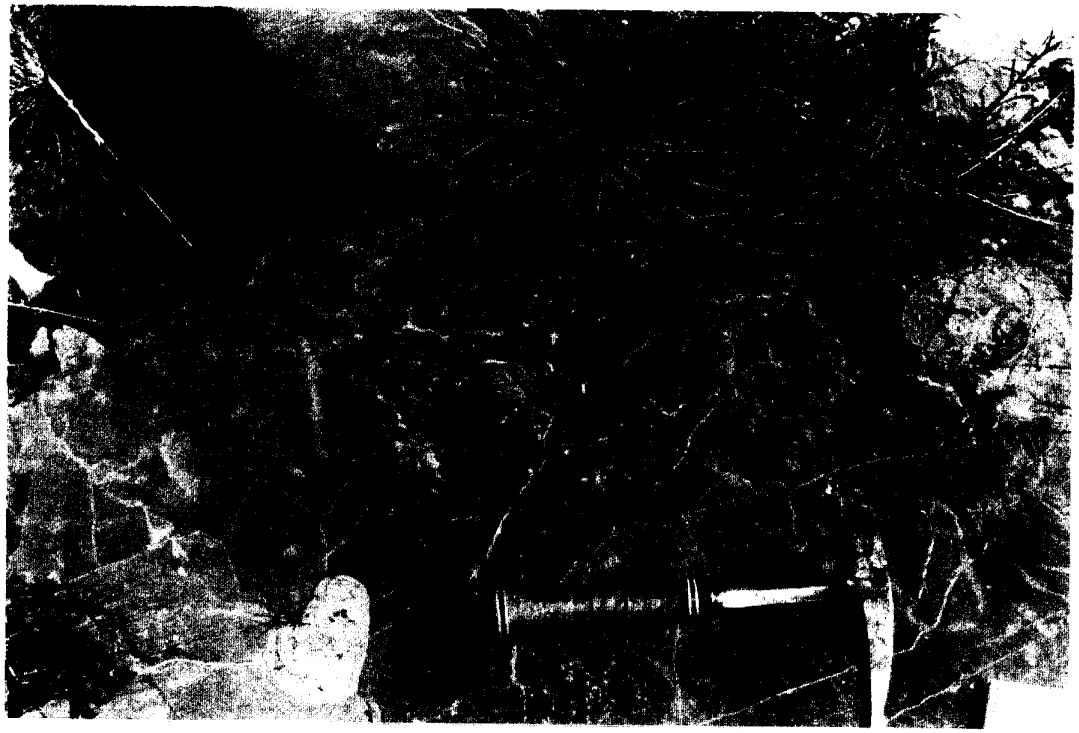


Figure 3.14 - Plan view of stromatolite heads growing around silicified Chaetetids (brown) at the top of Zone B (Bioherm H, 6.0 m).

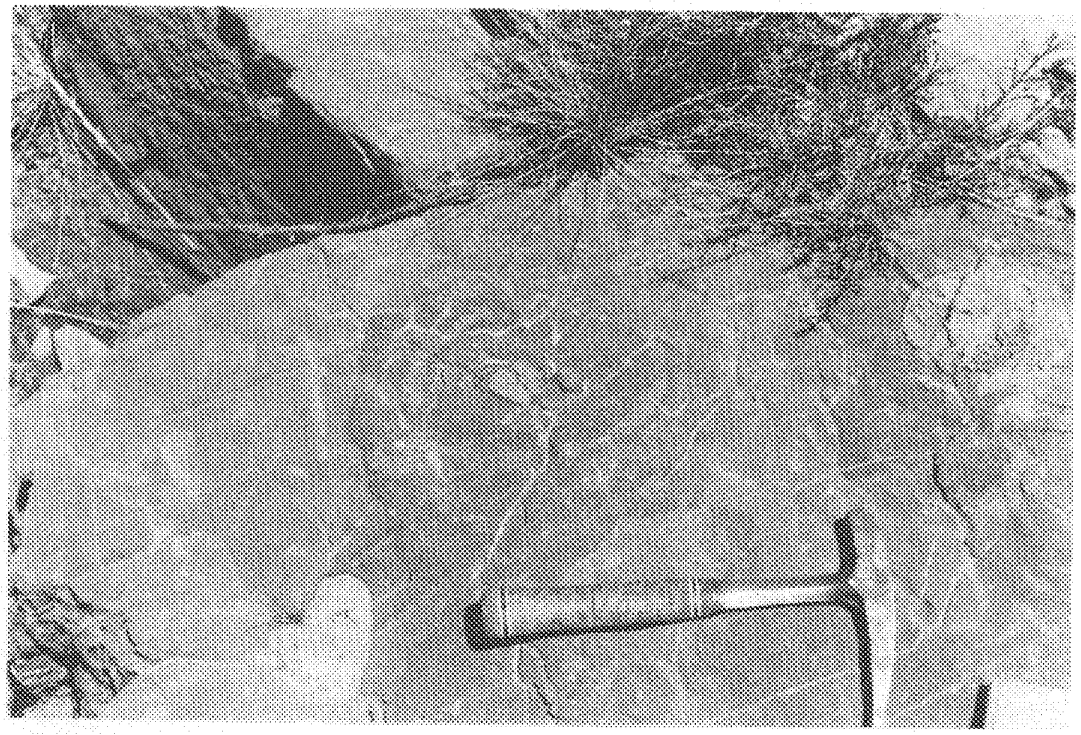


Figure 3.14 - Plan view of stromatolite heads growing around silicified Chaetetids (brown) at the top of Zone B (Bioherm H, 6.0 m).

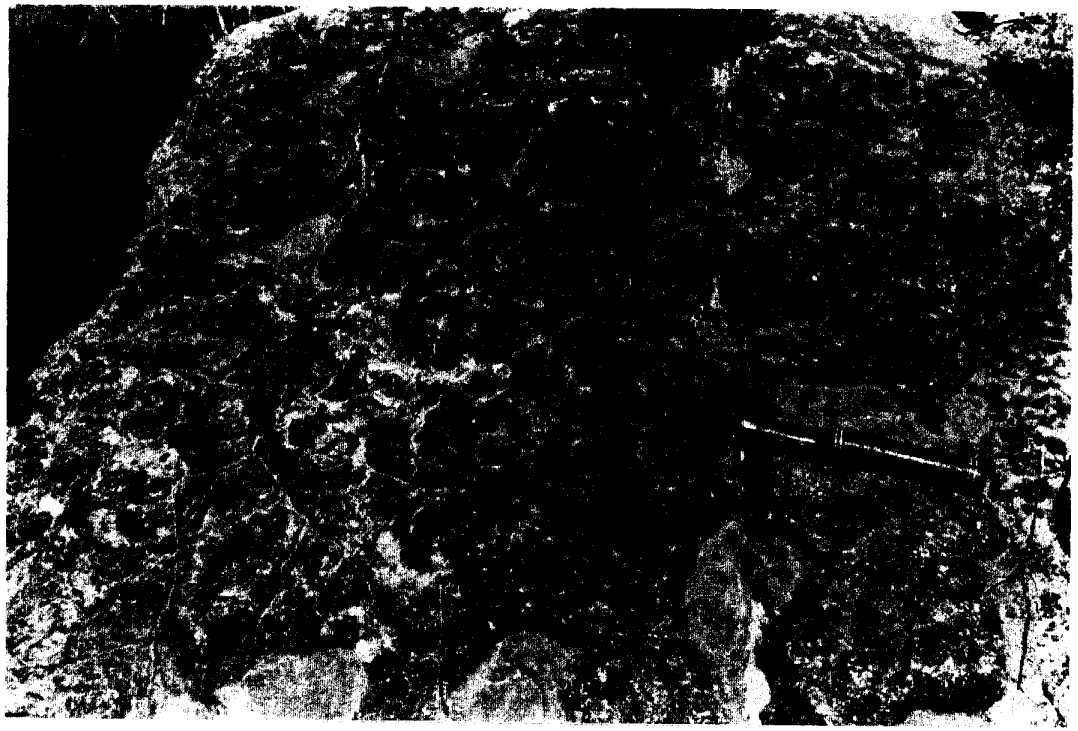


Figure 3.15 - Plan view of abundant stromatolites at the top of Zone B (Bioherm H, 6.0 m).

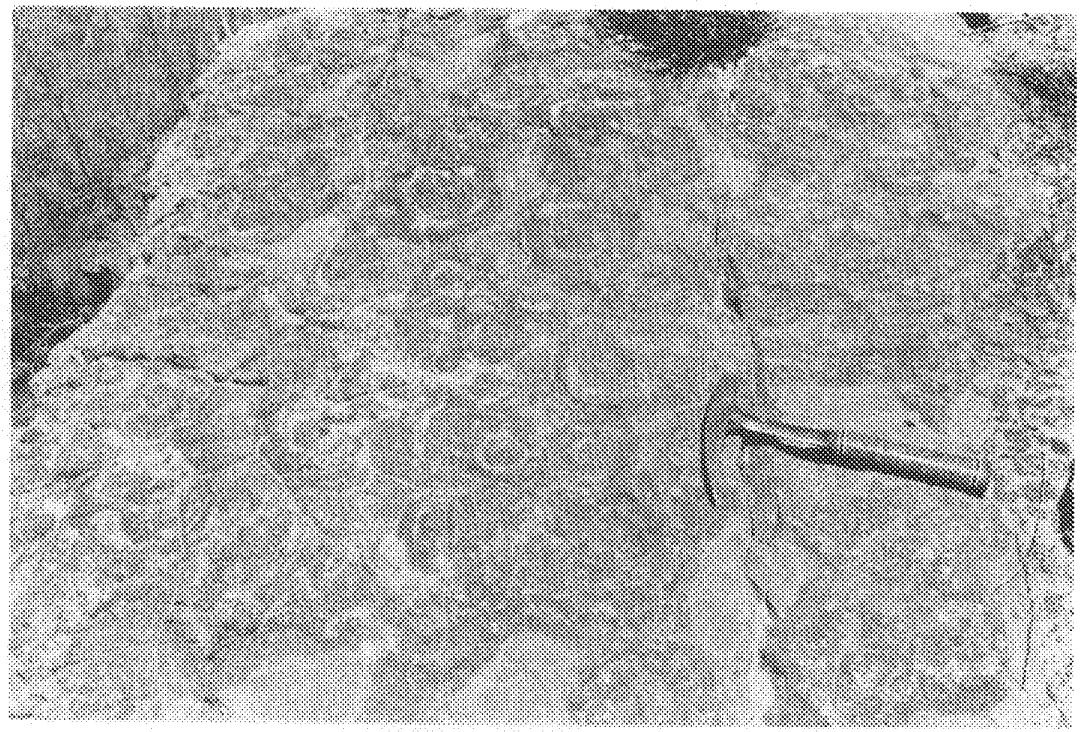


Figure 3.15 - Plan view of abundant stromatolites at the top of Zone B (Bioherm H, 6.0 m).



Figure 3.16 - Dark oncoid-like structures at the top of Zone A (Section P-1, 23.3 m).

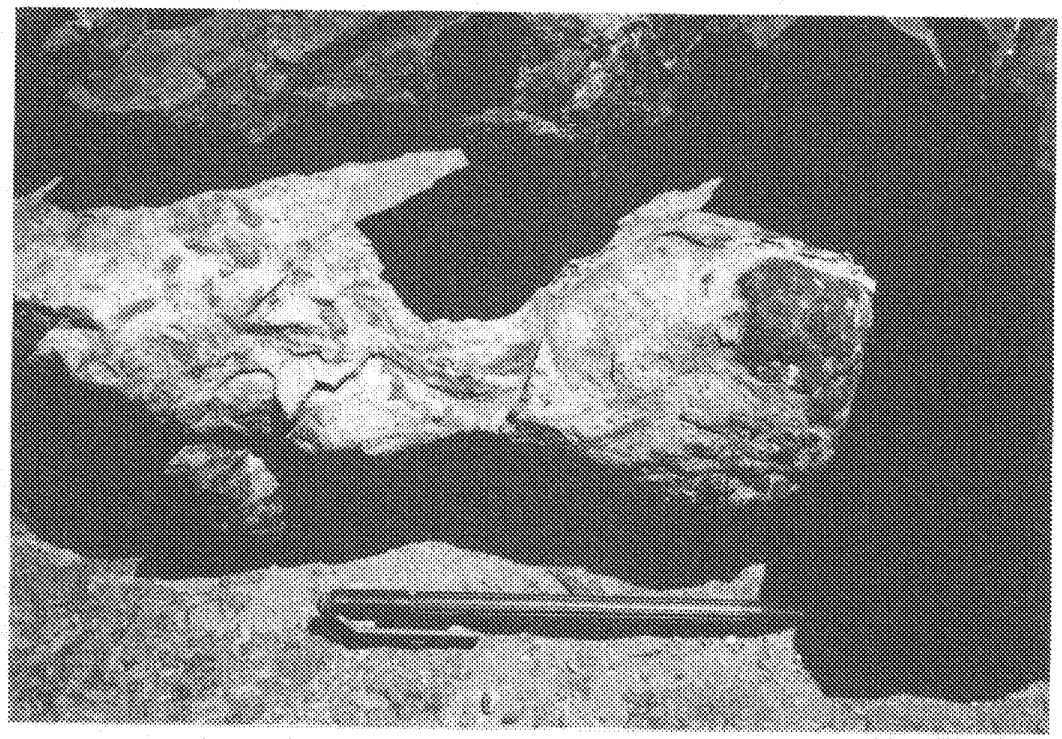


Figure 3.16 - Dark oncoid-like structures at the top of Zone A (Section P-1, 23.3 m).

coarse sand and granule sized clasts. They are dark black in color and have no internal structure and no visible cores. The oncoids are found within a white to light gray silty matrix.

The oncoid-bearing beds in Sections A-1 and G-2 are all within the upper three meters of Zone B in the BC2 interval. The oncoid bed in Section G-2 and the upper bed in Section A-1 both are grain supported bioclastic beds which contain questionable oncoids. The lower bed in Section A-1 is a silty bioclastic packstone containing an upper 10 cm thick oncoid-rich zone. The oncoids are dark gray to black and are approximately 1-2 cm in diameter.

The oncoids are found in association with algal laminites or are in positions which may be correlated with algal mats or stromatolites (at or near the top of Zone B, Figure 3.2). This suggests that the oncoids also were deposited within a restricted environment, and were forming in intermound or flanking positions while algal forms were growing on the mounds themselves. The lack of internal laminations suggests that this was a relatively quiet area of deposition.

Clastic Rock Type

(Sections A-1, C, F, G-1, and G-2)

Both conglomerates and intraclast units are present within the BC2 interval. The conglomerate beds are all present within bioherms and are near the contact between Zones A and B (Figure 3.1). A very continuous conglomerate is present above the bioherms, as pictured in Figures 3.1 and 3.2. This conglomerate is the basal unit of the BC3

interval, and as such is discussed with that interval. The intraclast units in the BC2 interval are not limited to within the bioherms, but they are only present within Zone B (Figures 3.1 and 3.2).

Several thin conglomeratic layers are present within the upper 50 cm of Zone A on the flanks of Bioherm F (adjacent to, but not within Section F). They contain reworked clasts of the underlying bioclastic limestone. A conglomeratic unit is found at the base of Zone B within the bioherms in Sections F and G-1 (Figure 3.1). The conglomerate in Section F is approximately 10 cm thick. Some of the clasts are black and rounded, others are lithoclasts derived from the underlying bioclastic limestone. The conglomerate is poorly sorted. The clasts range from coarse to very coarse sand to granule and gravel sized. The conglomerate in Section G-1 is 15 cm thick and is light gray in color. The conglomerate clasts are very coarse sand sized. Fossil hash is found within the matrix. Burrows are also present in the matrix of this conglomerate. Sorting of this unit is moderate.

Discontinuous intraclast layers are found in Sections A-1, C, and G-2 (Figures 3.1 and 3.2). Section C is located within a bioherm, Section G-2 is located on the flank of a bioherm, and Section A-1 is located in a between-bioherm position. The intraclast in Section C is found within the upper 1.5 m of Zone B. The 10 cm thick bed is found overlying a massive Chaetetid-rich foram boundstone within Bioherm C. The dark gray angular intraclasts, derived from the underlying grainstone, are coarse sand to granule sized. They, along with reworked Chaetetid fragments, are found within a light gray poorly sorted matrix. The intraclast-containing zone within Section G-2 is at

the base of Zone B, above an algal laminite (Figures 3.2 and 3.17). This 25 cm thick zone contains intraclasts up to 1 cm in diameter (small pebble sized). The matrix in which the clasts are contained is micrite-rich. This unit is very poorly sorted. These intraclasts appear to be the product of desiccation rather than scour. The intraclast in Section A-1 is found within the top 50 cm of Zone B (Figures 3.2 and 3.18). The intraclasts are found within a 10 cm zone, and are composed of the underlying foram-rich pack- to grainstone.

The clastic units within the BC2 all appear to be coincidental with or adjacent to the upper and lower boundaries of Zones A and B. They are in a correlative position with other rock types found at boundaries, such as the algal and oncolitic rock types, which are interpreted to indicate a restriction of the environment. The presence of clastic units at these boundaries suggest that the change of environment may have been caused by an increase in energy, causing scour of beds and transport of clasts. The conglomerate in Section G-2 suggests that the change in environment at the Zone A / Zone B boundary was also caused by a relative lowering of sea level, causing desiccation. The blackened appearance of clasts in Section F support the idea of lowered relative sea level.

Sandstone and Siltstone Rock Type

(Sections A-1, A-2, C, G-1, G-2, P-1, P-3, and P-4)

Both continuous and discontinuous siltstones are found in the BC2 interval. Eight thin discontinuous siltstones are found in Sections A-1, C, G-1, G-2, P-1, P-3, and P-4 (Figures 3.1 and 3.2). These range



Figure 3.17 - Intraclasts near the base of Zone B (Section G-2, 3.0 m). These intraclasts are interpreted to be the product of desiccation.



Figure 3.17 - Intraclasts near the base of Zone B (Section G-2, 3.0 m). These intraclasts are interpreted to be the product of desiccation.



Figure 3.18 - Intraclast unit near the top of Zone B (Section A-1, 12.0 m).

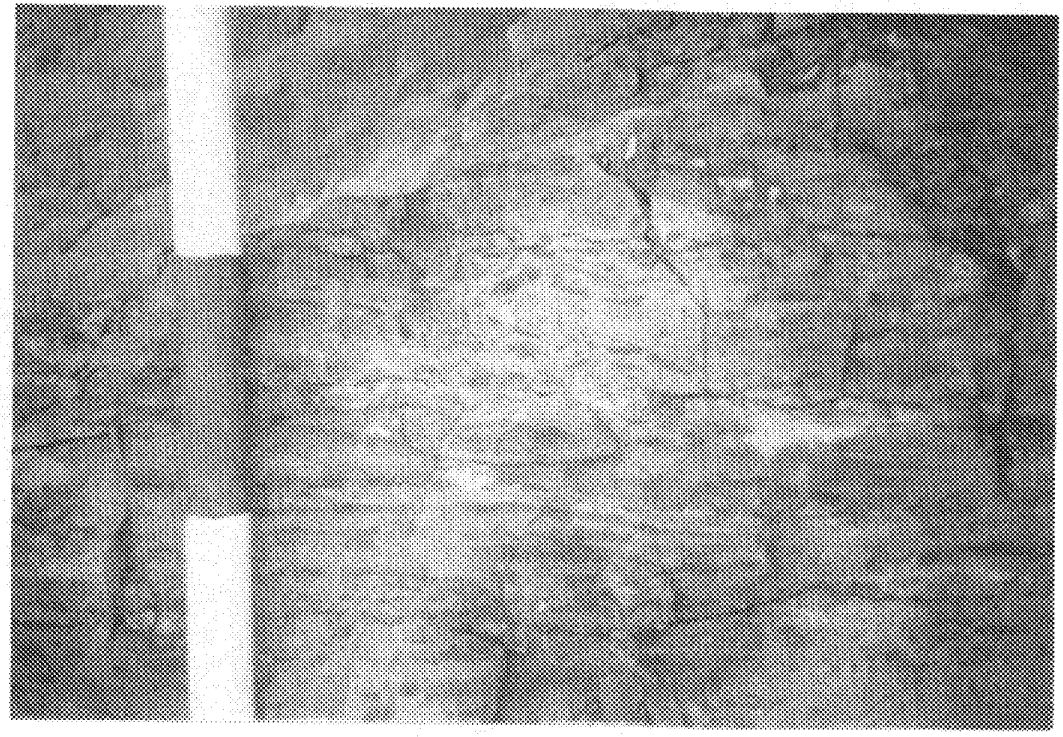


Figure 3.18 - Intraclast unit near the top of Zone B (Section A-1, 12.0 m).

in thickness from 4 to 35 cm. The recessive units are poorly sorted and appear to contain a variety of quartz silt, argillaceous mud, and carbonate mud or cement. Some of the very dark gray units resemble shaley units. Thin covered intervals within measured sections are probably also discontinuous, recessive siltstones.

Two thick greenish siltstones are also found in the BC2 interval. The lower of these is found at the very base of the BC2, exposed in Sections A-2 and P-1 (Figures 3.2 and 3.19). This greenish-gray siltstone is the more laterally extensive of the two. Elsewhere in the study area it forms a distinctive covered interval. This covered interval can be traced over approximately 3.5 km. It ranges in thickness from 1.6 m (Section P-3, thickness of covered interval) to 1.9 m (Section P-1, direct measurement). It is composed of well sorted silt-sized quartz grains and fine-grained carbonate material. No fossils are found within this greenish-gray siltstone. The only organic structures found in the siltstone are thin black organic stringers which are parallel to bedding. These are interpreted to be compressed plant material.

The upper greenish siltstone, exposed only in Sections P-1 and P-3, is located on the southeastern flank of the largest bioherm in the study area (Bioherm P) (Figures 3.1 and 3.2). It is found at the base of Zone B. It is a maximum of 75 cm thick, and thins to zero as it approaches the core of Bioherm P (Figure 3.20). This unit contains fine quartz silt and sand, as well as carbonate mud or cement. There are no fossils present in this unit. This siltstone is discontinuous; it is only found adjacent to this one bioherm.

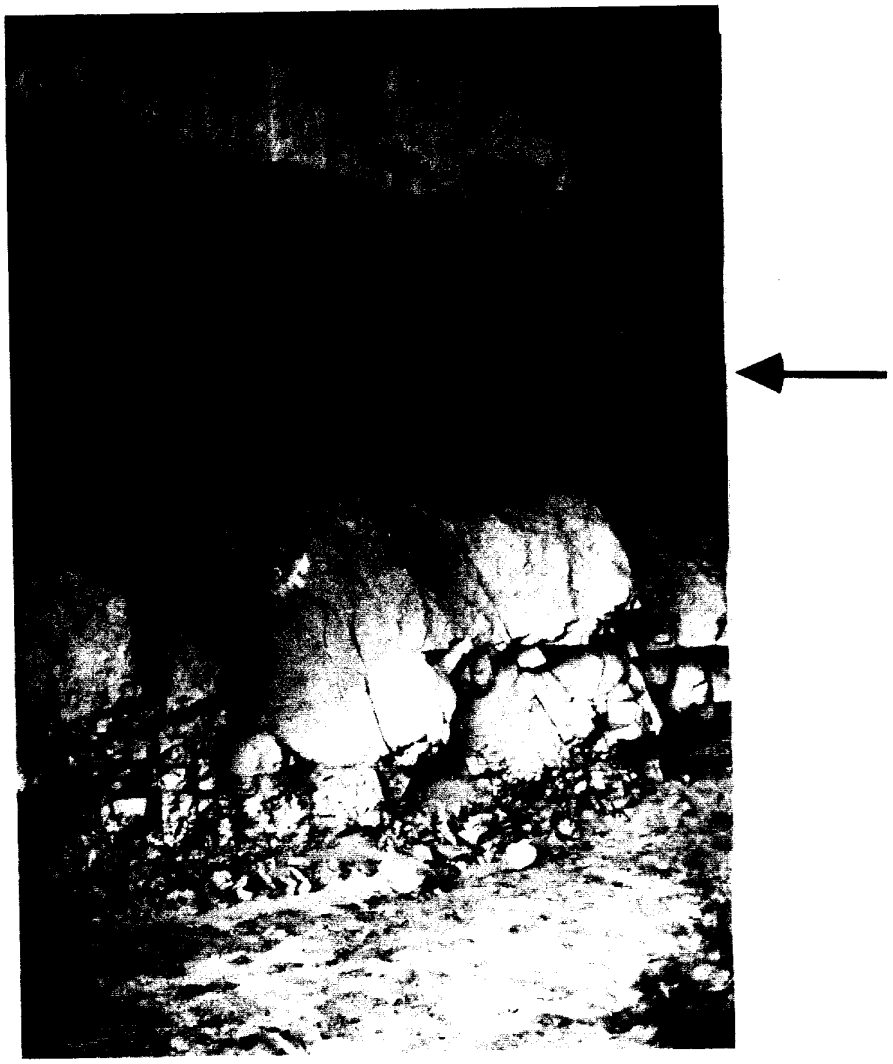


Figure 3.19 - Recessive greenish-gray siltstone (Section P-1, 13.5 m). Here the siltstone is 1.9 m thick. Arrow indicates 2 cm shale deposited on an undulatory surface, 20 cm above the siltstone.

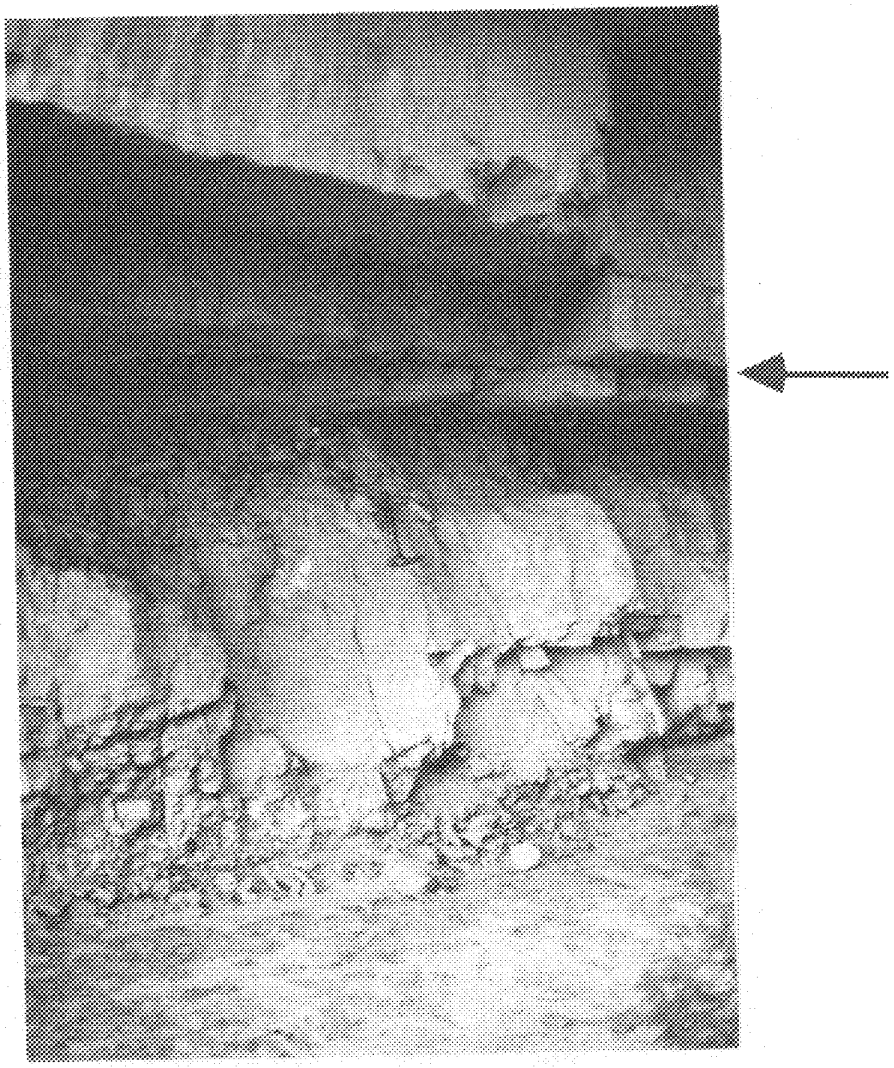


Figure 3.19 - Recessive greenish-gray siltstone (Section P-1, 13.5 m). Here the siltstone is 1.9 m thick. Arrow indicates 2 cm shale deposited on an undulatory surface, 20 cm above the siltstone.



Figure 3.20 - Discontinuous siltstone on the southeastern flank of Bioherm P at the base of Zone B (arrow). The siltstone can be seen thinning to zero as it approaches the core, towards the right of the photograph.

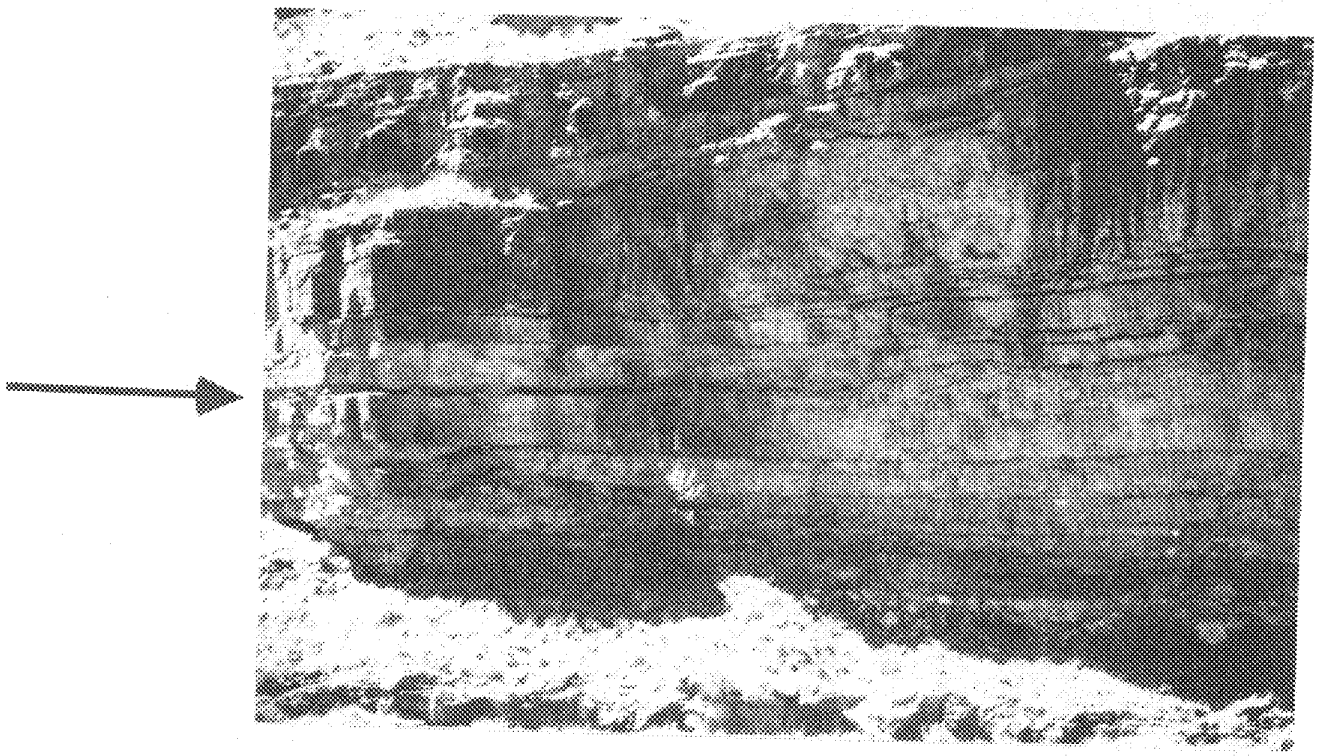


Figure 3.20 - Discontinuous siltstone on the southeastern flank of Bioherm P at the base of Zone B (arrow). The siltstone can be seen thinning to zero as it approaches the core, towards the right of the photograph.

The lower, laterally extensive siltstone could have been formed by either marine or non-marine processes. There is no evidence within the field area to suggest one interpretation over the other. Outside of the field area, there is evidence suggesting a non-marine origin of this unit. Within this green siltstone rootlets are present at river mile 45.2 (river left), and rhizoliths are present at river mile 53.6 (river right). The presence of these structures, in conjunction with the greenish color suggests that this unit is a paleosol.

There is also no evidence within the field area to indicate whether the upper greenish siltstone was formed by marine or non-marine processes. The greenish color suggests that this bed may too be a paleosol.

The thin discontinuous siltstones may reflect local terrigenous pulses. The fact that they are not continuous suggests that they originate from some local point source, such as a nearby fluvial source.

Dolostone Rock Type

(Sections A-1, A-2, C, D, F, G-1, G-2, M-1, P-1, P-2, P-3, P-4, and P-8)

Dolostones and dolomitic limestones in the BC2 interval are only found below the bioherm-rich zone. The lower dolostone units are commonly covered. There are three distinct dolostone units separated from each other by grainy limestones, as seen in sections P-1 and P-4 (Figure 3.1). As measured in Section P-1, the lowest silty dolomite is 1.52 m thick, the middle is 1.22 m thick, and the upper is 1.06 m thick.

The majority of these dolostones are monotonously very finely crystalline (microcrystalline), containing euhedral rhombohedra of dolomite (coarse silt sized, approx. 0.02 mm in diameter) (Figure 3.21). They also contain approximately 1% or less coarse quartz silt. Other dolostones and dolomitic limestones are quite grainy and appear to be dolomitized bioclastic limestones.

The dolostones are commonly bioturbated. They may contain small millimeter-scale burrows(?), or larger chert-filled burrows (approximately 1 cm in diameter, and several centimeters long) (Figure 3.22). Anhydrite nodules and chert beds or nodules are also common within the dolomites. Anhydrite nodules are most common in the uppermost dolostone. The nodules are large pebble to small cobble sized (averaging approximately 10 cm in diameter), and are elongated in a horizontal direction. The anhydrite nodules are often weathered out leaving large molds, but they are generally preserved under overhangs and in other sheltered locations. Chert nodules are oval to disk-shaped, also elongated in a horizontal direction. They are generally 10 cm or more wide, and only 5 to 10 cm tall. Digitate chert beds (from 5 to 10 cm thick) along bedding planes are found throughout the field area wherever the dolomites are exposed.

In thin section, one can see numerous small (approx. 0.1 mm, very small sand sized) round cement-filled bodies distributed throughout the dolomitic matrix (Figure 3.23). They are very rarely elongated. These bodies may be recrystallized sponge spicules. If this is so, they appear to be very well oriented. Because the bodies appear rounded in cross-section the majority of the time (approximately

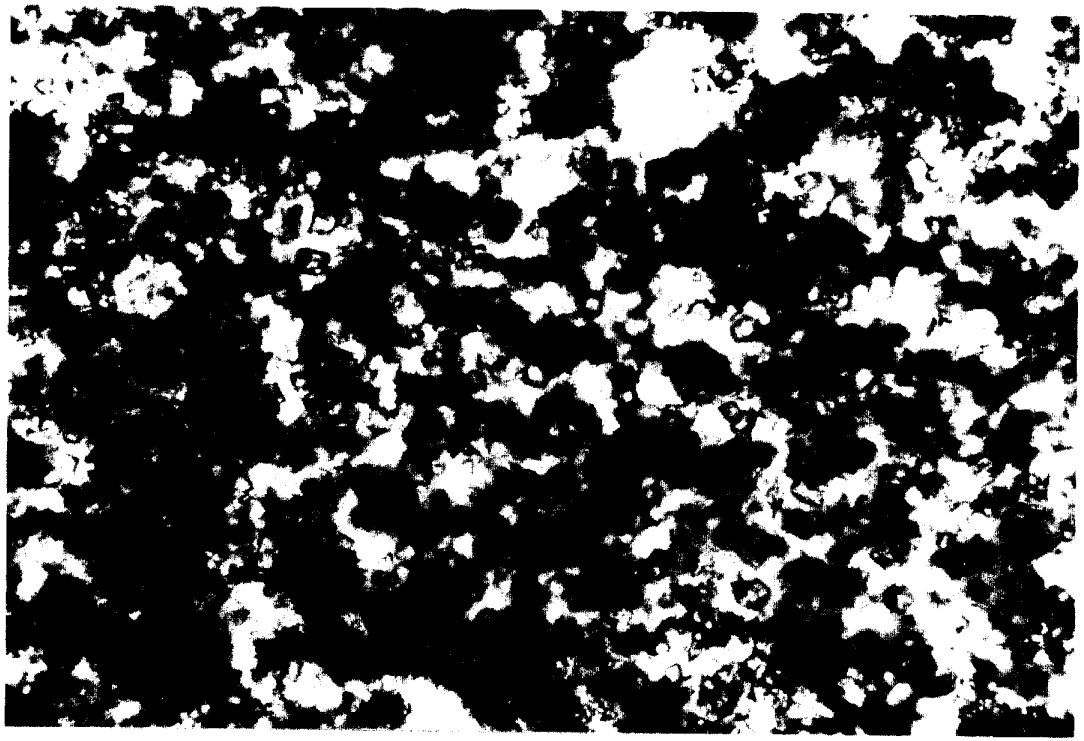


Figure 3.21 - Euhedral dolomite rhombs within a microcrystalline dolostone (Section P-4, 4.6 m, UW1884/111). (Width of view is 1.25 mm.)

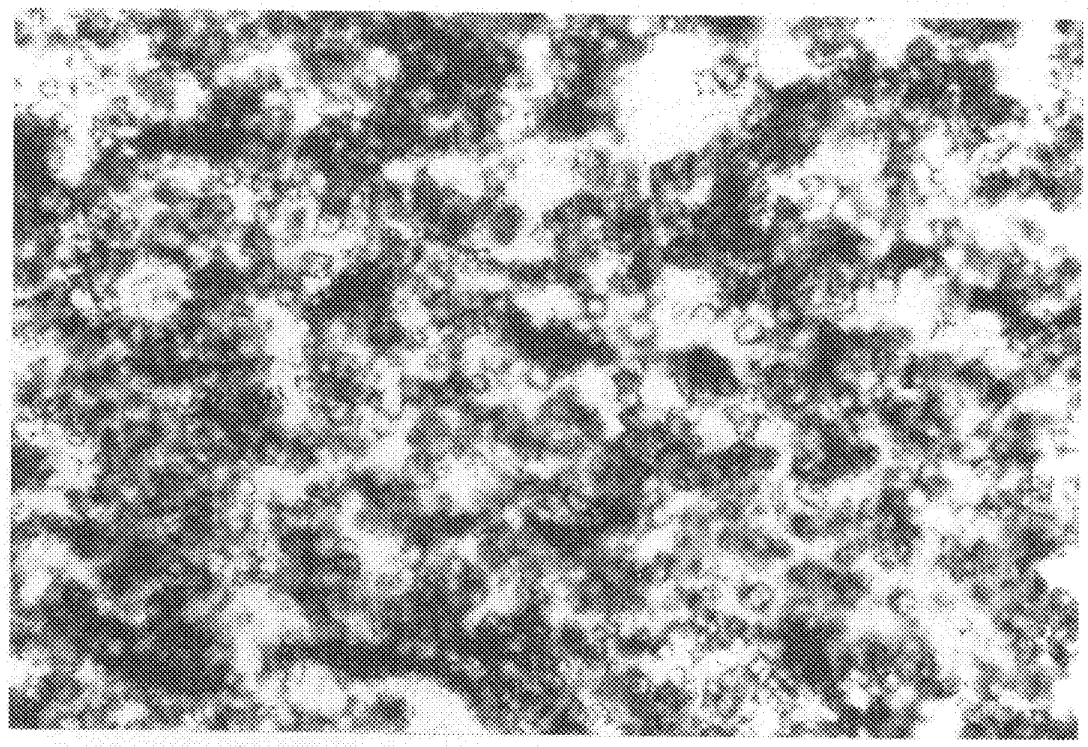


Figure 3.21 - Euhedral dolomite rhombs within a microcrystalline dolostone (Section P-4, 4.6 m, UW1884/111). (Width of view is 1.25 mm.)

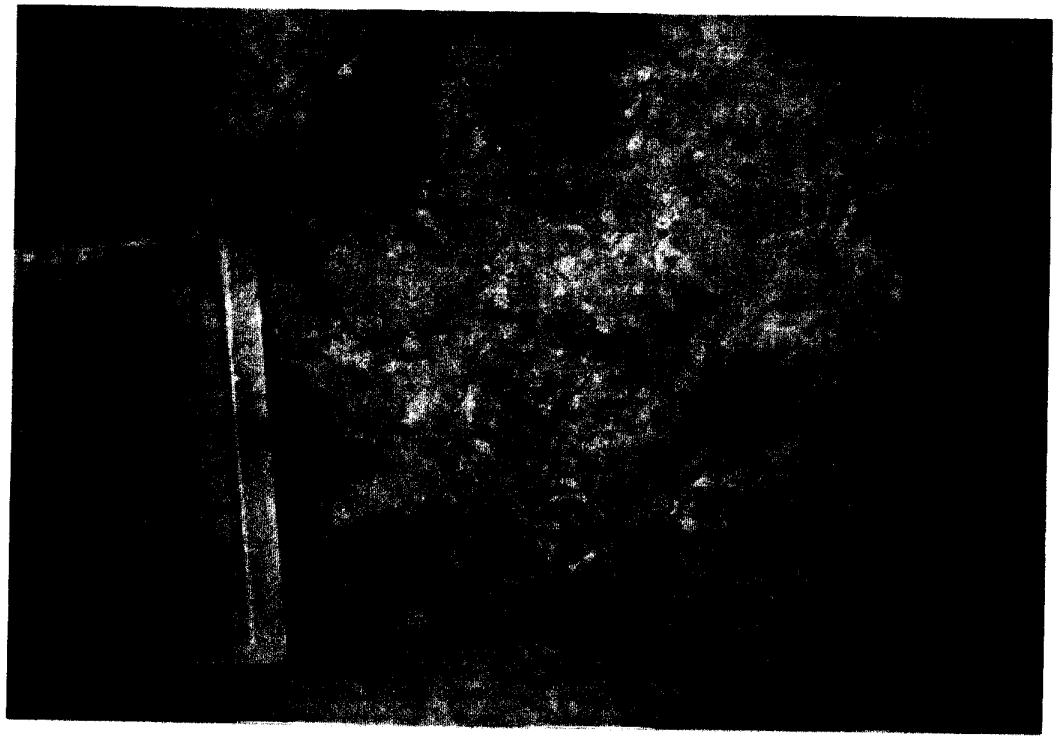


Figure 3.22 - Fine burrows (white) in a silty dolostone (Section P-1, 17.5 m).

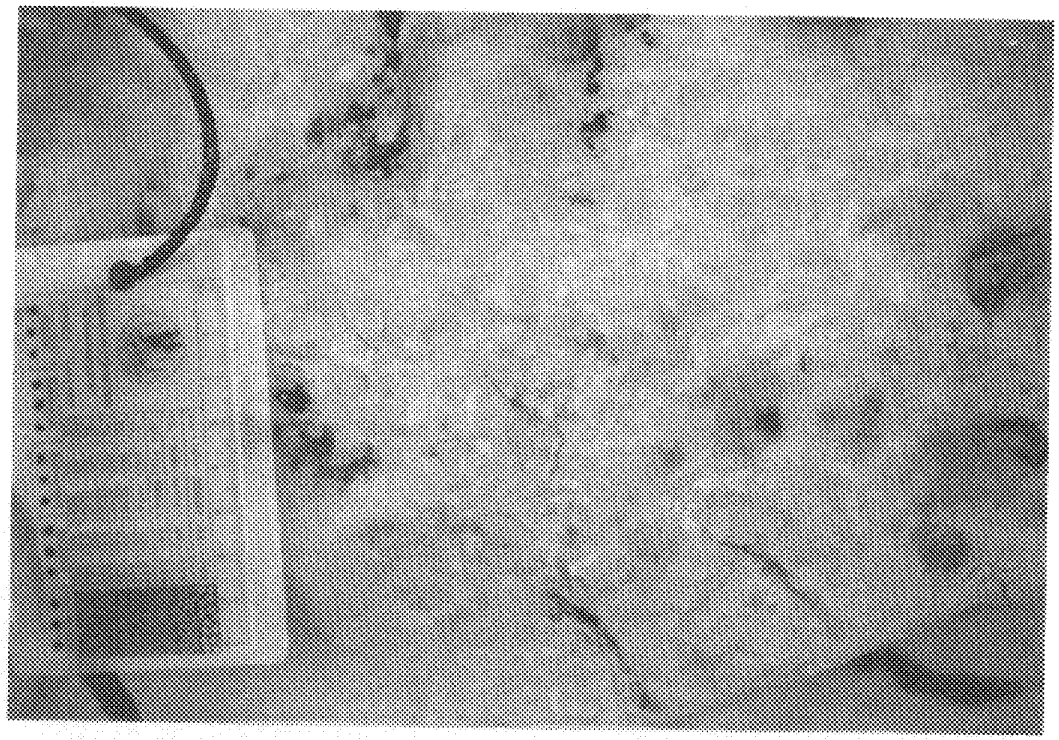


Figure 3.22 - Fine burrows (white) in a silty dolostone (Section P-1, 17.5 m).

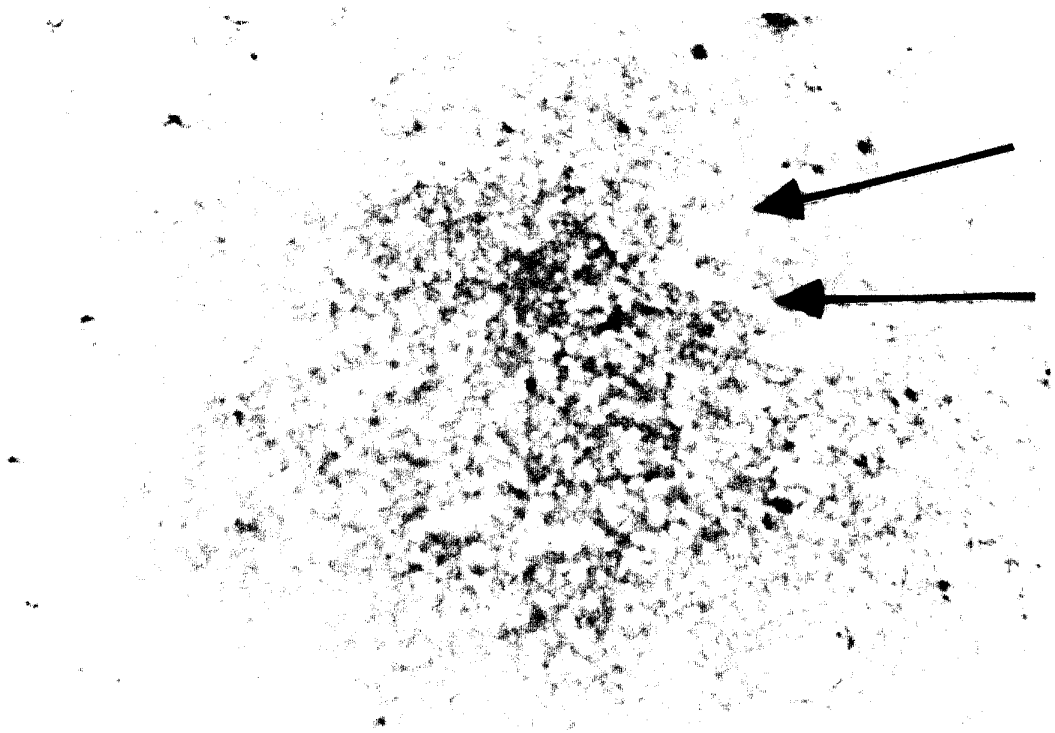


Figure 3.23 - Round and elongated cement-filled sponge spicules (?) within a dolostone (arrows) (Section P-3, 3.0 m, UW1884/112). (Width of view is 5 mm.)

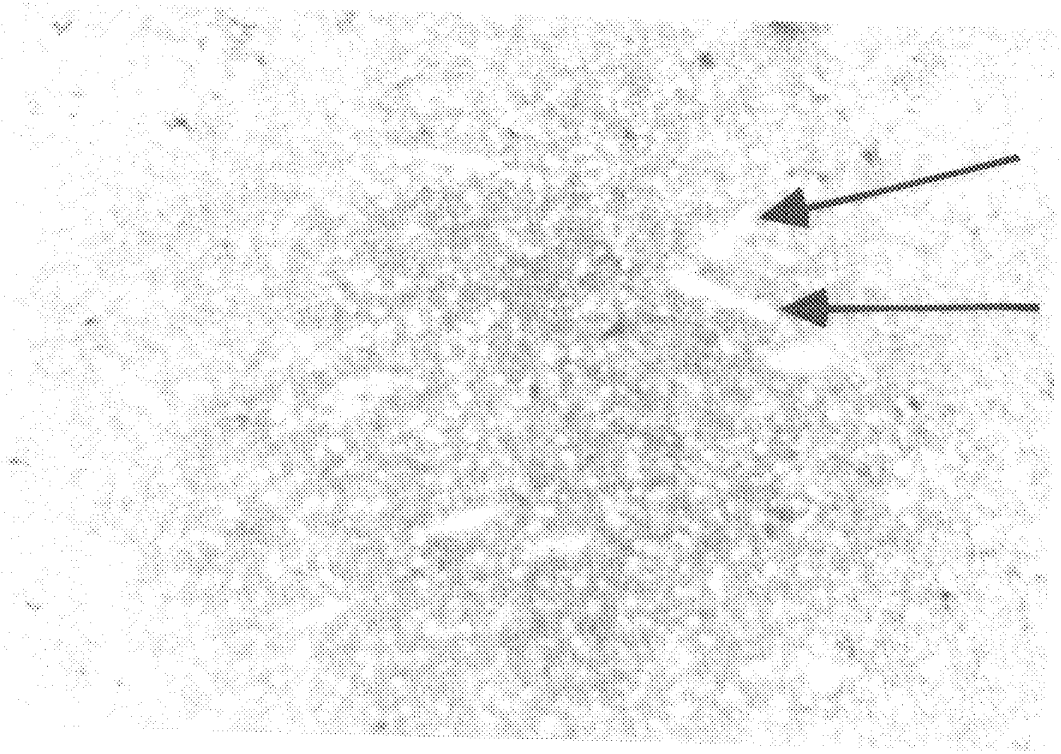


Figure 3.23 - Round and elongated cement-filled sponge spicules (?) within a dolostone (arrows) (Section P-3, 3.0 m, UW1884/112). (Width of view is 5 mm.)

90%), even in un-oriented samples, it is more likely that they are actually spherical forms.

The dolostones contain a combination of normal water and restricted water characteristics. The presence of (questionable) sponge spicules and chert nodules suggests deposition in a restricted or deep-water environment. The laminations which are suggestive of algal structures suggest a shallow water origin, specifically within the photic zone. Grainy bioclastic laminations suggest deposition in a shallow normal marine environment. This alternation between deep water silty dolomites and shallow water grainy dolostones and dolomitic limestones suggests that these units may have been deposited throughout periods of changing sea levels.

Shale Rock Type

(Section P-1)

The 1-2 cm fissile black shale in Section P-1 is found above the lowermost dolostone in the BC2 interval (Figure 3.2). The surface upon which the shale was deposited is undulating, as if it were rippled (Figure 3.19). The shale is of equal thickness both in the "troughs" and on the "crests" of the undulations. Coarse sand sized chips of the black shale are found within the lower 10 cm of the overlying dolostone (Figure 3.24). Neither fossils nor bioturbation are seen in this shale.

The fine grain size of a shale implies that it must be deposited in a very quiet water environment, usually in a deep-water environment. The equal thickness of the shale over both high and low



Figure 3.24 - Dolostone overlying black shale, containing coarse sand-sized chips of the shale (Section P-1, 15.5 m).

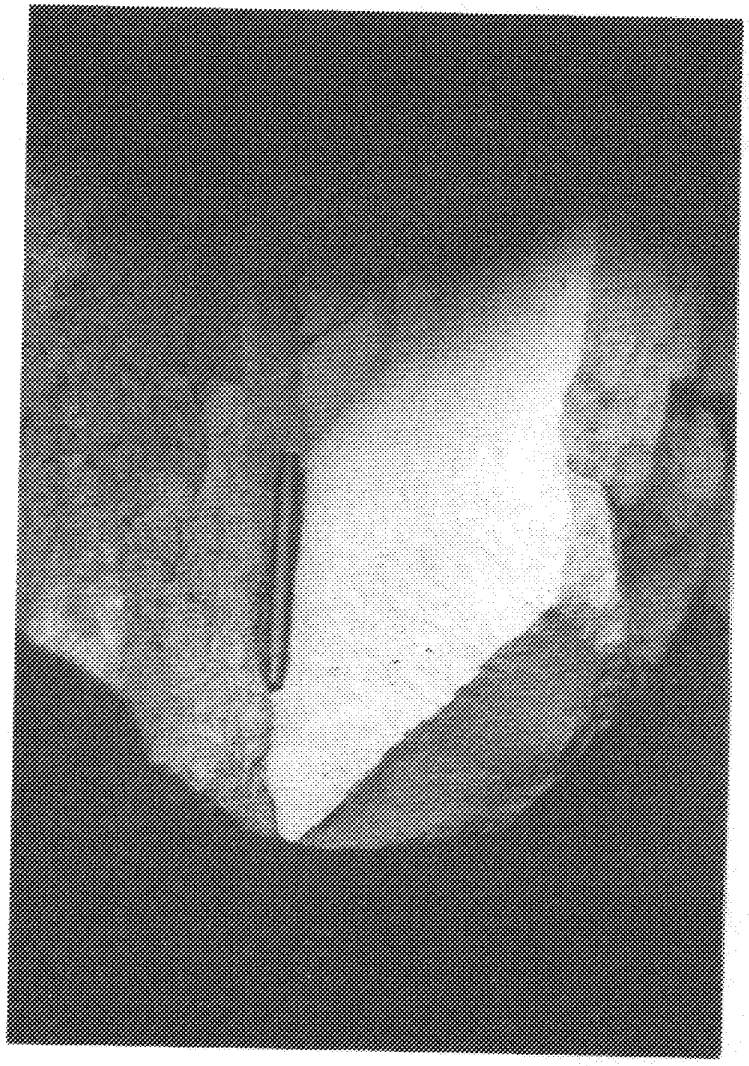


Figure 3.24 - Dolostone overlying black shale, containing coarse sand-sized chips of the shale (Section P-1, 15.5 m).

points on the underlying surface also suggests slow deposition, as suspended material slowly sank to the bottom of the water column, under the influence of no current activity which might have swept material into the "troughs". The black color of the shale indicates that it is organic rich.

- CYCLES IN THE BC2 INTERVAL -

The sequence of rock types in the BC2 can be divided into two cycles (Cycles BC2-1 and BC2-2, Figures 3.25 and 3.26). Exposure surfaces found in this interval include rooted surfaces (Figures 3.27 and 3.28), paleosols, fissured surfaces (Figure 3.29), and conglomerates with blackened clasts. Structures which suggest very shallow water and/or desiccation, such as algal laminites and fenestral porosity, are found in association with some of the exposure features. The cycle breaks within the BC2 appear to occur along two distinct surfaces: the surface at the top of Zone A and the surface at the top of Zone B.

Cycle BC2-1 extends from the base of green siltstone to the top of Zone A (Figures 3.25 and 3.26). Rootlets and rhizoliths are present within the green siltstone outside of the field area (at river miles 45.2 and 53.6), indicating exposure and a terrestrial environment. The green siltstone itself may be a paleosol. The dolostone and limestone package found below the bioherm-rich zone presents an enigmatic succession. Fine-grained dolostones, containing chert nodules and possible evidence of a deep-water fauna (sponge spicules?), alternate

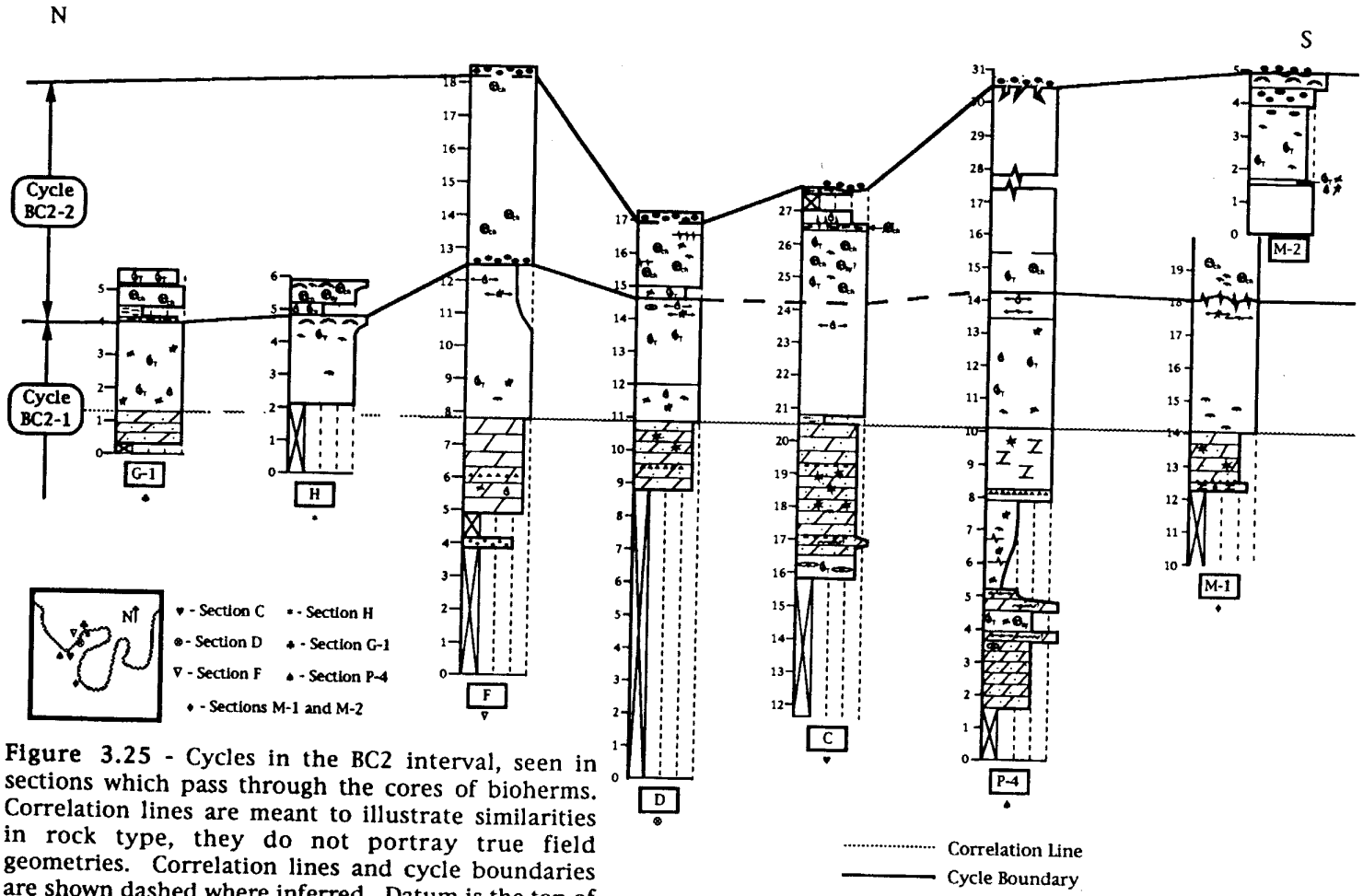


Figure 3.25 - Cycles in the BC2 interval, seen in sections which pass through the cores of bioherms. Correlation lines are meant to illustrate similarities in rock type, they do not portray true field geometries. Correlation lines and cycle boundaries are shown dashed where inferred. Datum is the top of the uppermost dolomite. (For entire sections and key see Appendix A.)

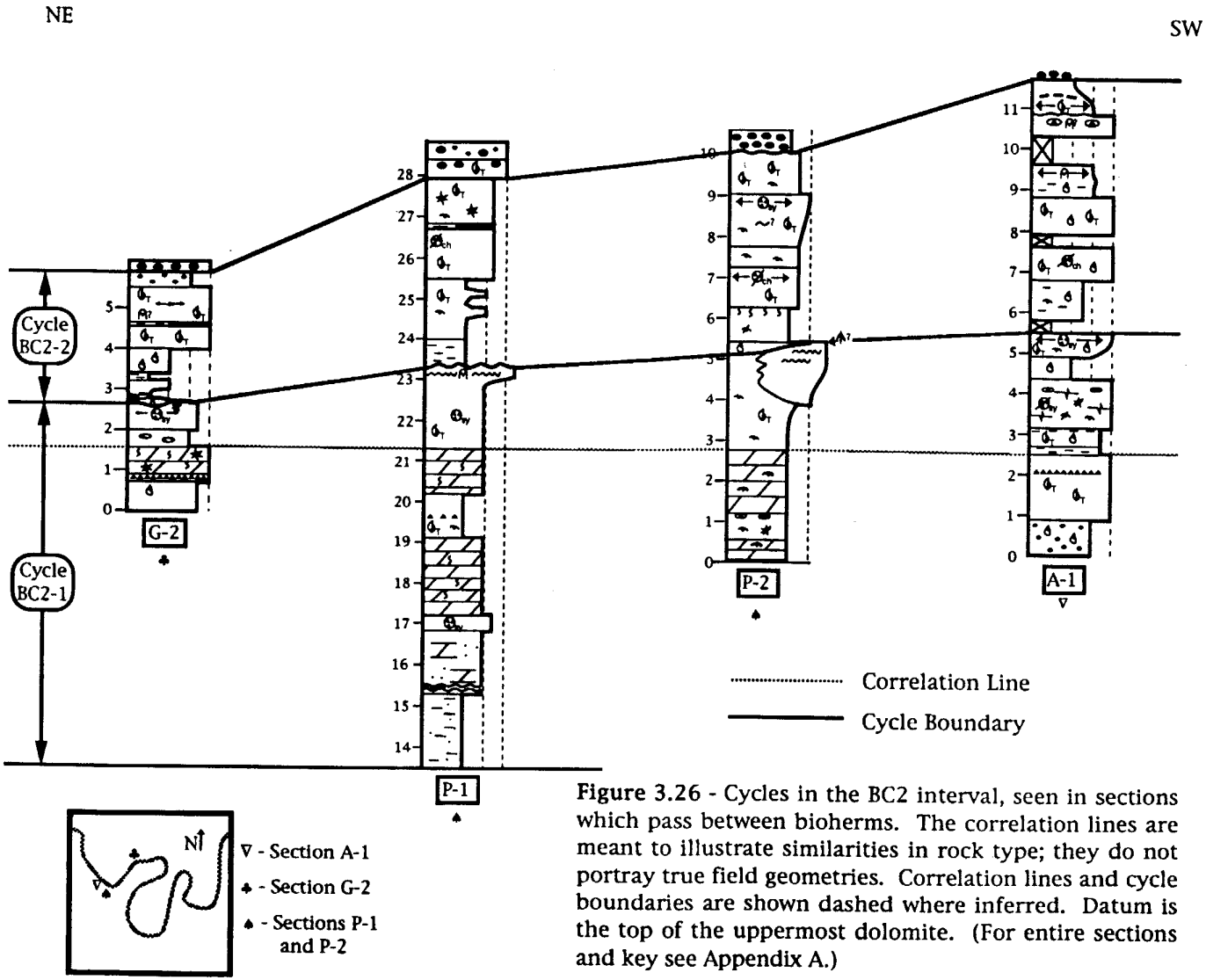


Figure 3.26 - Cycles in the BC2 interval, seen in sections which pass between bioherms. The correlation lines are meant to illustrate similarities in rock type; they do not portray true field geometries. Correlation lines and cycle boundaries are shown dashed where inferred. Datum is the top of the uppermost dolomite. (For entire sections and key see Appendix A.)



Figure 3.27 - Rhizolith found at the top of Zone A (Section P-2, 5.3 m).



Figure 3.27 - Rhizolith found at the top of Zone A (Section P-2, 5.3 m).



Figure 3.28 - Rhizolith found at the top of Zone B (Bioherm L).



Figure 3.28 - Rhizolith found at the top of Zone B (Bioherm L).

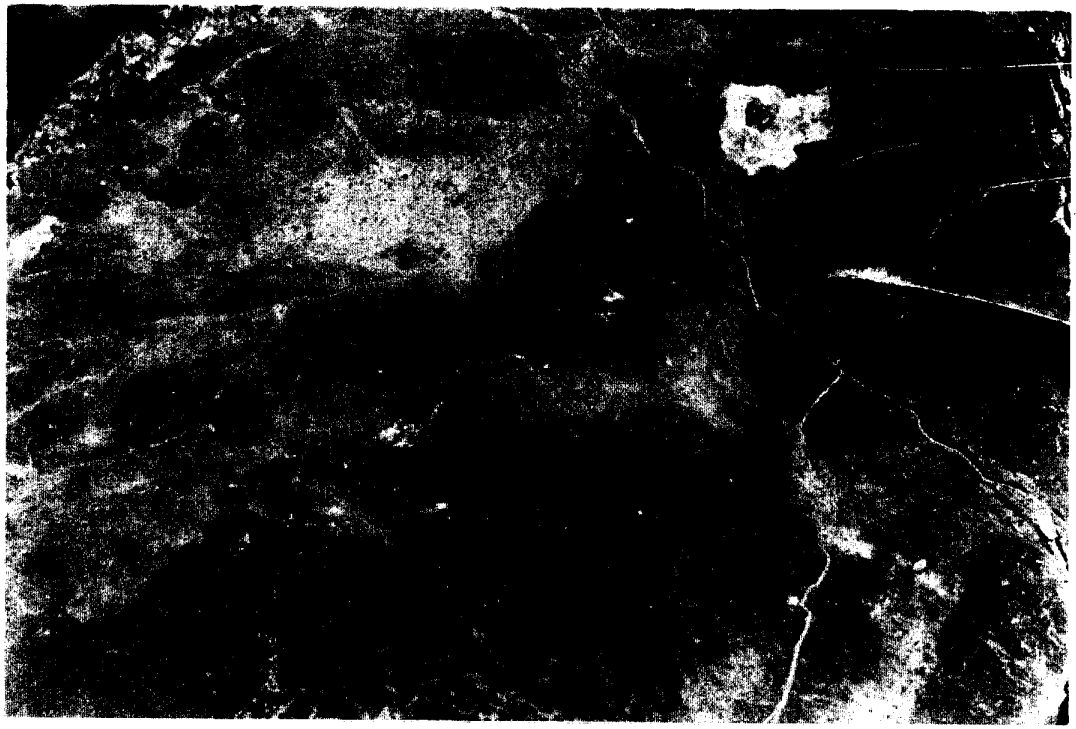


Figure 3.29 - Fissures in the upper surface of Zone B (Bioherm H, 6.0 m). The irregular fissures are filled with light grey to tan sediments. Also notice dark grey algal (?) structures at the bottom center and upper right hand corner of the photo.

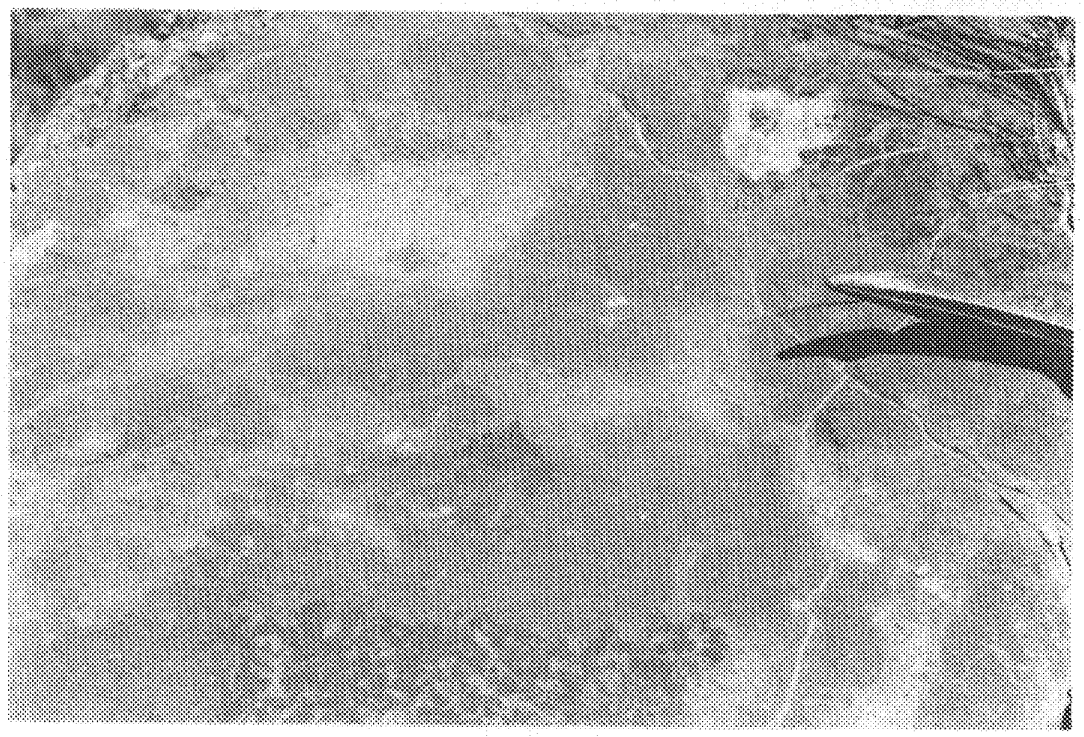


Figure 3.29 - Fissures in the upper surface of Zone B (Bioherm H, 6.0 m). The irregular fissures are filled with light grey to tan sediments. Also notice dark grey algal (?) structures at the bottom center and upper right hand corner of the photo.

with thin grainy bioclastic limestones containing a normal marine fauna. Three shallowing-upward events appear to be represented by this alternation. First, the lowest (deeper-water) dolostone gives way to a (shallower) thin *Syringipora* and tubular foraminifera-rich bioclastic limestone. Next, the second (deeper-water) dolostone gives way to a (shallower) brachiopod- and crinoid-rich bioclastic wackestone or dolomitic limestone. Finally, the upper (deeper-water) dolostone gives way to the (shallower) bioclastic limestones of Zone B which are capped by oncolitic rocks and algal laminites with fenestral porosity.

The upper bounding surface of Zone A is interpreted to be the lower boundary of cycle BC2-2 (Figures 3.25 and 3.26). This surface is overlain by intraclasts, suggesting desiccation (Section G-2, Figure 3.17), and black-pebble conglomerates (Sections C and F); and contains root-like structures (Section P-2, Figure 3.27). Evidence of exposure is not present in every section in the BC2 interval, but the surface can be easily correlated because of the break in bedding and the different fauna present in Zones A and B.

The growth of Chaetetid framestones and tubular foraminifera boundstones in Zone B, as well as the thin black shale in Section P1 (Figure 3.2), indicate a return to a marine environment. A shallowing upward trend within Zone B is shown by the Chaetetid fauna being replaced by stromatolites (Sections H, P-7, Figures 3.1, 3.2, 3.25, and 3.26). The upper surface of Zone B however marks another environmental restriction and a second exposure surface. A rhizolith found at the top of Bioherm L indicates exposure occurred (Figure

3.28). Furthermore, a laterally continuous conglomerate is found lying on top of the upper surface of Zone B, at the very base of the BC3 interval. This black pebble conglomerate is discussed with the BC3 interval, but is included at the top of all BC2 sections (Figures 3.1, 3.2, 3.25, and 3.26).

- BIOHERMS IN THE BC2 INTERVAL -

Thirteen bioherm exposures were seen in the BC2 interval (Figure 3.30). The thirteen exposures represent cuts through eight to ten individual bioherms. The size of the bioherms varies widely in the study area (Table 3.2). The heights of bioherms was measured either by directly measuring a section through the bioherm, by throwing a flagged rope over the edge of a bioherm, or by estimation. The maximum thickness of individual exposures ranges from 3.8 m (Bioherm H) to approximately 20 m (Bioherm P). Bioherm widths range from 15 m (Bioherm S) to 170 m (Bioherm P). Note that these are the maximum dimensions of the exposures, not necessarily the maximum dimensions of the bioherms.

Because most of the bioherms outcrop as cliffs, access to the cores is limited. This makes it difficult to determine the distribution of biota within the bioherm cores. Access to many of the smaller bioherms (ex. Bioherms G and H) is much easier. Thus, the detailed description of fauna which follows is based on one of the smallest (Bioherm H) (Figure 3.31), and is compared to portions of other bioherms observed in the field. The bioherms are subdivided into two

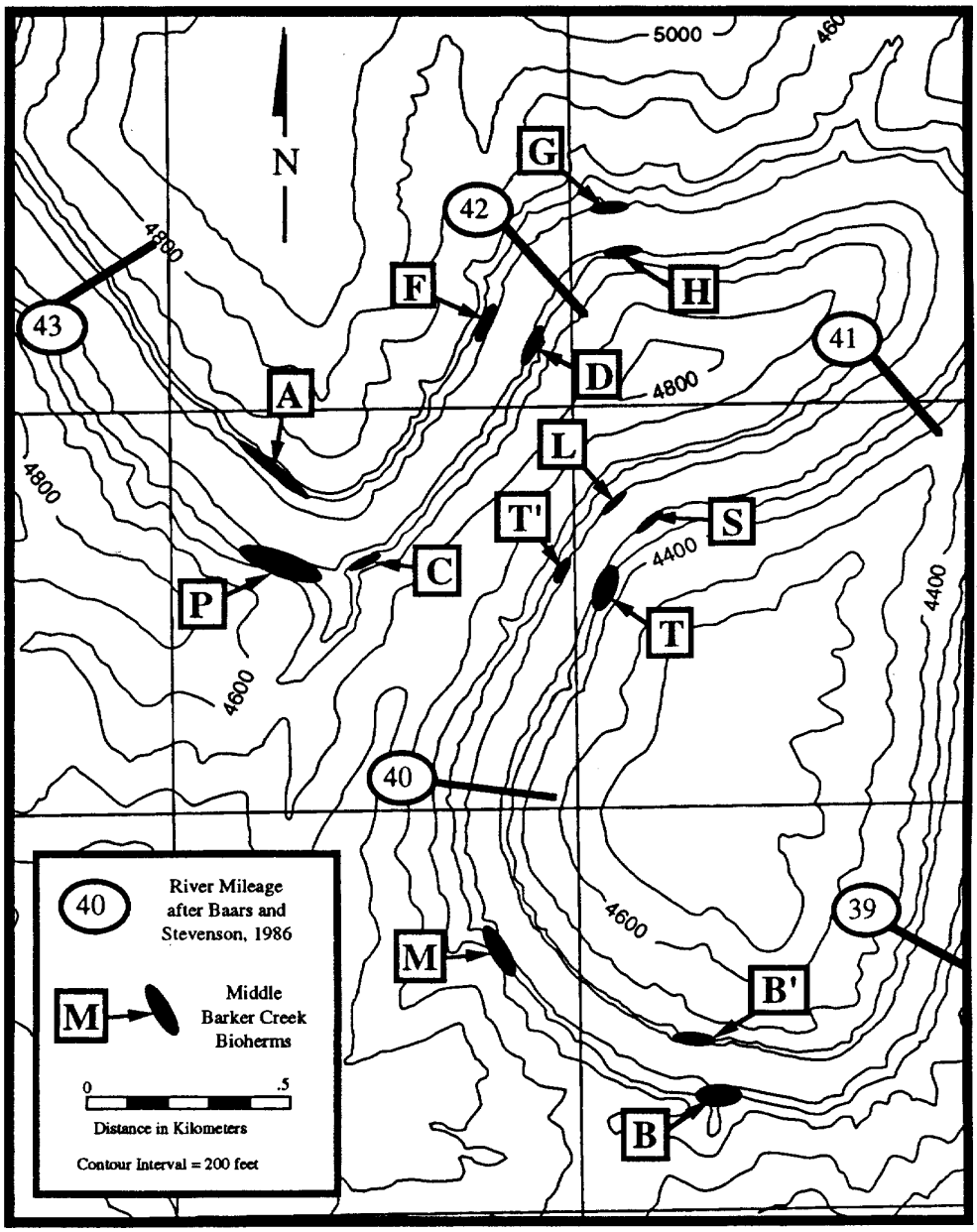


Figure 3.30 - Topographic map of the field area, showing location of bioherms in the BC2 interval.

Bioherm	Maximum Thickness (in meters)	Estimated Width (in meters)
A	5.5	120
B	9	18
B'	>4.25	20
C	7.2	70
D	8.35	45
F	11.5	50
G	4.3	35
H	3.1	20
L	>1.5	15
M	18	120
P	20	170
S	>2	15
T	>9	100

Table 3.2 - Data on the dimensions (in meters) of the thirteen bioherm outcrops. Bioherms B', L, and S were all partially under river level. The minimum height of these bioherms has been recorded. The actual height of Bioherm T was not measured in the field, but a minimum estimate was made based on what was measured. Widths were estimated either while in the field or later from photographic panoramas.

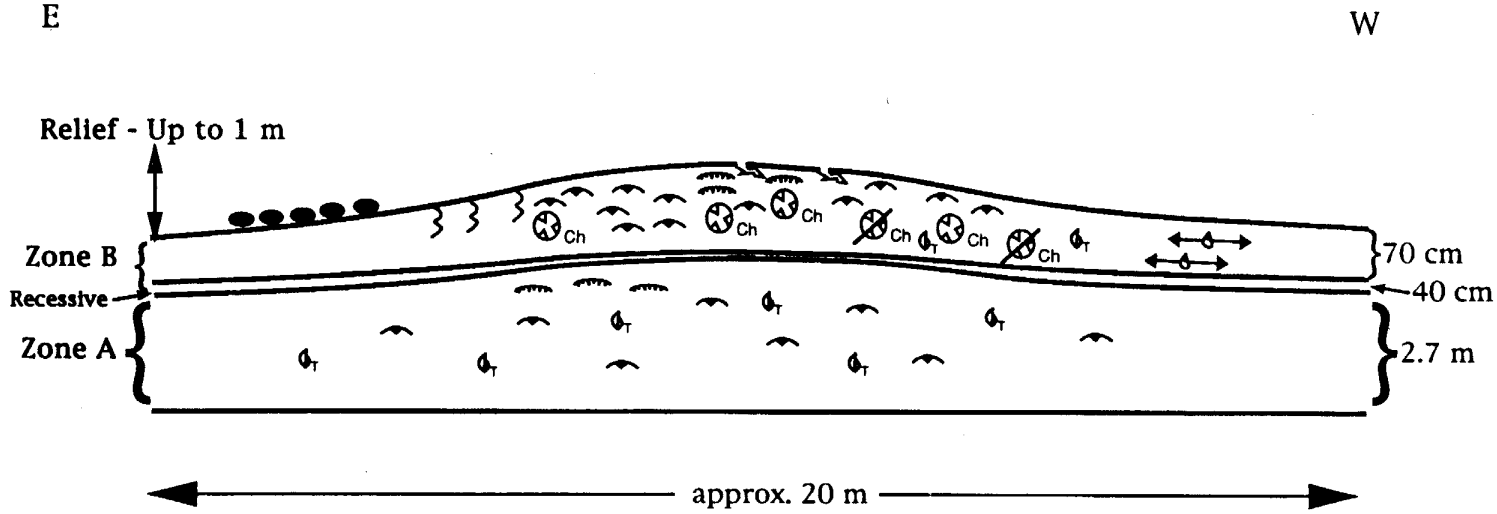


Figure 3.31 - Diagram showing growth history of Bioherm H. Zone A is made up primarily of tubular foraminifera, brachiopod fragments, and fossil hash. There is no obvious zonation of biota in Zone A. Stromatolites and other dark grey to black algal structures are seen at the top of Zone A. Zone B contains Chaetetids as well as articulated and reworked brachiopods, tubular foraminifera, and fossil hash. The western flank of this bioherm contains grainy laminations of fossil hash. Further toward the "core" of the bioherms, broken and reworked Chaetetid heads are seen. The core of the bioherm contains in plance Chaetetids and articulated brachiopods. The brachiopods are found between and above the Chaetetid heads. Numerous Chaetetid heads are surrounded by stromatolitic structures. Towards the northeast, fewer and fewer Chaetetids are seen. Sediments are burrowed. Capping the northeastern-most part of the exposure, conglomerate clasts are seen. (See Appendix A for key.)

zones, Zone A and B, on the basis of sedimentary structures and fauna. Zone A is less well exposed in the smaller bioherms than Zone B, and therefore there is less information about this zone.

Zonation of Lithofacies within Bioherm H

Zone A is a packstone to grainstone, containing tubular foraminifera, reworked brachiopod fragments, and fossil hash. Fossil molds, especially brachiopod molds, are common within this zone. The majority of grains are reworked. In this particular bioherm there are no sedimentary structures indicative of high energy. Algal structures are present at the top of Zone A in Bioherm H, both as algal mats and as stromatolites (Figures 3.31 and 3.32).

A relatively thin recessive bed is present at the base of Zone B (Figures 3.31 and 3.33). This bed ranges in thickness from 40 cm on the flanks of the bioherm to only 1-2 cm in the core. The lithology found within this recessive, or found in lieu of the recessive, varies from bioherm to bioherm. In Bioherm H the recessive bed is a tubular foram / fossil hash wackestone. Its weathering pattern however resembles siltstones seen in the field area.

Zone B in the core of the bioherm is dominated by large (10's of cm) Chaetetid heads (Figures 3.31 and 3.33) surrounded by articulated brachiopods (Figures 3.31 and 3.34). The Chaetetids are estimated to make up 70% of the total rock in the core. Within the core, the majority of the Chaetetid heads are in place. At the top of the bioherm, stromatolites are found encrusting Chaetetid heads (Figure 3.14).

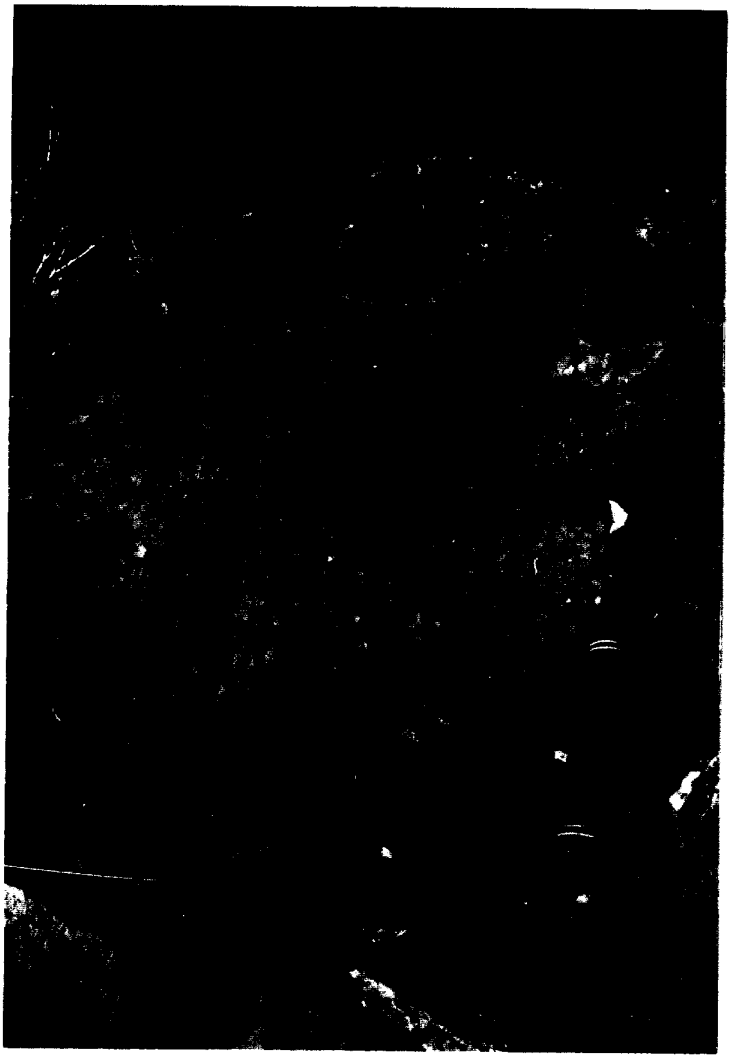


Figure 3.32 - Stromatolite heads found at the top of Zone A (Bioherm H, 6.0 m).

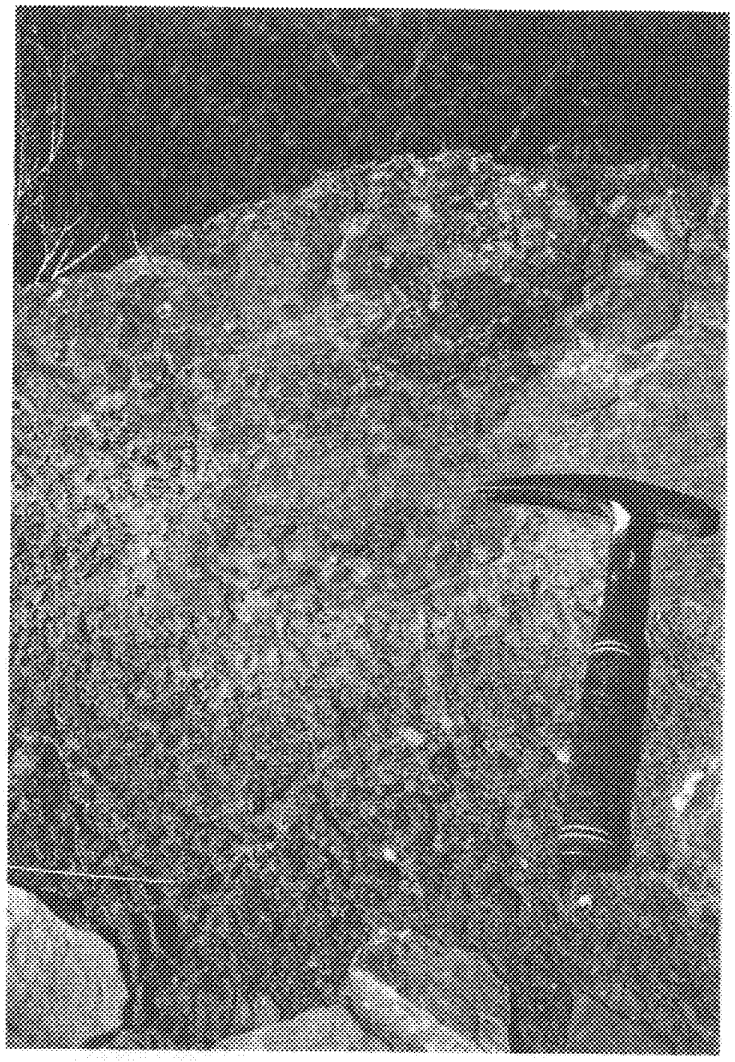


Figure 3.32 - Stromatolite heads found at the top of Zone A (Bioherm H, 6.0 m).



Figure 3.33 - Thin recessive between Zones A and B (Bioherm H, 5.0 m). The recessive bed is a tubular foram / fossil hash wackestone. Above the recessive, within Zone B, Chaetetid heads can be seen. The Chaetetids are silicified and range in size from 10 to 30 cm tall.



Figure 3.33 - Thin recessive between Zones A and B (Bioherm H, 5.0 m). The recessive bed is a tubular foram / fossil hash wackestone. Above the recessive, within Zone B, Chaetetid heads can be seen. The Chaetetids are silicified and range in size from 10 to 30 cm tall.



Figure 3.34 - Large (1-2 cm) articulated brachiopods near the top of Zone B (Bioherm H, 6.0 m).



Figure 3.34 - Large (1-2 cm) articulated brachiopods near the top of Zone B (Bioherm H, 6.0 m).

Zone B on the flanks of the bioherm contains fewer and more fragmented Chaetetids. These beds contain fragmented bioclastic material, including tubular foraminifera and brachiopod and echinoderm fragments. Zone B on the western flank is markedly different from Zone B on the eastern flank. On the western flank of the bioherm a greater percentage of the Chaetetid heads are reworked (Figures 3.31 and 3.35). Articulated brachiopods are still present above the Chaetetid heads. At the very edge of the western flank, Chaetetids are no longer present. Average overall grain size is much smaller (sand sized) and is much more well sorted. Grainy laminations are common within this flank. Chaetetid heads are rare in the eastern flank of the bioherm. The dominant biota are tubular foraminifera and brachiopods. The sediments contain large (several cm diameter) burrows (Figure 3.36).

The upper surface of the bioherm, near the core, is fissured (Figures 3.29 and 3.31). The fissures are filled in by light gray to tan carbonate sand and mud sized sediments. Conglomerate clasts are seen overlying the far eastern flank.

Zonation of Lithofacies within Other Bioherms

The distribution of rock types and fauna described in Bioherm H appears to be true for the majority of the bioherms in the study area, including the largest, Bioherm P (Figures 3.37 and 3.38). Within Bioherm P, as in all other bioherms, Zone A is made up primarily of reworked tubular foraminifera and brachiopods, as well as crinoid columnals (Figures 3.37 and 3.38). Bioherm P is unique in displaying



Figure 3.35 - Overturned Chaetetid heads on the western flank of Bioherm H, Zone B (approximately 5.5 m). Note the orientation of growth lines within the Chaetetids.

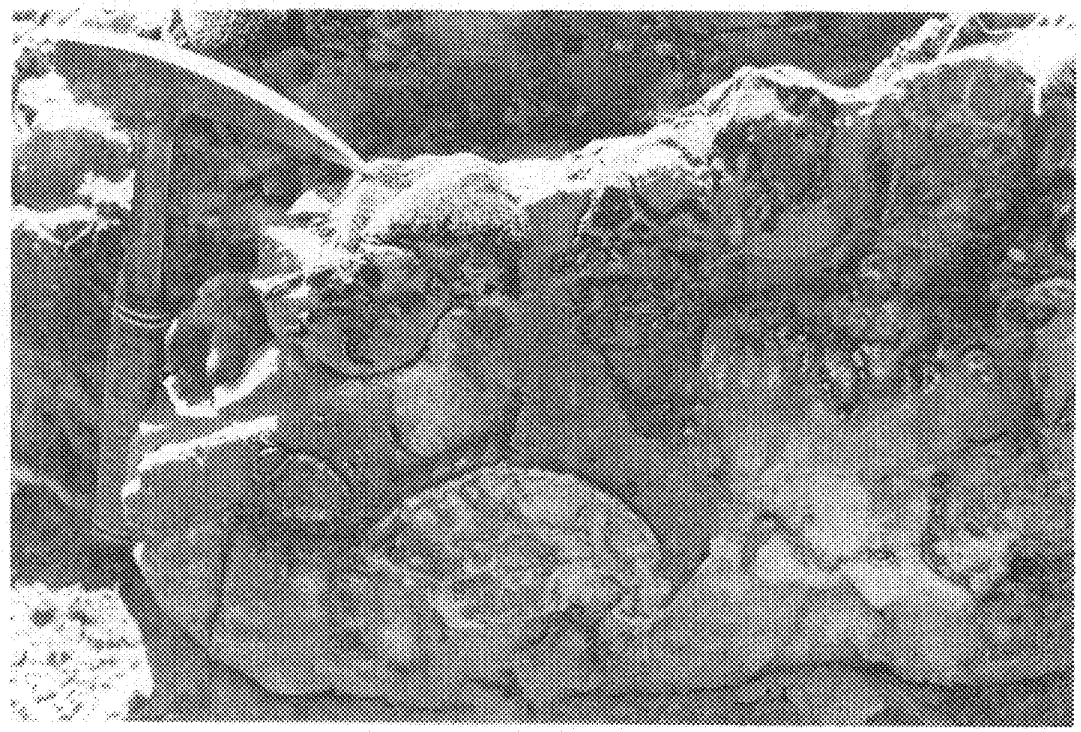


Figure 3.35 - Overturned Chaetetid heads on the western flank of Bioherm H, Zone B (approximately 5.5 m). Note the orientation of growth lines within the Chaetetids.

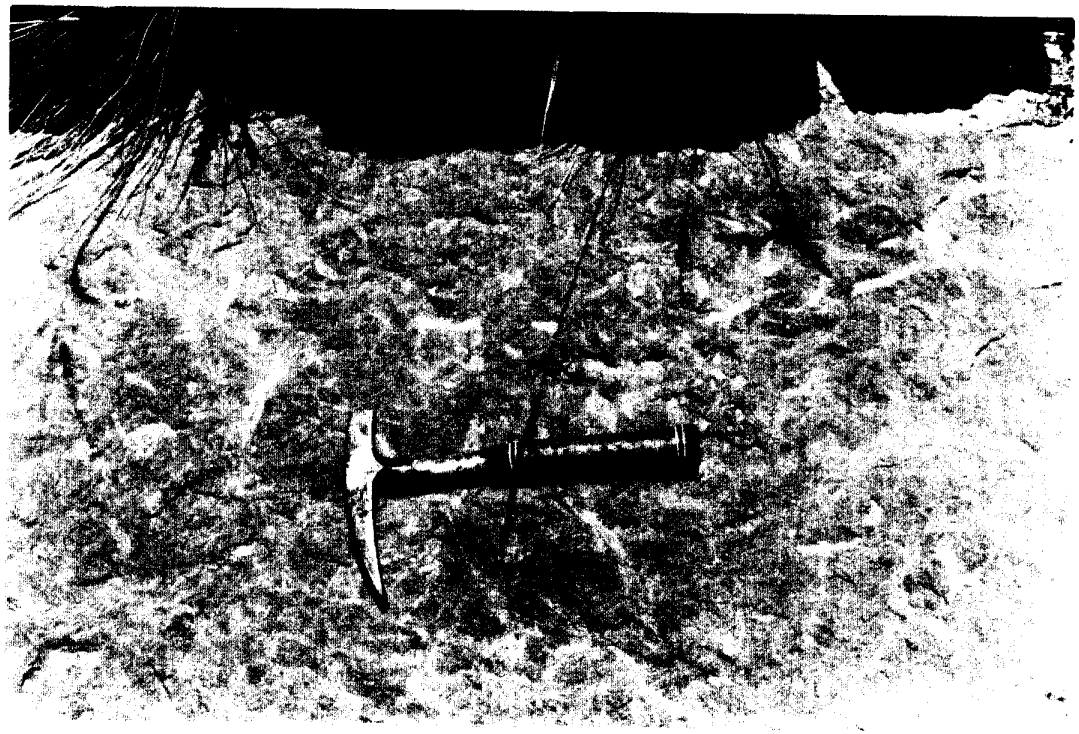


Figure 3.36 - Plan view of a bioclastic pack- to grainstone within Zone B containing large burrows (Section H, 15.8 m).

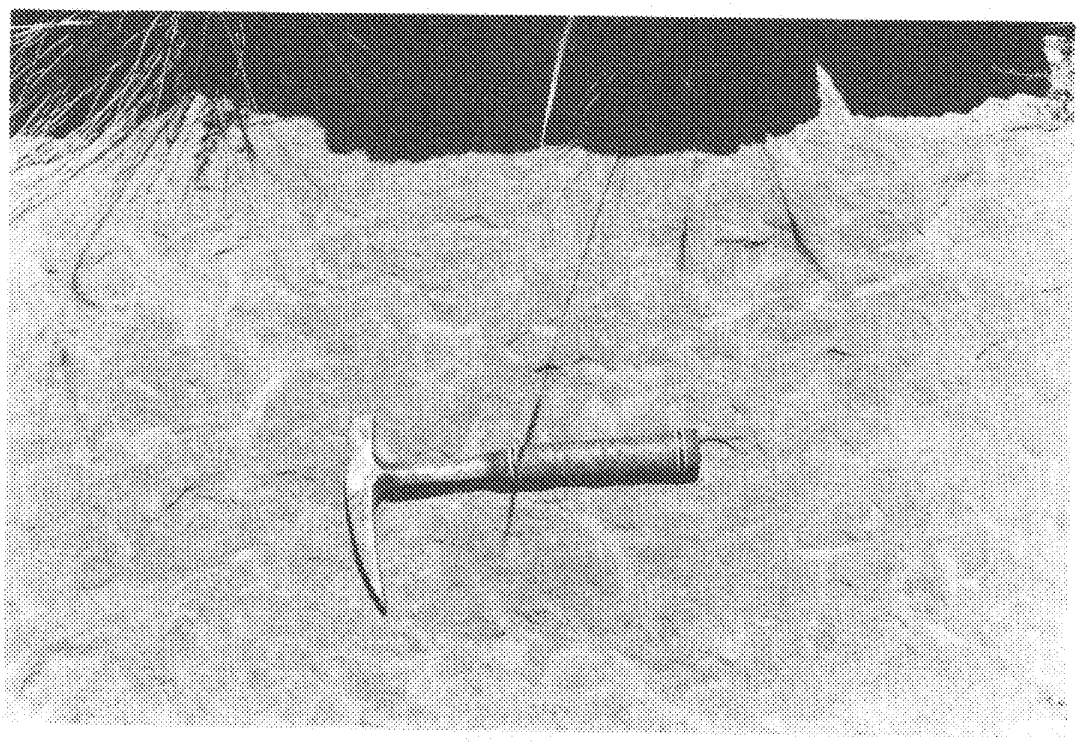


Figure 3.36 - Plan view of a bioclastic pack- to grainstone within Zone B containing large burrows (Section H, 15.8 m).

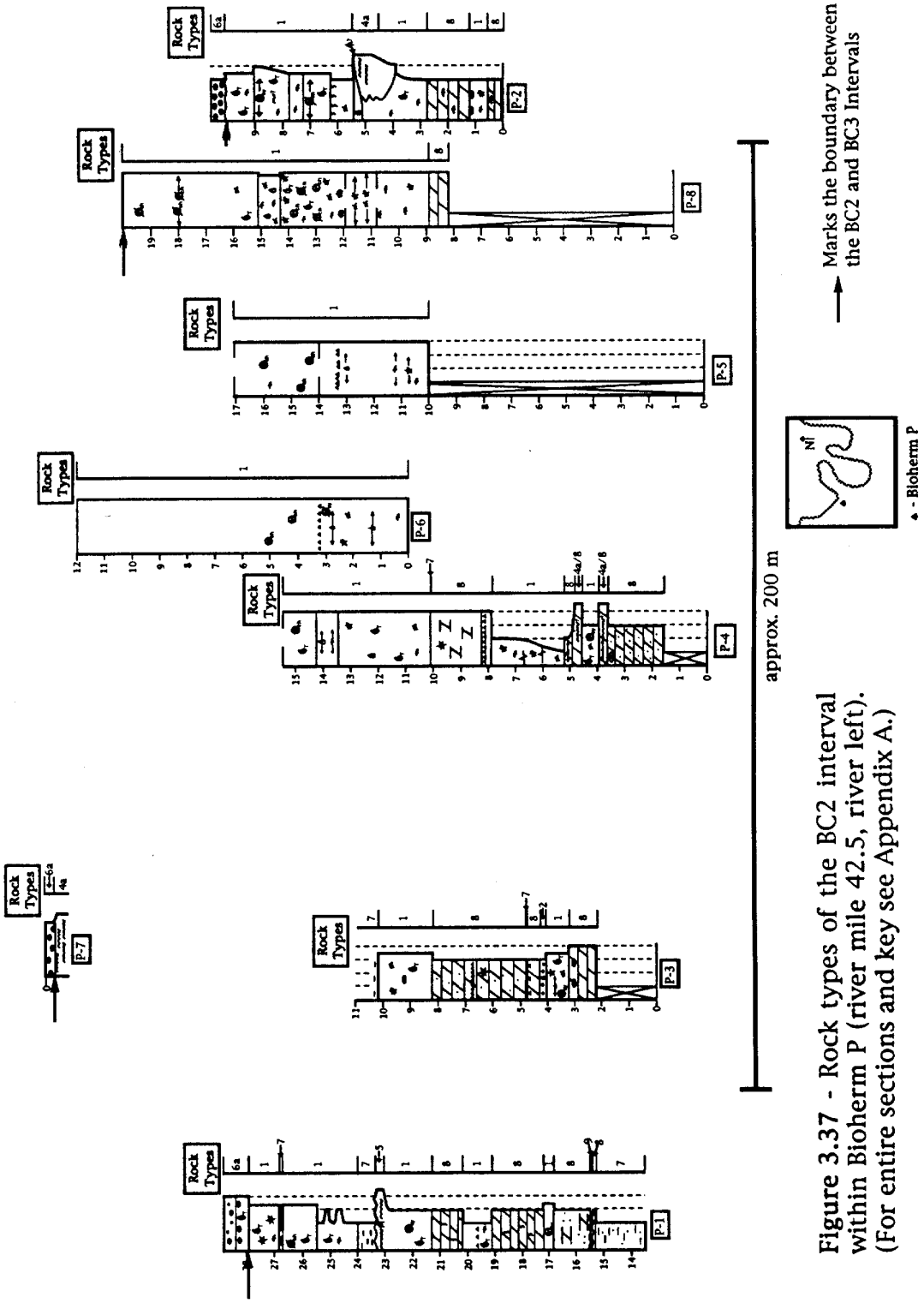


Figure 3.37 - Rock types of the BC2 interval within Bioherm P (river mile 42.5, river left). (For entire sections and key see Appendix A.)

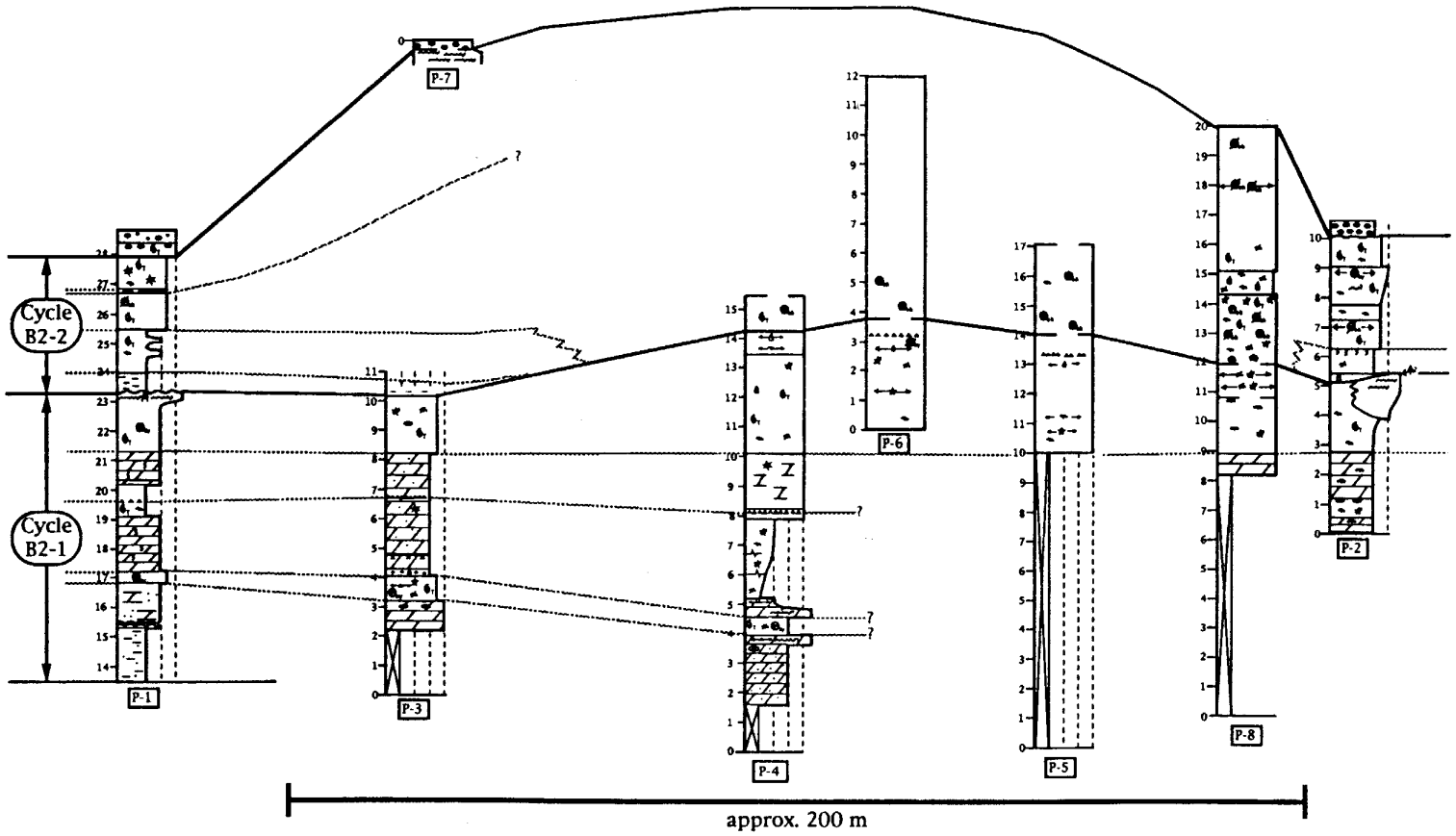


Figure 3.38 - Cycles in the BC2 interval, seen in relation to Bioherm P (river mile 42.5, river left). Correlation lines and cycle boundaries are shown dashed where inferred. Datum is the top of the uppermost dolostone. (For entire sections and key see Appendix A.)

cross bedding within this zone (Figure 3.5). No stromatolites are seen at the top of Zone A in the core of Bioherm P, but algal bumps and an algal laminite are seen at the upper surface of this zone on the southeastern flank (Figures 3.10 and 3.11), and silicified algal structures are seen on the northwestern flank (Figure 3.12). Root-like structures are found at the top of Zone A in Section P-2 (Figure 3.27).

A greenish siltstone is found forming the recessive at the base of Zone B on the southeastern flank of Bioherm P (Figures 3.19, 3.37, and 3.38). The recessive thins to zero within the core of the bioherm (Figures 3.20, 3.37, and 3.38). Here the contact between Zones A and B is represented by a continuous stylolite. In other bioherms, the recessive may be formed by a combination of mud-rich carbonates (Section D), silty carbonates (Sections C and G-1), or conglomeratic units (Sections F and G-1) (Figure 3.1).

Zone B contains Chaetetids in all bioherms in the study area. The other biota found in this zone likewise resembles that found in Bioherm H. In Bioherm P, Chaetetids are seen within the core of the bioherm, as well as in the northwestern flank (Figures 3.37 and 3.38). Clasts of Chaetetids can be traced up to 500 m away from Bioherm P to the northwest. Only one reworked Chaetetid head is seen to the southeast of the core however (Section P-1) (Figure 3.2). Stromatolites are found around Chaetetid heads in Bioherm S as well as H (Figure 3.14). Algal structures not associated with Chaetetids are present in Bioherms F, M, and P (Figures 3.13, 3.15, and 3.39). The top of Zone B is marked by conglomerates in the majority of bioherms in the study area (see Conglomeratic Rock Type, BC2 interval).

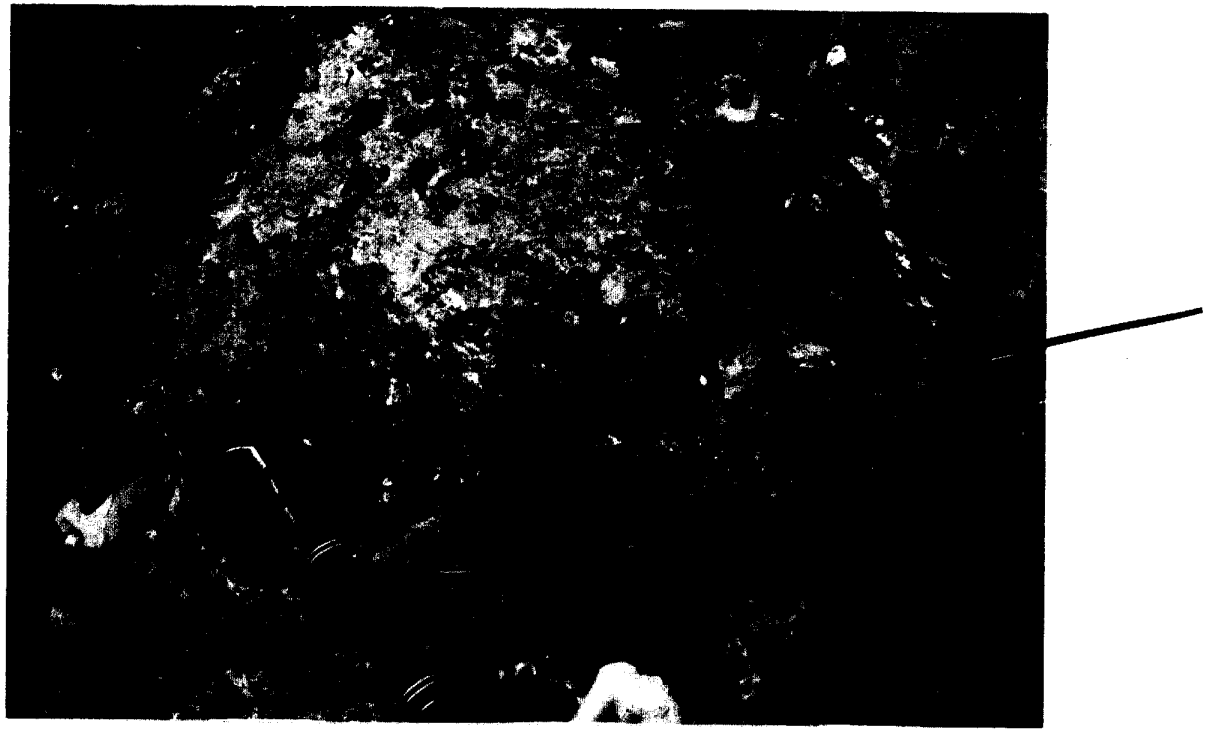


Figure 3.39 - Dark algal (?) structures at the top of Bioherm P (Section P-7, 0.0 m). The algal structures can be seen in the right hand side of the photo. Tan sediments are seen filling in fissures in the algal structures (arrow).

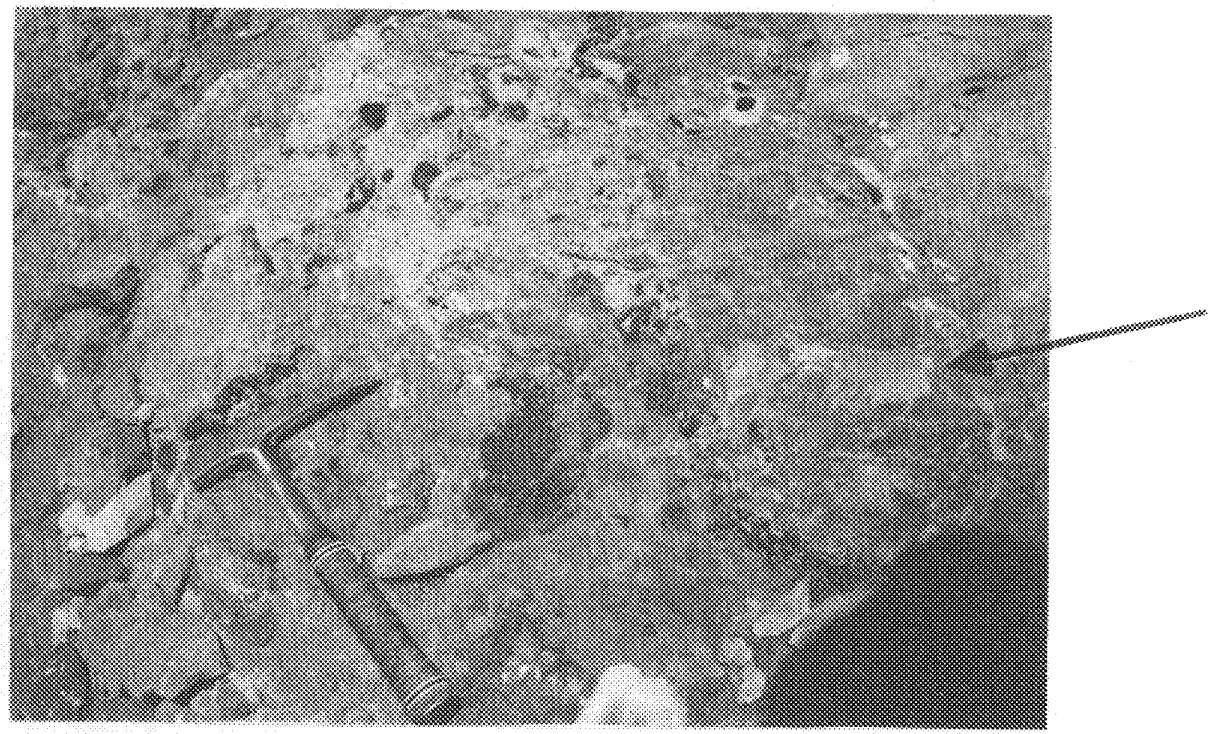


Figure 3.39 - Dark algal (?) structures at the top of Bioherm P (Section P-7, 0.0 m). The algal structures can be seen in the right hand side of the photo. Tan sediments are seen filling in fissures in the algal structures (arrow).

Fissures found at the top of Bioherm P are especially similar to those seen at the top of Bioherm H (compare Figure 3.29 with Figure 3.39).

Geometry and Distribution of Bioherms

The distribution of outcrops of Middle Creek bioherms is shown in Figure 3.30. Strike and dip measurements were taken on the flanks of five of these bioherms (Bioherms B, D, F, M and P) in an attempt to understand the geometries in three dimensions (Table 3.3). The measurements were taken on the upper surfaces of both Zones A and B. The strike and dip data was difficult to collect because of the low angles involved, and because the erosional relief on the surface of any one bed was almost as great as the angle at which the surface was dipping.

The bioherms generally show low angles of relief. When one looks at the direction of dip on the flanks of Bioherms B, F, M, and P, it is seen that they all dip down and away from the outcrop. This indicates that the core of these bioherms, the thickest portion, is further back in the cliff. This is true for even the two largest bioherms in the study area, Bioherms M and P. Of these four bioherms, three have smaller bioherms located opposite the river from them. It is therefore quite likely these pairs, Bioherms B and B', Bioherms P and A, and Bioherms F and D, are each separate exposures of one bioherm.

The beds within Zones A and B are seen to thicken within bioherms. An isopach map showing the thickness of the mounds within Zone A is shown in Figure 3.40. Bioherms S and L are not

Bioherm	Strikes and Dips		Average	Corrected
B	Eastern Flank:	N 11 E, 11°SE N 21 W, 22°NE N 24 W, 26°NE N 42 W, 11°NE	N11W, 16°NE	N12W, 14°NE
	Western Flank:	N 41 W, 9°NE N 72 W, 22°NE	N62W, 12°NE	N72W, 12°NE
D	Northern Flank:	*N 10 W, 19°NE*	N10W, 19°NE	N10W, 13°NE
F	Northern Flank:	N11W, 12°NE N 21 W, 13°NE N 40 W, 24°NE	N22W, 16°NE	N26W, 13°NE
	Southern Flank:	N 59 E, 24°NW N 88 E, 14°NW N 69 W, 20°SW	N84E, 18°NW	N74E, 18°NW
M	Northern Flank:	N 52 E, 15°NW N 67 E, 7°NW N 85 E, 9°NW N 64 W, 13°NE	N74E, 11°NW	N66E, 12°NW
	Southern Flank:	N 4 E, 12°SE N 28 E, 17°SE N 30 E, 20°SE N 33 E, 18°SE N 49 E, 19°SE	N31E, 16°SE	N36E, 14°SE
P	Eastern Flank:	N 42 W, 16°NE N 51 W, 25°NE	N48W, 20°NE	N52W, 18°NE
	Western Flank:	*N 8 E, 19°NW* *N 70 W, 4°NE* *N 73 W, 19°SW* N 13 E, 9°NW N 38 E, 5°NW N 44 E, 8°NW N 75 W, 13°SW	N3W, 6°SW	N5W, 8°SW

Table 3.3 - Strike and Dip measurements from the flanks of bioherms. Data in italics were taken at the top of Zone A. Data in normal print were taken at the top of Zone B. Average strike and dips were found by plotting the raw data for each flank on a stereonet and visually determining the location of the average. Numbers in the "Corrected" column are the average values corrected for a regional structural dip of N4W, 1.6°NE.

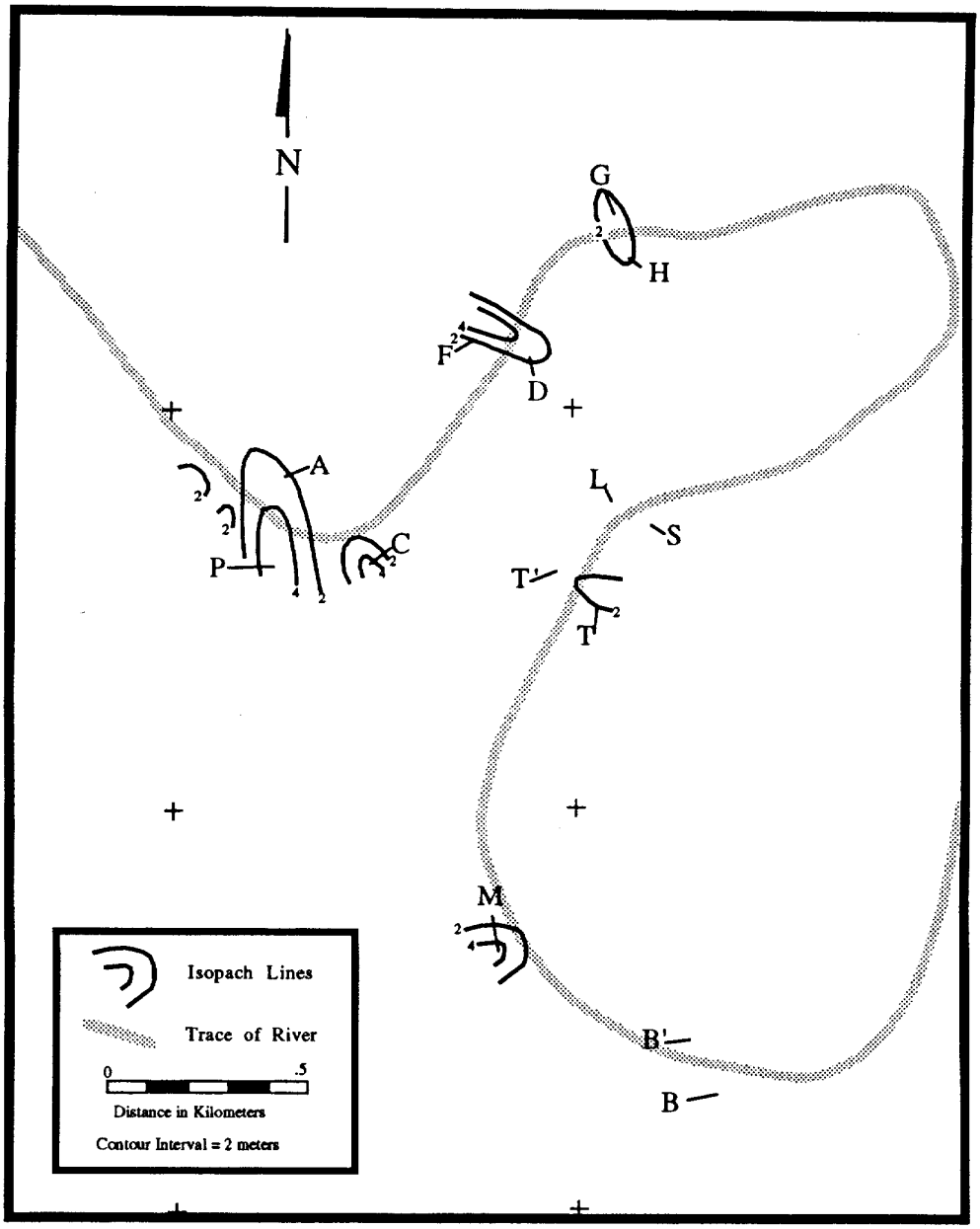


Figure 3.40 - Isopach map showing thickness of Zone A. The isopach lines are spaced at intervals of 2 m. Data on the thickness of Bed A within Bioherm B is not known. Bed A is under river level in Bioherms S and L. Compare with Figure 3.30.

shown because Zone A was under river level at both of these locations. Bioherm B is not shown because the thickness of Bed A in this location is unknown. An isopach map showing the total thickness of bioherms (the thickness of Zone A plus Zone B) is shown in Figure 3.41. It can be seen when comparing these two figures that mounds in Zone B formed only above mounds in Zone A. This implies that the mounds within Zone A controlled the location of formation of mounds in Zone B, and therefore the location of Chaetetid growth.

Figure 3.42 combines strike and dip information (Table 3.3) with information from the isopach maps (Figures 3.40 and 3.41) to recreate how the bioherms may have been arranged in the study area. Where the margin of a bioherm is unknown (i.e. within a cliff) it is drawn with a dotted line. With a lack of information on whether the bioherms were asymmetrical or not, they have all been drawn roughly concentric.

Bioherms are seen to be elongated, oriented along a northwest-southeastern trend, between N10°W and N60°W (Figure 3.42). The presence of broken and reworked Chaetetid heads on the northwestern flanks of Bioherms H and P suggest that wave and or tidal currents were coming from the northwest.

Growth History of Bioherms in the BC2 Interval

Zone A beds within the bioherms in the BC2 interval formed quite differently than Zone B beds. Beds within Zone A contain sedimentary structures which suggest accumulation in a high energy environment. These structures, including cross-bedding, oolitic

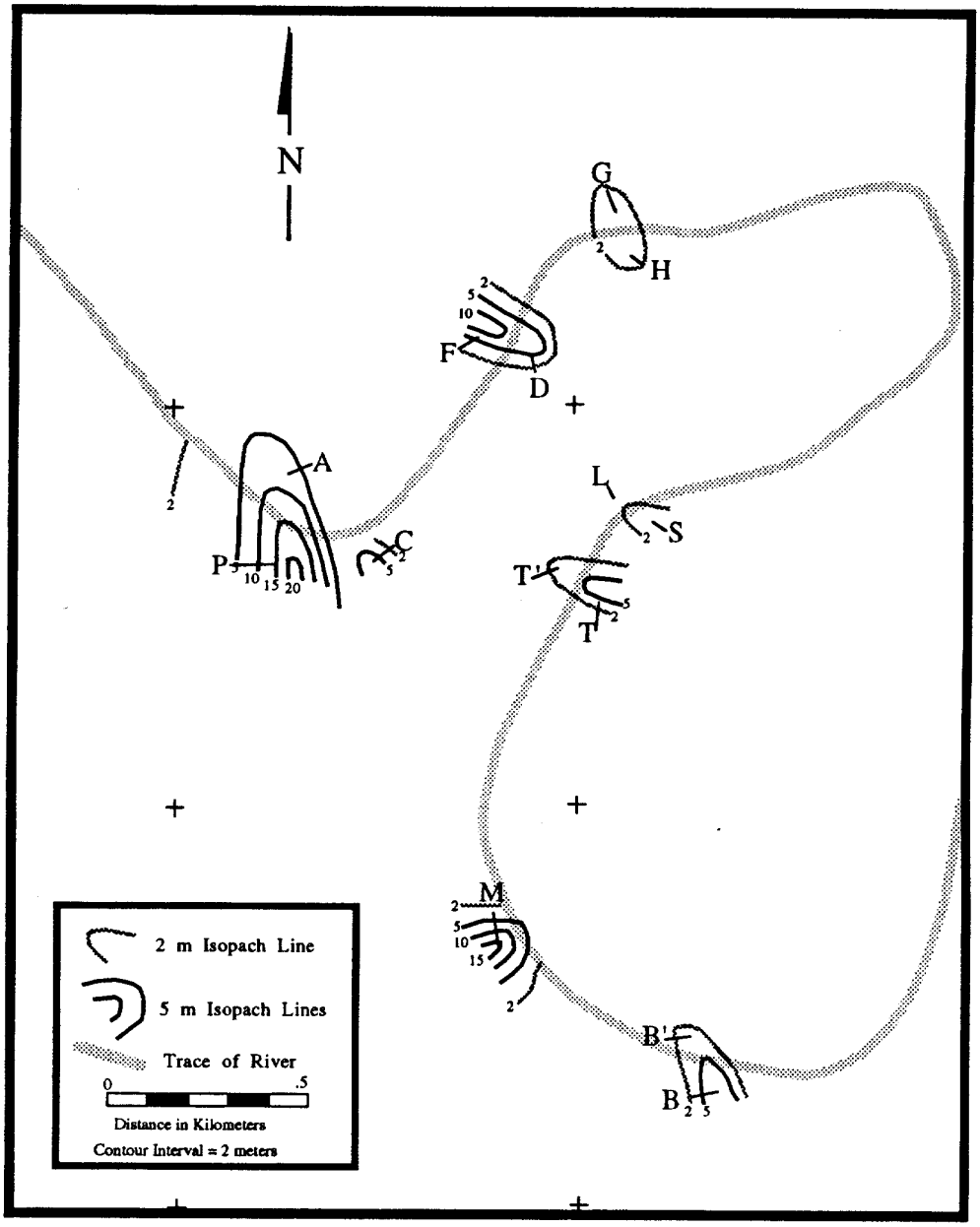


Figure 3.41 - Isopach map showing bioherm thickness. Dashed lines represent a thickness of 2 m. Solid lines are spaced every 5 m. Compare with Figure 3.30.

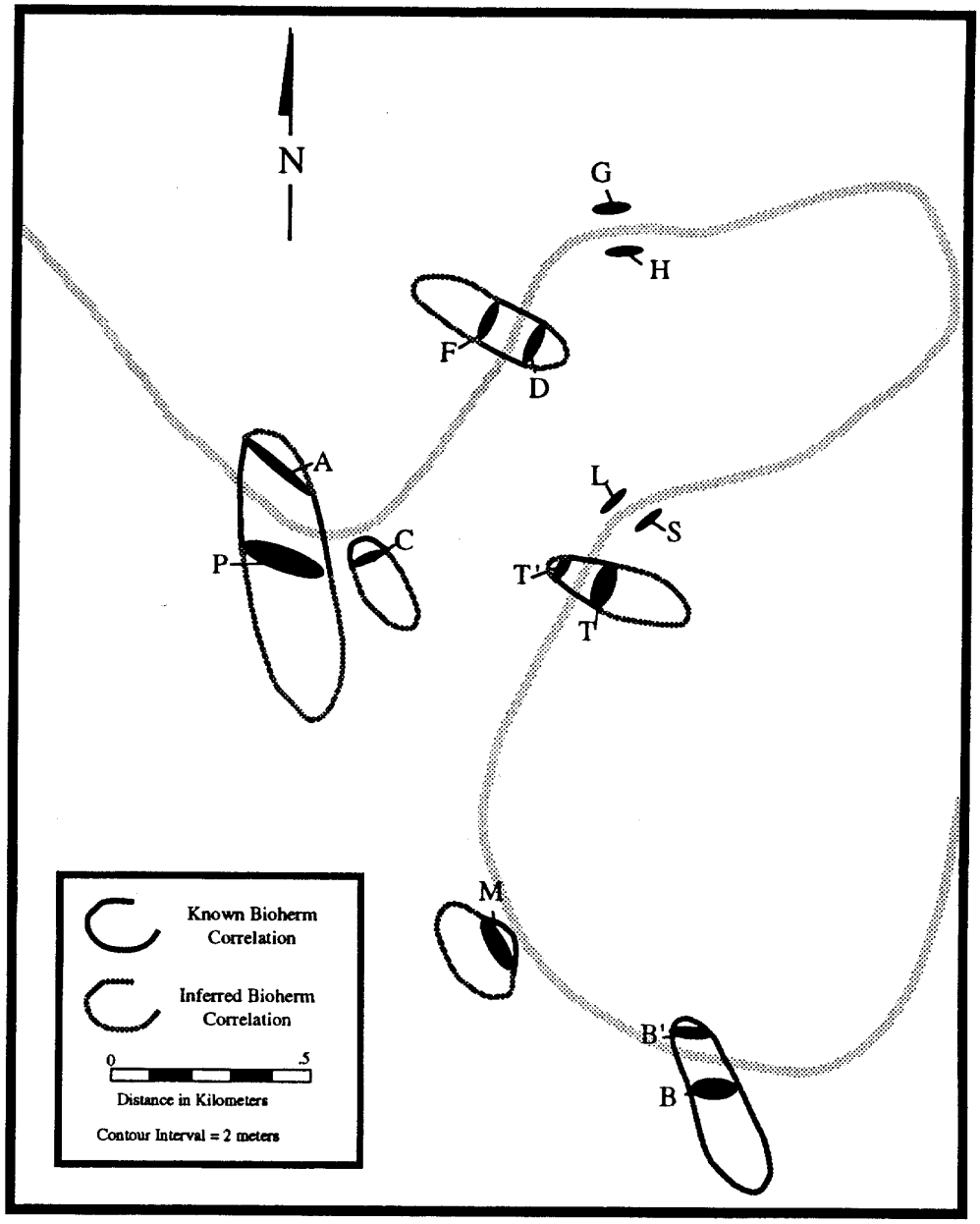


Figure 3.42 - Diagram interpreting the possible distribution and orientation of bioherms within the study area. Compare with Figure 3.30.

coatings around grains, and grainy laminations, suggests that the mounds are mechanically produced shoals. Considering the abundance of reworked normal marine fauna found within these shoal-like bodies, it can be concluded that they formed in a freely circulating shallow marine shelf. These conditions became more restricted during the later deposition of Zone A. Evidence of this change is seen in the appearance of stromatolites, algal mats, and oncolites (Figures 3.1, 3.2, 3.37, 3.38, and 3.31). The restriction was most likely associated with a drop in relative sea level, as evidenced by exposure surfaces marked by conglomerates, rhizoliths, and possible paleosols seen in the study area (Figures 3.25, 3.26, and 3.38).

Relative sea level rose once again, and normal marine conditions were resumed, as indicated by the diverse fauna found within Zone B. The mounds within Zone B are clearly biologically produced, as evidenced by the presence of large frame-producing Chaetetid heads and encrusting foraminifera. Growth of Zone B mounds occurs only above the Zone A mounds. This suggests that the minor paleo-relief of the Zone A mounds (1 to 3 meters) was enough initiate growth of Zone B mounds. This seemingly insignificant topography provided enough sunlight, current activity, or nutrient input for Chaetetids to grow and provide a stable framework for the rest of the mound fauna. Towards the end of Zone B restriction of the environment occurred again, and stromatolites and algal mats appeared. Conglomerates, fissures, and rhizoliths mark the upper surface of Zone B, indicating that exposure was the end result of the relative sea level change.

Chapter 4

BC3 and Akah Intervals

- INTRODUCTION -

The BC3 interval is present in eight measured sections: Sections P-1, P-2, P-7, A-1, C, D, G-2, and M-2. It ranges in thickness from 2.8 m (Section P-7) to approximately 9 m (Section G-2). This range in thickness is due to the BC3 beds filling in relief created by bioherms in the BC2 interval. The BC3 interval is thickest in a between-bioherm position and thinnest directly over a bioherm. The base of this interval is a relatively thick (10 cm to 1.14 m) conglomerate found draping the BC2 bioherms, and the top is defined as the base of the black shale which separates the Barker Creek and Akah. Where there is more than one black shale (Sections P-1 and P-7) the lowest black shale is considered to be the boundary.

Because the emphasis of this study was rocks within the Barker Creek, detailed sections through the Akah were rarely made. The distance from the top of the exposed Barker Creek to one of two key beds in the Akah was measured, to provide a datum when correlating measured sections. These two key beds are the black shale that marks the base of the Akah (which is often covered), and a distinctive framestone referred to as the continuous digitate bed or "CDB". Only four sections include detailed information about rocks found in the

Akah. Three of these sections (Sections P-1, P-2, and P-3) are within approximately 200 meters of each other. The fourth section (Section M-2) is located 1.1 km away.

The BC3 interval and the Akah intervals are discussed together because the stratigraphic boundary (the black shale) between them does not correspond to a cycle boundary. The location of sections and distribution of rock types is illustrated in Figure 4.1. The abundance of different rock types within the BC3 and Akah intervals in Section P-1, and the thickness of beds of each rock type within this section, are displayed in Table 4.1.

- ROCK TYPES IN THE BC3 AND AKAH INTERVALS -

Bioclastic Limestone Rock Type

(Sections A-1, C, D, G-2, M-2, P-1, P-2, and P-7)

The bioclastic beds found in the BC3 and Akah intervals generally contain more quartz silt or fine sand and are more poorly sorted than those in the BC1 and BC2 intervals (Table 4.1). Individual beds range in thickness from 10 cm to 1.22 m thick. Common fossils found in these beds include tubular foraminifera (coarse sand sized) and whole and fragmented brachiopods (very coarse sand to pebble sized). Other fossils include crinoid fragments (coarse to very coarse sand sized), *Syringipora* (coarse sand to granule sized), and fossil hash (medium to coarse sand sized). An unusual segmented algal (?) form is found within the BC3 interval at 31.8 m in Section P-1 (Figure 4.2). A digitate frame-builder is found within the "CDB" in the Akah. The

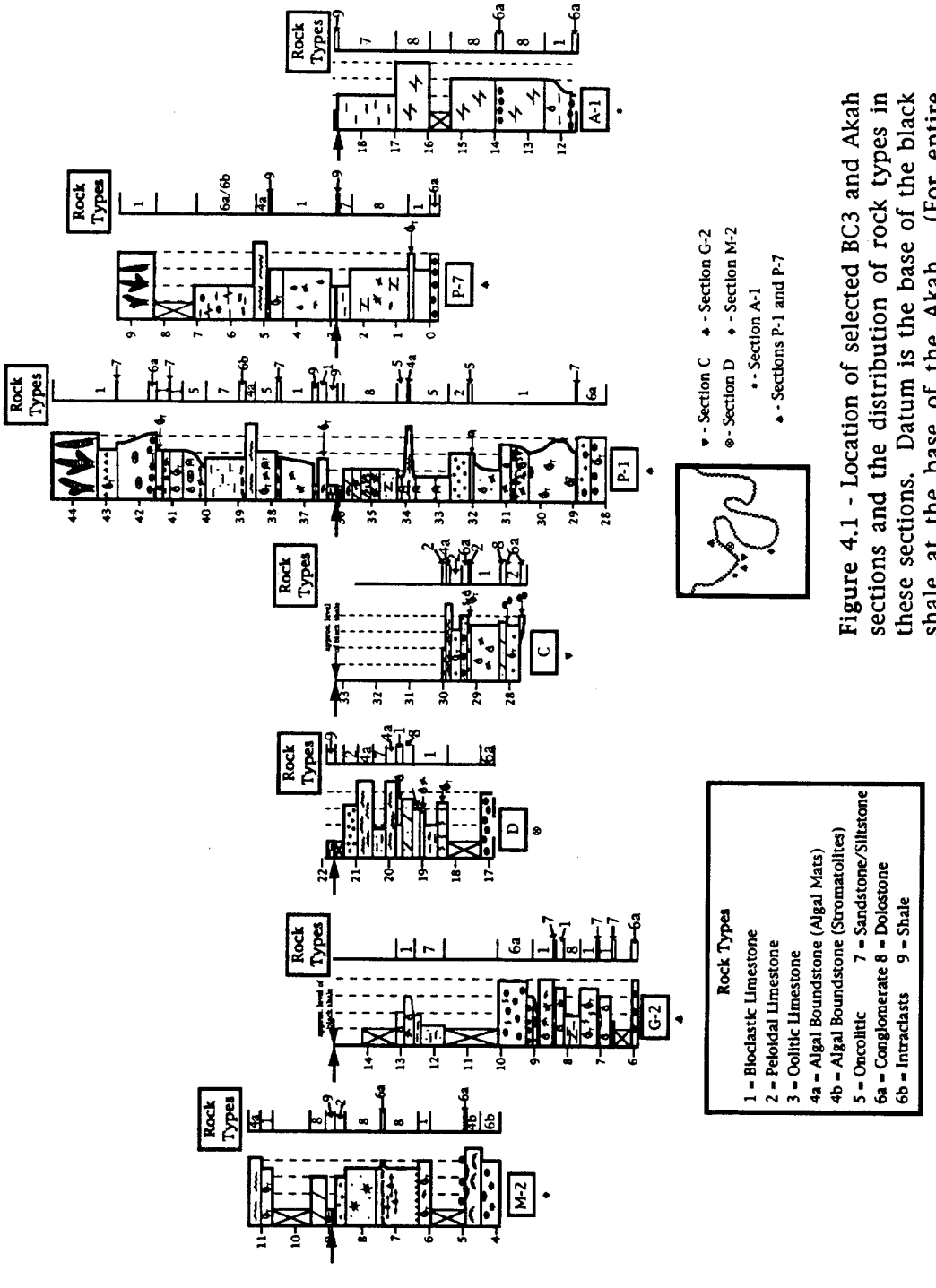


Figure 4.1 - Location of selected BC3 and Akah sections and the distribution of rock types in these sections. Datum is the base of the black shale at the base of the Akah. (For entire sections and key see Appendix A.)

Rock Type	Number of Beds	Total Thickness (in meters)	Percentage of Section (Thickness)	Minimum Bed Thickness (in meters)	Average Bed Thickness (in meters)	Maximum Bed Thickness (in meters)
Bioclastic Limestone (1)	11	7.13	45.04	0.23	0.64	1.07
Peloidal Limestone (2)	1	0.46	2.91	-	0.46	-
Oolitic Limestone (3)	0	0	0	-	0	-
Algal Boundstone (Algal Mat) (4a)	1	0.23	1.45	-	0.23	-
Algal Boundstone (Stromatolitic Heads) (4b)	0	0	0	-	0	-
Oncolitic (5)	4	2.96	18.70	0.15	0.74	1.68
Clastic (Conglomerates) (6a)	3	1.34	8.46	0.20	0.45	0.61
Clastic (Intraclasts) (6b)	1	0.10	0.63	-	0	-
Fine Sandstone/ Siltstone (7)	4	1.70	10.74	0.10	0.43	1.35
Dolostone (8)	2	1.53	9.67	0.46	0.77	1.07
Black Shale (9)	2	0.38	2.40	0.15	0.19	0.23
Total:	29	15.83				

Table 4.1 - Relative abundance of rock types in the BC3 and Akah intervals. Data from Section P-1.

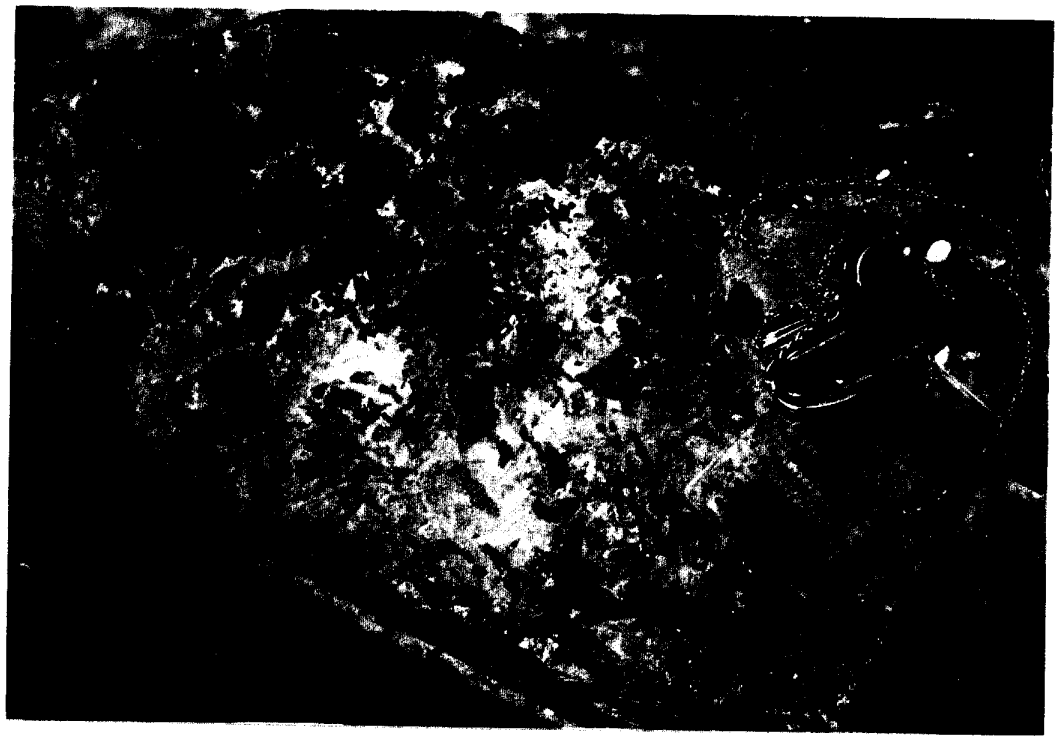


Figure 4.2 - Articulated algae-like structures (Section P-1, 31.8 m).

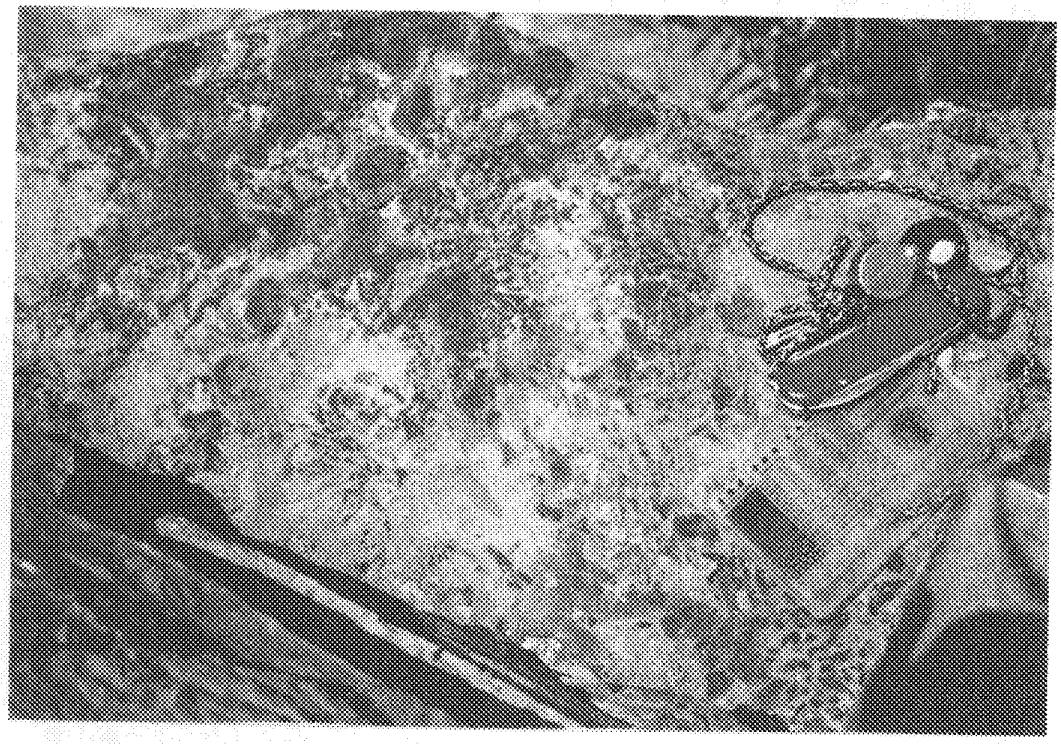


Figure 4.2 - Articulated algae-like structures (Section P-1, 31.8 m).

identity of this organism is not known. It is dark gray in color, with pronounced growth lines as well as septa-like structures. It is uncertain whether this organism is a type of coral or even a variety of sponge (the internal texture is similar to Chaetetid sclerosponges). Fossil material in both intervals is commonly fragmented and reworked. Sorting is moderate to poor.

The majority of bioclastic limestone beds in the BC3 and Akah intervals are grain-supported, indicating that reworking and fragmentation of skeletal material during high energy events, such as storms, was common in the area of deposition. The package of grain-supported rocks is thicker in between-bioherm positions than in above-bioherm positions. This suggests that current activity was strong in a between-bioherm position. As material accumulated in this position and the topography leveled out, lower-energy environments dominated as evidenced by the appearance of matrix-supported units (Figure 4.1).

Peloidal Limestone Rock Type

(Sections C, D, M-2, and P-1)

Peloidal packstones are found only in the BC3 interval. These beds range in thickness from 10 to 46 cm (Figure 4.1). They do not appear to correlate between sections. Fine sand sized fossil grains include tubular foraminifera and unidentifiable fossil hash. The packstones are moderately to well sorted. The porosity within these beds is poor. The uppermost peloidal packstone at Section C (at 29.15 m) contains fine burrows. The lower half of the packstone at Section

P-1 contains fine laminations. There are no other sedimentary structures within the peloidal packstone beds.

These peloidal packstones are very similar to those in the BC1. Like those packstones, these are interpreted to have been deposited in a shallow, normal marine protected shelf.

Algal Boundstone Rock Type

(Sections C, D, M-2, P-1, P-2, and P-7)

Algal laminites (Rock Type 4a) are common within the BC3 and Akah intervals. They have very little relief, and in the field grade both laterally and vertically into structure-less mudstones. No grains larger than mud-sized are seen trapped within the algal mats within the BC3 interval. One algal boundstone can be correlated between all four sections in the Akah. This bed ranges in thickness from 23-60 cm. Mud is the dominant grain size, but some grainy laminae are trapped within the muddy algal matrix. Fenestral porosity is seen within this algal laminite in Section P-7, and in the upper laminite within the BC3 interval in Section D.

One stromatolitic bed (Rock Type 4b) is present between two conglomerates in Section M-2. The stromatolites in this bed are dark gray to black in color. They are hemispherical in shape (suggesting a stromatoform relationship) and 20 to 30 cm in diameter. The domed heads are surrounded by a wackestone to packstone containing very small articulated, in place brachiopods or ostracodes (2-3 mm in diameter). The upper surface of the wackestone/packstone is

fractured, and the fractures are filled in with a poorly sorted conglomerate.

The large amount of mud present in these rocks suggests that they were deposited in a predominantly quiet environment. The fissured surface at the top of the stromatolite bed (Section M-2) indicates that a period of shallow marine deposition was followed by subaerial exposure. The presence of fenestrae in Sections D and P-7 indicates that, at least in these two locations, deposition occurred in an intertidal or supratidal setting.

Oncolitic Rock Type

(Sections P-1 and P-2)

Four distinct oncolite layers are present in the BC3 interval within two wackestones to packstones in Section P-1 (between 31.9 and 34.2 m above river level) (Figures 4.1 and 4.3). The oncolites are from approximately 0.5 to 2 cm in diameter, and have irregular, but roughly concentric laminations. They are very dark gray to almost black in color. They are disk to bladed in shape (Zingg, 1935 classification) with irregular outlines, often oval or pear-shaped. The long axes of the oncolites are parallel to bedding. The cores of these oncolites, where visible, are either lithoclasts or masses of calcite spar. The oncolites are found within a poorly sorted matrix, which also makes up the rock between the oncolite layers. The grains found within the matrix appear to be made up of the same algal material that makes up the oncolites (Figure 4.3). They are fine to medium sand sized. It is unclear whether these grains are primary algal

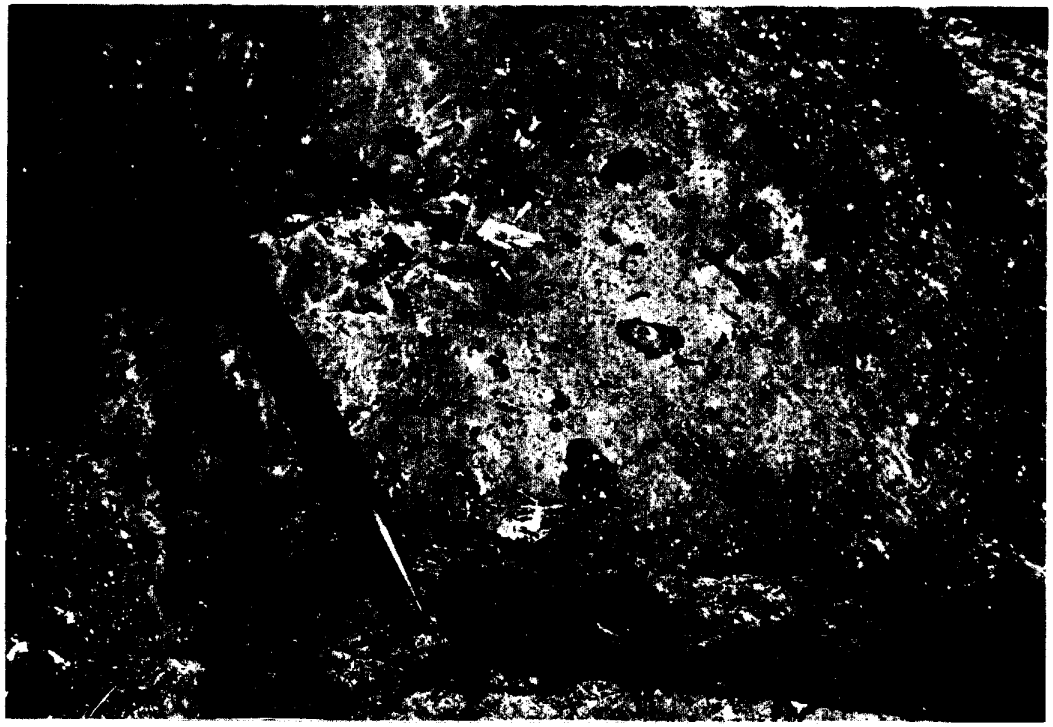


Figure 4.3 - Oncoids in a poorly sorted clastic limestone matrix (Section P-1, 33.0 m). The majority of the clasts appear to be reworked oncoid material.

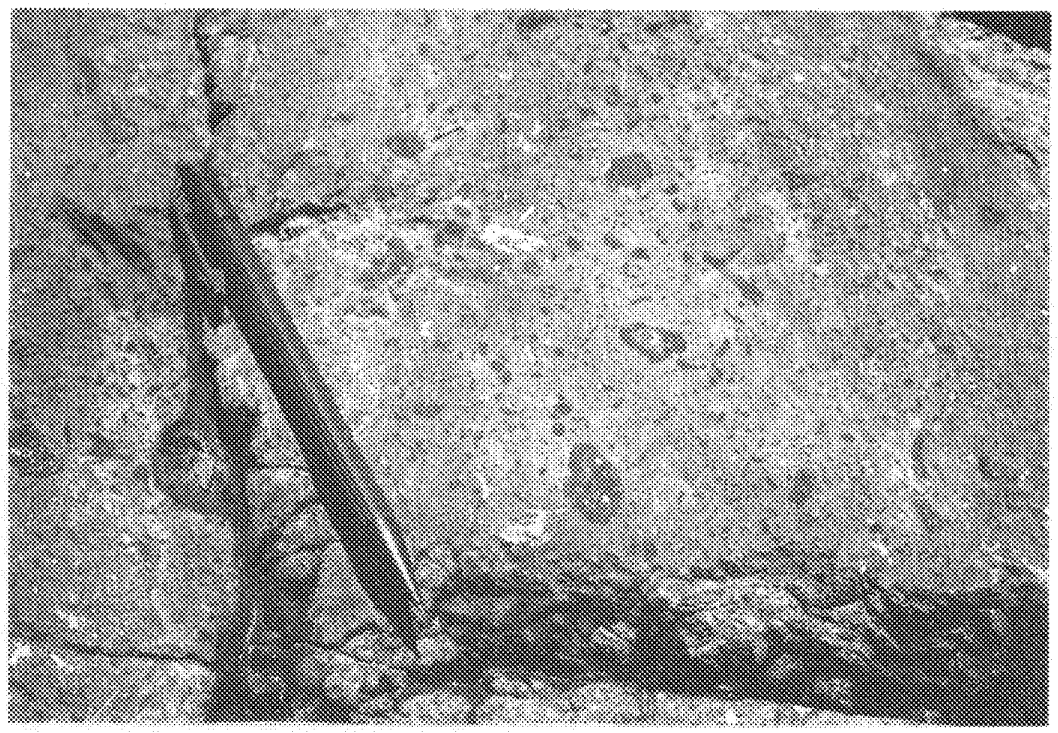


Figure 4.3 - Oncoids in a poorly sorted clastic limestone matrix (Section P-1, 33.0 m). The majority of the clasts appear to be reworked oncoid material.

structures or are oncoids which have been reworked and eroded. The presence of oncolites with semi-concentric laminations, in combination with fine grains which appear to be fragmented oncolites, suggests deposition in a turbulent marine environment.

Three oncoid-containing beds are found in Sections P-1 and P-2 in the Akah, ranging in thickness from 46 cm to 1.0 m. The beds do not appear to correlate between sections. The oncoids are found in bioclastic wackestones to packstones. Fossil grains, ranging from fine to very coarse sand sized, include tubular foraminifera, brachiopod fragments, and fossil hash. Grainy laminations are present within these units. The oncoids measure up to 8 mm in diameter. Sorting is poor. Chert nodules are found within the two beds in Section P-1. The presence of oncoids was noted in these beds, but not the type of internal laminations. Therefore it is not clear whether these oncoids formed in a calm or agitated marine environment.

Clastic Rock Type

(Sections A-1, C, D, G-2, M-2, P-1, P-2, and P-7)

Two types of conglomerates are found in the BC3 interval: 1) those which are part of the laterally continuous conglomerate which forms the boundary between the BC2 and BC3 intervals, and 2) other discontinuous conglomeratic beds (Figure 4.1).

The conglomerate found at the base of the BC3 interval forms a thin, laterally continuous package which overlies both bioherms and equivalent inter-biohermal rocks of the BC2. It is traceable over a distance of approximately 2 km. This conglomerate, and correlative

sandstones, often overlie fissured surfaces (with only a few cm of relief) at the top of the BC2. The conglomerates are clast supported units, and thickness varies (where complete thickness can be measured) from 10 cm (Section C) to 1 m (Section M) on top of bioherms, and from 15 cm (Section G-2) to 1.06 m (Section P-1) between bioherms. The subangular to subrounded clasts within the conglomerates are either clasts of muddy limestone or chert and are characteristically dark gray to black in color. The matrix between the clasts is muddy, and is lighter in color than the clasts. Above bioherms, average clast size is generally granule to small pebble sized, but clasts may be up to 4 cm in diameter. Most clasts appear to be reworked lithic fragments, although clasts of silicified Chaetetids and other fossil grains have been seen. The clasts are generally smaller in a between-bioherm position, ranging from lower medium sand to very coarse sand to granule sized. The composition of these smaller clasts is unrecognizable in the field. Fine fossil hash is common in the mud-rich matrix of these finer grained conglomerates, which also contains fine quartz sand and silt. At Sections M-2 and P-7 the conglomerates are found filling in fractures in the underlying algal material (Figures 4.4 and 4.5). There is no apparent stratification within the conglomerates. Interpenetration of clasts is common.

Erosive surfaces are found above stromatoform growths at the top of the BC2 interval in Sections P-7 and M-2 (see Figures 3.1 and 3.25). This, in conjunction with roots, fissures, and evidence of scour at the top of the BC2 interval suggests a restriction of environment and eventual exposure. The conglomerate clasts at the base of the BC3



Figure 4.4 - Plan view of a clast supported conglomerate above a stromatolite bed (Bioherm M, 4.9 m). Clasts are medium to dark gray, are angular in shape, and are coarse sand to pebble and cobble sized. Clasts appear to be derived from the underlying bioclastic rocks.

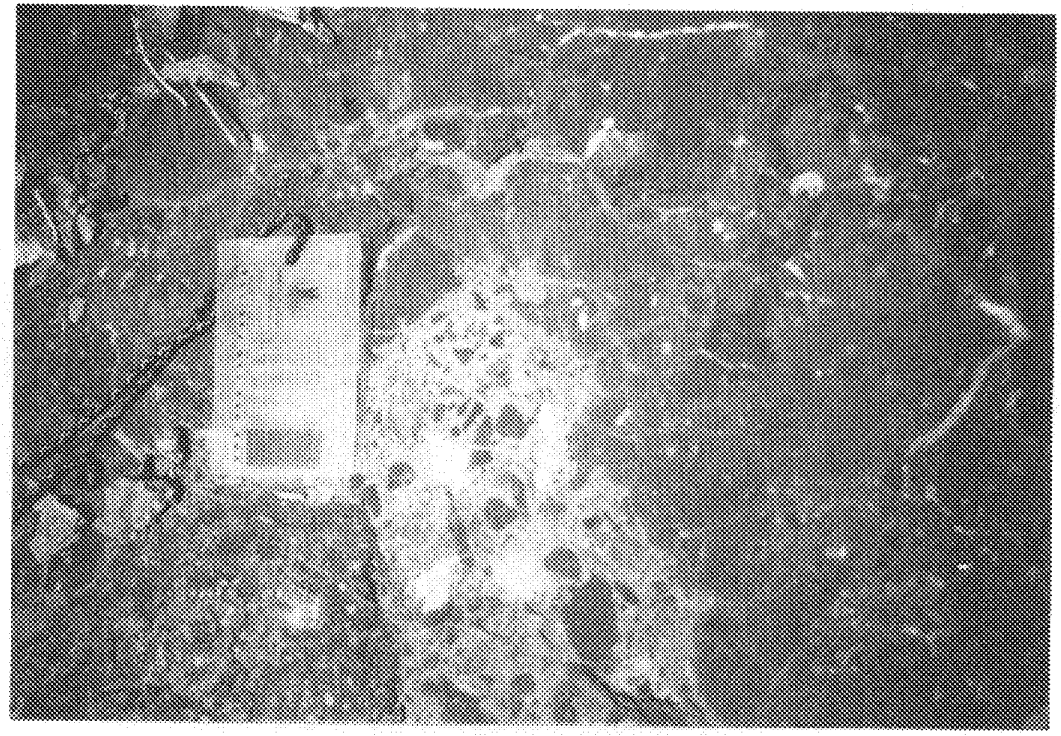


Figure 4.4 - Plan view of a clast supported conglomerate above a stromatolite bed (Bioherm M, 4.9 m). Clasts are medium to dark gray, are angular in shape, and are coarse sand to pebble and cobble sized. Clasts appear to be derived from the underlying bioclastic rocks.

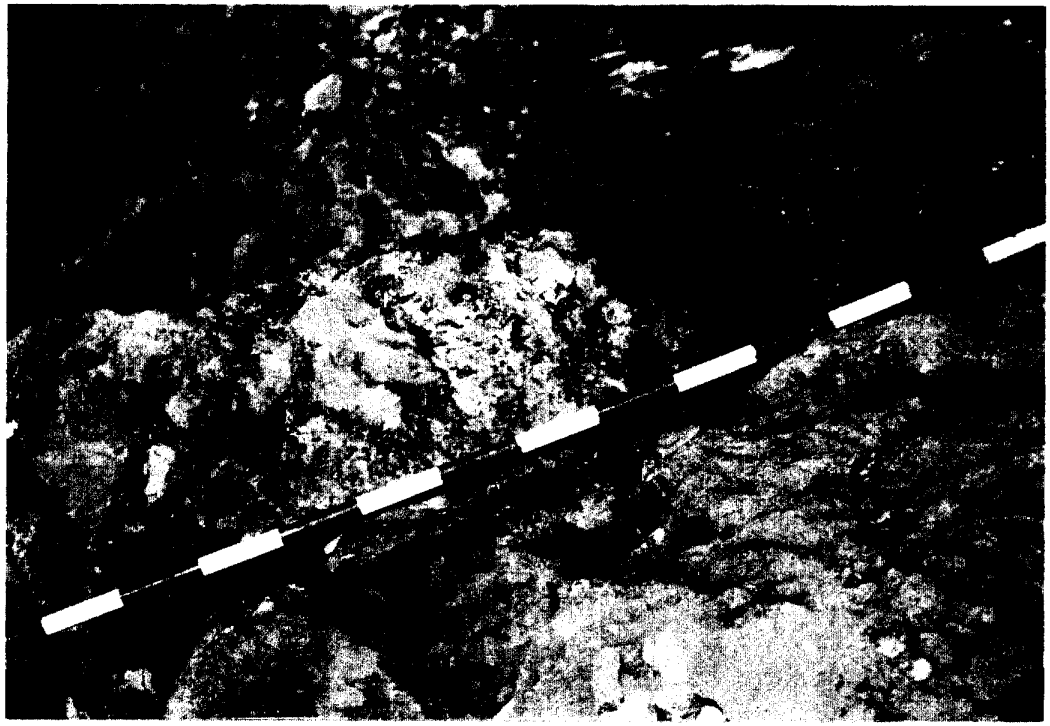


Figure 4.5 - Sandstone to fine conglomerate filling in a fissured surface at the top of Bioherm P (Section P-7, 0.0 m).

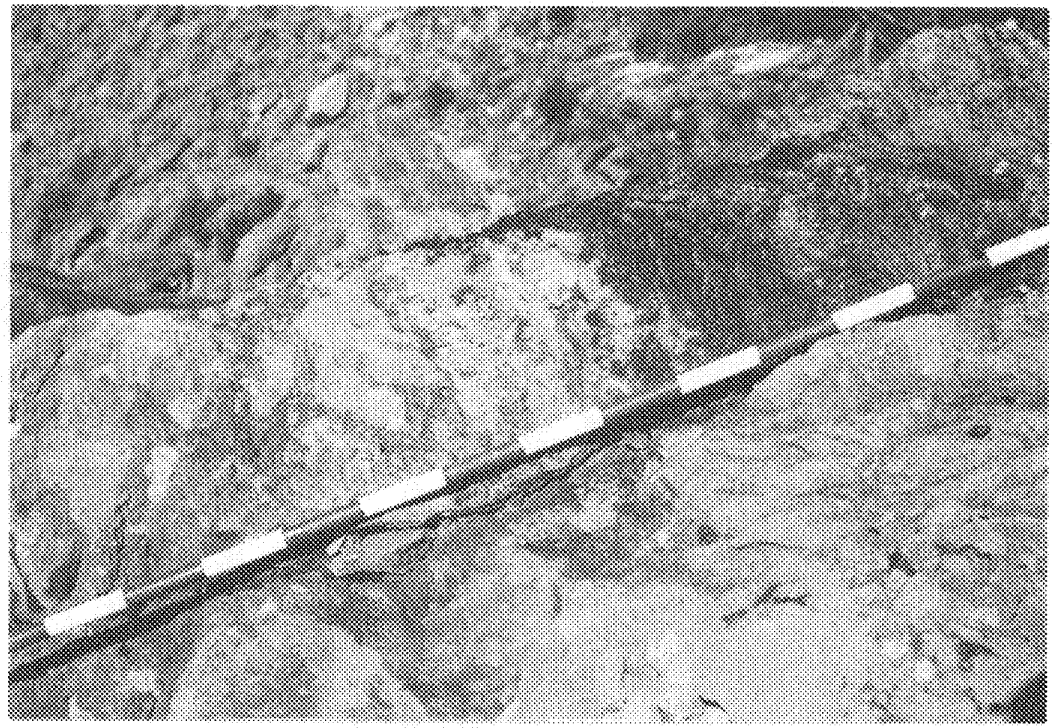


Figure 4.5 - Sandstone to fine conglomerate filling in a fissured surface at the top of Bioherm P (Section P-7, 0.0 m).

interval appear to be derived from the underlying bioclastic packstone / grainstone to boundstone facies, suggesting that the sediments within the bioherms were at least well "stiffified" at the time of exposure. The blackened appearance of many of the clasts also suggests that they have been subaerially exposed. The fact that the basal contact is not erosive at smaller bioherms and in a between-bioherm position suggests that any relative sea-level drop was not great. The interpenetration of grains indicates compaction during later diagenesis.

Discontinuous conglomerates are present in Sections A-1, C, and G-2. These beds do not correlate between sections. The beds range in thickness from 20-85 cm. The clasts range from coarse and very coarse sand sized, up to pebbles 2 cm in diameter. Fine quartz sand is present in the matrix of the conglomerate at Section C. The base of the upper conglomerate in Section G-2 is characterized by a tan silty matrix. The majority of the clasts within this uppermost conglomerate in Section G-2 are overly closely packed, suggesting compaction. The lower half of this same bed displays good porosity, probably late dissolutional in origin.

The discontinuous conglomerates are not associated with any fissured surfaces or any other evidence of exposure. The presence of reworked clasts indicates that high energy currents operated to rip them up, probably from the underlying limestone units. The distribution of the discontinuous conglomerates does not appear to be connected to paleo-topography, as two of them (those in Sections C

and G-2) are directly above or adjacent to bioherms in the BC2, while the third (in Section A-1) is in an inter-bioherm position.

Two conglomerates and one intraclast unit are present in the Akah (Figure 4.1). The 1.8 m thick conglomeratic bed in Section P-7 is unusual because of its varied nature. The clasts are not of the underlying laminite bed, and it is unclear from where they are derived. The clasts are not blackened. The conglomerate is matrix supported and the matrix is very silty. The character of the weathering varies greatly on the outcrop scale, from very massive to recessive. The bed contains numerous chert nodules and is cut by stylolites. Similar sediments occur in Section P-1, where a 10 cm thick zone of intraclasts is found at the base of a 1.35 m siltstone. The angular intraclasts are derived from the underlying bioclastic limestone. The intraclasts are approximately granule sized. A conglomerate in Section P-1 forms a 20 cm thick recessive interval. The matrix of this bed is a green siltstone. The clasts are well rounded and are derived from the underlying bioclastic limestone. The conglomerate is clast supported. Broken brachiopods are found within the matrix in the top 5-10 cm. The silty nature of these three clastic units suggests a terrigenous or fluvial origin.

Sandstone and Siltstone Rock Type

(Sections A-1, D, G-2, P-1, P-2, and P-7)

The siltstones found in the BC3 interval are recessive beds which range in thickness from 20 cm to 1.75 m thick, and are light to medium gray in color. They contain fine to very fine sand and silt

sized quartz grains, as well as very fine-grained lime mud. These beds are moderately to well sorted and contain no discernible sedimentary structures. Section G-2 contains five siltstones, the lower three of which are merely thin (<10 cm) intervals. The upper siltstones in Sections G-2 and D appear to correlate with one each other, as do those in Sections P-7 and A-1.

Four siltstone beds are seen in the Akah interval (Section P-1, Figure 4.1; Section P-2, not shown). Three of these siltstones are thin silty recessives no more than 10 cm thick (Section P-1, Figure 4.1). They appear to be discontinuous and are interpreted to be products of local terrigenous input. One thick siltstone bed can be correlated between Sections P-1 and P-2. It also appears to correlate with a thick silty conglomerate in Section P-7. These siltstone beds contain very fine sand to silt sized quartz grains. The siltstone in Section P-1 is greenish in color.

The BC3 siltstone found in Sections P-7 and P-1 overlies the thick conglomerate interpreted to be a cycle boundary. The BC3 siltstone found in Sections D and G-2 is found underlying an algal boundstone in Section D displaying fenestral porosity. The thick siltstones in the Akah are correlated with a silty conglomerate and overlie a supratidal algal laminite. These associations suggest that these siltstones all represent shallow water or terrestrial deposits.

Dolostone Rock Type

(Sections A-1, C, D, G-2, M-2, P-1, P-2, and P-7)

The dolostone beds present in the BC3 interval range in thickness from 20 cm to 1.75 m. Most contain fine-grained quartz sand. The dolostone beds are well to moderately sorted. The majority of these beds are also marked by high porosity, created either by large (2 cm) vugs or by fossil molds. Some molds can be identified as brachiopods and crinoid columnals, while others are unidentifiable, presumably fossil hash. Rarely (5% to 10% of the time) the molds are filled with coarse calcite spar. Within one bed (Section P-7) the original fossil grains (brachiopods and crinoids) are still present. The dolostone bed found in Section P-1 contains fine burrows, such as those found in the dolostones of the BC2. If one assumes that these two dolostones represent all the original rock types, then one can interpret this rock type as the bioclastic wackestone to grainstone rock type - as being deposited in shallow normal marine waters. The presence of silt and fine sand suggests that there is an additional terrigenous input. The majority of these beds are only partially dolomitized, suggesting late replacement. Within three of the dolomite beds (Section A-1, 13.5 m; Section M-2, 7.5 m; Section P-1, 34.3 m) there are indistinct laminations (Figure 4.1). It is unclear whether these laminations are due to algal growth, irregular dolomitization, or weathering processes.

Both of the dolostone beds in the Akah are found directly above the black shale. Both are fine-grained dolomites containing fine quartz sand. The dolostone in Section P-2 contains fine sand-sized

tubular foraminifera. Both appear to be dolomitized bioclastic wackestones to packstones. They are therefore interpreted to represent shallow normal marine deposition.

Shale Rock Type

(Sections M-2, P-1, and P-7)

No shales are found in the BC3 interval. The fissile shale which marks the lower boundary of the Akah is found in three of the four measured sections. It ranges from 7-30 cm thick. It is black in color, and contains ramiform conodont elements. The black shale at the base of Section P-1 is unusual in that it contains a tubular-foraminifera-rich wackestone to packstone and a nodular micrite within the shale itself. The thickness of the shale-limestone package is 68 cm. A second 10 cm black shale is found 2 m above the first in Section P-7. This fissile shale forms a thin recessive interval. The black color of these shales and the presence of conodonts indicates that this shale was deposited in a deep water setting. The lack of bioturbation within these shales suggests that they were deposited in an anoxic setting. The presence of fossiliferous bioclastic limestones within the black shale in Section P-1 suggests that there were fluctuations in the dissolved oxygen content of the water, perhaps indicating relative sea level fluctuations.

- CYCLES IN THE BC3 AND AKAH INTERVALS -

The lack of confident correlations one can make between the sections measured in the BC3 and Akah intervals, due to the lack of good exposure in these intervals, makes it difficult to draw cycle breaks through these intervals. Only fissured surfaces and conglomerates with blackened clasts are present in these sections, and these are found predominantly at the base of the BC3 interval. Information from outside of the field area (from Gianniny, 1994) is therefore tied in with shallow water deposits to divide the Barker Creek and Akah intervals into two cycles (Figure 4.6).

The lowest cycle (BC/A-1) is contained within the BC3 interval. The lower boundary of this cycle is marked by the continuous conglomerate with blackened clasts found at the base of the BC3. Fissures are found cutting into the underlying bioherms at Sections P-7 and M-2 (Figures 4.4 and 4.5). The upper boundary of this cycle is marked by conglomerates with blackened clasts correlated with siltstones from outside of the study area. To the northwest of the field area a siltstone is seen truncating the beds below it to a depth of 2.1 m, containing roots, and overlying a paleosol (Toni Simo, personal communication). This siltstone is approximately one meter thick, and is overlain by several carbonate beds which range from 0.5 to 2 m thick. This siltstone is interpreted to correlate with the siltstones in Sections A-1 and P-7 (Figure 4.6). This cycle boundary is correlated with the shallowest water environments within the other five sections. These include algal laminites (Sections P-1 and D),

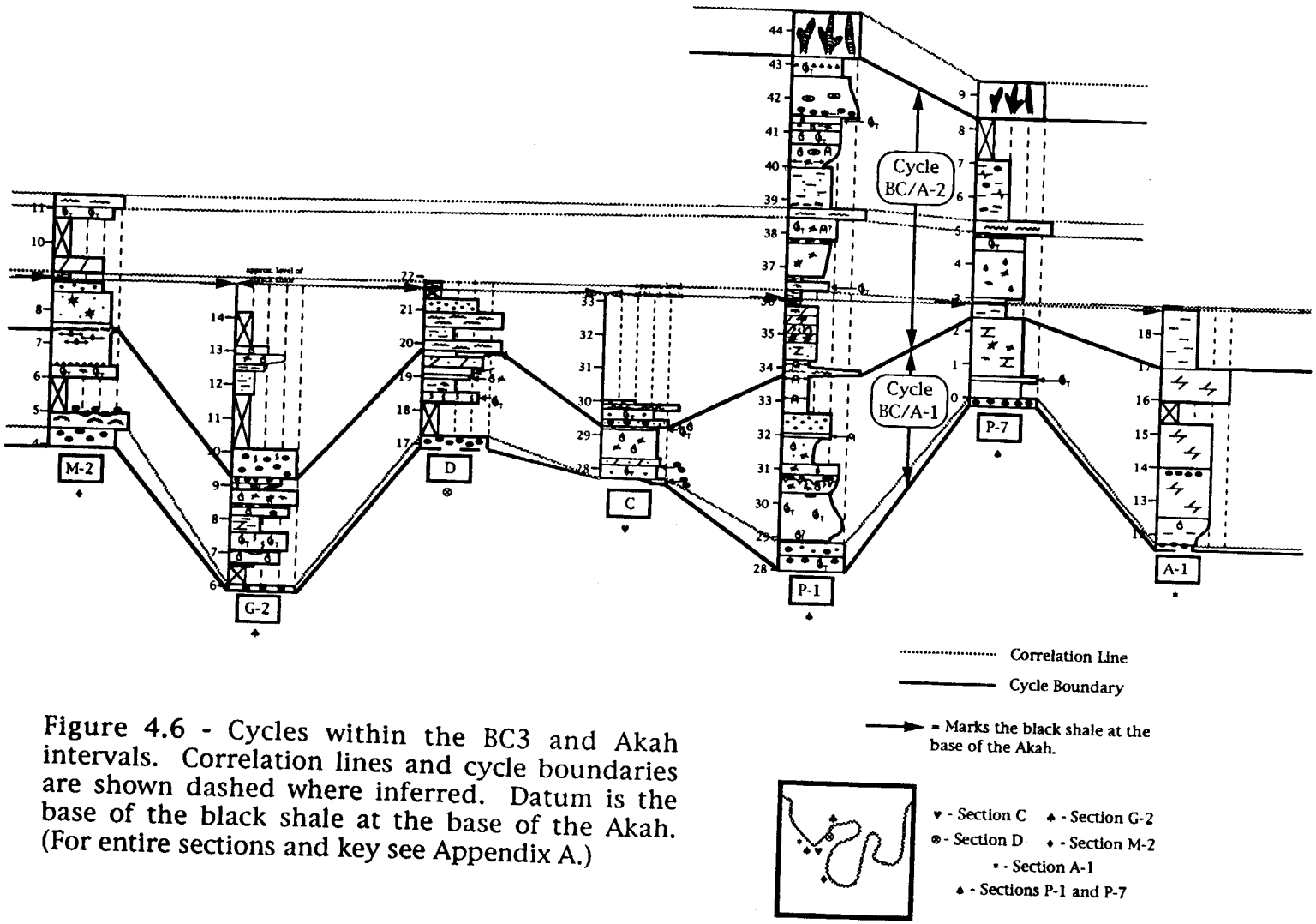


Figure 4.6 - Cycles within the BC3 and Akah intervals. Correlation lines and cycle boundaries are shown dashed where inferred. Datum is the base of the black shale at the base of the Akah. (For entire sections and key see Appendix A.)

conglomerates with blackened clasts (Sections C and G-2), and an intraclast unit (Section M-2) (Figure 4.6). The beds contained within this cycle do not appear to show any definite shallowing upward trend.

The second cycle (BC/A-2) bridges the Barker Creek and Akah break (Figure 4.6). Two successions representing fluctuating sea level are present within this cycle. The lowest succession contains a deepening trend followed by a shallowing trend. Normal marine carbonates and dolomites are overlain by the black shale which marks the boundary between the Barker Creek and Akah intervals (Figure 4.6). This shale is interpreted to be a maximum flooding surface. A relative drop in sea level is interpreted to follow the deposition of this shale, as evidenced by the presence of normal marine carbonates. This succession is capped by an algal laminite. This laminite contains fenestral porosity within Section P-1, further evidence of a very shallow environment. The second succession is marked by clastic units and a siltstone at its base, interpreted to represent a relatively shallow environment (Sections P-1 and P-7, Figure 4.6). These clastic units are overlain by normal marine carbonates interspersed with siliciclastic and clastic units within Section P-1. The normal marine carbonates are interpreted to represent a relatively deeper water environment. The upper boundary of this cycle is marked by an exposure surface at the base of the "CDB" bed. Channeling is seen outside of the field area at this stratigraphic interval.

Both of these cycles (BC/A-1 and BC/A-2, Figure 4.6) appear to be dominated by low energy deposits, containing much carbonate mud

and quartz silt. Cycle BC/A-1 and the lower shallowing upward succession within cycle BC/A-2 are both capped by algal laminites, further evidence of a low energy environment. Grain-supported bioclastic rocks are found predominantly in between-bioherm positions, and at the base of sections (Sections A-1, C, G-2, and P-1, Figure 4.1). This suggests that as material accumulated between and on bioherms and as the topography leveled out, lower energy environments became dominant.

Chapter 5

Conclusions

- INTRODUCTION -

In this chapter I will discuss the objectives originally stated at the beginning of the thesis: lithologic repetition and cyclicity, growth history of the bioherms, bioherm orientation and distribution, and controls on bioherm growth. The data supporting the conclusions below have been provided in previous sections.

- LITHOLOGIC TRENDS IN THE STRATIGRAPHIC COLUMN -

Trends in bed thickness, ratios of carbonate vs. clastic rocks, and ratios of grain vs. matrix supported rocks are present in the stratigraphic section studied. Figure 5.1 summarizes rock type data (from Section P-1) within the cycles of each informal stratigraphic interval. Cycle BC1-1 was not included because it is an incomplete cycle. In this analysis, carbonate beds include bioclastic limestone, peloidal limestone, oolitic limestone, algal boundstone, oncolitic, and dolostone rock types. Clastic beds include clastic, fine sandstone/siltstone, and black shale rock types. Grain supported and matrix supported rocks include beds from only the carbonate facies listed above. Grain supported rocks include packstones and

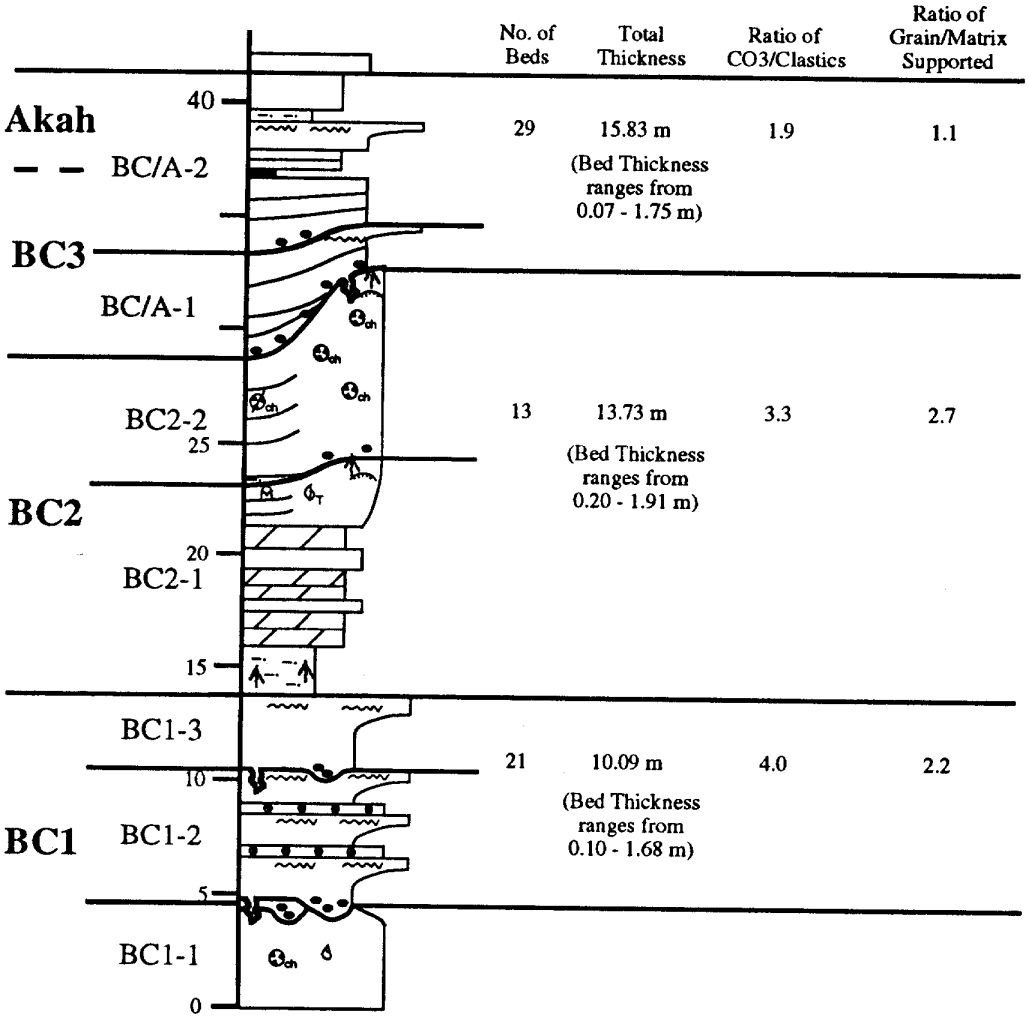


Figure 5.1 - Idealized cycles and rock data (from Section P-1) from each informal stratigraphic interval. Rock data includes number of beds, total thickness of beds, ratio of carbonate to clastic beds, and ratio of grain supported to matrix supported units within the cycles of each informal stratigraphic interval. Cycle BC1-1 is not included because data from only the top of this cycle is exposed. (For key see Appendix A.)

grainstones. Matrix supported rocks include mudstones, wackestones, and algal boundstones.

The beds within cycles BC2-1 and BC2-2 are the most thickly bedded (13 beds in 13.73 m of section, average bed thickness is approximately 1 m). Beds within cycles BC1-2, BC1-3, and within cycles BC/A-1 and BC/A-2 are about half as thick on average (21 beds in 10.09 m of section in the BC-1, and 29 beds in 15.83 m of section in the BC-3 and Akah, Figure 5.1). These differences in bed thickness may be due simply to the fact that Section P-1 is located on the flanks of Bioherm P. Bioherm formation took place within cycles BC2-1 and BC2-2. Carbonate beds in this location within these two cycles may therefore be thicker because they include the edge of the bioherm.

The highest ratio of carbonate to clastic rocks is seen in cycles BC1-2 and BC1-3 (ratio of 4.0, Figure 5.1). In these cycles, clastic units are present at the cycle boundaries, but they are very thin units with respect to the rest of the interval. There is also a high ratio of carbonates to clastics in cycles BC2-1 and BC2-2 (ratio of 3.3, Figure 5.1). Relatively thick green siltstones are present in these cycles, but they are few in number. The lowest ratio of carbonate to clastic rocks is seen in cycles BC/A-1 and BC/A-2 (ratio of 1.9, Figure 5.1). A decrease in the ratio of carbonate vs. clastic beds is seen as one moves upsection. This increase in clastic deposition could be caused by a shallowing trend upsection, a change to a relatively more shoreward position on the shelf, or a change to a position closer to the source area.

There are over two times more grain supported beds than matrix supported beds in cycles BC1-2 and BC1-3, and cycles BC2-1 and BC2-2 (ratios of 2.2 and 2.6 respectively, Figure 5.1). The ratio in the BC1 interval is higher than one might expect, considering the presence of algal laminites which would suggest deposition in a quiet environment. The presence of oolitic grainstones within these cycles however raises the ratio. Likewise, the ratio in the BC2 interval is lower than one might expect, considering the presence of bioclastic packstones and grainstones in the bioherms which are interpreted to be deposited in a higher energy environment. The presence of fine-grained dolostones within the lower cycle lowers the ratio. There is roughly the same number of grain supported and matrix supported beds in cycles BC/A-1 and BC/A-2 (ratio of 1.1, Figure 5.1). As discussed in Chapter 4, the increase in matrix supported vs. grain supported carbonate beds may be due to the fact that the carbonates are filling in topography created by the bioherms of the BC2 interval. The grain supported carbonate beds appear near the base of the stratigraphic section in between-bioherm positions. Matrix supported carbonate beds appear near the top of the section where the topography has been substantially decreased.

- CYCLICITY IN THE STRATIGRAPHIC COLUMN -

The stratigraphic interval within the study area has been divided into several shallowing upwards cycles, separated by surfaces or beds which contain compelling evidence of exposure. These

exposure features include fissures, roots and rhizoliths, paleosols, and conglomeratic beds with blackened clasts. Cyclicity within each informal stratigraphic subdivision has already been discussed at length in previous chapters. Figure 5.2 summarizes cycles and shallowing upward successions in the interval studied, as well as what evidence of exposure there is at each cycle boundary. In summary, six complete cycles are seen in the study area. The top of another cycle (BC1-1) is also seen, whose base is under river level.

Two types of cycles and shallowing upwards successions are seen within the study area (Figure 5.3). The first type shows a transition from high energy to low energy environments. This type is found in cycles BC1-2, BC1-3, BC/A-1, and BC/A-2 which show a transition from oolite beds or other normal water carbonates to algal laminites. Both of these are relatively shallow water deposits. The second type of cycle shows a transition from low energy to high energy environments. This type includes cycles BC2-1 and BC2-2 which show a transition from relatively deep fine-grained dolomites to shallower bioclastic limestones. The second type of cycle appears to indicate a greater change in relative sea level. It is also within these second type of cycles that bioherms appear. This suggests that bioherms formed because of a greater amount of initial accommodation space available to them.

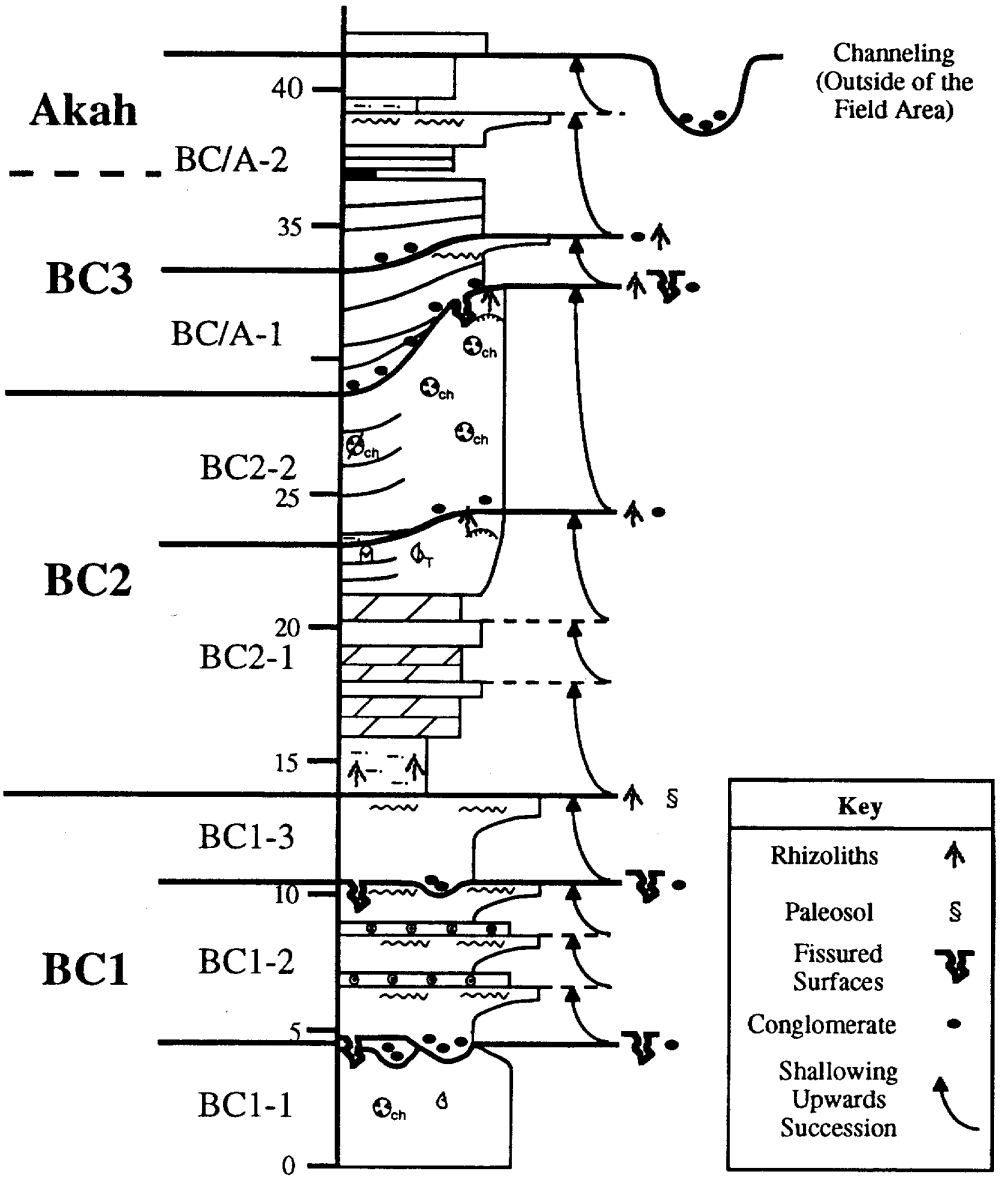


Figure 5.2 - Diagram illustrating idealized cycles and shallowing upward successions within the study area. Cycle numbers correspond with those used throughout. Meter scale is approximate. (For key see Appendix A.)

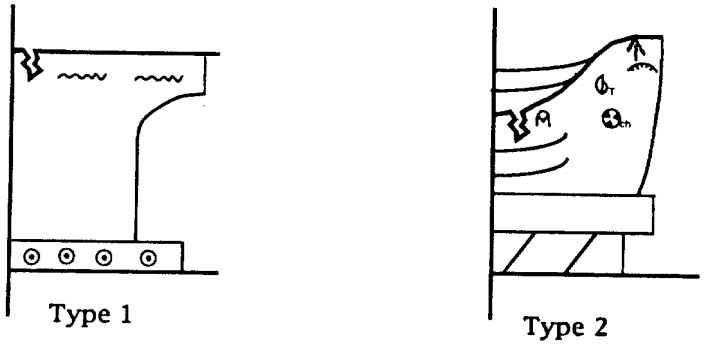


Figure 5.3 - Idealized cycle models. Type 1 - shows a transition from a high energy oolitic grainstone to a low energy mudstone or wackestone and algal laminite. Type 2 - shows a transition from low energy dolostones to high energy buildup facies. This cycle type is also capped with algal laminites or stromatolites. Both cycle types terminate with either an exposure surface or a surface which marks a return to deeper water facies.

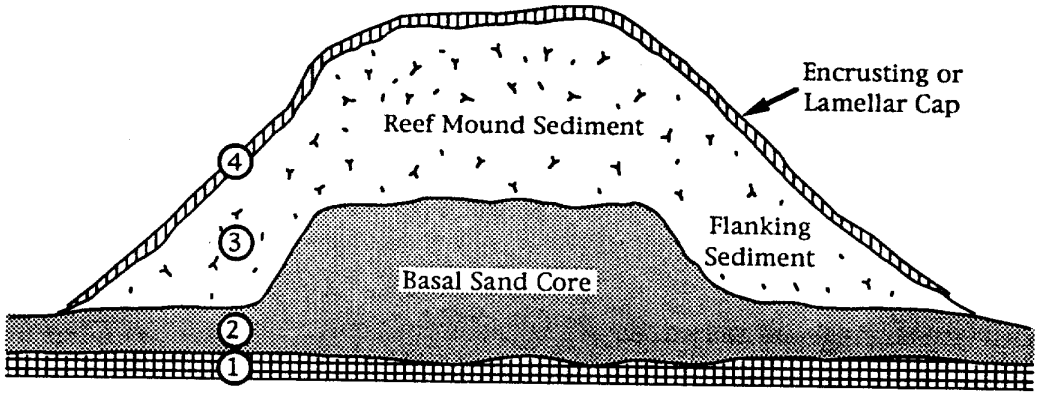


Figure 5.4 - Model of reef mound growth, after James, 1984. 1 = original sea floor, 2 = basal bioclastic pile, 3 = mudstone or bafflestone core, and 4 = encrusting or lamellar cap.

- GROWTH HISTORY OF THE BIOHERM COMMUNITY -

This summarizes the discussion in Chapter 3 on the growth history of bioherms in the BC2 interval. Bioherm orientation, distribution, and size will be discussed below. The beds within buildups can be subdivided into two different zones based on texture, fossil content, and sedimentary structures. The lower zone, Zone A, represents mechanical accumulations formed on the floor of the shallow shelf. These accumulations within Zone A were small, never exceeding a height of 3 m (see Figure 3.40, Chapter 3). Relative sea level fell as these accumulations were forming, causing a restriction in environment. As a result, stromatolites and other algal structures grew, forming an algal cap. Sea level continued to fall, resulting in exposure and forming the cycle boundary between cycles BC2-1 and BC2-2 (Figure 5.2). When sea level deepened once again, the mechanical accumulations within Zone A formed local areas of relief which were preferentially chosen as sites for Zone B mound initiation (see Figure 3.41, Chapter 3). Zone B mounds are biologically formed, primarily by *Chaetetids* and tubular foraminifera. The size of the Zone B mounds varies greatly (see Figure 3.41, Chapter 3). Relative sea level fell once again, causing another restriction in environment. Stromatolites and algal structures once again formed. Exposure occurred once again, forming the cycle boundary between cycles BC2-2 and BC/A-1. Evidence for this cycle boundary includes fissures, rhizoliths, and clastic units found at the top of the bioherms (Figure 5.2).

The overall growth pattern then is as follows: 1) establishment of a mechanically formed mound, 2) formation of an algal cap and exposure, 3) colonization by an organic community, and 4) formation of another algal cap and exposure. James' (1984) model of "reef mound" growth is similar in many aspects to the one seen in the Barker Creek bioherms. His three stage sequence is as follows (Figure 5.4): 1) accumulation of a basal bioclastic pile, 2) formation of a lime mudstone or bafflestone core, and 3) formation of a cap, often by encrusting or lamellar organisms. The difference between this model and the bioherms studied, is that the mounds in the model are formed within one sea level cycle, whereas the bioherms in the field area formed within two sea level cycles.

- BIOHERM ORIENTATION AND DISTRIBUTION -

Bioherms in the field area are oriented along a northwest-southeastern trend, approximately N10°W to N60°W This trend is similar to that noted by Wengerd (1955) of between N40°W and N65°W. Wengerd also proposed that the bioherms form continuous barrier reef-like bars, like "beads on a string" (Wengerd, 1955). This study suggests that the bioherms are not located along such discrete lines. Rather, they are more randomly distributed (see Figure 3.42, Chapter 3).

This orientation is interpreted to result from the shaping effects of currents. Zone A mounds, mechanically produced, would have been shaped by current activity within the basin. The orientation of Zone B

mounds (controlled by those in Zone A), and the distribution of fauna within these mounds would also have been affected by current activity. The orientation of cross-bedding in Zone A, Bioherm P (from 1° to 6°, N11E); and the presence of broken and reworked Chaetetid heads on the northwestern flanks of Bioherms H and P suggest that currents were directed toward the east.

- CONTROL OF BIOHERM SIZE -

There is as yet no satisfactory answer as to what factors control the size of the bioherms. All bioherms in the study area, both large and small, contain both Zones A and B, and therefore formed during two relative sea level cycles (Figure 5.2, see Figures 3.25, 3.26, and 3.27, Chapter 3).

It is possible that the disparity in bioherm size is simply a factor of exposure. It has been shown that the cores of the medium (D-F) and large (P and M) sized bioherms in the field area are back within the cliff. It is possible that within the cliffs, out of view, the medium bioherm (D-F) expands to a size equal to that of Bioherms P and M. This answer is not satisfactory because it cannot explain the smaller bioherms (G, H, L and S), and it cannot be tested.

A second explanation is based on the distribution of the larger versus the smaller bioherms. A definite trend in size can be seen in the bioherms, with the largest being in the southwestern corner of the study area and the smallest being within the northeastern corner (see Table 3.2 and Figures 3.40, 3.41, and 3.42, Chapter 3). If one assumes

that all bioherms grew to fill available accommodation space, this trend suggests that water depth was increasing to the southwest. The difference in bioherm height requires that the shelf was sloping 1.0° to the southwest. The major problem with this explanation is that, if one looks at large scale trends, the shelf should be dipping in the opposite direction (see Figure 1.1, Chapter 1 for regional map of the Paradox Basin). It is possible that this gentle dip reflects a local perturbation in the southwest dipping shelf which is true of local geometries. A gently northeastern dipping shelf may then be characteristic of the basin on a large scale.

References

ATCHLEY, S.C. AND LOOPE, D.B., 1993, Low-stand aeolian influence on stratigraphic completeness: upper member of the Hermosa Formation (latest Carboniferous), southeast Utah, USA. IAS Spec. Pub. 16, p. 127-149.

BAARS, D. AND STEVENSON, G., 1981, Tectonic evolution of the Paradox Basin, Utah and Colorado. in Wiegland, D.L. (ed.), Geology of the Paradox basin, Rocky Mountain Assoc. Geol. 1981 Field Conf., p. 23-31.

BAARS, D. AND STEVENSON, G., 1986, San Juan Canyons, A river runner's guide and natural history of the San Juan River canyons, Canon Publisher Ltd., Evergreen, Colorado, 64 pp.

DAHANAYAKE, K., 1983, Depositional environments of some Upper Jurassic oncoids. in Peryt, T.M. (ed.), Coated Grains, Springer-Verlag, New York, p. 377-385.

GIANNINY, G.L., 1994, (in preparation), Desmoinesian carbonate buildups and platform evolution, Paradox basin, Utah. PhD Thesis, Department of Geology and Geophysics, University of Wisconsin-Madison.

GOLDHAMMER, R.K., OSWALD, E.J., AND DUNN, P.A., 1991, The hierarchy of stratigraphic forcing: an example from Middle Pennsylvanian shelf carbonates of the Paradox Basin, Kansas Geological Survey. in Fransen, E.K., Watney, W.L., Kendal, C.G., and Ross, W., (eds.) Sedimentary modeling: computer simulations and methods for improved parameter definition, Bulletin 233, Kansas Geological Survey, p. 361-413.

HOFFMAN, P., 1976, Stromatolite morphogenesis in Shark Bay, western Australia. in Walter, M.R. (ed.), Stromatolites, Elsevier Sci. Pub., Netherlands, p. 261-271.

HITE, R.J., 1960, Stratigraphy of the saline facies of the Paradox Member of the Hermosa Formation of southeastern Utah and southwestern Colorado. in Geology of the Paradox basin fold and fault belt, Four Corners Geol. Soc. Guidebook, 3rd Field Conf., 1960, p. 86-89.

JAMES, N.P., 1984, Reefs. in Walker, R.G. (ed.), Facies Models, Second Edition, Geological Association of Canada, p. 229-244.

LOUCKS, R.G. AND HANDFORD, C.R., 1992, Origin and recognition of fractures, breccias, and sediment fills in paleocave-reservoir networks. in Candelonia, M.P. and Reed, C.L. (eds.), Paleokarst karst-related diagenesis, and reservoir development, PBS Publication 92-93, p. 31-44.

PETERSON, J.A. AND OHLEN, H.R., 1963, Pennsylvanian shelf carbonates, Paradox basin. in Bass, R.O. (ed.), Shelf carbonates of the Paradox basin, Four Corners Geol. Soc. 4th Field Conf. Guidebook, p. 65-79.

PRAY, L.C. AND WRAY, J.L., 1963, Porous algal facies (Pennsylvanian) Honaker Trail, San Juan Canyon, Utah. in Bass, R.O. (ed.), Shelf carbonates of the Paradox basin, Four Corners Geol. Soc. 4th Field Conf. Guidebook, p. 204-234.

SEE, P.D., 1963, Nomenclature Chart of the Four Corners Area. in Bass, R.O. (ed.), Shelf carbonates of the Paradox basin, Four Corners Geol. Soc. 4th Field Conf. Guidebook, p. 2-4.

WENGERD, S.A., 1951, Reef limestones of Hermosa Formation, San Juan Canyon, Utah, AAPG Bulletin, v. 35, p. 1038-1051.

WENGERD, S.A., 1955, Biohermal trends in Pennsylvanian strata of San Juan Canyon, Utah. in Four Corners Geological Society Guidebook, First Field Conference, Geology of Parts of the Paradox, Black Mesa, and San Juan Basins, p. 70-77.

WEST, R.R., 1988, Temporal changes in Carboniferous reef mound communities. Palaios, v. 3, p. 152-169.

WEST, R.R. AND CLARK, G.R., 1983, Chaetetids. in Broadhead, T.W. (ed.), Sponges and Spongiomorphs, Notes for a Short Course, Studies in Geology 7, p. 130-140.

WILSON, J.L., 1975, Carbonate facies in Geologic history, Springer-Verlag, New York, 417 p.

Appendix A

Measured Sections

During the field season of 1992, 19 sections were measured in the field area. All of these sections have been computer drafted and are included in this appendix. Maps of the field area are shown in Figures A-1, A-2, and A-3. The location of each of these sections is illustrated in Figures A-3 and A-4. Most sections include the following: 1) a textural profile (for both carbonate and siliciclastic rocks), 2) sampling locations, 3) information on sorting, porosity, and bioturbation, and 4) when the section was measured and with whom. A key to symbols used in the sections is located in Figure A-5, and a guide to reading the sections is located in Figure A-6. Most sections were measured from river level, as indicated on the individual sections. Exceptions to this include Sections P-2 through P-8, A-1, and M-2. Figure A-4 shows where the base of Sections P-1 through P-8 are located in relation to Bioherm P and the river. Figure A-7 is a profile of the side canyon in which Section P-1 is located, to assist those who visit the field area in orienting themselves. Attempts were made when measuring the sections to measure up to the top of the "CDB" within the lower Akah, so that this unit could be used as a datum. Occasionally the distance from the top of the upper Barker Creek and "CDB" was noted without the intervening section being measured.

Exceptions to the above generalizations are as follows.

Section P-1 - This very complete section, covering the entire stratigraphic interval of interest in this study, includes a weathering profile and a listing of individual bed thicknesses. Figure A-7 also indicates how the section is distributed in relation to benches and slopes within the side canyon. This will help enable those interested in going back to this section to locate themselves within the side canyon.

Section P-2 - This section was measured very quickly, and as a result little was noted other than lithology, thickness, presence of fossils, and any other particularly striking information. Therefore, the sorting and porosity columns are only filled where that information was recorded in the field.

Section P-6 - This section was measured from a large (12 m tall) float block which was located at the base of Bioherm P. Only the lower half and the very top of the block were accessible and could be measured. Because he upper middle section of the block could be observed, albeit from a distance, and because the lithology and texture of this part of the section were known from other measured sections, the lithology and texture of this gap were inferred when drafting; but the sorting, porosity, and bioturbation columns were left blank.

Section G-1 - This section was measured on a day with particularly oppressive weather, and as such, when it became apparent that the

facies of interest had already been measured, it was simply noted where this section "tied into" the section closest to it - Section G-2. The comment at the top of this section refers to the exact height at which it ties into Section G-2.

Section M-2 - This section is an extension of Section M-1. Section M-1 is of the core of Bioherm M, Section M-2 is of the eastern flank. The base of Section M-2 is roughly equivalent to the top of Section M-1.

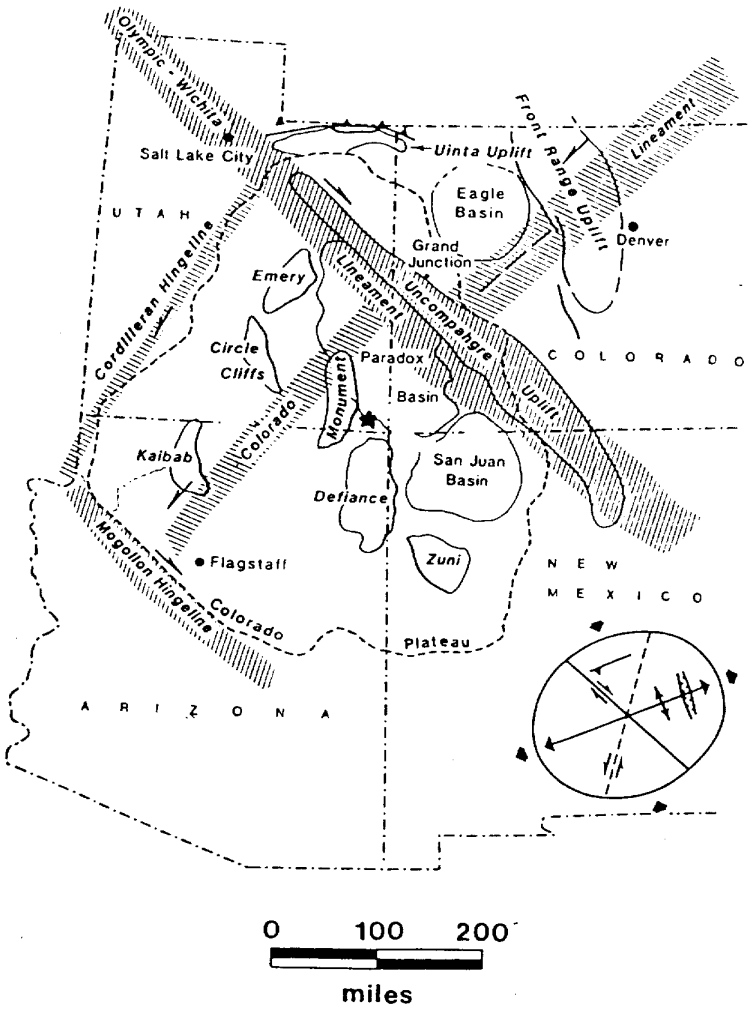


Figure A-1 - Regional map, showing location of Paradox Basin. The Paradox Basin is a pull-apart basin, aligned along right-lateral NW-SE faults and NE-SW faults. The star marks the location of the field area in southeastern Utah, on the southwestern margin of the Paradox Basin. (From Baars and Stevenson, 1981, p 26.)

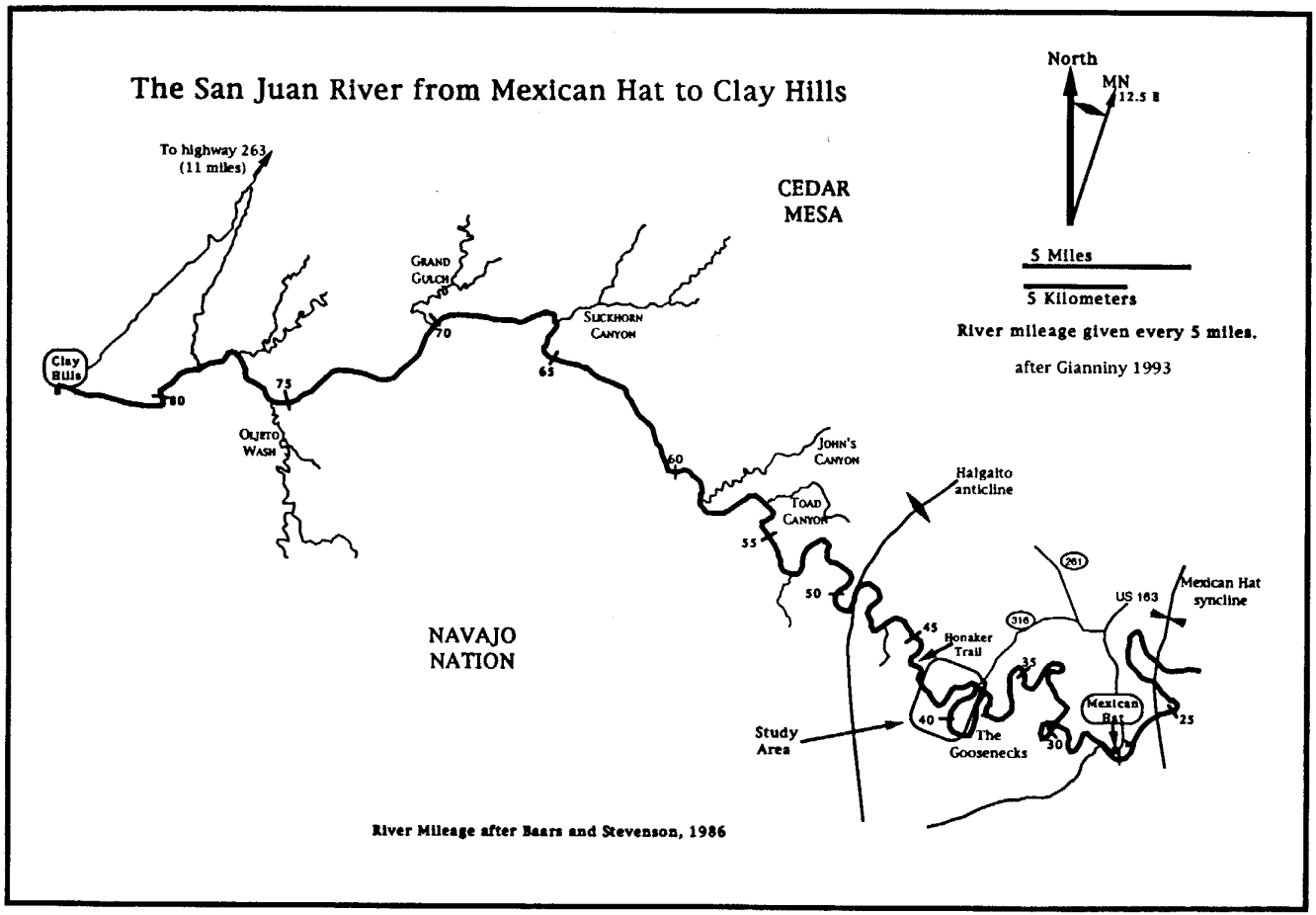


Figure A-2 - Map of the San Juan River showing location of the field area.

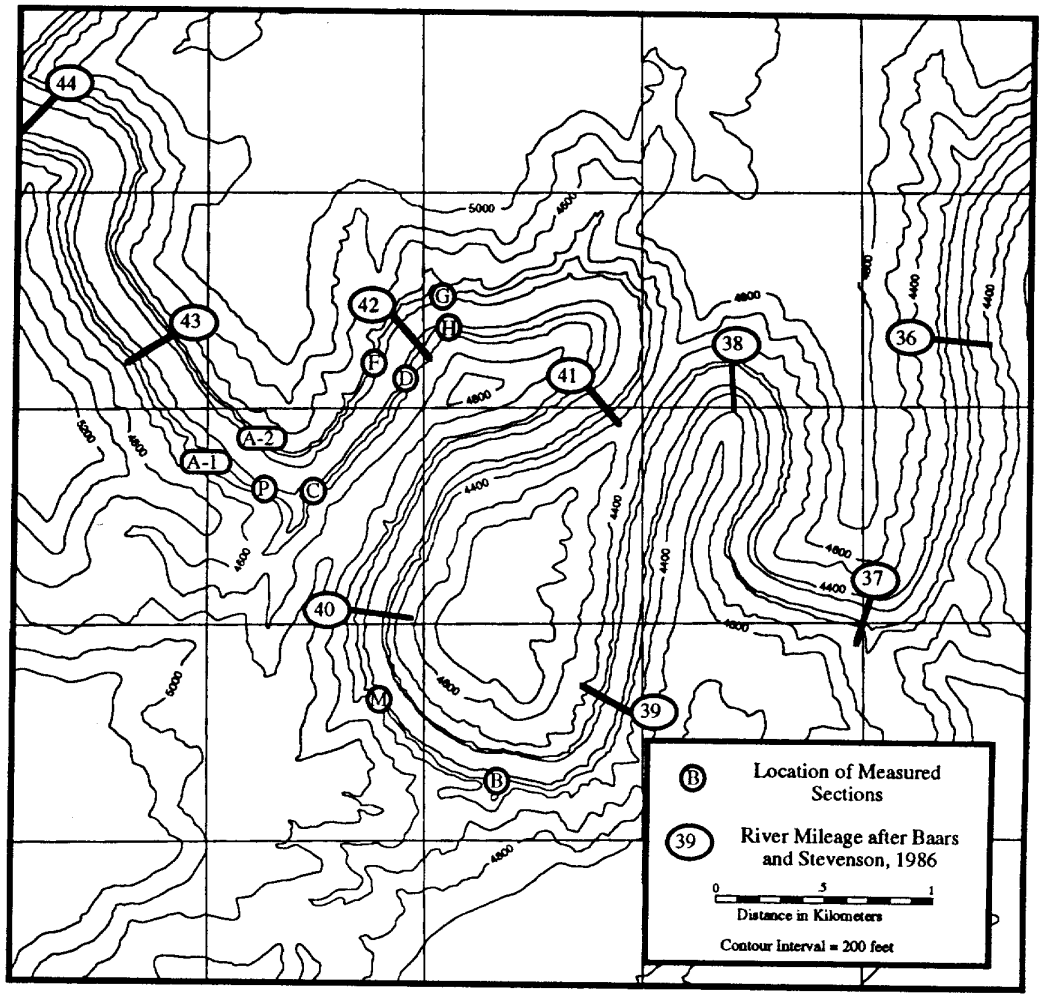


Figure A-3 - Topographic map of Goosenecks area from river mile 36 to 44, showing the location of measured sections within the BC1 interval. Both G-1 and G-2, and M-1 and M-2 are located at their respctive letters. All P sections are located in the vicinity of the circled P. For more information on the distribution of Sections P-1 through P-8, see Figure A-4.

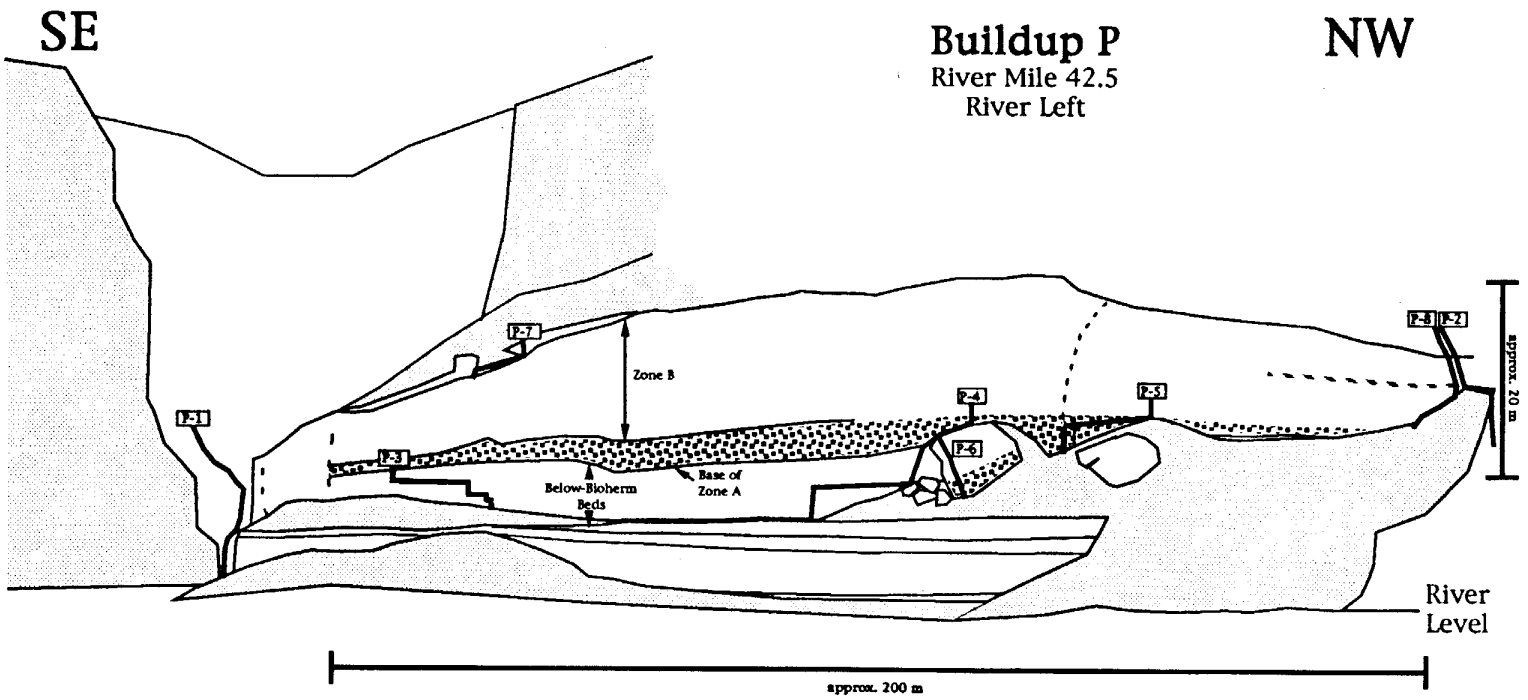


Figure A-4 - Sketch of Buildup P as viewed from downstream, river right. Locations of measured sections P-1 through P-8 are shown. Buildup is approximately 200 m wide and 20 m high.

Rock Types

- limestone
- sandy/silty limestone
- dolomitic limestone
- sandy/silty dolomitic limestone
- dolostone
- sandy/silty dolostone
- siltstone
- shale

Fossils

- algal laminite
- brachiopods
- brachiopod hash
- brachiopod mold
- bryozoa, fenestrate
- bryozoa, ramose
- chaetetids
- crinoid columnals
- crinoid hash
- "Continuous Digitate Bed" (stratiform layer)
- stromatolite
- fusulinid
- oncolite
- syringipora
- tubular foraminifera
- fossil hash

Nonskeletal Grains and Sedimentary Features

- breccia clast
- burrow
- chert
- chert nodule
- conglomerate clast
- evaporite mold
- intraclasts
- oolite
- peloid
- roots
- sand
- shale
- silt
- trough cross bedding

Figure A-5 - Rock Types and Grain Types for sections in Appendix A.

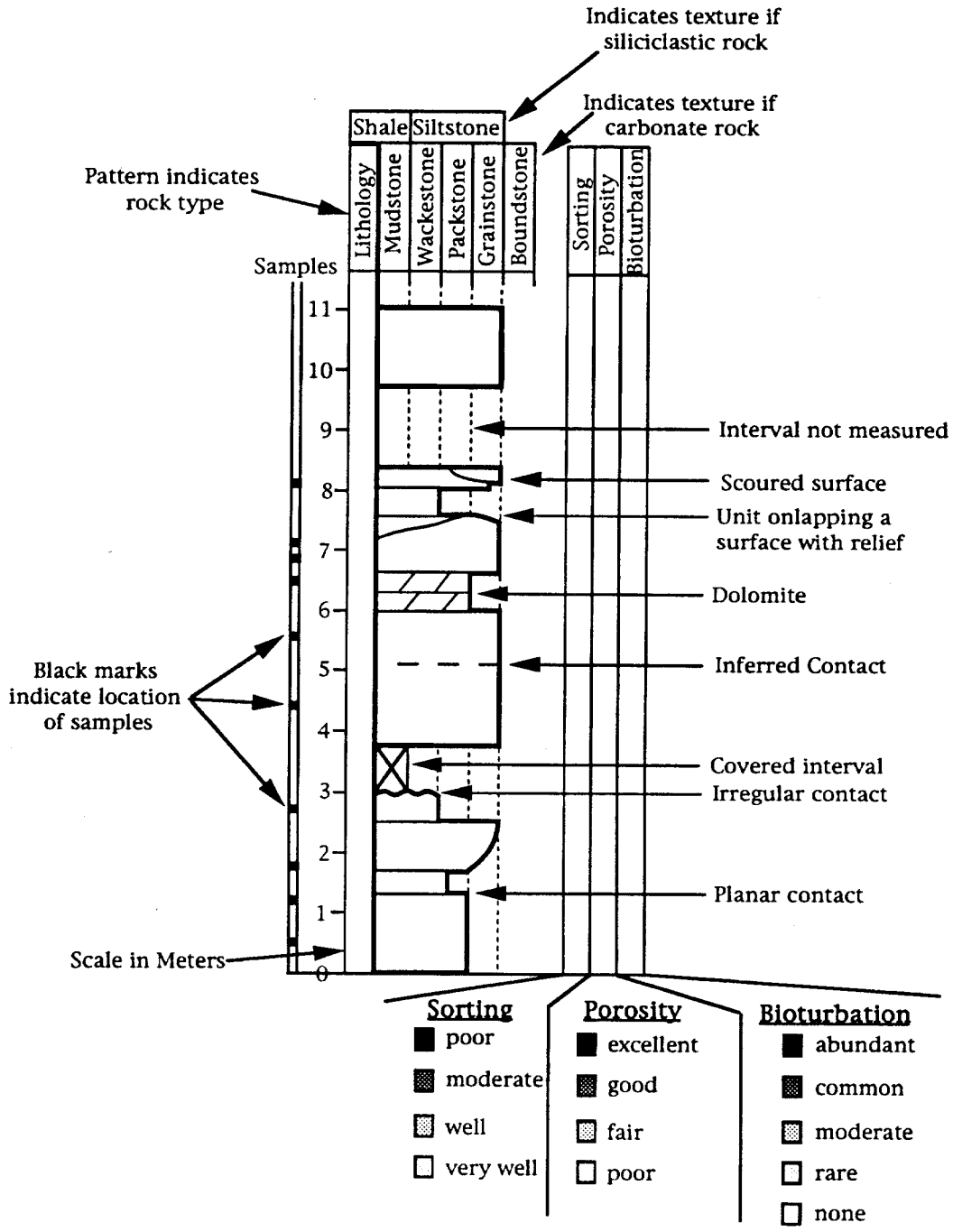


Figure A-6 - Guide to reading the sections in Appendix A.

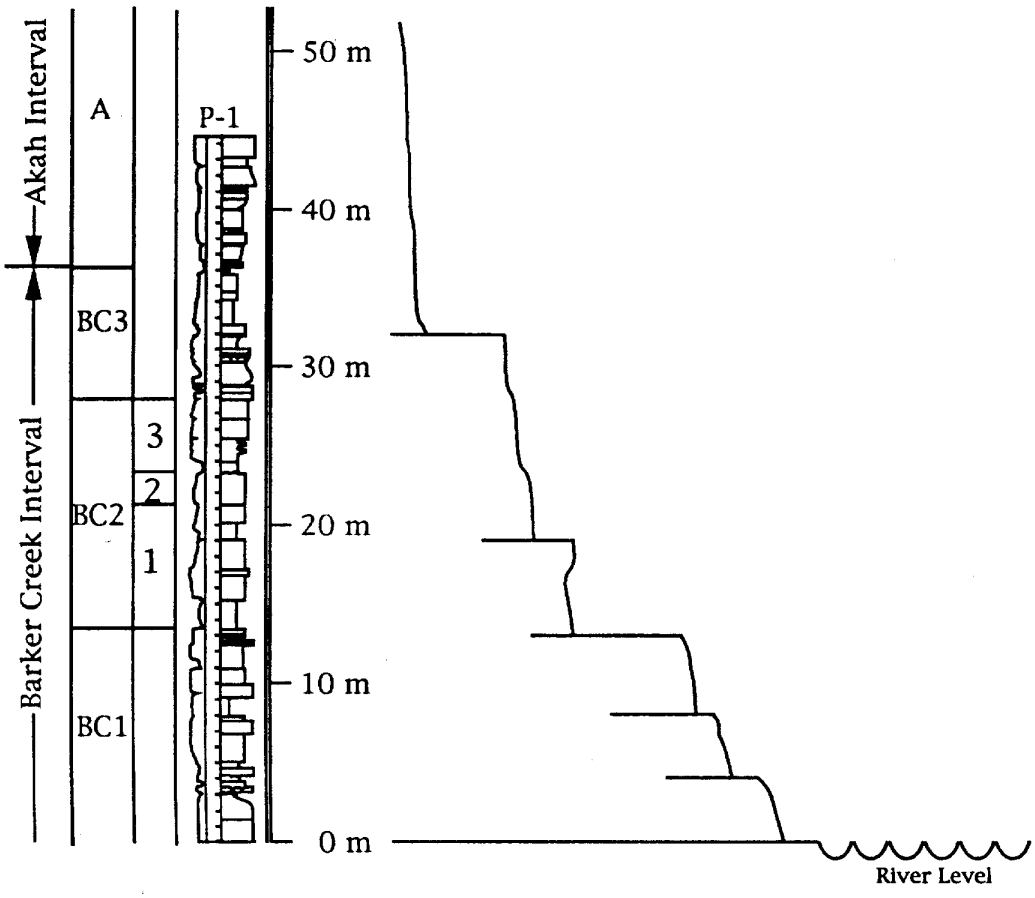


Figure A-7 - Profile of side canyon in which Section P-1 was measured. Flat areas indicate major benches in the side canyon. Included are the textural and weathering profiles of Section P-1 to aid in locating oneself in the side canyon. Also included are the two intervals emphasized in this study as well as their informal subdivisions (BC1, BC2, BC3, and Akah). The division of the BC2 interval into rock types is also shown (1 = siltstone, dolomites and grainy limestones, 2 = Zone A bioclastic pack- to grainstones, and 3 = Zone B boundstones to grainstones).

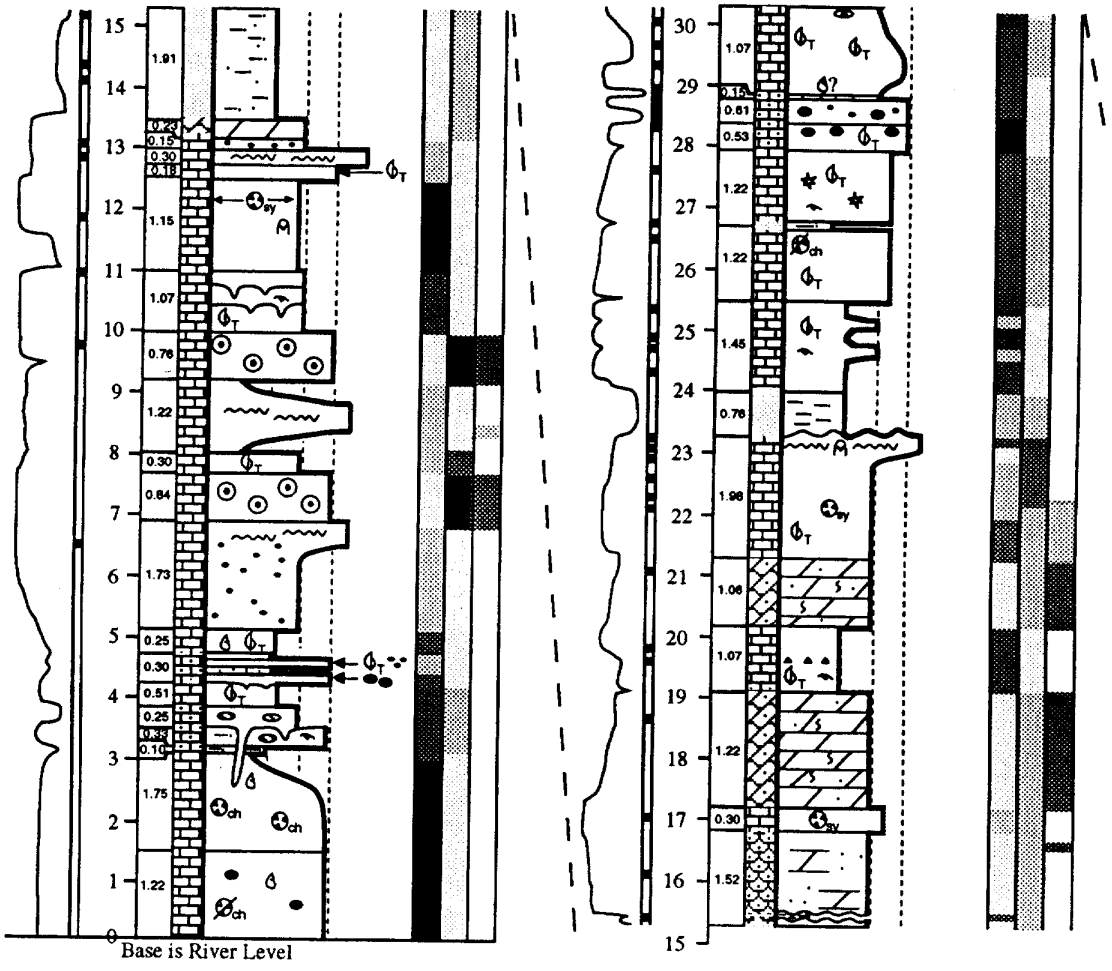
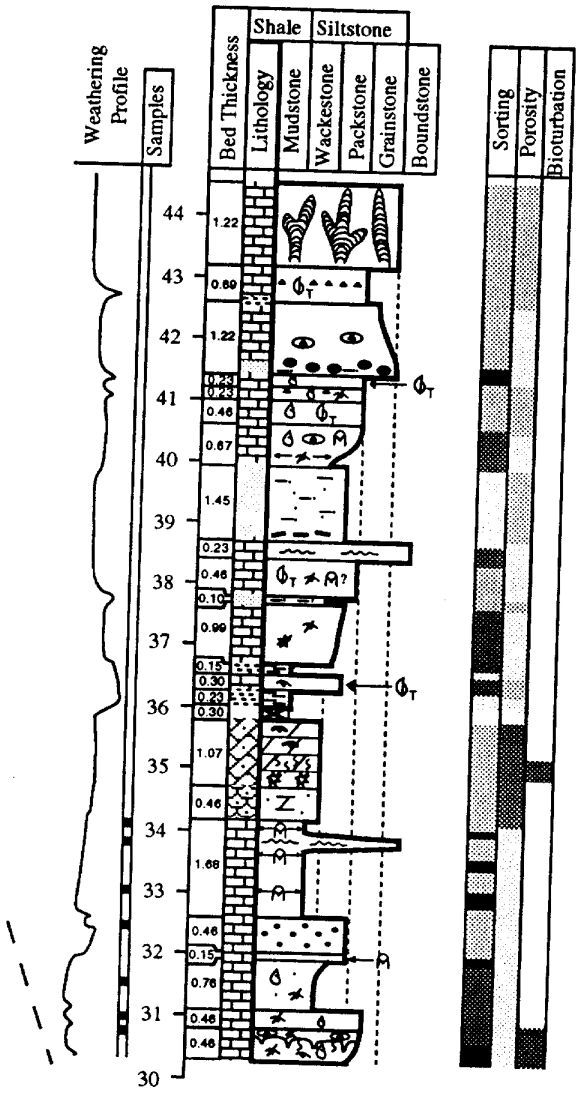


Figure A-8 - Section P-1, measured May 28, 29, 30, and June 1 and 2, with Kathy O'Neil. Continued on next page.


Weathering Profile
Samples
Bed Thickness
Lithology
Shale
Siltstone
Mudstone
Wackestone
Packstone
Grainstone
Boundstone
Sorting
Porosity
Bioturbation
44
43
42
41
40
39
38
37
36
35
34
33
32
31
30
1.22
0.69
1.22
0.23
0.23
0.46
0.67
1.45
0.23
0.46
0.10
0.99
0.15
0.30
0.23
0.30
1.07
0.46
1.68
0.46
0.15
0.76
0.46
0.46

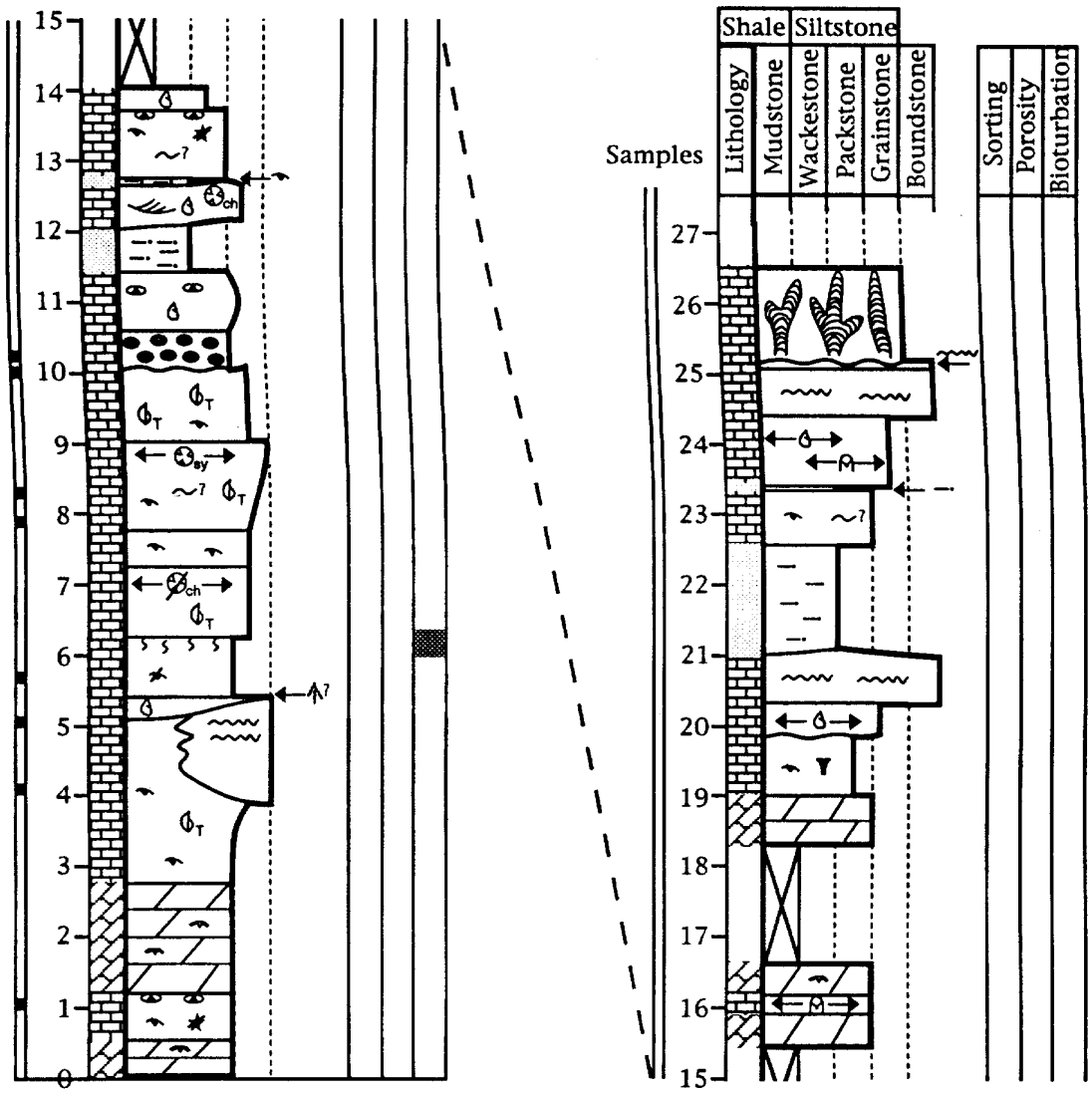


Figure A-9 - Section P-2, measured June 1 with Toni Simo.

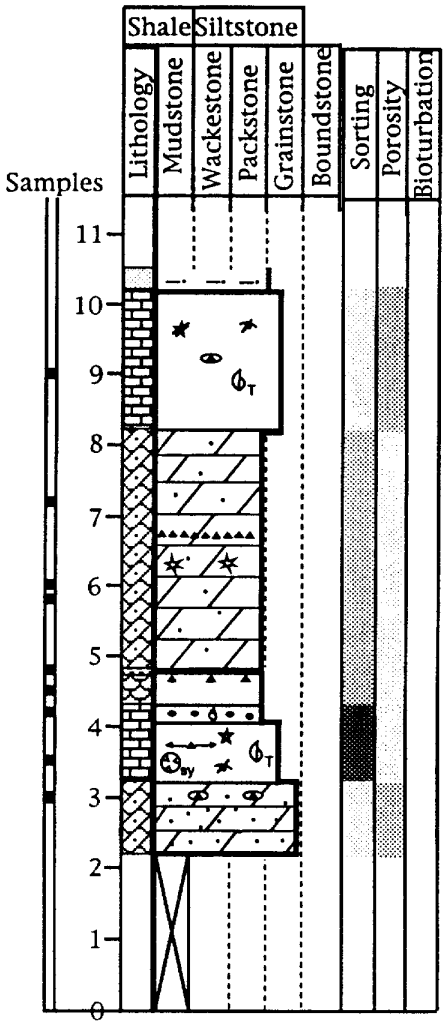


Figure A-10 - Section P-3, measured June 8, 1992 with Kathy O'Neil.

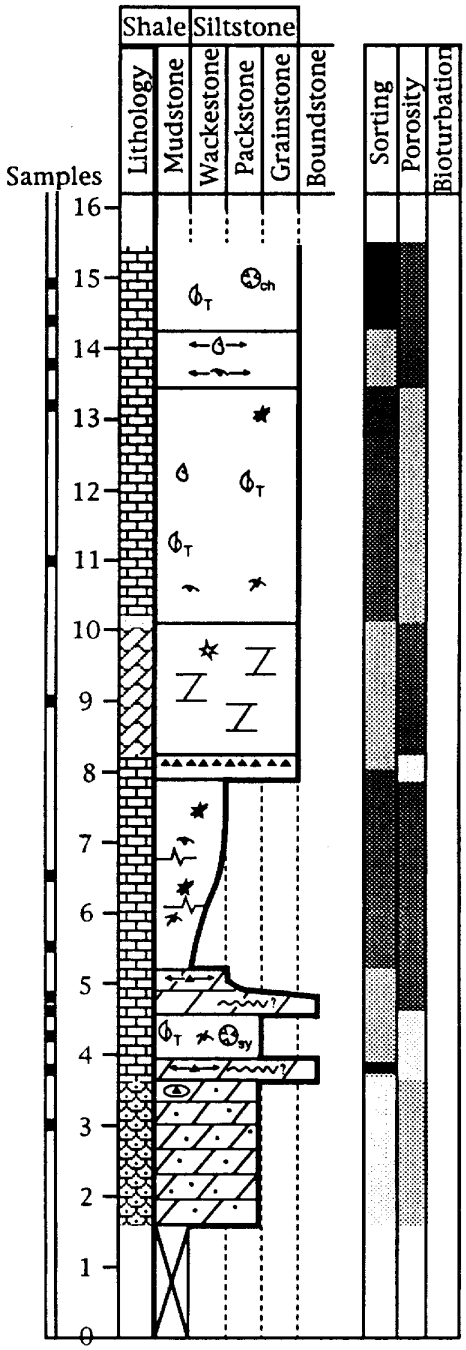


Figure A-11 - Section P-4, measured June 9 and 10 with Kathy O'Neil

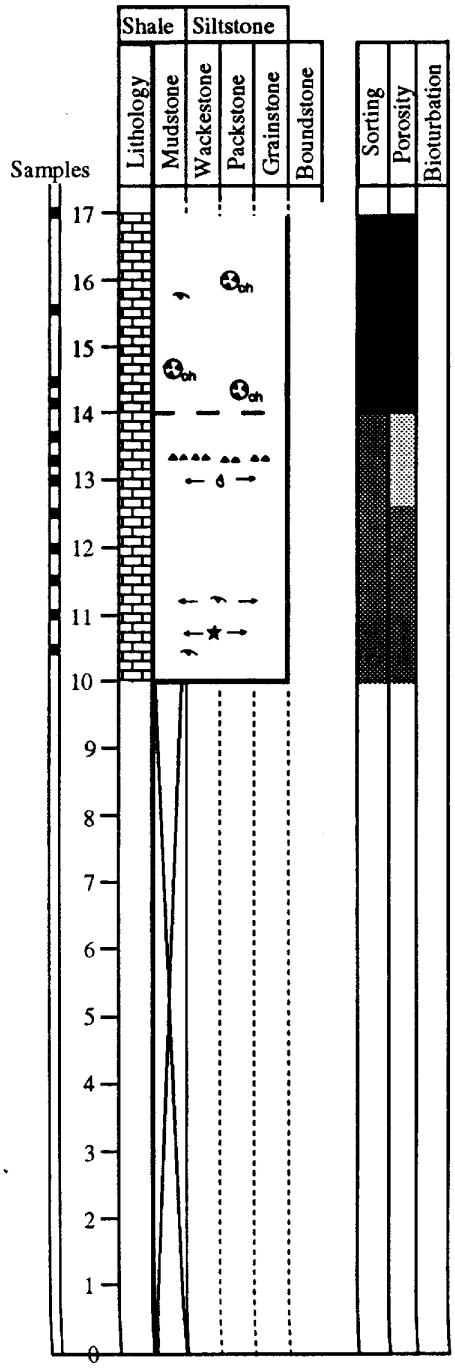


Figure A-12 - Section P-5, measured June 9 with Kathy O'Neil.

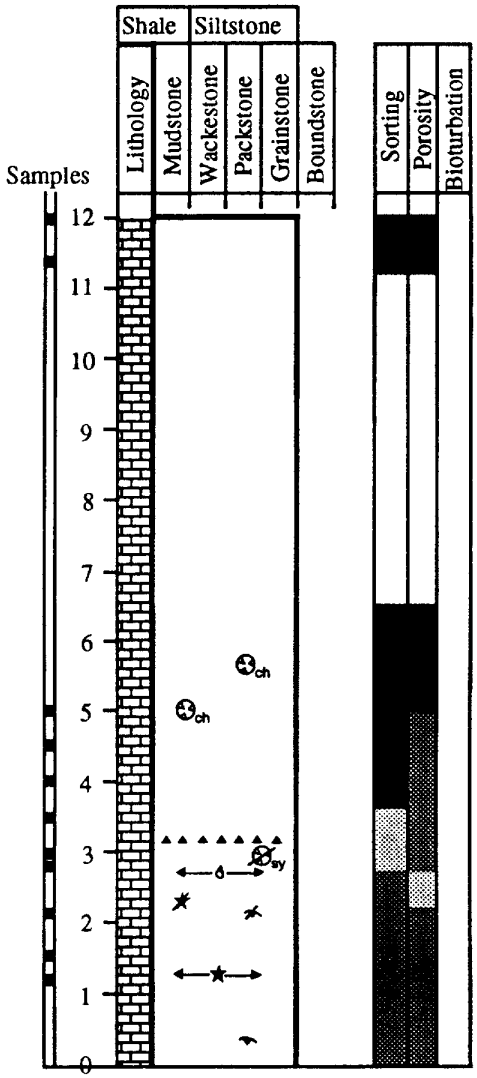


Figure A-13 - Section P-6, measured June 10 with Kathy O'Neil.

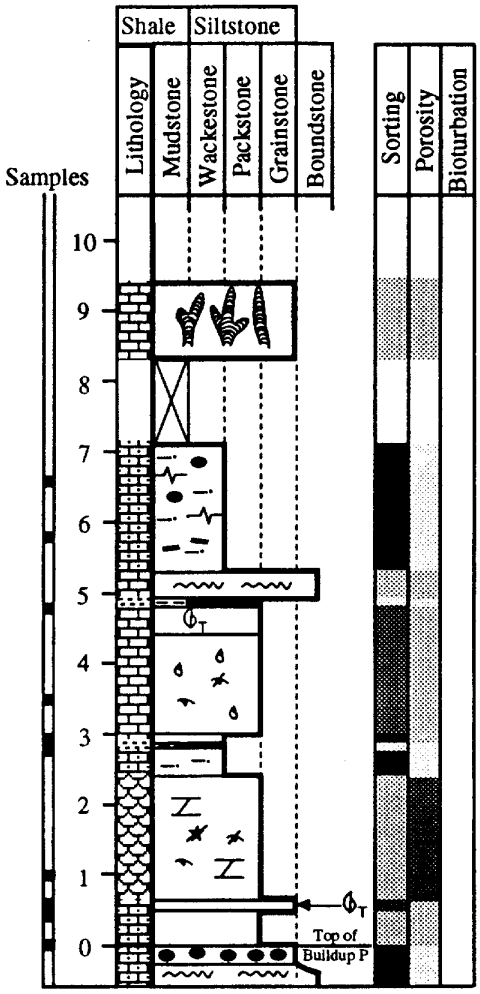


Figure A-14 - Section P-7, measured June 12 with Kathy O'Neil.

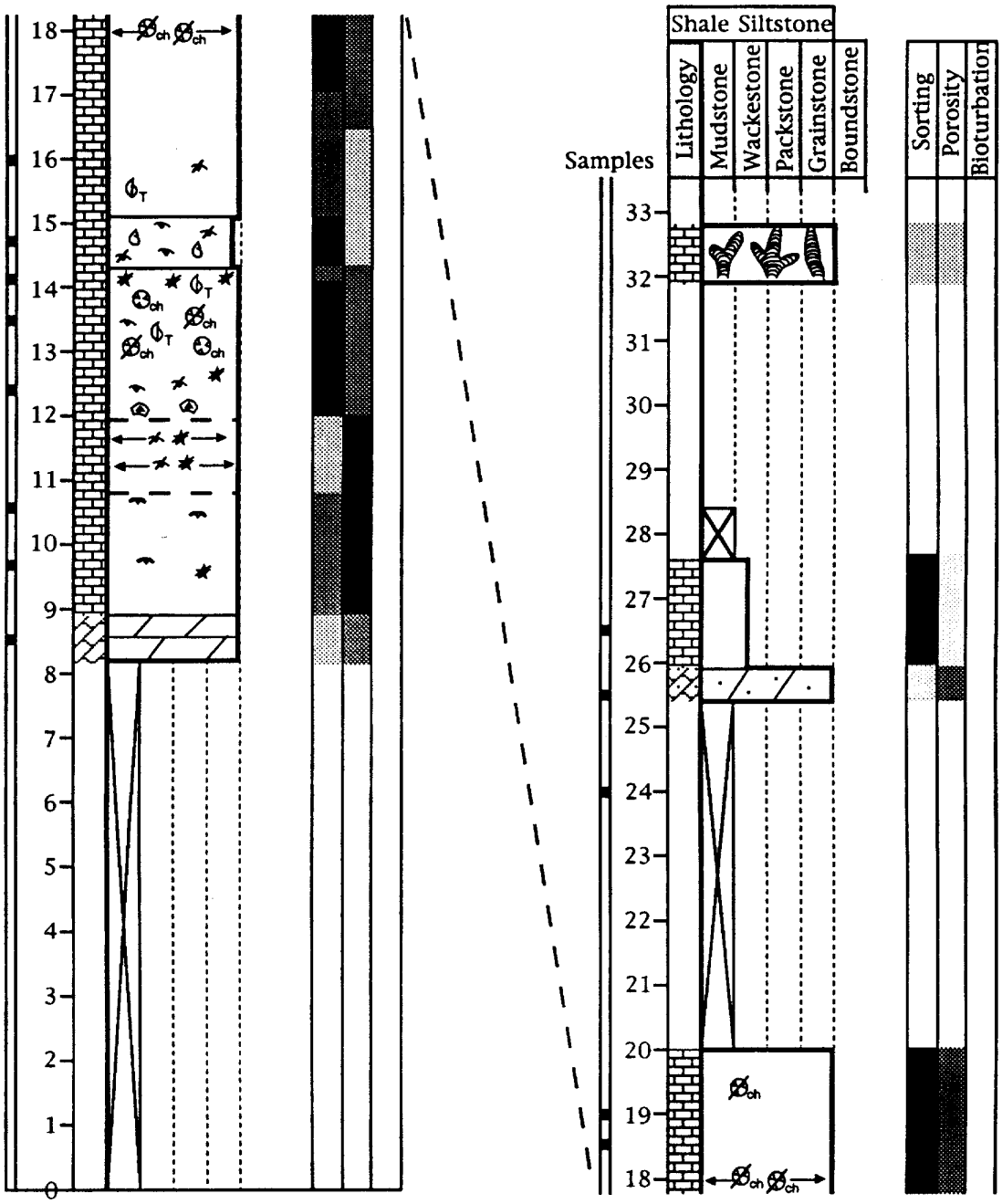


Figure A-15 - Section P-8, measured June 24 with Kathy O'Neil.

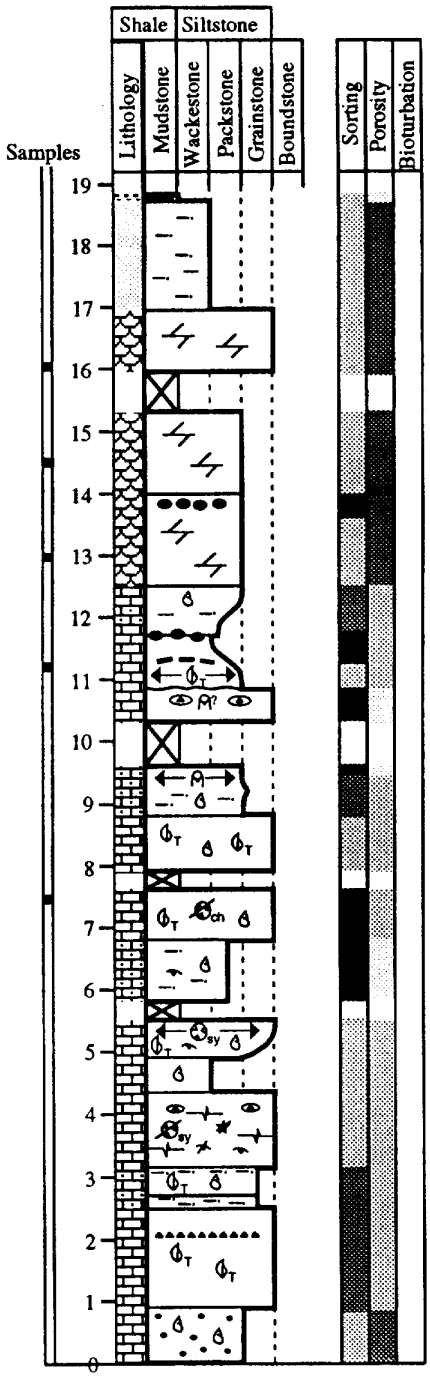


Figure A-16 - Section A-1, measured June 11 with Kathy O'Neil.

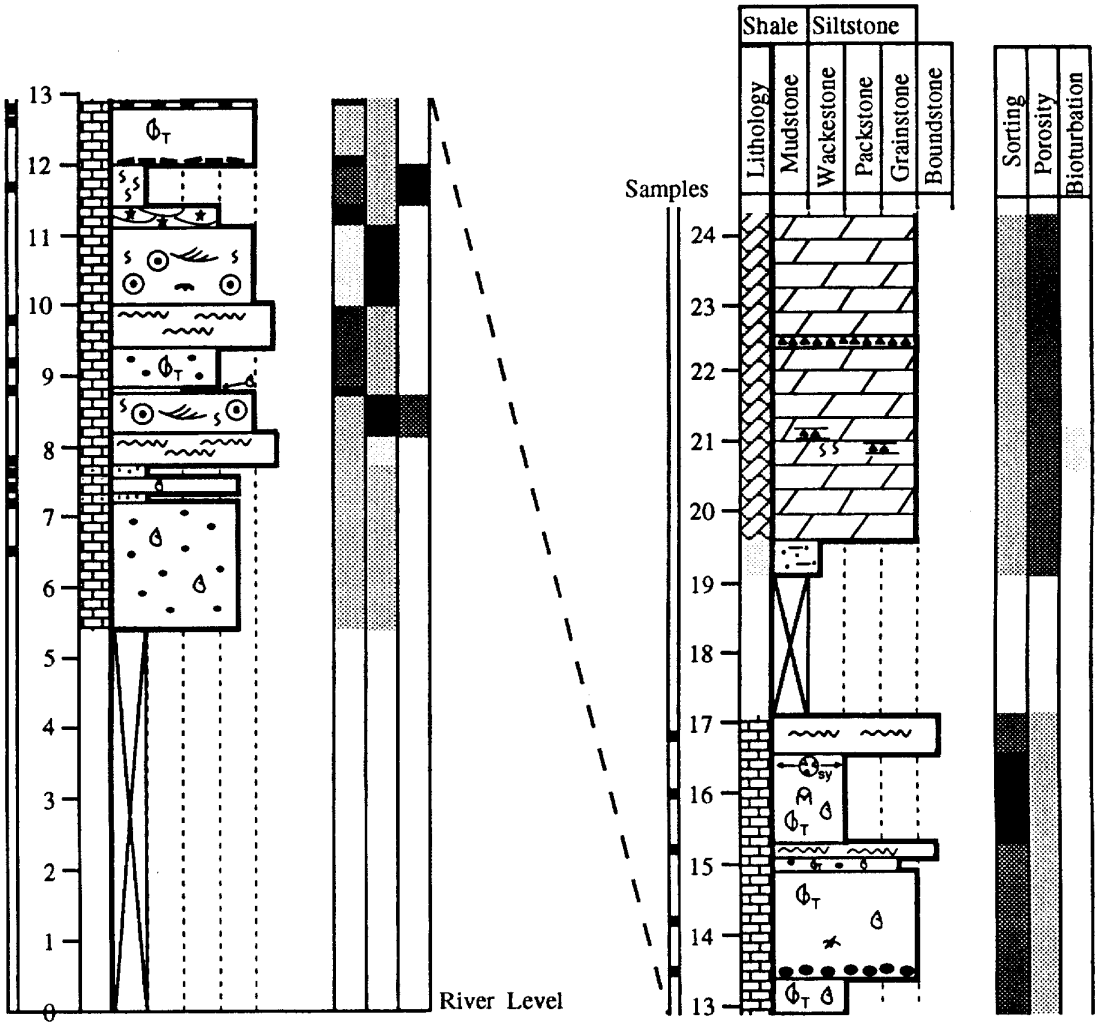


Figure A-17 - Section A-2, measured July 1 and 14 with Kathy O'Neil.

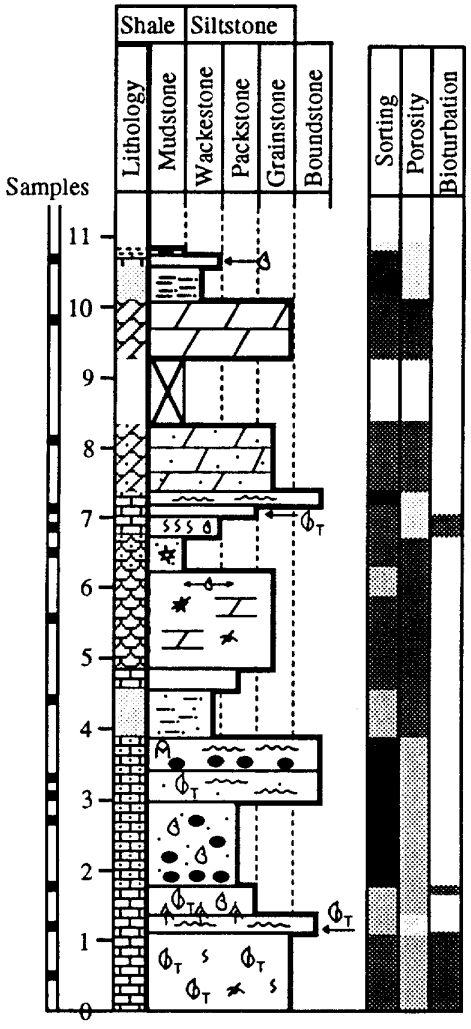


Figure A-18 - Section B, measured July 9 with Kathy O'Neil.

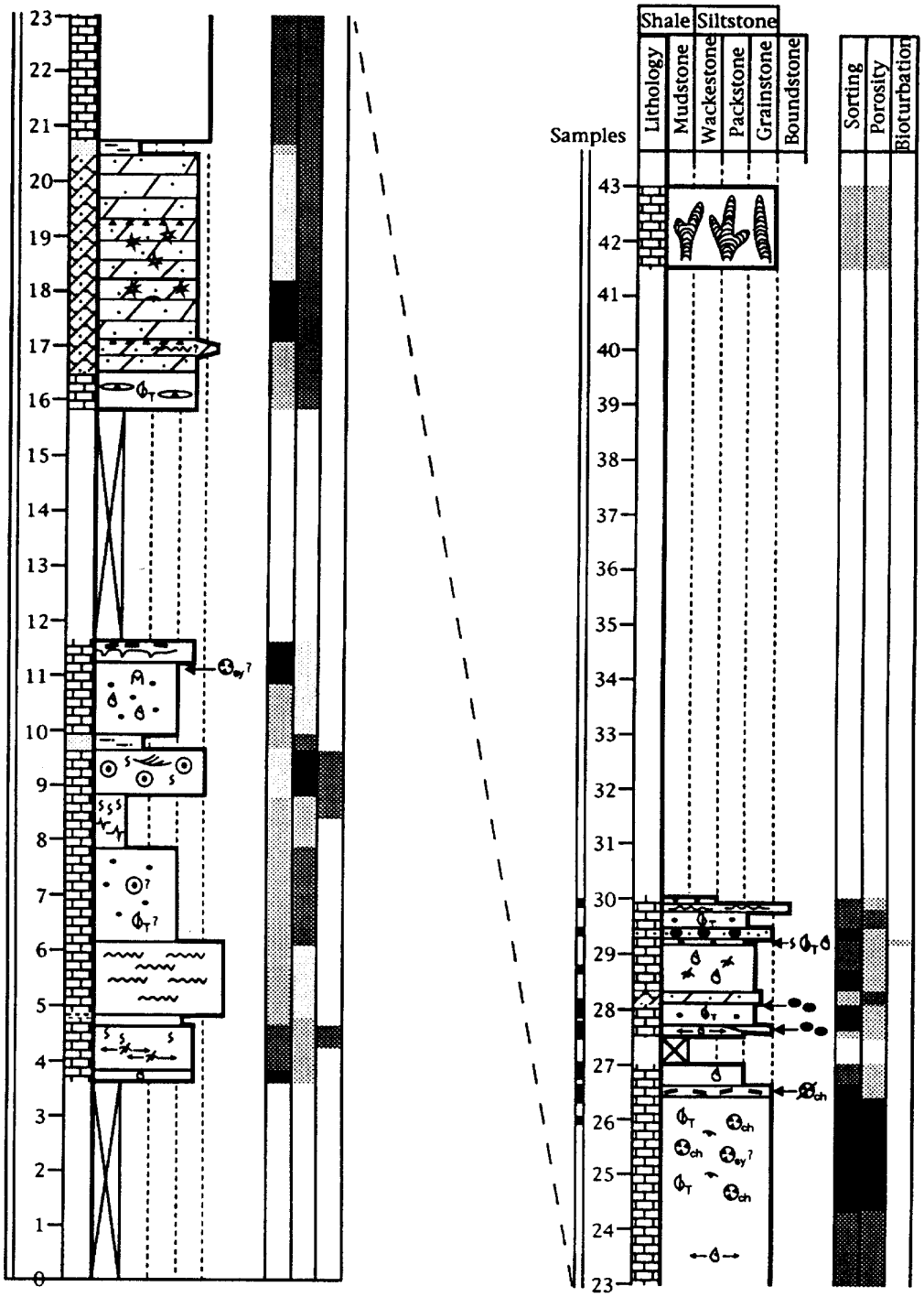


Figure A-19 - Section C, measured June 25 and 26 with Kathy O'Neil.

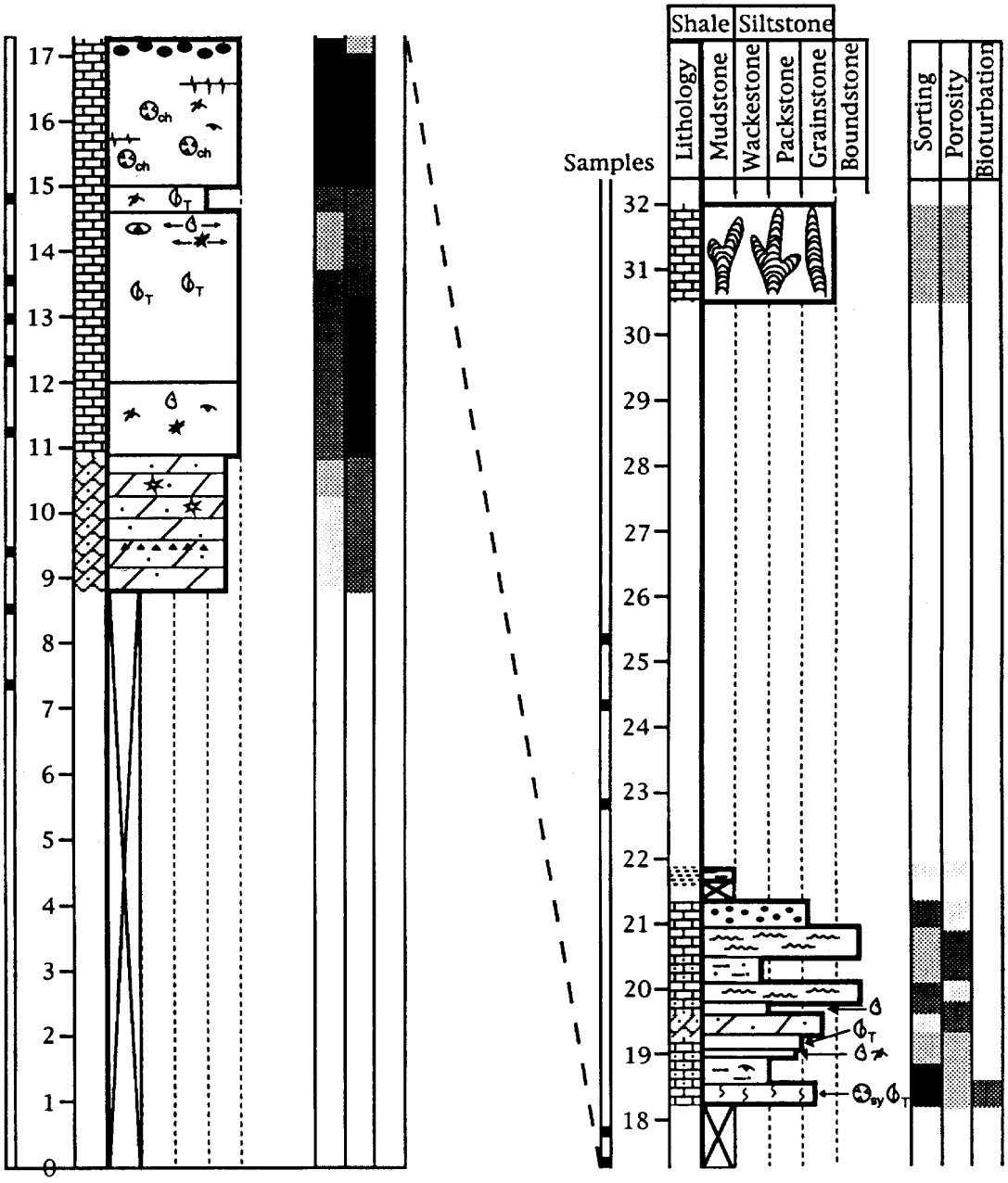


Figure A-20 - Section D, measured June 27 with Kathy O'Neil.

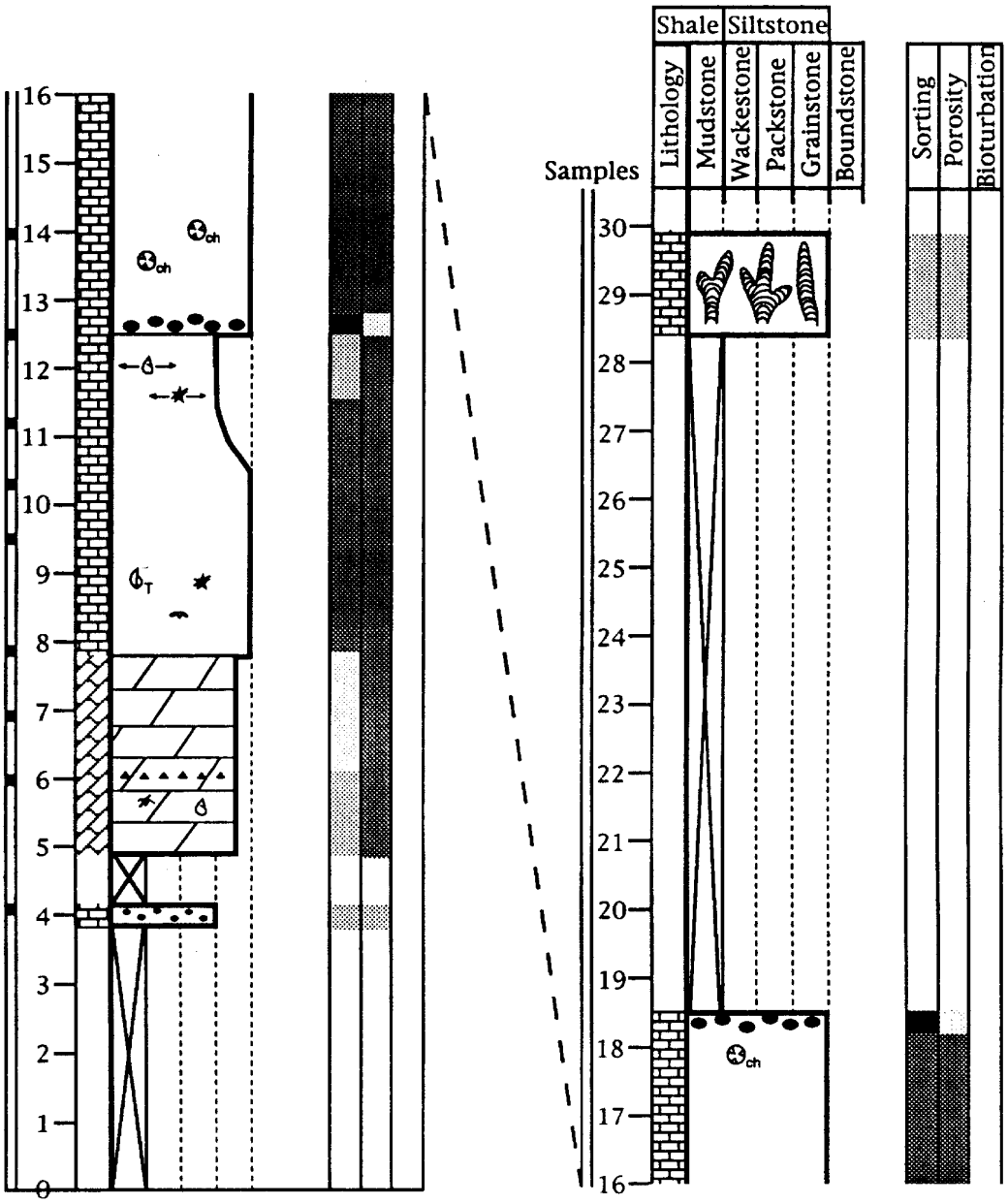


Figure A-21 - Section F, measured July 13 with Kathy O'Neil.

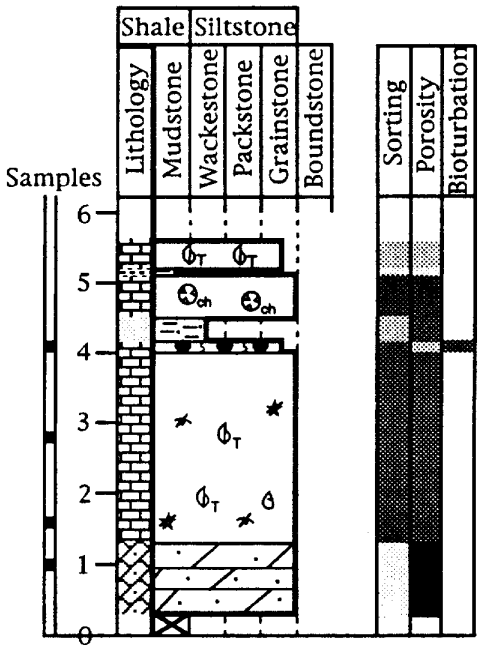


Figure A-22 - Section G-1, measured July 13 and 27 with Kathy O'Neil.

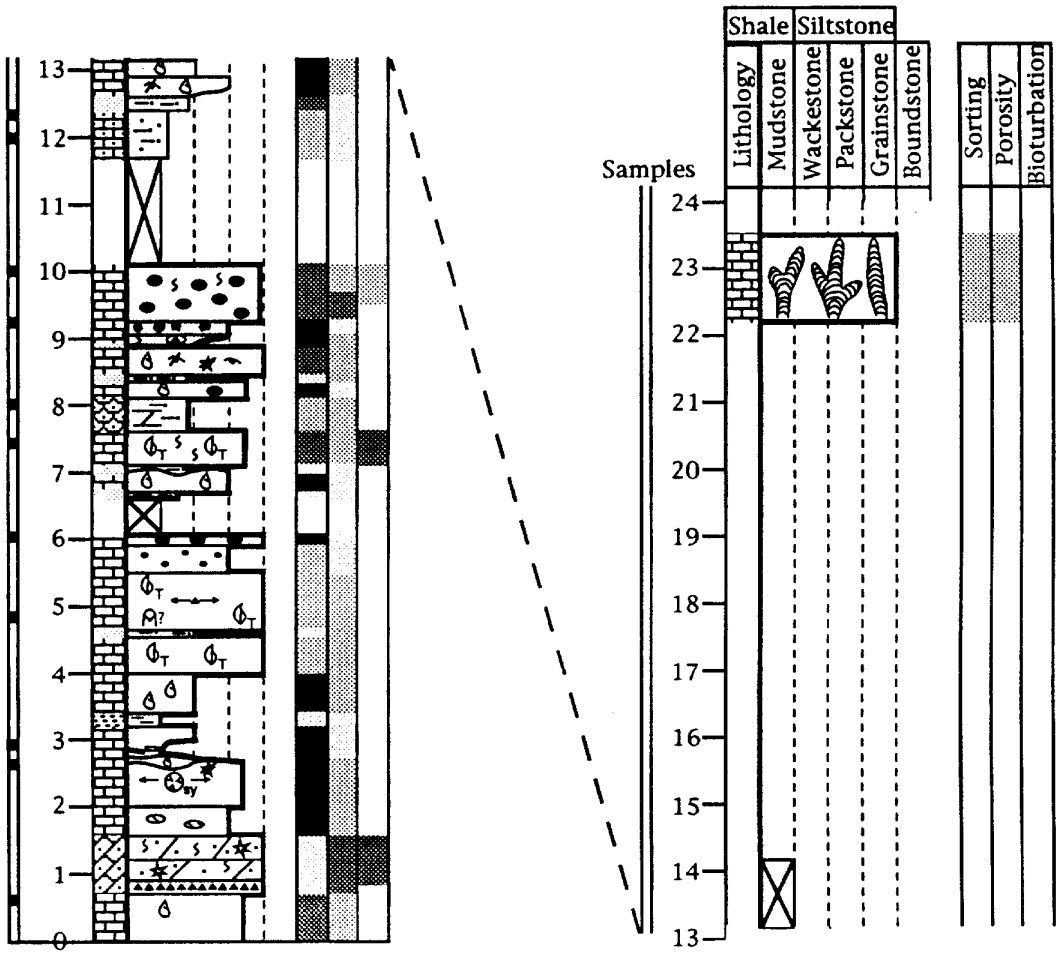


Figure A-23 - Section G-2, measured July 28.

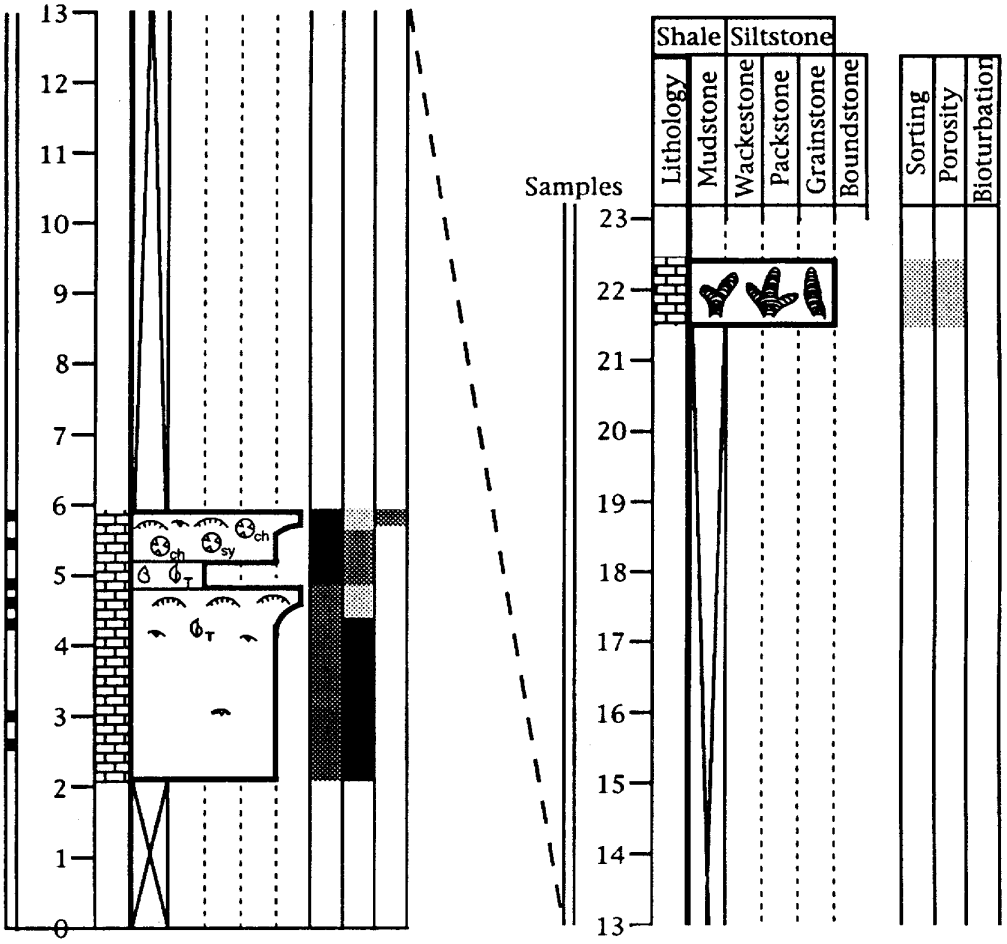


Figure A-24 - Section H, measured July 11 with Kathy O'Neil.

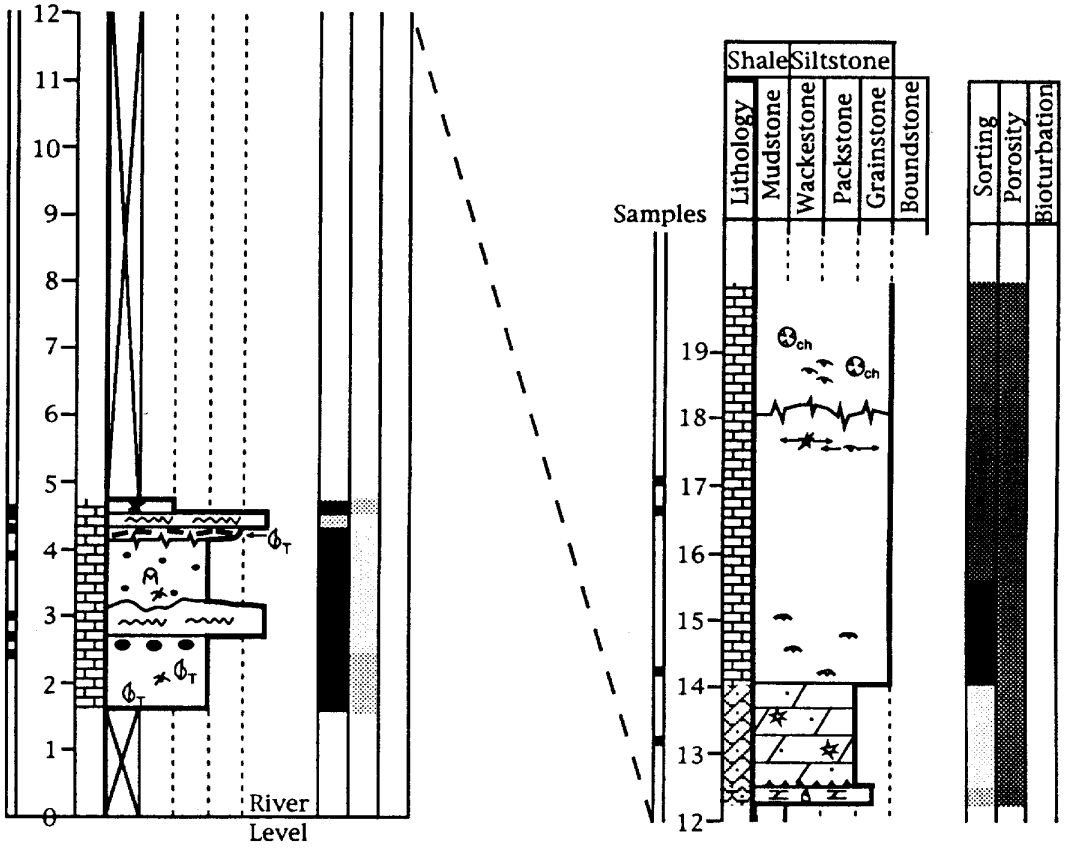


Figure A-25 - Section M-1, measured July 10 with Kathy O'Neil.

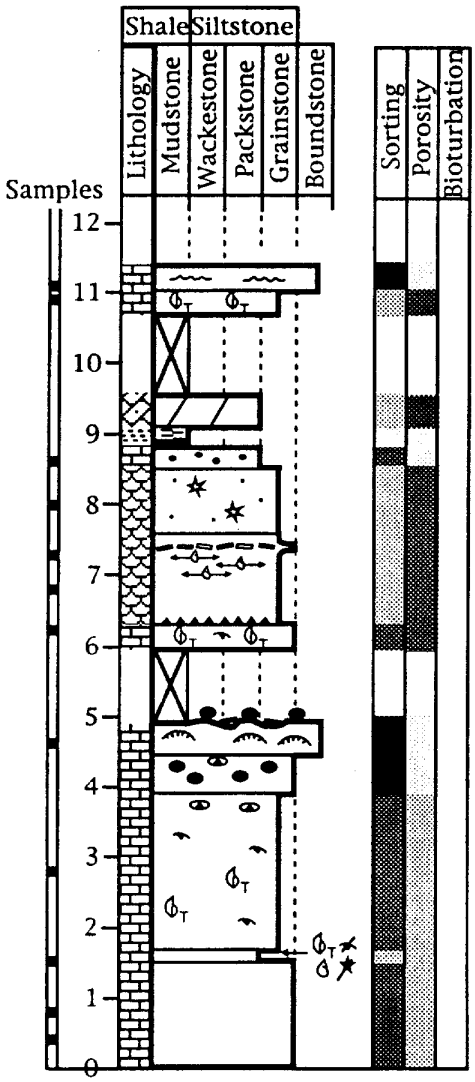


Figure A-26 - Section M-2, measured July 10 with Kathy O'Neil.

Appendix B

Description of Hand Samples

In agreement with the Navajo Nation, all samples collected on Navajo land (on the southern side of the river) are deposited in the collections of the Department of Geology and Geophysics, University of Wisconsin - Madison, under file number U.W. 1884. This appendix contains descriptions of these samples. They are from Sections A-1, C, D, H, P-1, P-2, P-3, P-4, P-5, P-6, P-7, and P-8. The different rock features that are described include the lithology, color, rock classification, grain size, sorting, grain support, grain type, fossil type, cement, porosity, compaction, bioturbation, and sedimentary structures. A symbol or abbreviation is used to describe each feature. If no abbreviation is present in a certain category, it means that feature is not present in that sample (ex. there will be no grains in a mudstone, some samples have no evidence of bioturbation or compaction, etc.). A key to the abbreviations used follows. See Appendix A for the location of each sample within a section.

Key to Rock Descriptions

UW Number (UW No.) gives the number under which the sample is catalogued in the collections of the Department of Geology and Geophysics, University of Wisconsin - Madison.

Section Number (Sect.) gives the section from which the sample is from (ex. P-1, C, M-2).

Sample Number (Sam. #) gives the elevation from which the sample was collected (in meters). Some samples were given letter names. If known, the approximate elevation of these samples is given in parentheses after the letter. Samples P-Ph 1, P-Ph 2, P-Ph 3, and PB-IB are all samples of the bioclastic limestones of Zone A, taken between Sections P-2 and A-1. Sample LP-F is a block from the core of Bioherm P (elevation unknown). Sample D-EF is taken from the eastern flank of Bioherm D (elevation unknown). Sample HA is taken from the western flank of Bioherm H, from the top of Zone A.

Lithology (Lith.) describes the composition of the rock (ls=limestone, d=dolostone, si=siltstone, ss=sandstone; x/y=combination of two rock types, ex. d/ls=dolomitic limestone, si/d=silty dolostone, si/d/ls=silty dolomitic limestone).

Color (Col.) describes the color of the sample on a fresh surface (dg=dark grey, mg=medium grey, lg=light grey, t=tan, b=black).

Rock Type (R. Type) gives the Dunham '62 classification of the sample (ms=mudstone, ws=wackestone, ps=packstone, gs=grainstone, bs=boundstone; cg=conglomerate).

Grain Size (G. Size) gives the variety of grain sized found in the sample (m=mud sized, si=silt sized, vfs=very fine sand sized, fs=fine sand sized, ms=medium sand sized, cs=coarse sand sized,

vcs=very coarse sand sized, gr=granule sized, pb=pebble sized, cb=cobble sized).

Grain Type (G. Type) lists the different types of grains which are present in the sample (fo=fossils, ic=intraclasts, oo=ooids, pe=peloids, qu=quartz sand or silt, oc=other clasts).

Fossils (Foss.) lists the different fossil grains which are present in the sample (al=algal laminations or stromatolites, br=brachiopods, by=bryozoans, ch=Chaetetids, cr=crinoids, ec=echinoderms, fh=unidentified fossil hash, on=oncolites, ph=phylloid algae, sy=*Syringipora*, tf=tubular foraminifera;). If a fossil grain is broken or fragmented, its symbol is in italics. If it is whole but reworked, its symbol is underlined. If in is whole and in place, its symbol is written normally. Ex. "*ec* br ch" indicates that this sample contains reworked fragments of echinoderms, reworked whole brachiopods, and in place Chaetetids.

Sorting (Sort.) describes the sorting of the sample (p=poorly sorted, m=moderately sorted, w=well sorted, vw=very well sorted).

Cement (Cem.) describes the type of cement present and its abundance in the sample (c=calcite cement, d=dolomitic cement). If a cement type is rare, the symbol is in italics. If the cement type is predominant, the symbol is in bold. Otherwise, the symbol is written normally.

Porosity (Por.) describes the type of porosity present and its abundance within the sample (fe=fenestral, fr=fracture, gr=growth framework, ir=interparticle , ia=intraparticle, mo=moldic, sh=shelter). If the porosity is rare, the symbol is in italics. If the porosity is very abundant, the symbol is in bold. If the original porosity has been filled in by cement, the symbol is struck through with a line. Otherwise the symbol is written normally.

Compaction (Comp.) indicates if there is any evidence of compaction in the sample (cb=compressed burrows, cf=compressed fossils, ps=pressure solution, sy=stylolites).

Bioturbation (Turb.) indicates whether or not there is any evidence of bioturbation and its abundance in the sample (r=rare, m=moderate, c=common, a=abundant).

Sedimentary Structures (Sed. St.) lists the various types of sedimentary structures present in the sample (al=algal laminations, cb=cross-bedding, gb=graded bedding, gl=grain laminations, oi=oil stains, sc=evidence of scour).

Appendix B

Hand Sample Descriptions

Sec. No. = Section Number
Sam. No. = Sample Number
Lith. = Lithology
Col. = Color
R. Type = Rock Type

G.S. = Grain Size
Sort. = Sorting
G. Supp. = Grain Support
G. Type = Grain Types
Foss. = Fossil Grain Types

Cem. = Cement
Por. = Porosity
Comp. = Compaction
Turb. = Bioturbation
Sed. St. = Sedimentary Structures

UW No.	Sect.	Sam. #	Lith.	Col.	R. Type	G. Size	G. Type	Foss.	Sort.	Cem.	Por.	Comp.	Turb.	Sed. St.
UW1884/1	P-1	6.4	ls	dg	ws/ps	m, ms	pe, fo	fh	w				m	al?
UW1884/2	P-1	9.8	ls	lg/mg	gs	fs, ms	oo		vw		**mo**			cb
UW1884/3	P-1	11.9	ls	mg	ps	fs, ms, vcs	fo	tf, fh, *on, br*	m					
UW1884/4	P-1	12.8	ls	mg	ms	m			vw					
UW1884/5	P-1	12.9	ls	dg	ps	m, vfs, fs	pe		w					gl
UW1884/6	P-1	14.O	si	gg		m, si, vfs	qu, fo		w			cf		
UW1884/7	P-1	14.3	si	gg		m, si, vfs	qu, fo		w			cf		
UW1884/10	P-1	15.2	si	gg		m,si,vfs	qu		w					
UW1884/8	P-1	15.3	ls	t/mg	ps	fs, ms, vcs	fo	tf, al?, fh	m, p					
UW1884/9	P-1	15.4 b	d/ls	t	ms/ws	m, c-vcs			w					
UW1884/11	P-1	16.O	d/ls	t	ms	m, vfs	qu, fo		vw			sy	r	
UW1884/12	P-1	16.9	ls	mg	ps	m, fs, ms	fo, oc	fh, *cr*	m, w		mo		r	gb
UW1884/15	P-1	18.6	d/ls	lg	ps	m, fs, vfs	qu, fo	fh	w				r	
UW1884/13	P-1	19.7	ls	lg	ws/ps	m, ms, cs	fo	tf, *ph?*	m				m?	
UW1884/14	P-1	20.7	ls/d	lg	ws	m, fs	fo	fh	w					
UW1884/16	P-1	21.O	ls/d	lg	ms	m								
UW1884/17	P-1	22.1	ls	lg	ps	m, fs, ms	fo	fh	m, p		**mo**			
UW1884/18	P-1	23.2 a	ls	mg	bs	m, ms	fo	al	m					al
UW1884/19	P-1	23.2 b	ls	lg/mg	bs	m, cs	oc	al	g	c	**fe**			al
UW1884/20	P-1	24.8	ls	mg	ps	m, fs, cs	fo	tf, fh, *br*	m, p	*c*	~~*fe*~~			
UW1884/21	P-1	25.O	ls	mg	ps	m, ms, cs	fo	tf, fh, *br*	m, p					
UW1884/22	P-1	26.2	ls	lg	ps/gs	m?, fs, ms	fo	tf, *br, cr*	g	c				
UW1884/23	P-1	27.4	ls	mg	ps/bs	ms-vcs	fo	tf, *br*	m					
UW1884/24	P-1	28.8	ls	mg	ps/cg?	m, ms, cs, vcs	oc		p					

UW No.	Sect.	Sam. #	Lith.	Col.	R. Type	G. Size	G. Type	Foss.	Sort.	Cem.	Por.	Comp.	Turb.	Sed. St.
UW1884/25	P-1	29.O	ls	mg	ps/gs	fs, ms	oc		vw			ps		
UW1884/26	P-1	29.1	ls	mg/dg	ps/gs	fs, ms, pb	oc, fo	tf, on?	w					
UW1884/27	P-1	29.6	ls	mg/lg	ws/ps	m, fs, ms	fo	tf, fh	w					
UW1884/28	P-1	30.O	ls	mg/dg	ws/ps	m, fs, ms, cs	oc, fo	tf, on	m					gl, al?
UW1884/29	P-1	30.8	ls	mg	ws/ps	m, vfs, fs	pe, fo	fh	w				m?	gl
UW1884/30	P-1	32.3	ls	mg	bs	m, ms, cs	fo	al, fh	m, p				m	al
UW1884/31	P-1	32.8	ls	mg	ps	m, vcs, gr, pb	fo	on	p					gl
UW1884/32	P-1	33.8	ls	mg	ps	m, fs, vcs, pb	fo, oc	*on*	p					gl
UW1884/33	P-1	34.1	ls	mg	ps	m, ms, cs, pb	fo	on	m			ps		
UW1884/34	P-1	38.4	ls	lg	ps	m, vfs, fs, gr	fo	tf, fh	w				m	
UW1884/35	P-1	38.6	ls	lg/dg	cg	m, cs, gr	ic		p					
UW1884/36	P-2	4.1	ls	mg/t	bs	m, fs	fo	al, fh	w	c	~~fe, gr~~			al
UW1884/37	P-2	5.1	ls	mg	ps	m, cs, vcs	fo, oc	tf, fh	p				c	
UW1884/38	P-2	5.7	ls	lg	gs/bs	fs, ms, cs	fo	tf, fh	w	c		cb?	m	
UW1884/39	P-2	6.4	ls	mg	ps	m, fs, gr, cb	fo, oc	*br, tf, cr*	p					
UW1884/40	P-2	7.9	ls	lg	ps	m, vfs, fs, vcs	fo	tf, *br*	m	c				
UW1884/41	P-2	8.3	ls	mg	ps	m, vfs, fs, ms	fo, pe?, oc	tf, fh	m					
UW1884/42	P-2	8.8	ls	mg	ms, ps	m			w	c	~~fe?~~	sy		al?
UW1884/106	P-2	9.8 A	ls	mg	bs	m, cs	fo	tf, *tf*	p	c	fe?			
UW1884/43	P-2	9.8 B	ls	mg/dg	cg	fs, cs, gr, pb	oc		p	c		ps		
UW1884/44	P-2	10.4 A	ls	mg/dg	ws/ps	m, fs, ms	fo	fh?	p					
UW1884/45	P-2	10.4 B	ls	mg/dg	cg	m, ms, gr, pb	oc	al	p			ps		
UW1884/46	P-3	3.O	si/d/ls	lg	ms	m, si, vfs	qu		vw					
UW1884/47	P-3	3.5	ls	mg/dg	ps	fs, ms	pe, fo, oc	t f	m					gl
UW1884/48	P-3	4.2	ls	ms	ps	m, fs, ms	fo	tf, fh	p		mo			
UW1884/49	P-3	4.5	d	t	bs?	m, cs	fo	al?	w			sy		al?
UW1884/50	P-3	4.8	d/ls	t	ws	m, ms, cs	fo	br	p	*c*	~~mo~~		m	
UW1884/51	P-3	5.8	d	lg	ms	m			vw					
UW1884/52	P-3	6.O	d	lg	ms	m, si, vfs	qu		vw					
UW1884/53	P-3	7.2	d	lg	ms	m, vfs, fs	qu		vw					
UW1884/54	P-3	PB (9.0)	ls	lg	ps	m, fs, ms, cs	fo	tf, *cr, br*	m		mo			
UW1884/55	P-4	3.O	d	t	ms	m, si	qu		w		ir			
UW1884/56	P-4	3.8	d	t/mg	ws	m, fs, cs	fo	sy?, fh	w		ir			
UW1884/57	P-4	4.3	ls	mg	ps	m, fs, ms	pe, fo	tf, fh *sy, br*	w					gl

UW No.	Sect.	Sam. #	Lith.	Col.	R. Type	G. Size	G. Type	Foss.	Sort.	Cem.	Por.	Comp.	Turb.	Sed. St.
UW1884/58	P-4	4.5	ls	mg	ps	m, ms, pb	fo	br, tf, fh	p			cf		
UW1884/59	P-4	4.6	d/ls	dg	ws	m, ms, cs	fo, oc	*cr, br*	m/p					sc
UW1884/60	P-4	4.8	d	t	ms/ws	m, vfs	qu	al?	w	*c*				al?
UW1884/61	P-4	9.O	d/ls	t	ws	m, fs, ms	fo, qu	fh	w	c	ir, fr			
UW1884/62	P-4	11.O	ls	lg	ps	m, ms, vcs	fo	tf, fh, *br, cr*	p	*c*	**mo**			
UW1884/63	P-4	13.3	ls	lg	ps	m, fs, ms, pb	fo, pe?	tf, br, *br, cr*	w			sy		
UW1884/64	P-4	13.8	ls	mg	ps	m, fs, ms, cs	fo	tf, fh	m					
UW1884/65	P-4	14.4	ls	lg	ps	m, fs	fo	tf, fh	w		**ia**			
UW1884/66	P-4	14.9	ls	lg	bs	m, cs, pb	fo	tf,al,ch, *ch*	p		**ia, gr**			
UW1884/67	P-5	11.O	ls	lg	ms	m			w	c	**fr**			
UW1884/68	P-5	11.5	ls	lg	ws/ps	m, mv, vcs, gr	fo, oc?	*cr, br, ph?*	p		*mo*	sy	m	oi
UW1884/69	P-5	12.O	ls	lg	ws/ps	m, fs, ms	fo	tf, fh	m		ia, mo			
UW1884/70	P-5	12.5	ls	lg	ws	m, fs, ms, cs	fo	tf, fh, *br*	p				m	
UW1884/71	P-5	13.O	ls	lg	ps	m, fs, cs, vcs	fo	tf, fh *ec, br*	p				p?	
UW1884/72	P-5	13.6	ls	lg/mg	ps	m, fs, ms	fo	tf, al?, fh	m					
UW1884/73	P-5	14.2	ls	lg	ps/bs	fs, ms, vcs, cb	fo	tf, fh, *ch*	p		ir			
UW1884/74	P-5	14.5	ls	lg	ps/bs	fs, ms, vcs, cb	fo	tf, fh, *ch*	m		ir			
UW1884/75	P-6	1.2	ls	lg	ws	m, cs	fo	fh	m		mo		m	
UW1884/113	P-6	1.5	ls	lg	ws	m, fs, ms, vcs	fo	tf, *cr*	p					
UW1884/76	P-6	2.2	ls	lg	ws/ps	m, fs, cs, gr	fo, oc	*cr*	w	c	*d?*			gl
UW1884/77	P-6	3.5	ls	lg	gs/bs	fs, cs	fo, oc, pe?	tf, *cr*	w		*ia*			
UW1884/78	P-6	4.O	ls	lg	gs/bs	ms, cs, gr, pb	fo	tf, fh, *ch, br*	m		ia, gr			
UW1884/79	P-6	7.5	ls	lg/mg	ps/bs	m, ms, vcs	fo, oc	tf, fh	p		ia, ia		m?	
UW1884/80	P-7	F (O.O)	ls/ss	mg/t	ws	m, fs, ms	fo?, qu	fh?, al?	m					
UW1884/81	P-7	I (0.O)	ls	dg/t	ps/cg?	m?, ms, cs	oc	al?	m	c				
UW1884/82	P-7	J(0.0)	ls/ss	mg/t	ws/ps	m, fs, ms	qu, oc	al?	m	c		sy		
UW1884/83	P-7	O (O.O)	ls	mg	ms?	m			w	c	**fr**			
UW1884/84	P-7	O.O	ls/ss	mg/t	ps	m, fs, cs	oc, fo?	fh?	m					
UW1884/85	P-7	0.4	ls	mg	ps	m, fs, ms, cs	pe, fo	tf, fh, *br*	m			sy	m	
UW1884/86	P-7	1.O	d	t	ws	m, si, fs, bp	qu, fo	*br,* br	w/m	c	mo			
UW1884/87	P-7	4.8	ls	mg	ps	m, fs, ms, cs	fo	fh	w					
UW1884/88	P-7	5.O	ls	lg	bs	m, fs	pe?	al	vw	c				al
UW1884/89	P-7	5.8	ls	mg	ws	m, s, cs, vcs	fo	fh, *br*	p					
UW1884/90	P-7	6.6	ls	mg	ps	m, fs, ms	fo	tf, fh, *br*	w					

UW No.	Sect.	Sam. #	Lith.	Col.	R. Type	G. Size	G. Type	Foss.	Sort.	Cem.	Por.	Comp.	Turb.	Sed. St.
UW1884/91	P-8	8.5	d	lg	ps/ws	m, cs, gr	fo?, oc	fh	p	*?*				
UW1884/92	P-8	9.7	ls	mg	ps	m, fs, ms, gr	fo	tf, *cr, br*	p		mo		r?	
UW1884/93	P-8	10.6	ls	mg	ps	m, ms, gr	fo	ph, tf, *br*	p		mo, ia			oi
UW1884/94	P-8	12.4	ls	lg	ws	m, vfs, fs, cs	fo	tf, fh, *cr, br*	m		*fr*		r	
UW1884/95	P-8	13.5	ls	lg	ps/gs	m?, fs, ms, pb	fo	tf, *ch, br*	m/p					
UW1884/96	P-8	15.5	ls	mg/dg	ps	m, fs	fo	t f	w	c	~~fe?~~		m?	
UW1884/97	P-8	16.5	ls	lg	ps	m, fs, ms, cs	fo, pe?	tf, fh, *cr, ec*	m		ia			
UW1884/98	P-8	16.5b	ls	lg	ps	m, ms, cs, vcs	fo, oc	tf, ph, f *br, cr*	m	c	ia			
UW1884/99	P-8	18.5	ls	mg	gr	fs, ms, cs, gr	fo	*br, by, cr, tf*	m	c	*ia, mo*			
UW1884/100	P-8	18.5b	ls	mg	cg	m, fs, gr, pb	bc, oc		p	c	ia?	ps		
UW1884/101	P-8	18.5c	ls	mg/dg	cg	m, ms, cs, p	fo, oc	t f	p		*fr*	ps		
UW1884/102	P-8	23.5	d	lg	ms/ps	m, ms, cs	oc		m	d	mo, fe?			gl?/al?
UW1884/103	P-8	26.O	ls	t/mg	ps	m?, ms, cs	fo, oc?	fh	m					
UW1884/104	P-8	1	ls	t	ps/gs	ms, cs, pb	fo	br	p					
UW1884/105	P-8	B	ls	mg/dg	cg	m?, fs, cs, pb	oc		p					
UW1884/114		P-Ph 1	ls	mg	ps	m, fs, ms, cs	fo, oc?	tf, fh, *cr*	m					
UW1884/115		P-Ph 2	ls	dg	cg?	m, cs, vcs, pb	oc		p	*c*	~~ir~~	ps		
UW1884/116		P-Ph 3	ls	dg	ps	m, fs, ms	fo	tf, fh, *br*	w					
UW1884/117		PB-IB	ls	lg	ws/ps	m, fs, vcs, pb	fo, oc	tf,ph?, *br*	p		mo			
UW1884/118		LP-F	ls	mg	ps/bs	m, fs, ms	fo	tf, al?	m	c	~~fr~~			
UW1884/119	A-1	4.O	ls	lg	ws/ps	m, fs, ms, vcs	fo	tf, br, *cr*	m/p					
UW1884/120	A-1	B-7.5	ls	mg	ps	m, fs, ms, vcs	fo, oc	t f	m					
UW1884/121	A-1	11.2	ls	mg	ps	m, fs, ms, gr	fo	tf, fh	w	c	~~*fr*~~			gl
UW1884/122	A-1	13.O	d	lg	ms	m, si	qu		vw		ir			
UW1884/123	A-1	14.5	ls	lg/t	ws	m, fs	fo?	fh?	vw	*c*	~~*mo*~~	sy		
UW1884/124	C	25.1	ls	lg	ps	m?, ms, cs	fo, oc	tf, fh, *br?*	m			ps		
UW1884/125	C	26.O	ls	lg	bs/ps	m?, fs, md, cs	fo	tf, fh, *br, sy*	w/m				r?	
UW1884/126	C	26.5	ls	mg	gs	fs, ms, cs	fo	tf, fh	w	c				
UW1884/127	C	27.O	ls	dg	bs/ps	m, gr	fo	on?, al	p	c	~~*fr, d*~~			al
UW1884/128	C	28.O	ls	mg	ps	m, fs, gr	fo	tf, br	w/m	c	~~mo~~			gl
UW1884/129	C	28.1	ls	mg/dg	ws/bs?	m, fs	fo?	al?, fh?	w		~~*gr?*~~			oi
UW1884/130	C	28.7	ls	mg/dg	ps	m, fs, ms, cs	fo	tf, fh	m					
UW1884/132	D	11.3	ls	lg	ws/ps	m, fs, cs	fo	tf, *br*	w		mo	ps?		
UW1884/131	D	12.1	ls	mg	ps/cg	m, cs, gr	fo, oc	*cr, ph?*	p		mo			oi

UW No.	Sect.	Sam. #	Lith.	Col.	R. Type	G. Size	G. Type	Foss.	Sort.	Cem.	Por.	Comp.	Turb.	Sed. St.
UW1884/133	D	14.1	ls	lg	ps, gs	m, fs, ms	fo, oc	tf, *cr, br?*	p	c	~~ia, mo~~		m	
UW1884/135	D	14.4	ls	mg	ps	m, fs, cs, vcs	fo	tf, fh, *cr*	p			sy, cf		
UW1884/136	D	16.O	ls	lg	ps	m, fs, ms, vcs	fo	tf, fh, *br*	m					
UW1884/137	D	16.3	ls	lg	gs/ps	m, vfs, ms, gr	fo, pe	tf,fh,al *br*	m			sy		
UW1884/138	D	17.1	ls	dg	ms/bs/cg	m, cs, gr	oc	al, *al*	p	c				al
UW1884/139	D	17.1b	ls	dg	cg?	m, gr	oc?		m		*fr*	ps		
UW1884/140	D	18.5	ls	dg	ws/ps	m, fs, ms	fo	tf, fh	w				m	
UW1884/141	D	19.2	ls	dg	ps	m, fs, ms	fo	tf, fh	w					
UW1884/142	D	20.8	ls	mg/t	bs	m, fs	qu, fo	on	p			ps		al
UW1884/143	D	D-EF	ls	lg/mg	bs	m, ms	fo	tf, al	w	c				al
UW1884/144	H	2.6	ls	t/lg	ps	m, fs, cs, gr	fo, oc	*br*	p	*c*	mo, ia			oi
UW1884/145	H	3.O	ls	lg	ws/ps	m, ms, vcs	fo, oc?	fh, *br, ph?*	p		mo			
UW1884/146	H	4.6	ls	mg	ps	m, ms, cs	fo, oc	fh, br	m/p			sy		
UW1884/147	H	HA	ls	mg	ps	m, fs, ms	fo	tf, fh	w					gl
UW1884/148	M-1	4.3	ls	mg	ws/ps	m, fs, ms	fo	fh	w					gl
UW1884/149	M-1	13.15	d	t	ms	m			w				m	
UW1884/150	M-2	10.9	ls	mg	ps	m, fs, ms	fo	tf, fh, cr	w			sy		

APPROVED: [redacted]

DATE: Jan 21, 1994